US 20080157732A1

(19) United States

(12) Patent Application Publication

Williams

(10) Pub. No.: US 2008/0157732 A1

(43) Pub. Date: Jul. 3, 2008

(54) HIGH-EFFICIENCY DC/DC VOLTAGE CONVERTER INCLUDING CAPACITIVE SWITCHING PRE-CONVERTER AND UP INDUCTIVE SWITCHING POST-REGULATOR

(75) Inventor: **Richard K. Williams**, Cupertino, CA (US)

Correspondence Address:
PATENTABILITY ASSOCIATES
P.O. BOX 9551
SAN JOSE, CA 95157

(73) Assignee: **Advanced Analogic Technologies, Inc.**, Sunnyvale, CA (US)

(21) Appl. No.: **11/890,941**

(22) Filed: **Aug. 8, 2007**

Related U.S. Application Data

(60) Provisional application No. 60/877,952, filed on Dec. 30, 2006, provisional application No. 60/877,720, filed on Dec. 30, 2006.

Publication Classification

(51) Int. Cl.
G05F 1/00 (2006.01)

(52) U.S. Cl. **323/266**; 323/271; 323/282

(57) **ABSTRACT**

A DC/DC converter includes a pre-converter stage, which may include a charge pump, and a post-regulator stage, which may include a boost converter. The duty factor of the post-regulator stage is controlled by a feedback path that extends from the output terminal of the DC/DC converter to an input terminal in the post-regulator stage. The pre-converter steps the input DC voltage up or down by a positive or negative integral or fractional value, and the post-regulator steps the voltage up by a variable amount depending on the duty factor at which the post-regulator is driven. The converter overcomes the problems of noise glitches, poor regulation, and instability, even near unity input-to-output voltage conversion ratios.

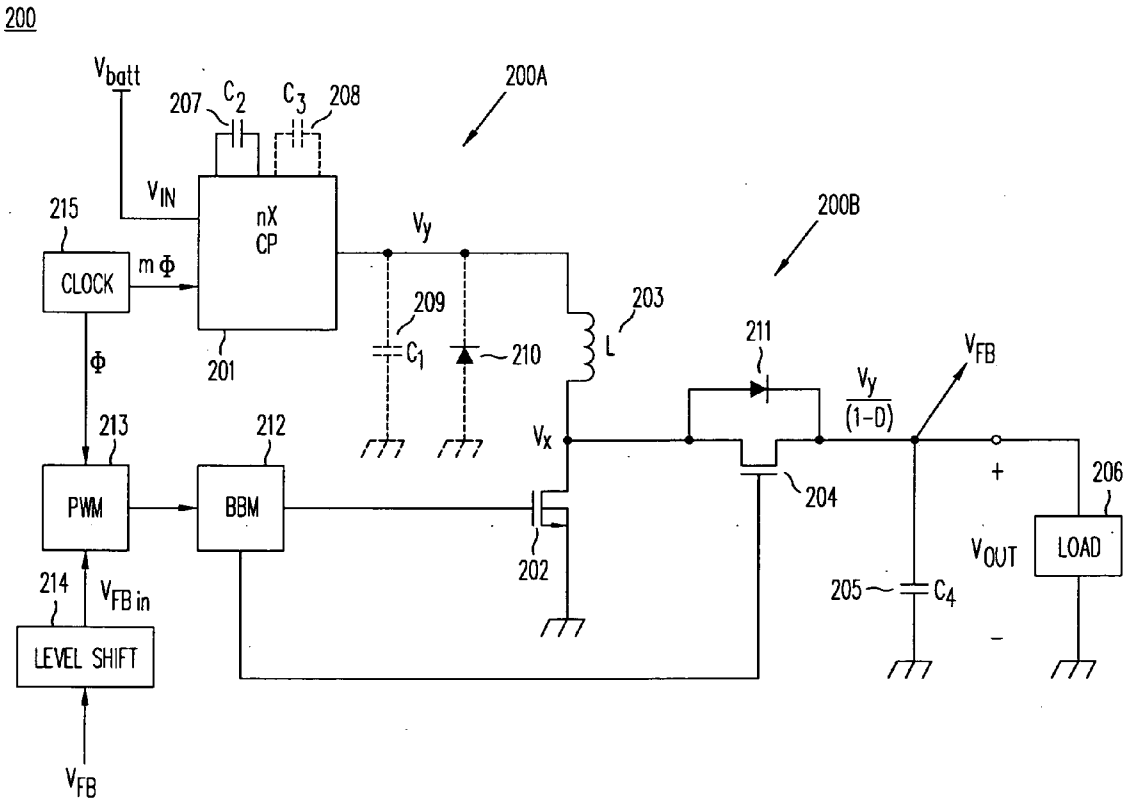

NOCO Exhibit 2011
ADC v. NOCO
IPR2024-00671

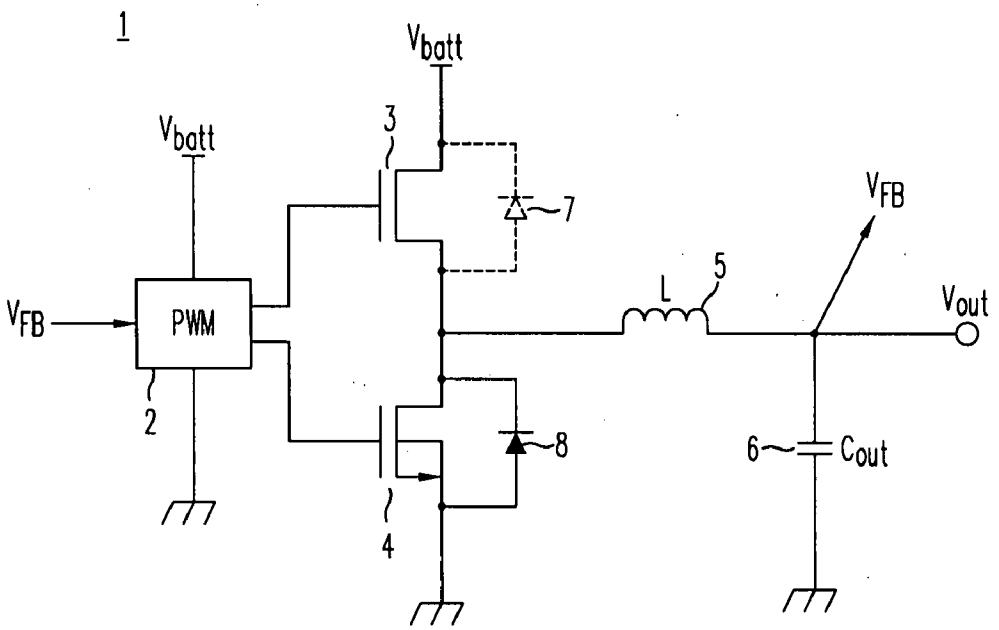

FIG. 1A
(Prior Art)

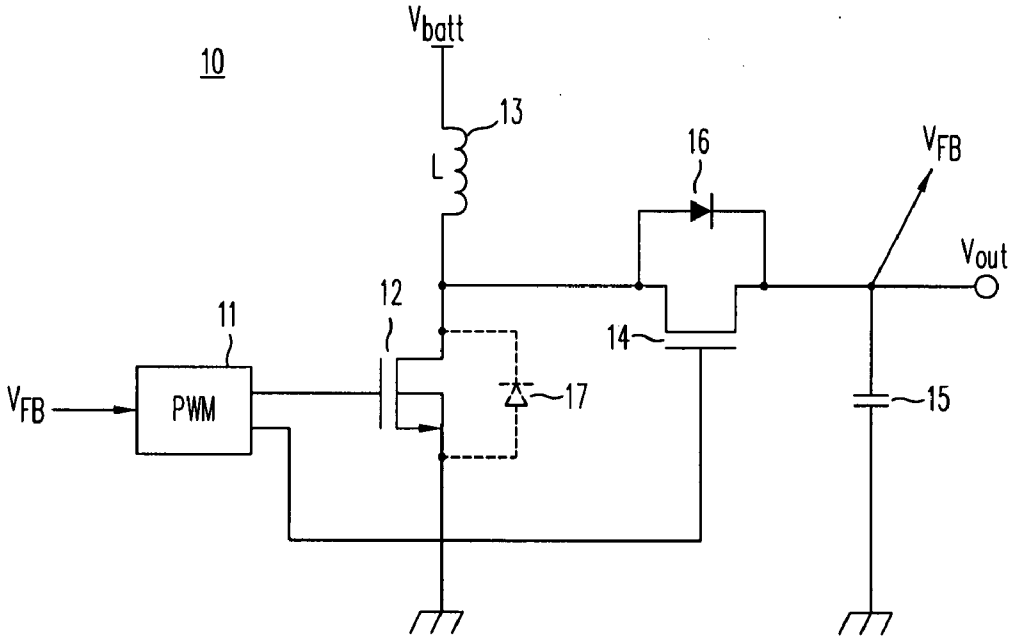

FIG. 1B
(Prior Art)

NOCO Exhibit 2011
ADC v. NOCO
IPR2024-00671

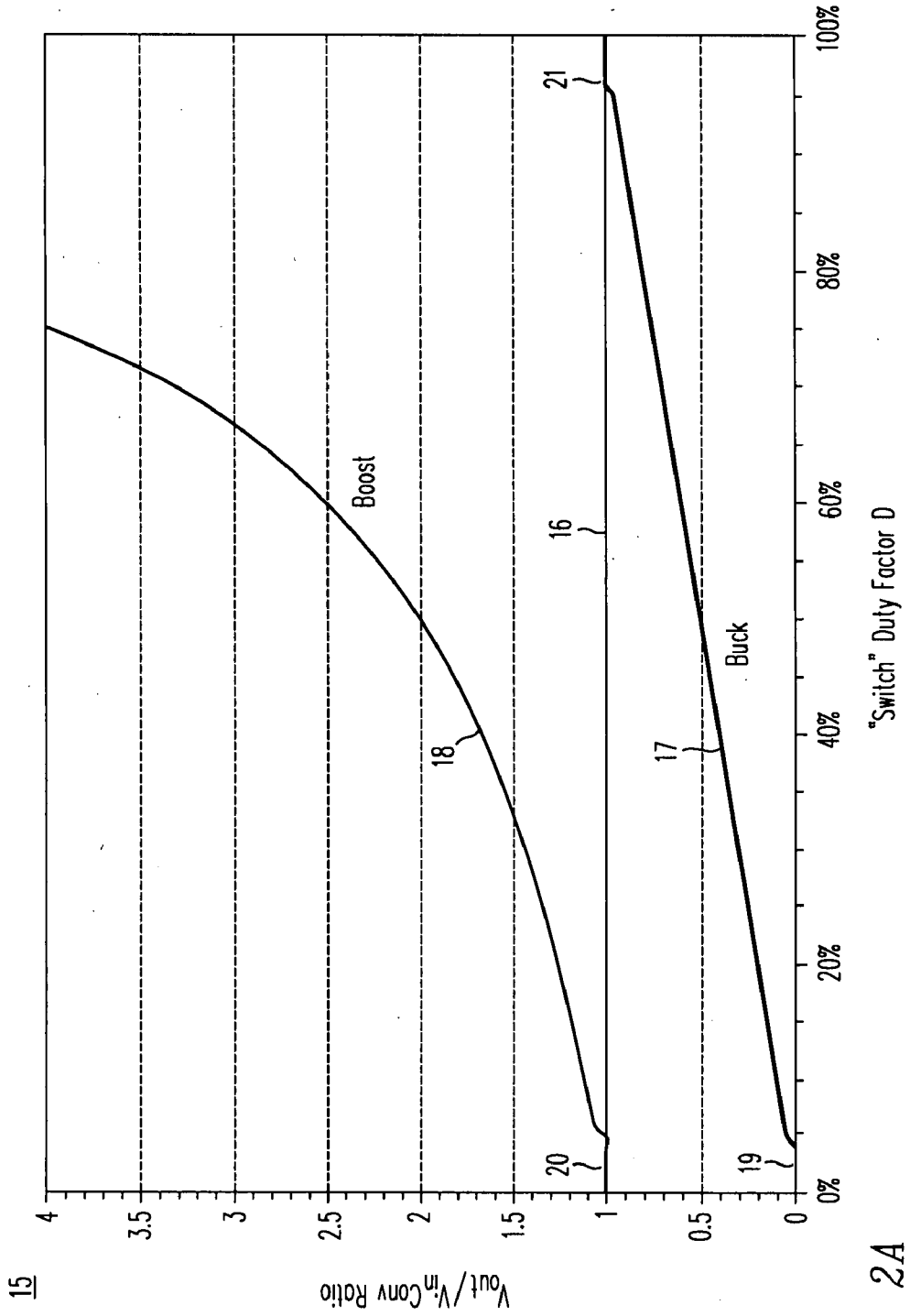
15
Vout/Vin Conv Ratio
4
3.5
3
2.5
2
1.5
1
0.5
0
0%
20%
40%
60%
80%
100%
"Switch" Duty Factor D
Boost
Buck
16
17
18
19
20
21

FIG. 2A

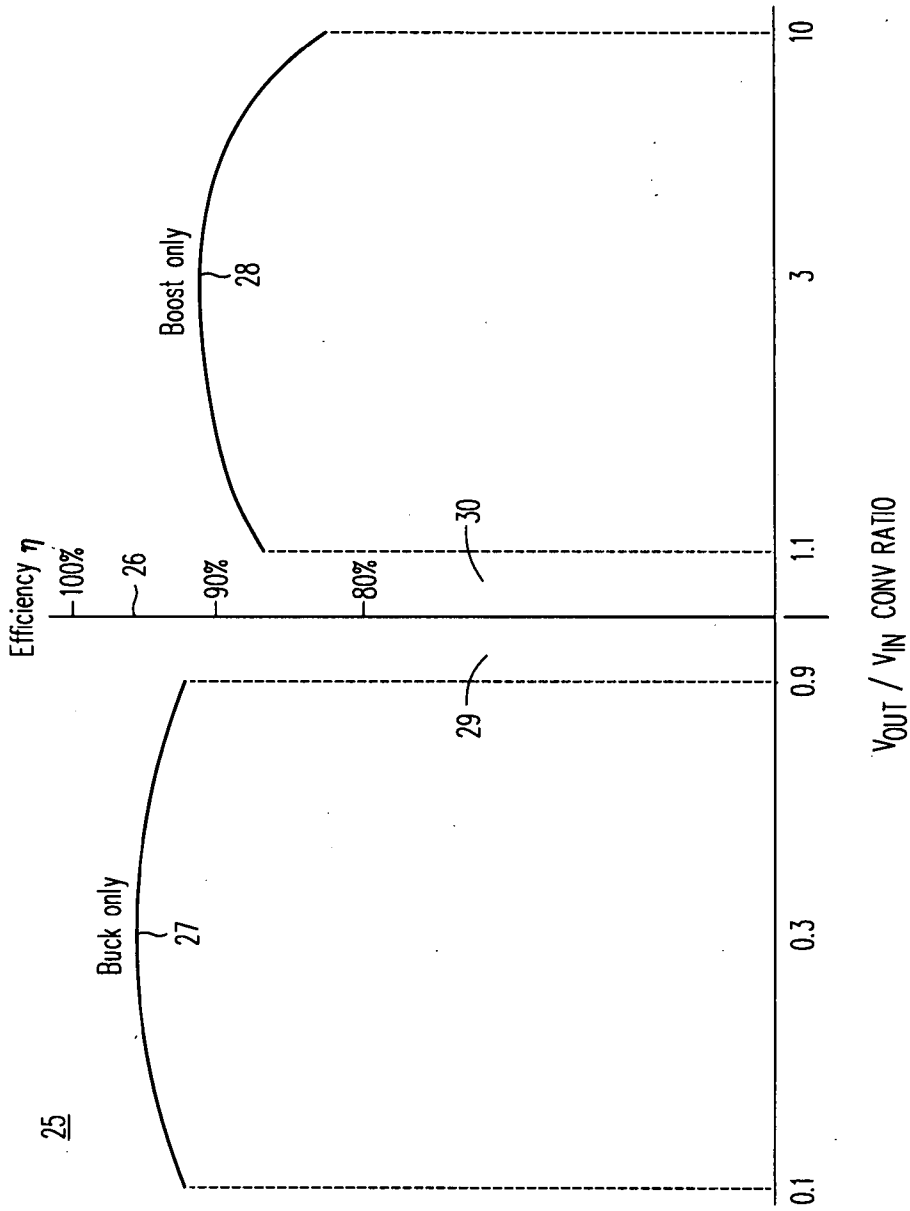
25
Efficiency η
100%
26
90%
80%
30
Boost only
28
Buck only
27
29
0.1
0.3
0.9
1.1
3
10
VOUT / VIN CONV RATIO

FIG. 2B

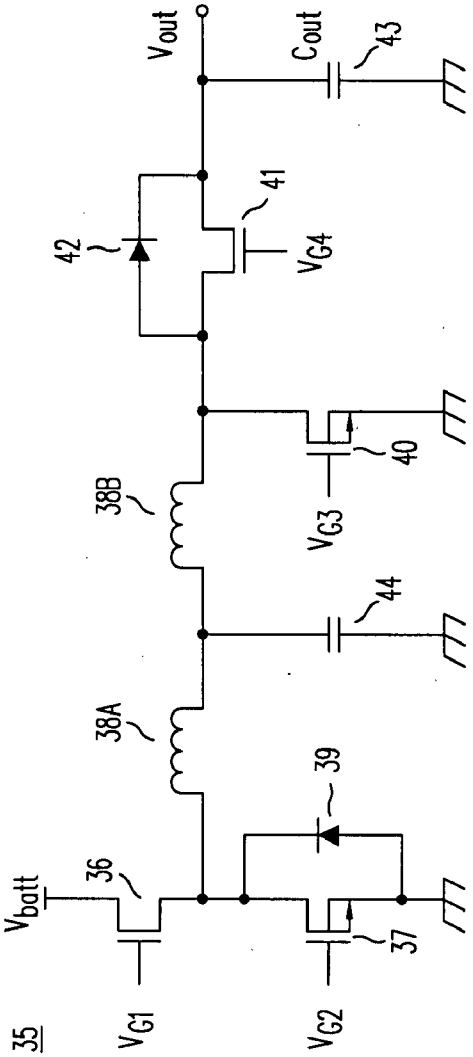

FIG. 3A
(Prior Art)

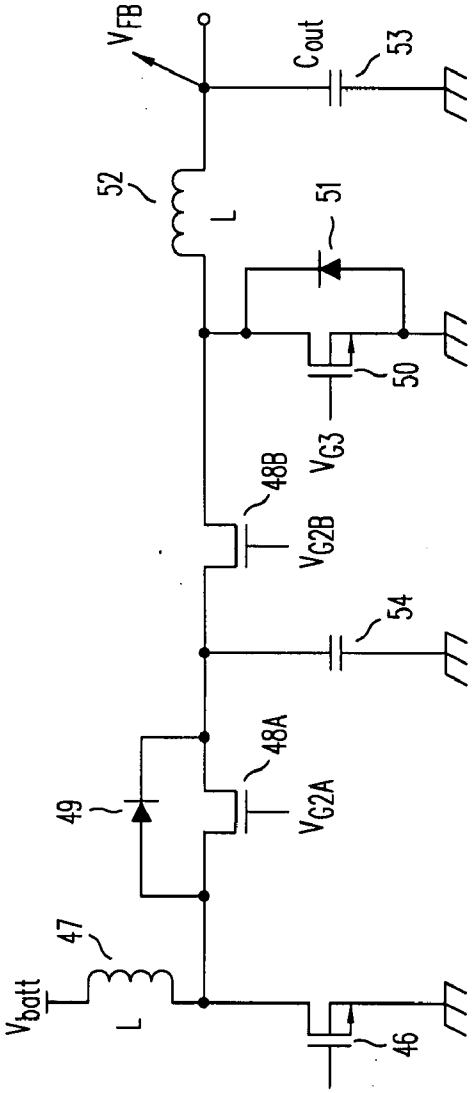

FIG. 3B
(Prior Art)

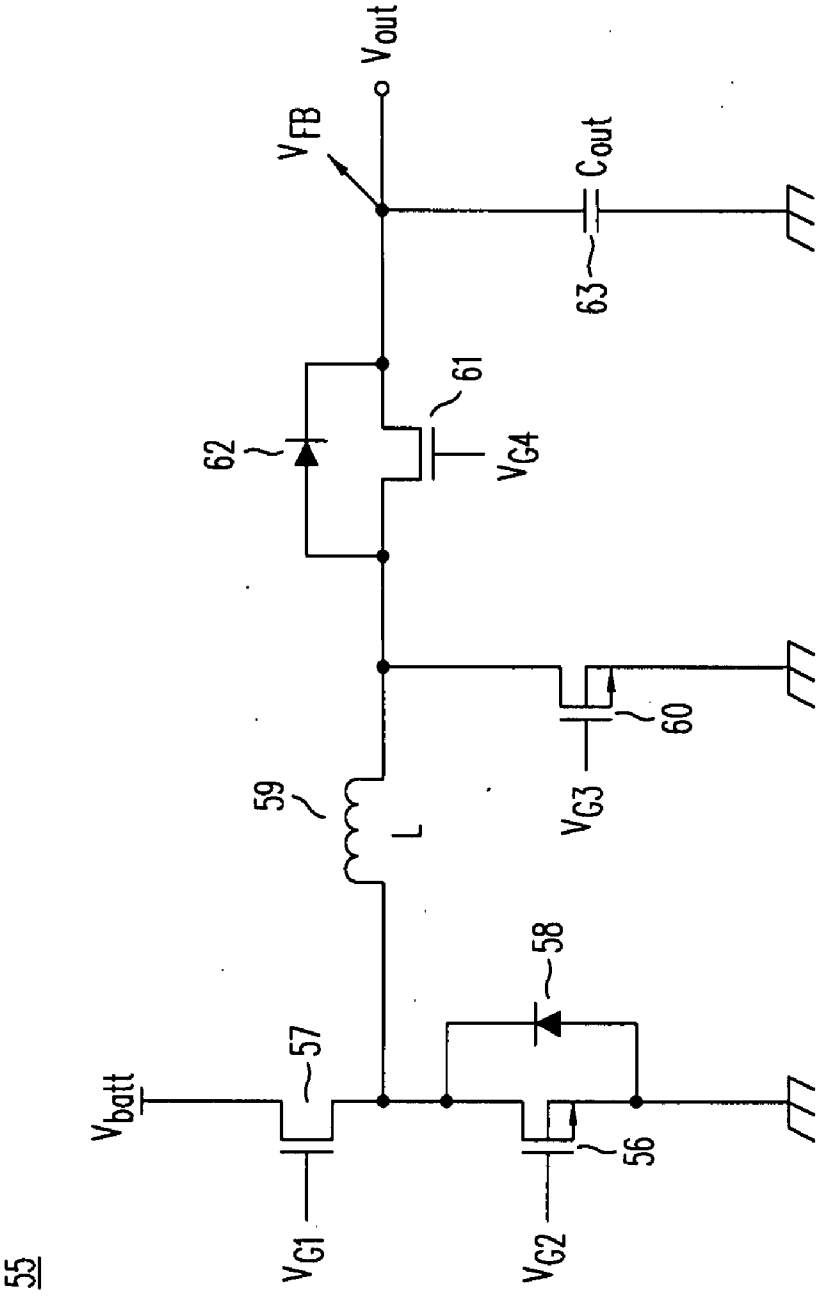

FIG. 3C
(Prior Art)

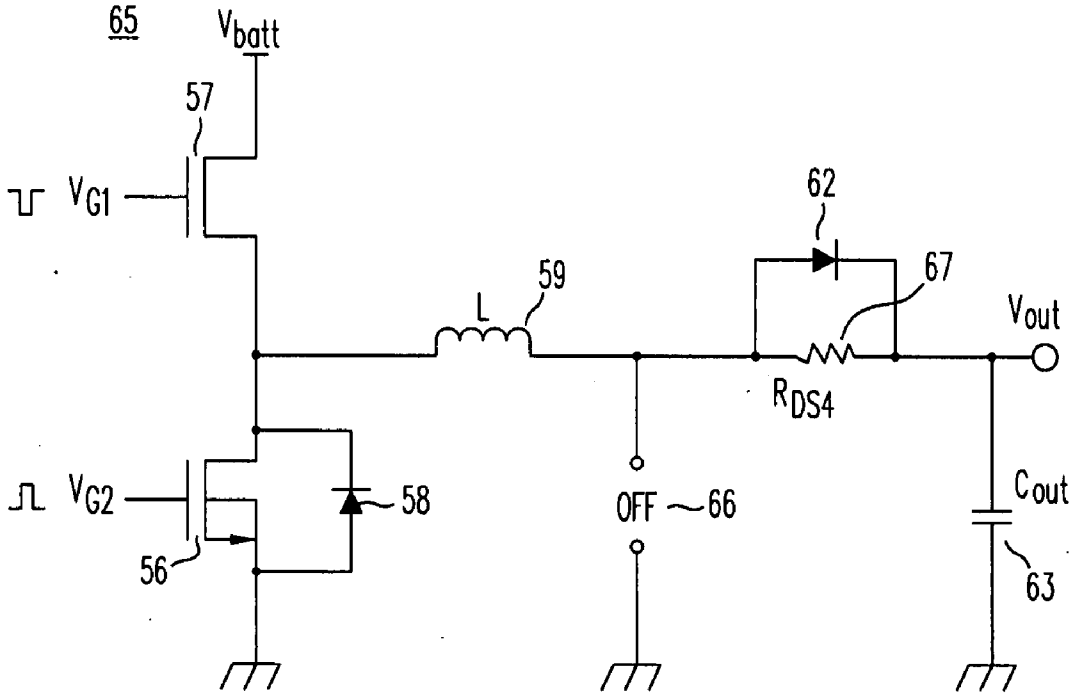

FIG. 3D
(Prior Art)

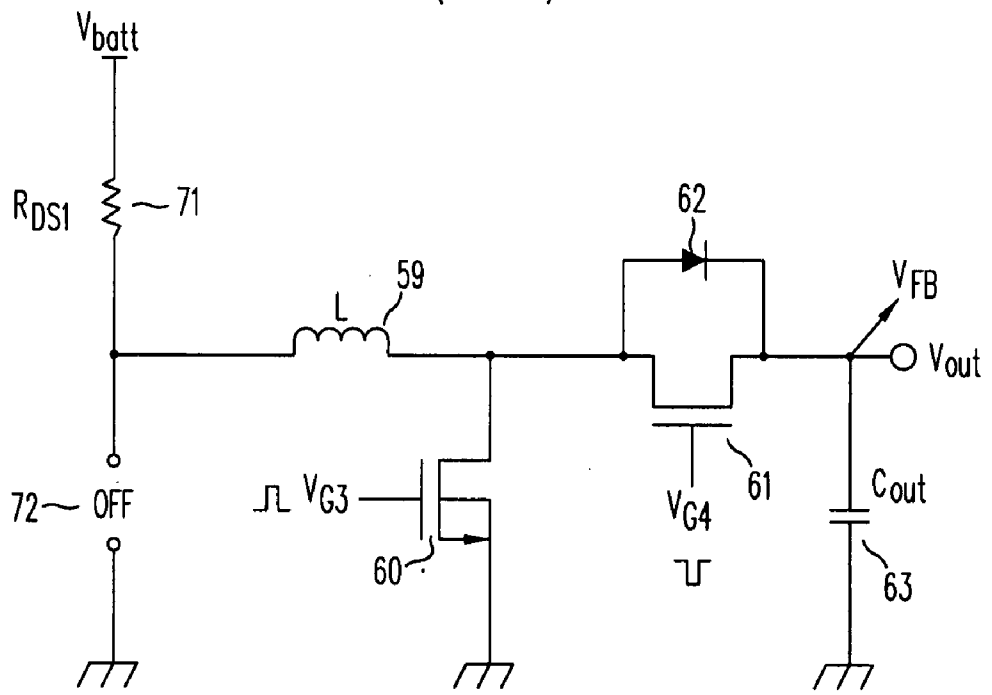

FIG. 3E
(Prior Art)

NOCO Exhibit 2011
ADC v. NOCO
IPR2024-00671

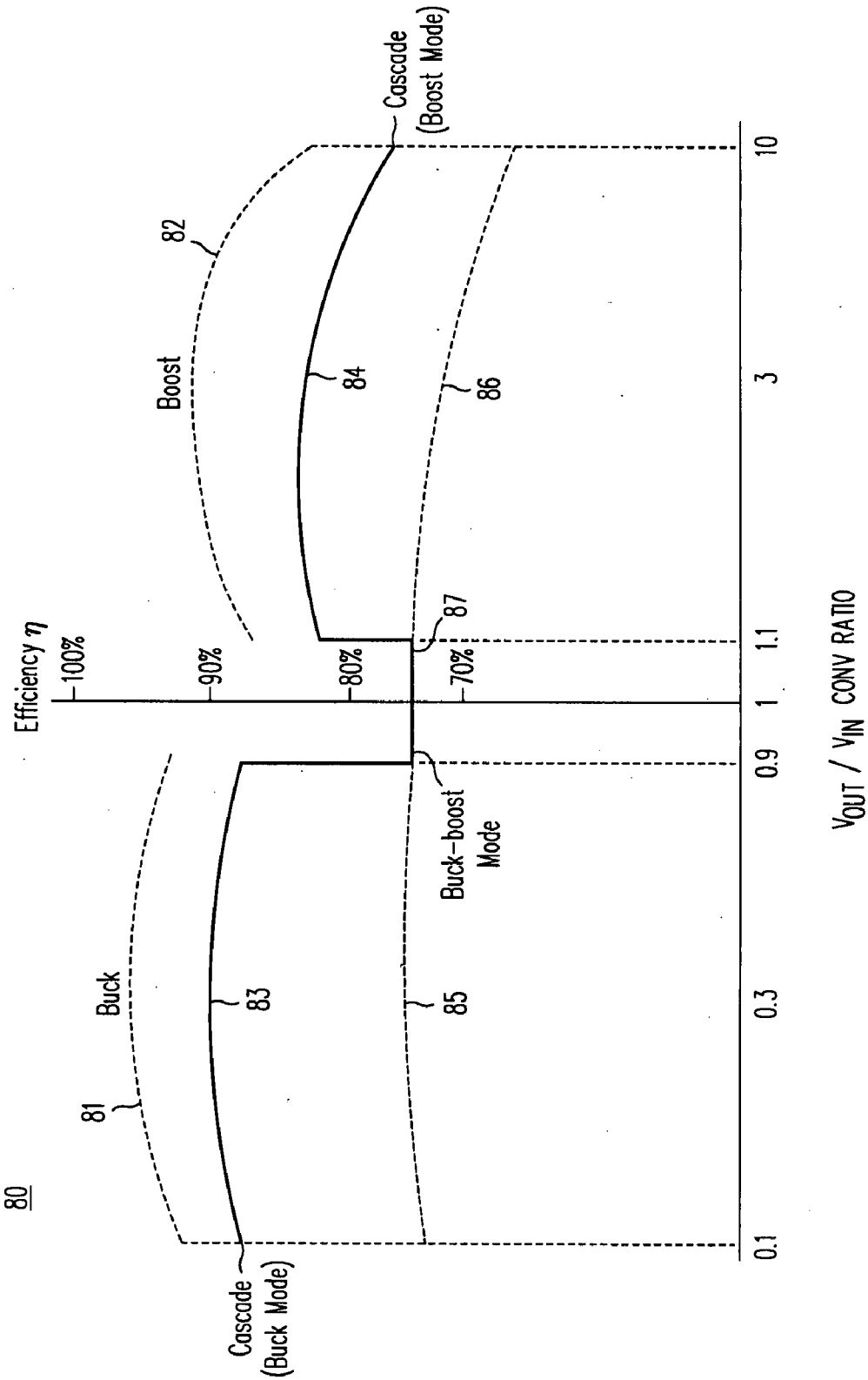

FIG. 4

NOCO Exhibit 2011
ADC v. NOCO
IPR2024-00671

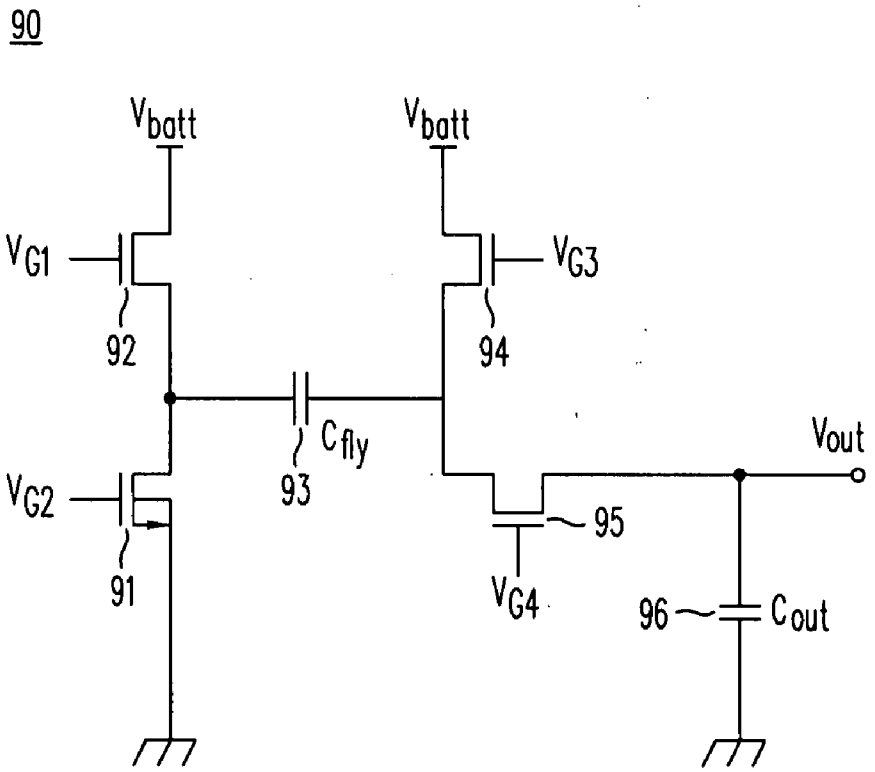

FIG. 5A
(Prior Art)

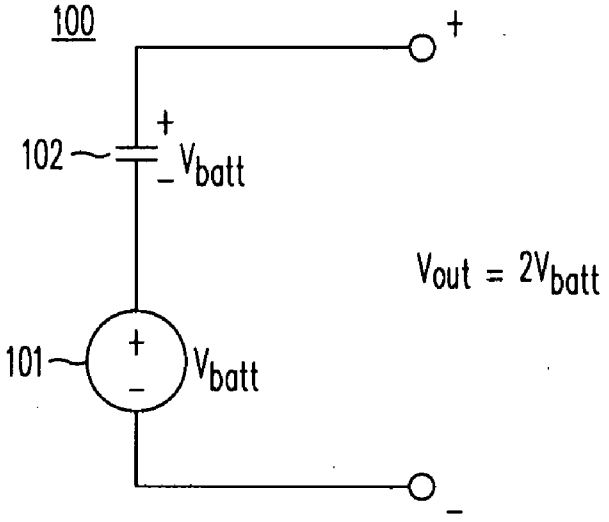

FIG. 5B
(Prior Art)

NOCO Exhibit 2011
ADC v. NOCO
IPR2024-00671

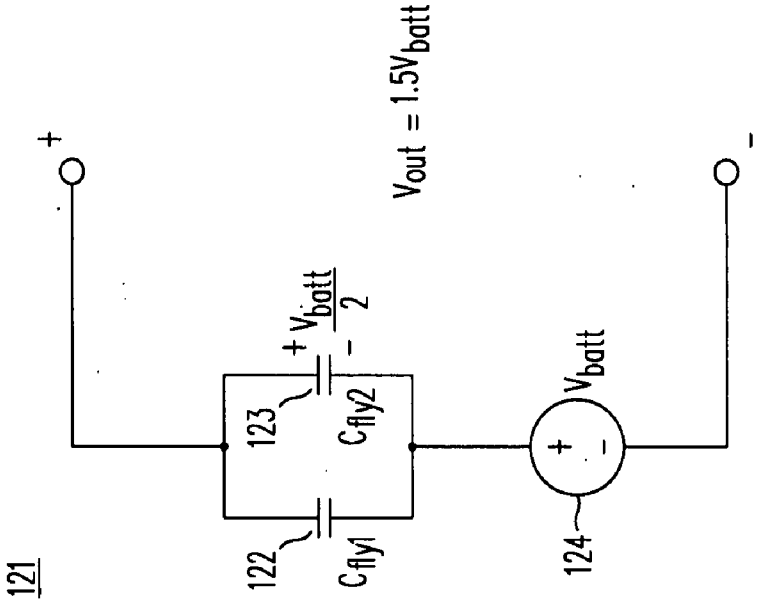

FIG. 5D
(Prior Art)

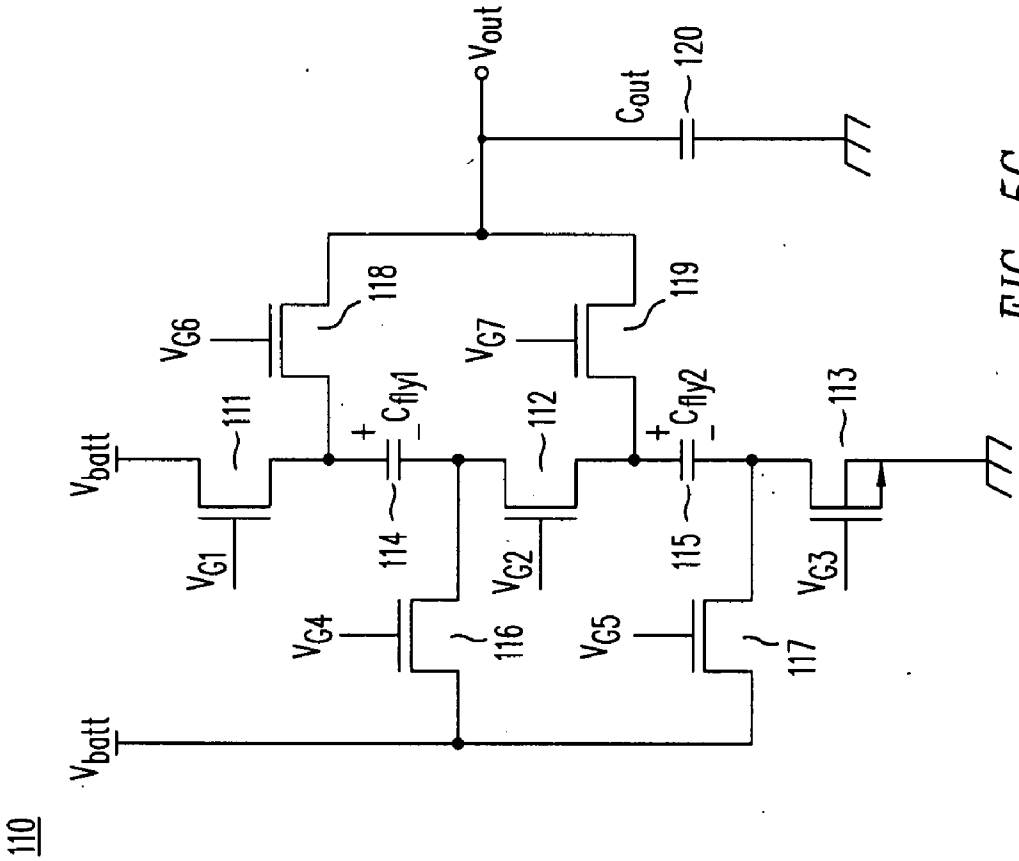

FIG. 5C
(Prior Art)

NOCO Exhibit 2011
ADC v. NOCO
IPR2024-00671

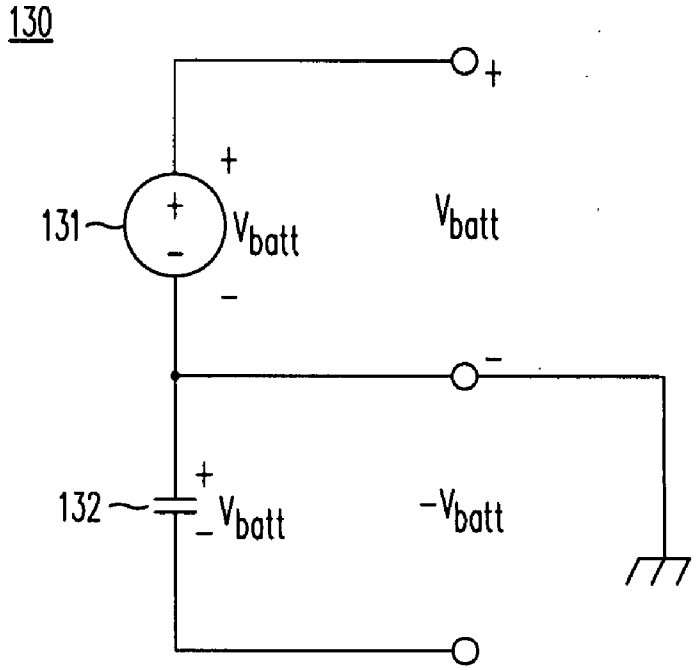

FIG. 5E
(Prior Art)

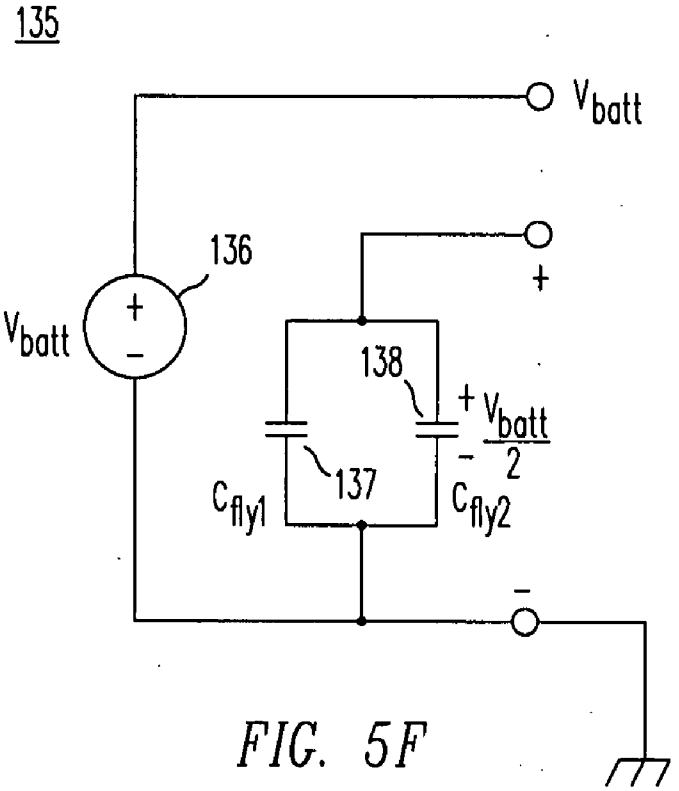

FIG. 5F
(Prior Art)

NOCO Exhibit 2011
ADC v. NOCO
IPR2024-00671

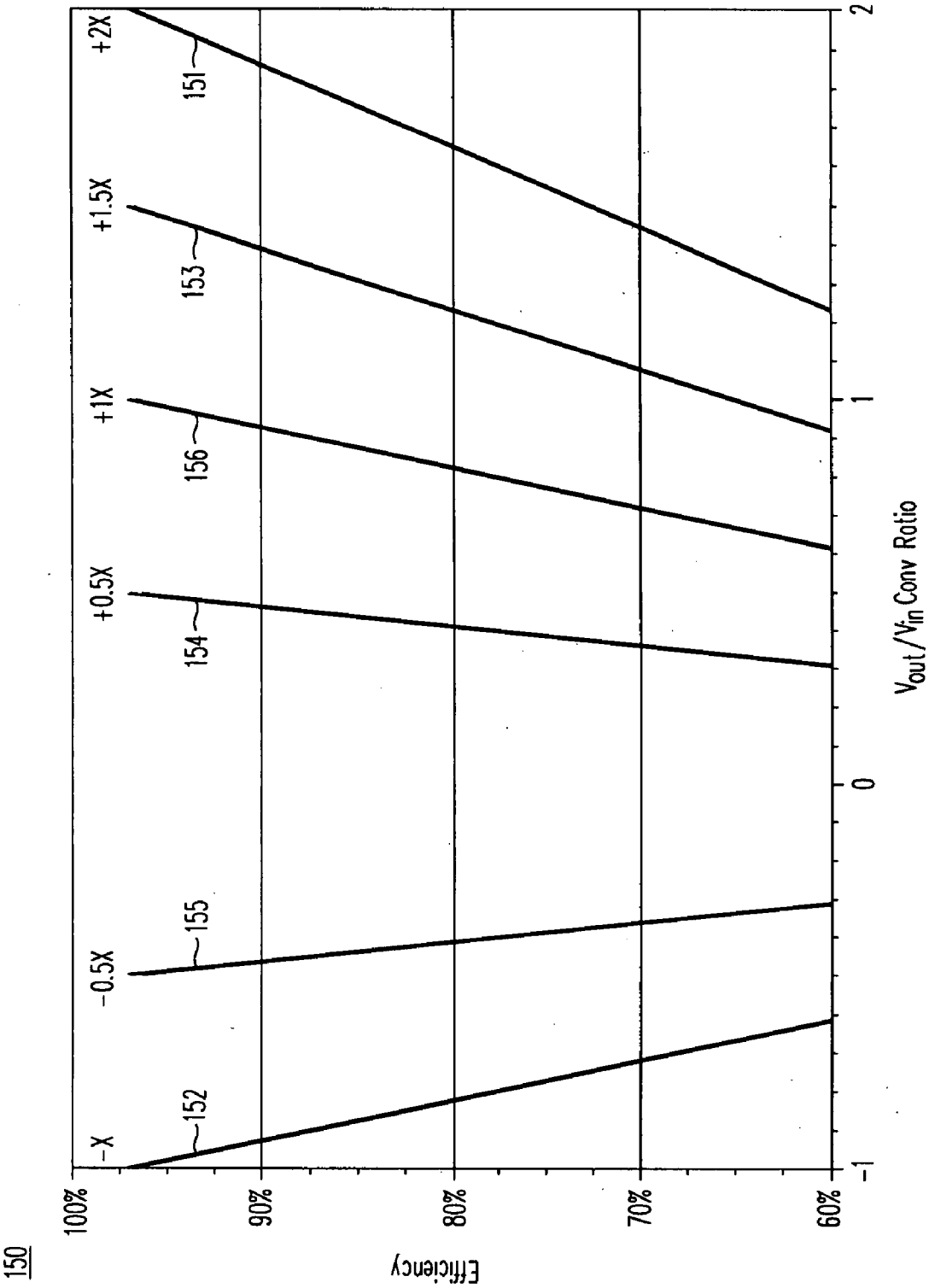

FIG. 6A

NOCO Exhibit 2011
ADC v. NOCO
IPR2024-00671

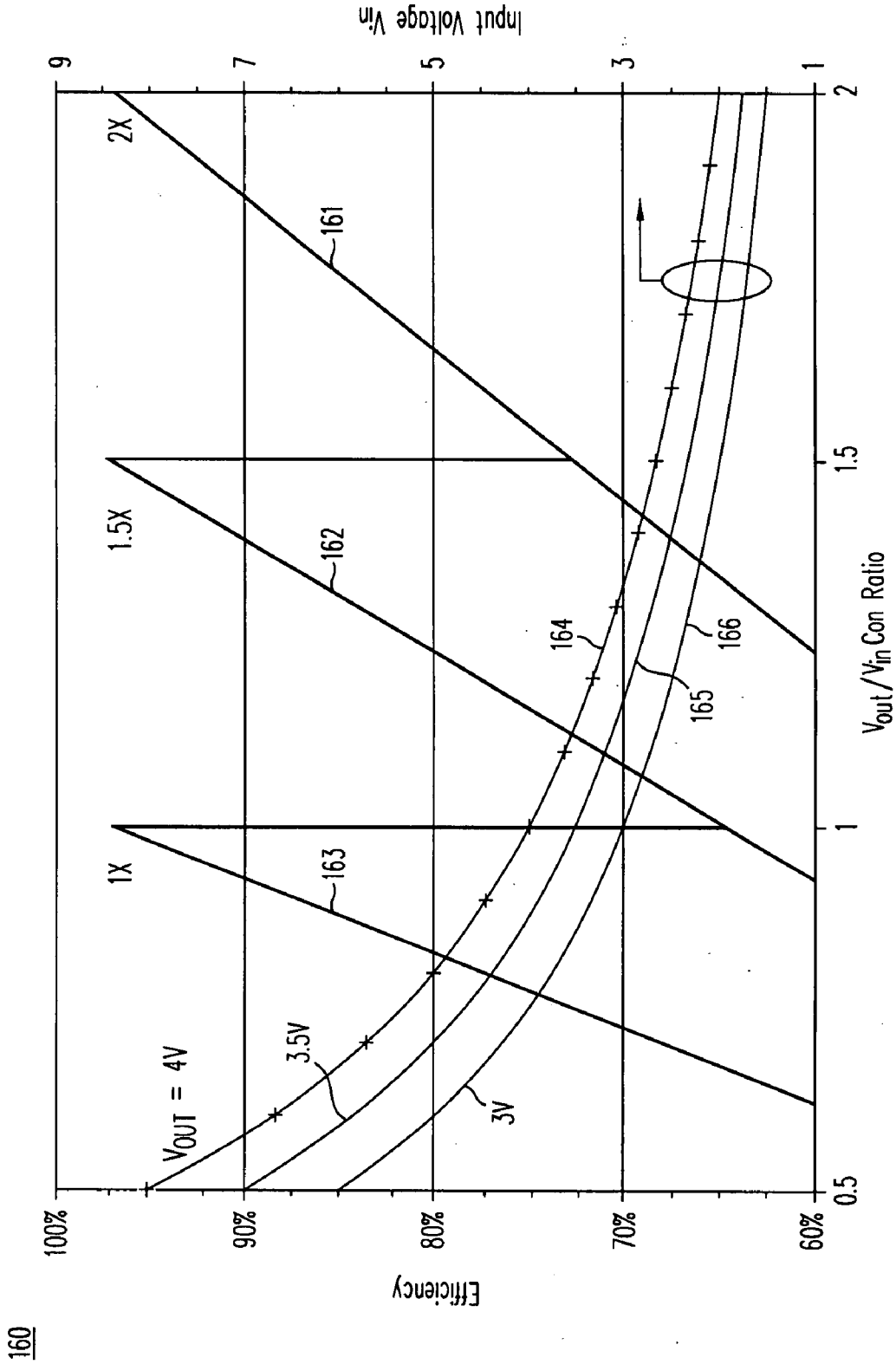
160
Efficiency
100%
90%
80%
70%
60%
Input Voltage Vin
9
7
5
3
1
0.5
1
1.5
2
Vout/Vin Con Ratio
1X
1.5X
2X
VOUT = 4V
3.5V
3V
161
162
163
164
165
166

FIG. 6B

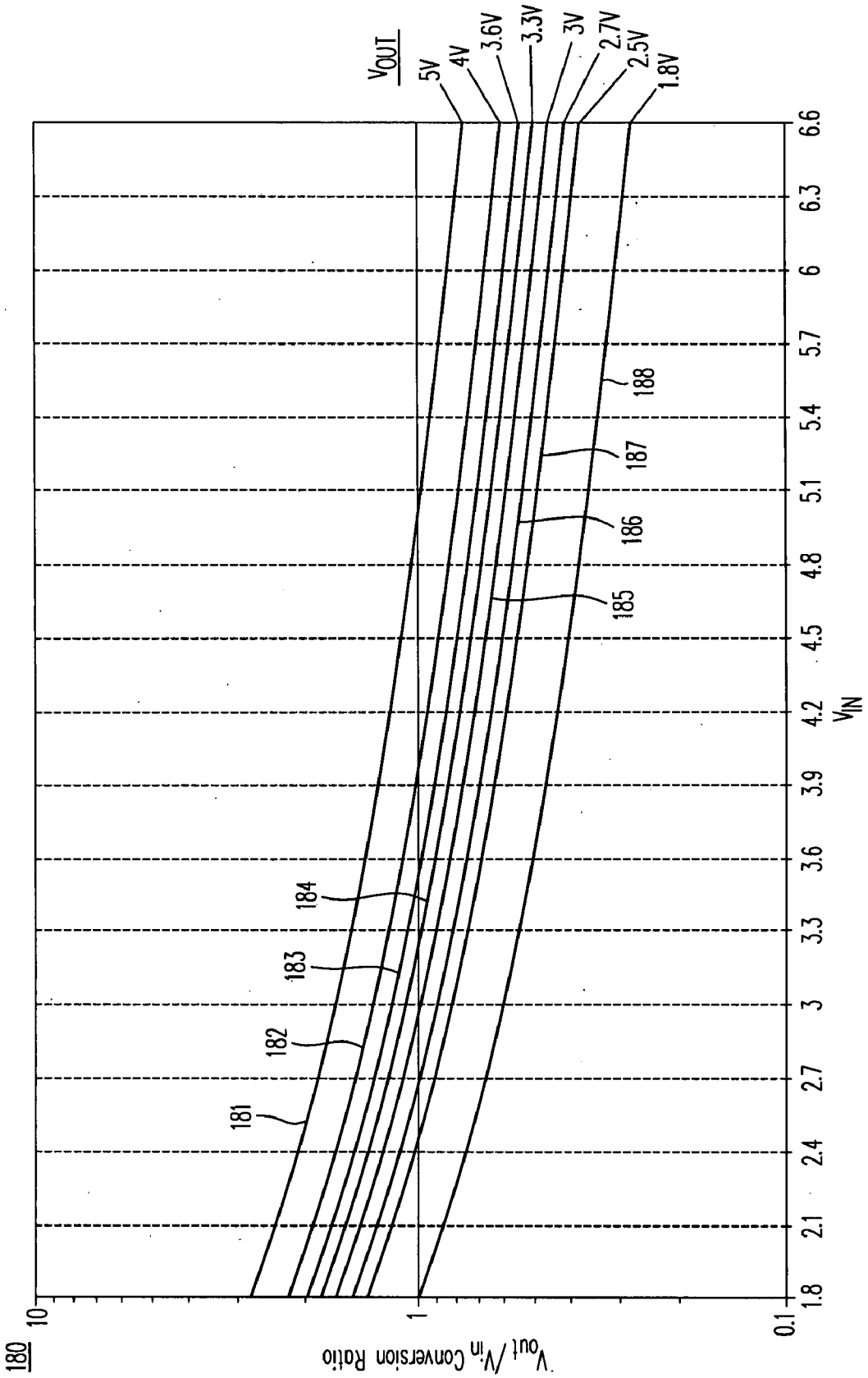
180
10
1
0.1
Vout /Vin Conversion Ratio
1.8
2.1
2.4
2.7
3
3.3
3.6
3.9
4.2
4.5
4.8
5.1
5.4
5.7
6
6.3
6.6
VIN
VOUT
5V
4V
3.6V
3.3V
3V
2.7V
2.5V
1.8V
181
182
183
184
185
186
187
188

FIG. 7

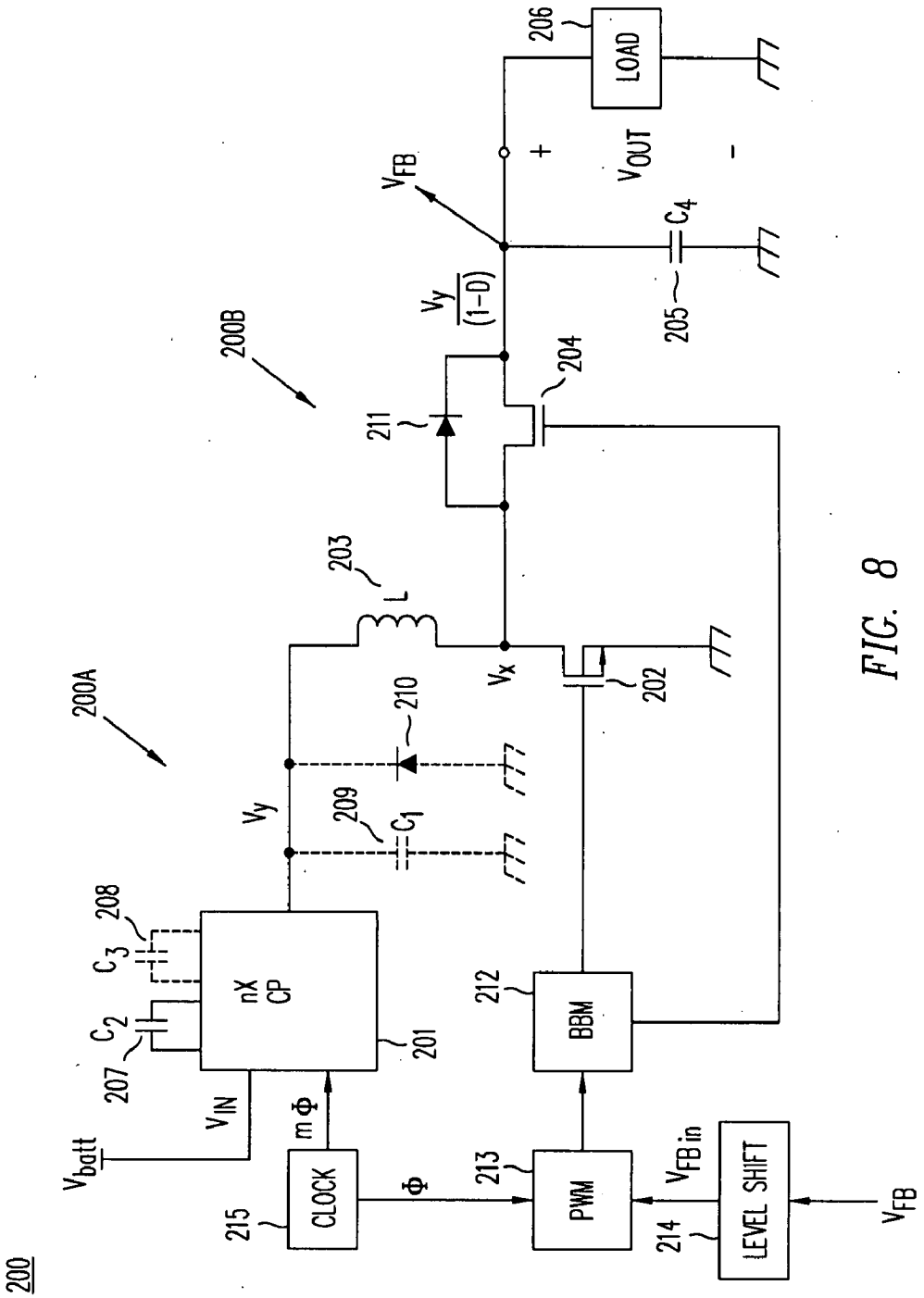

FIG. 8

NOCO Exhibit 2011
ADC v. NOCO
IPR2024-00671

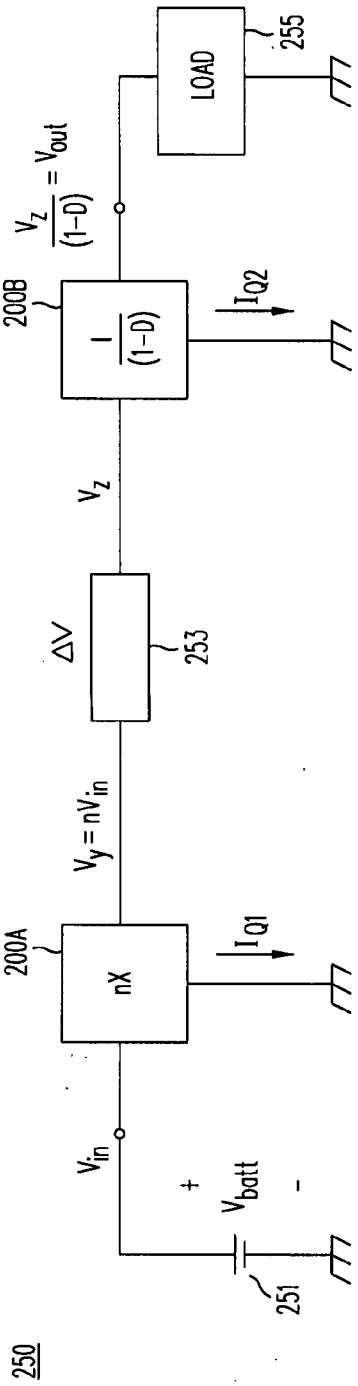
250
V_{in}
+
V_{batt}
-
251
200A
nX
I_{Q1}
$V_y = nV_{in}$
ΔV
253
V_z
200B
$\frac{1}{(1-D)}$
I_{Q2}
$\frac{V_z}{(1-D)} = V_{out}$
LOAD
255

FIG. 9

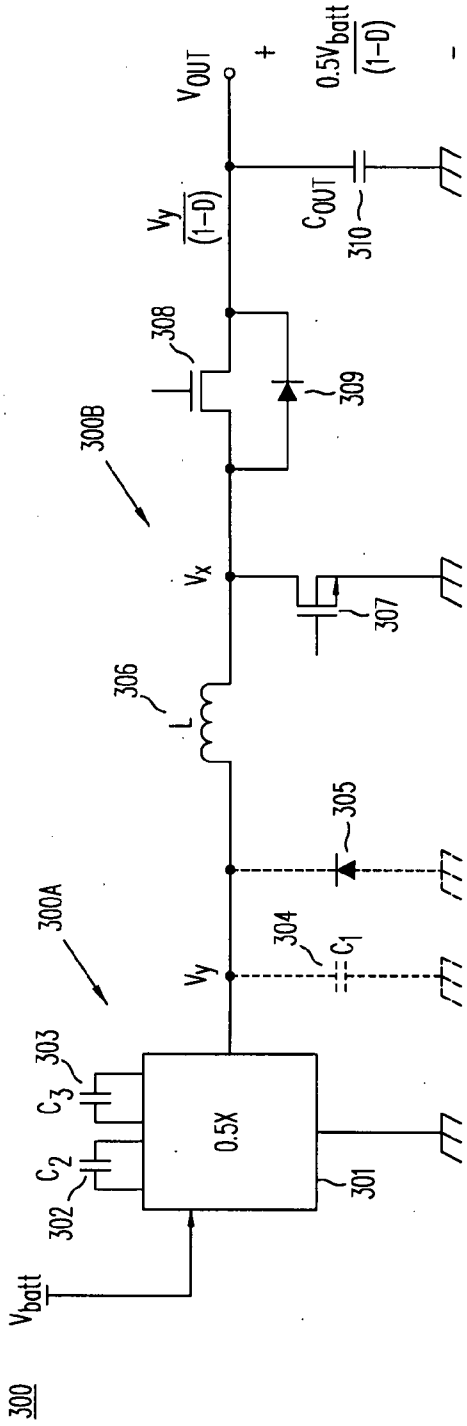
300
V_{batt}
302
C_2
303
C_3
0.5X
301
300A
V_y
304
C_1
305
306
L
V_x
307
300B
308
309
$\frac{V_y}{(1-D)}$
V_{OUT}
+
C_{OUT}
310
$\frac{0.5V_{batt}}{(1-D)}$
-

FIG. 10

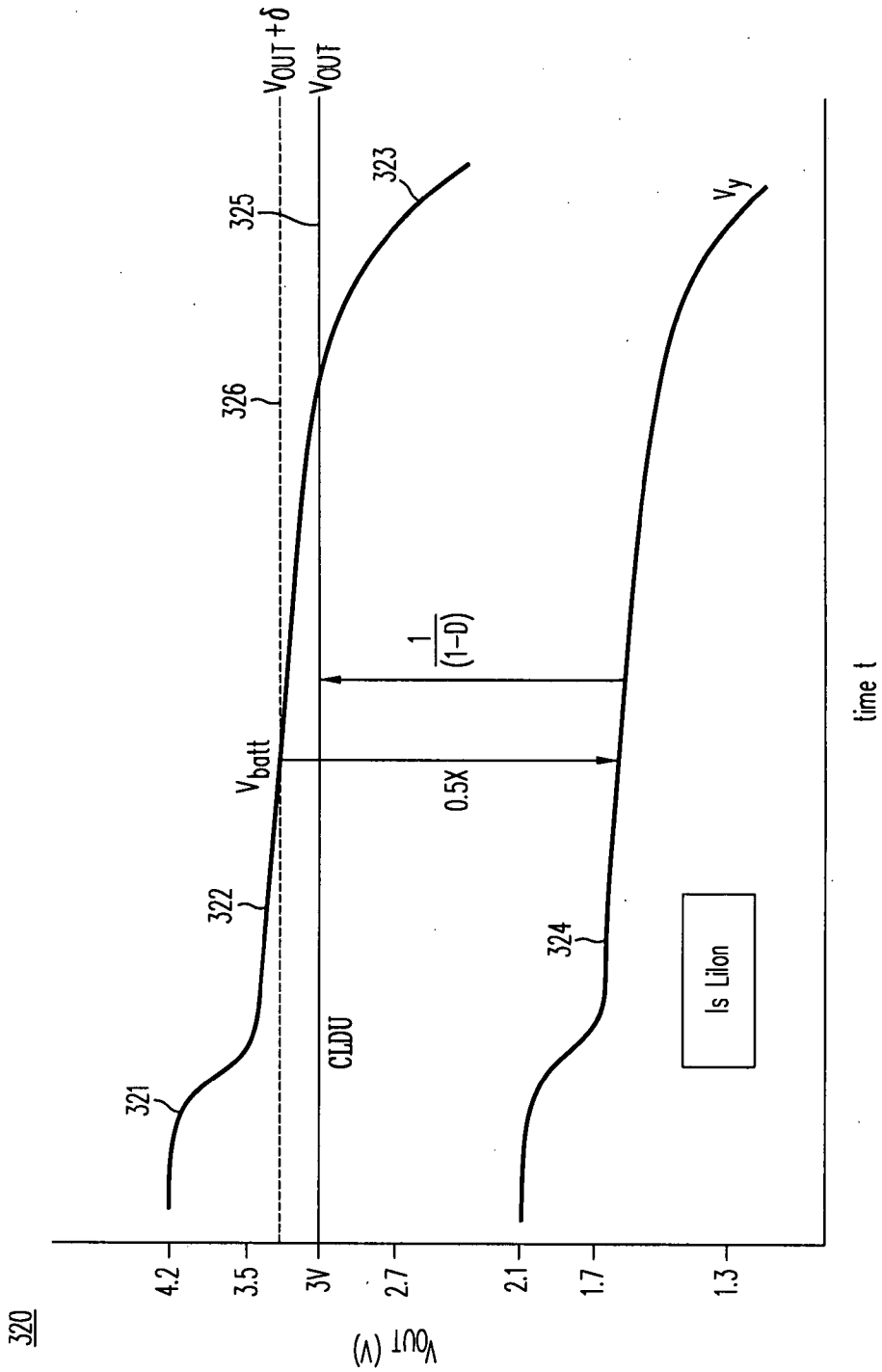
320
V_{OUT} (V)
4.2
3.5
3V
2.7
2.1
1.7
1.3
$V_{OUT}+\delta$
V_{OUT}
325
326
323
321
322
V_{batt}
CLDU
0.5X
$\frac{1}{(1-D)}$
324
Is LiIon
V_y
time t

FIG. 11A

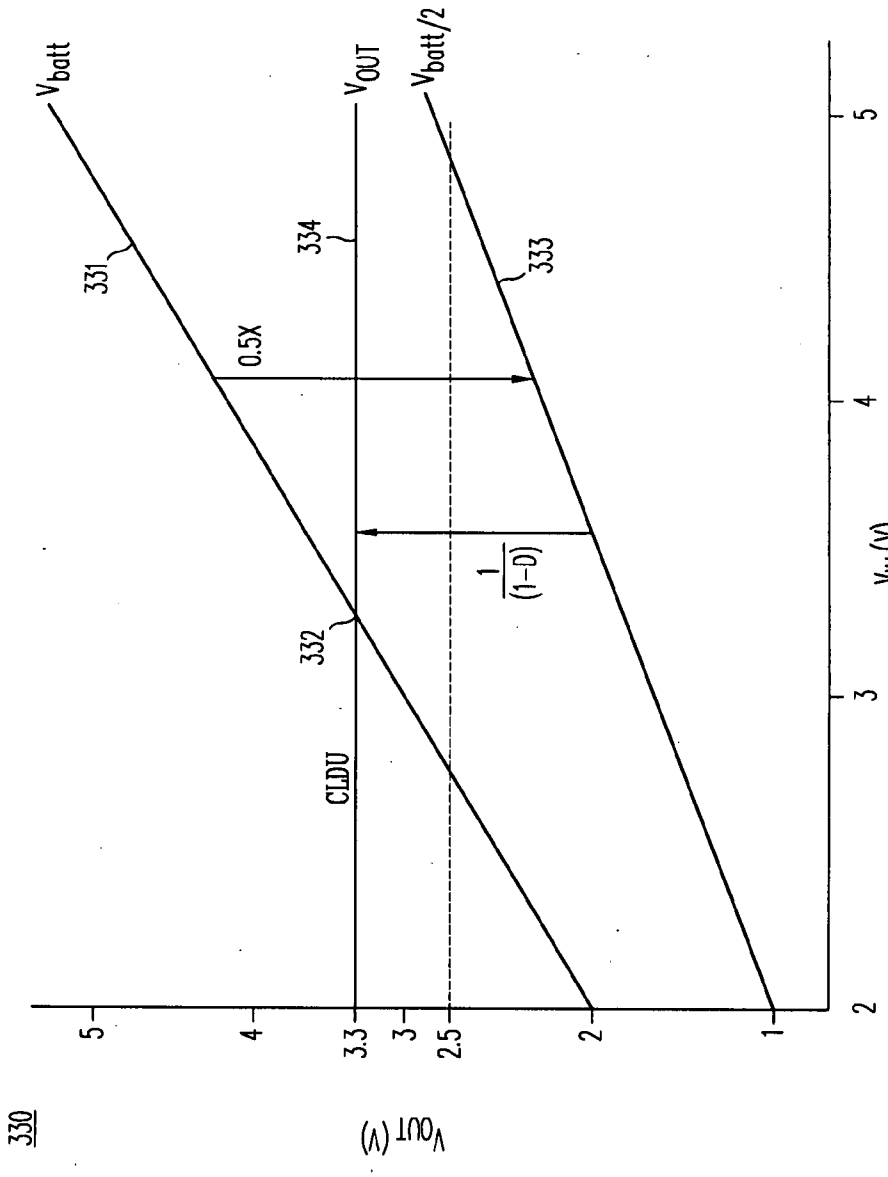
330
V_{OUT} (V)
5
4
3.3
3
2.5
2
1
V_{batt}
331
0.5X
332
CLDU
V_{OUT}
334
$V_{batt}/2$
333
$\frac{1}{(1-D)}$
2
3
4
5
V_{IN} (V)

FIG. 11B

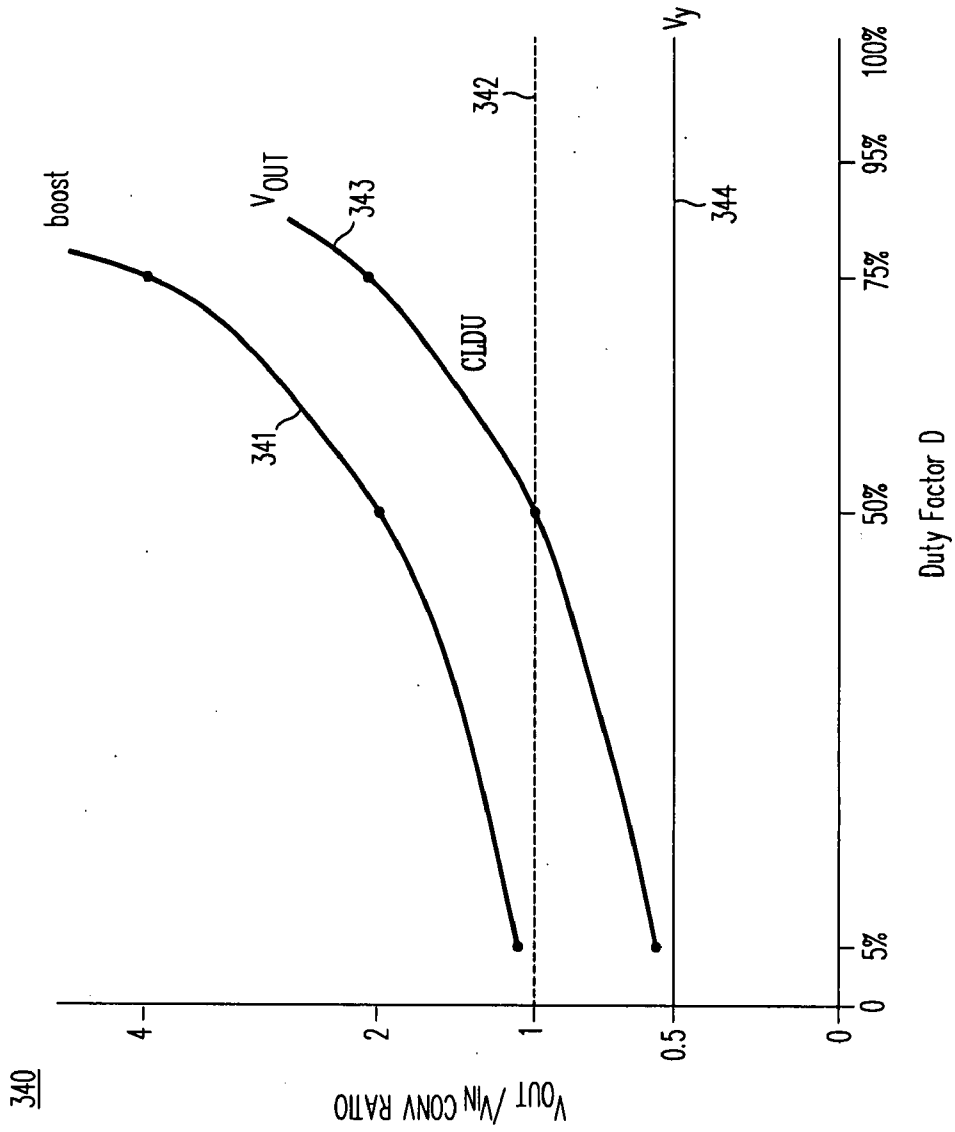
340
boost
341
V_{OUT}
343
CLDU
342
V_y
344
4
2
1
0.5
0
V_{OUT} /V_{IN} CONV RATIO
0
5%
50%
75%
95%
100%
Duty Factor D

FIG. 11C

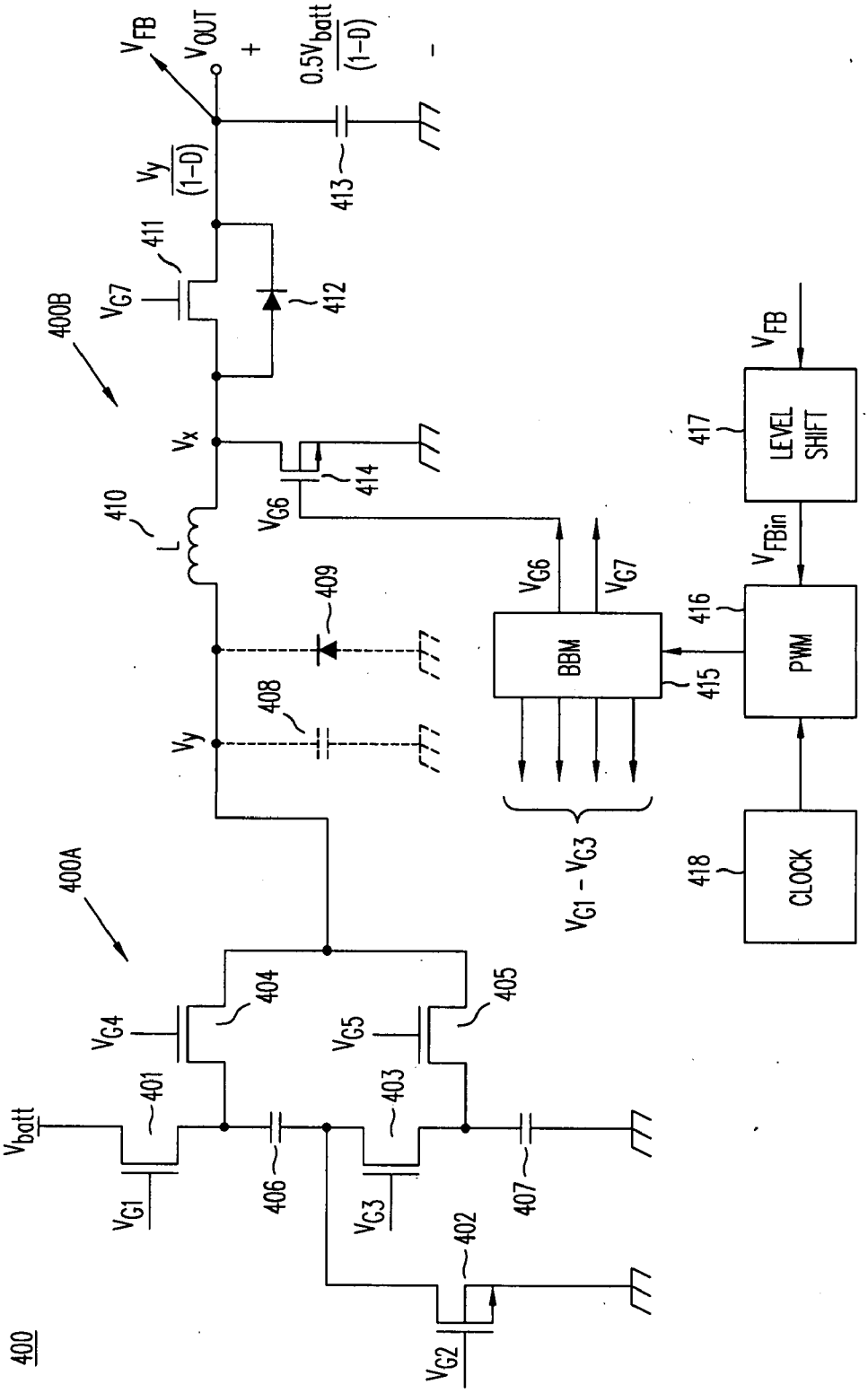
400
400A
400B
V_{batt}
V_{G1}
401
V_{G4}
404
406
V_{G3}
403
V_{G5}
405
407
402
V_{G2}
V_y
408
409
410
L
V_x
V_{G6}
414
V_{G7}
411
412
$\frac{V_y}{(1-D)}$
V_{FB}
V_{OUT}
+
413
$\frac{0.5V_{batt}}{(1-D)}$
-
BBM
415
$V_{G1} - V_{G3}$
PWM
416
V_{FBin}
LEVEL SHIFT
417
CLOCK
418

FIG. 12A

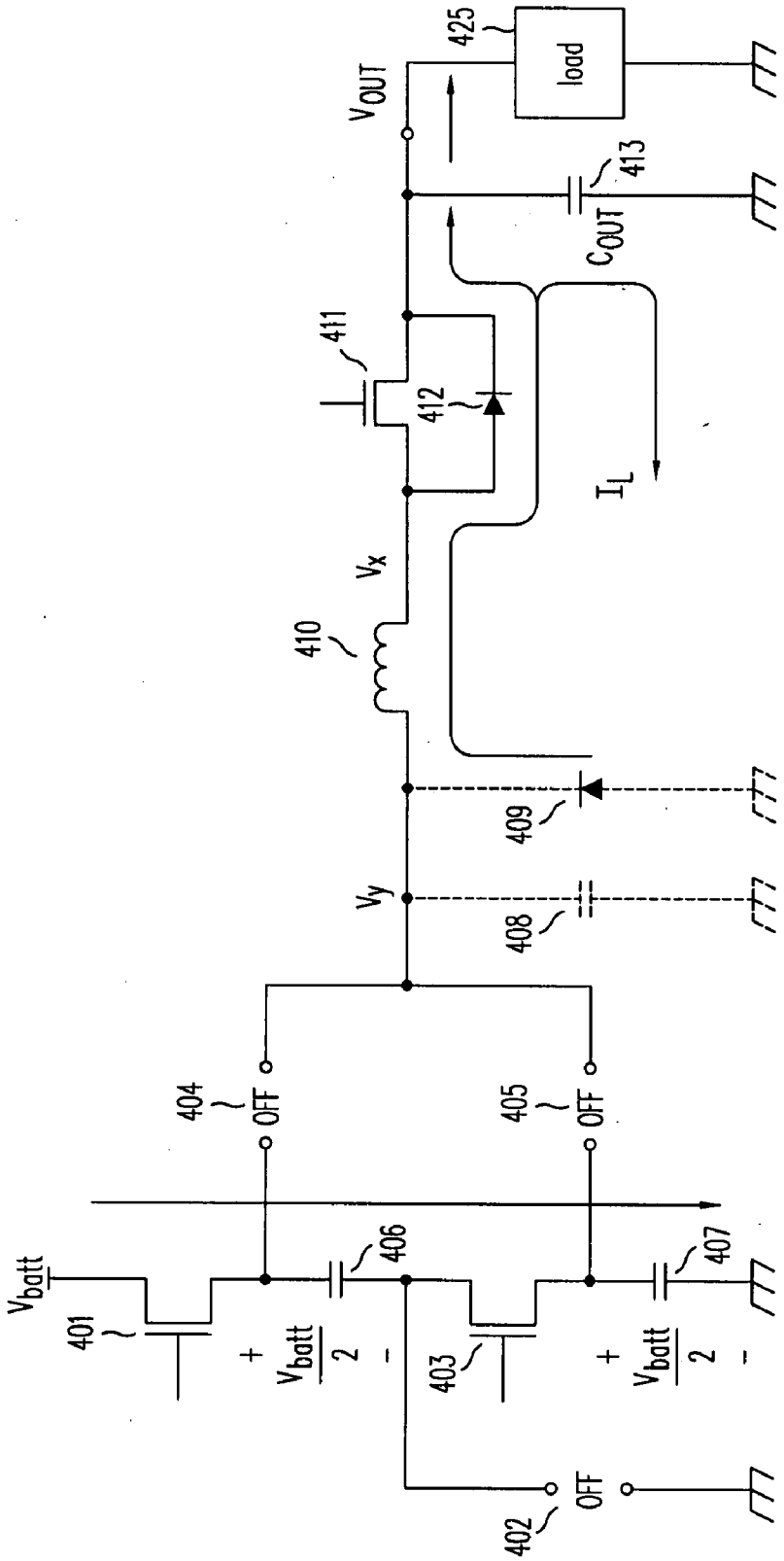

FIG. 12B

NOCO Exhibit 2011
ADC v. NOCO
IPR2024-00671

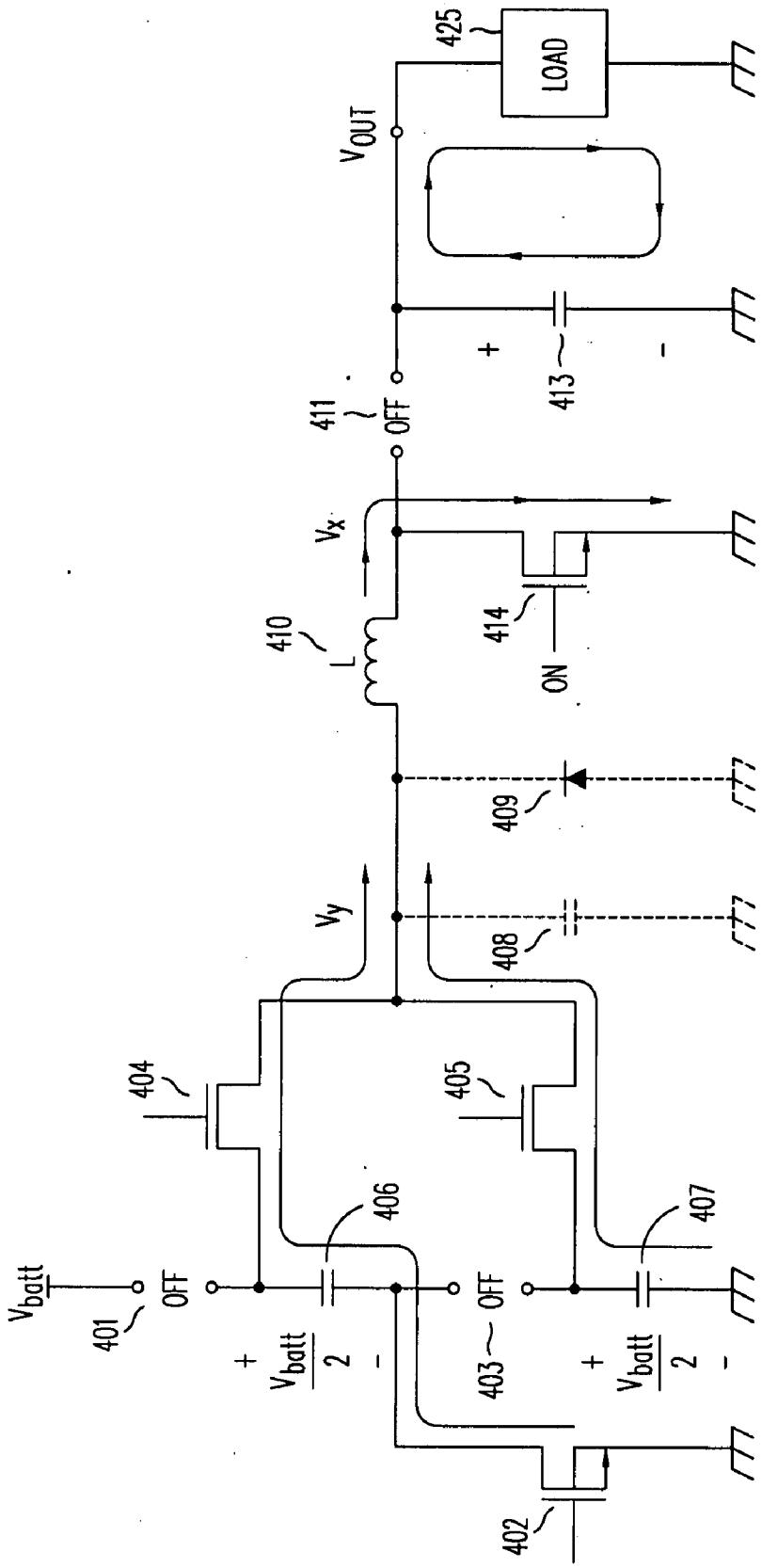

FIG. 12C

NOCO Exhibit 2011
ADC v. NOCO
IPR2024-00671

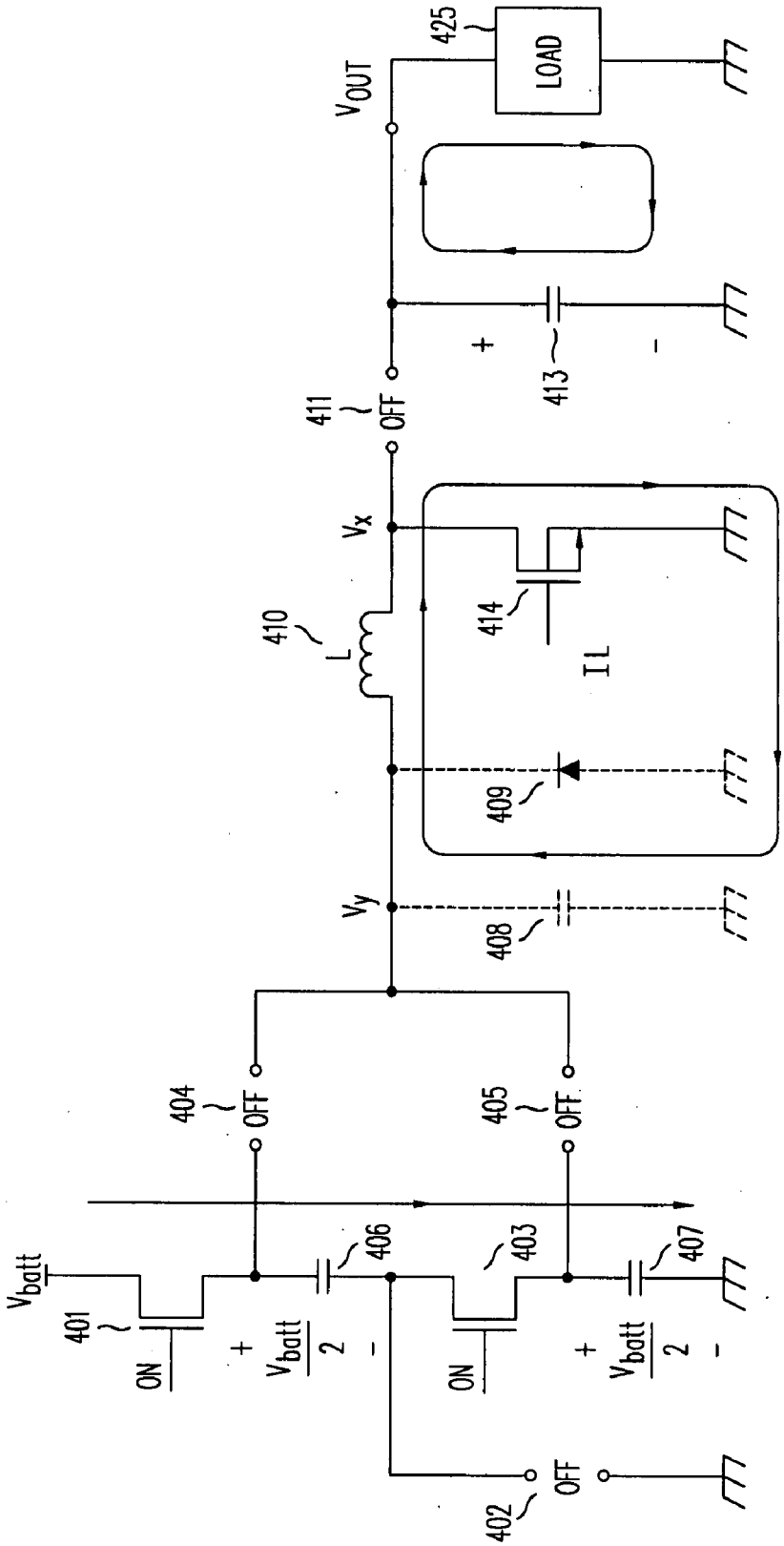
V_{batt}
401
ON
+
$\frac{V_{batt}}{2}$
-
406
404
OFF
402
OFF
403
ON
+
$\frac{V_{batt}}{2}$
-
407
405
OFF
V_y
408
409
410
L
V_x
414
IL
411
OFF
413
+
-
V_{OUT}
425
LOAD

FIG. 12D

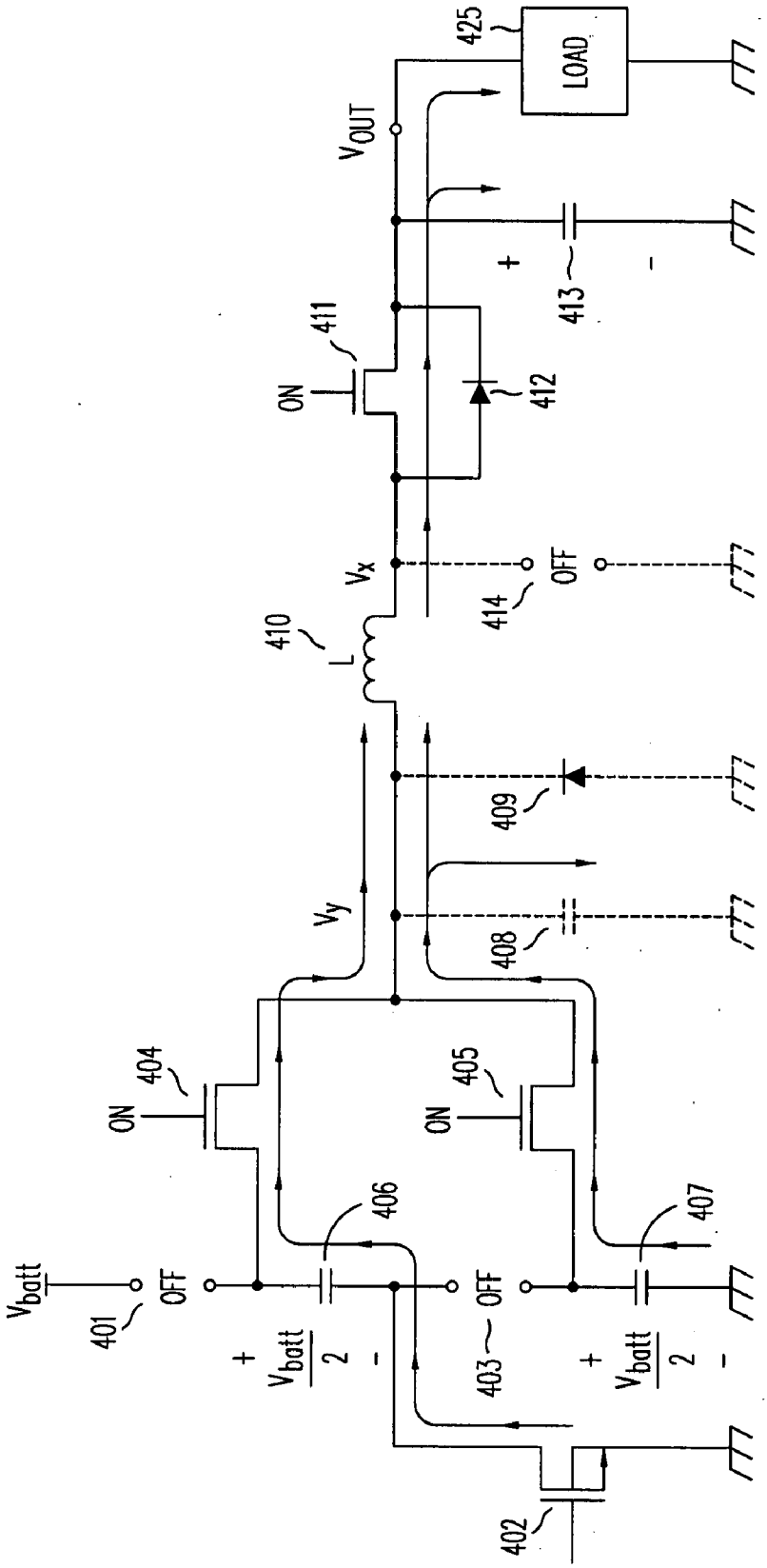
V_{batt}
401
OFF
+
$\frac{V_{batt}}{2}$
-
ON
404
406
V_y
ON
405
407
OFF
403
+
$\frac{V_{batt}}{2}$
-
402
408
409
410
L
V_x
OFF
414
ON
411
412
V_{OUT}
+
413
-
425
LOAD

FIG. 12E

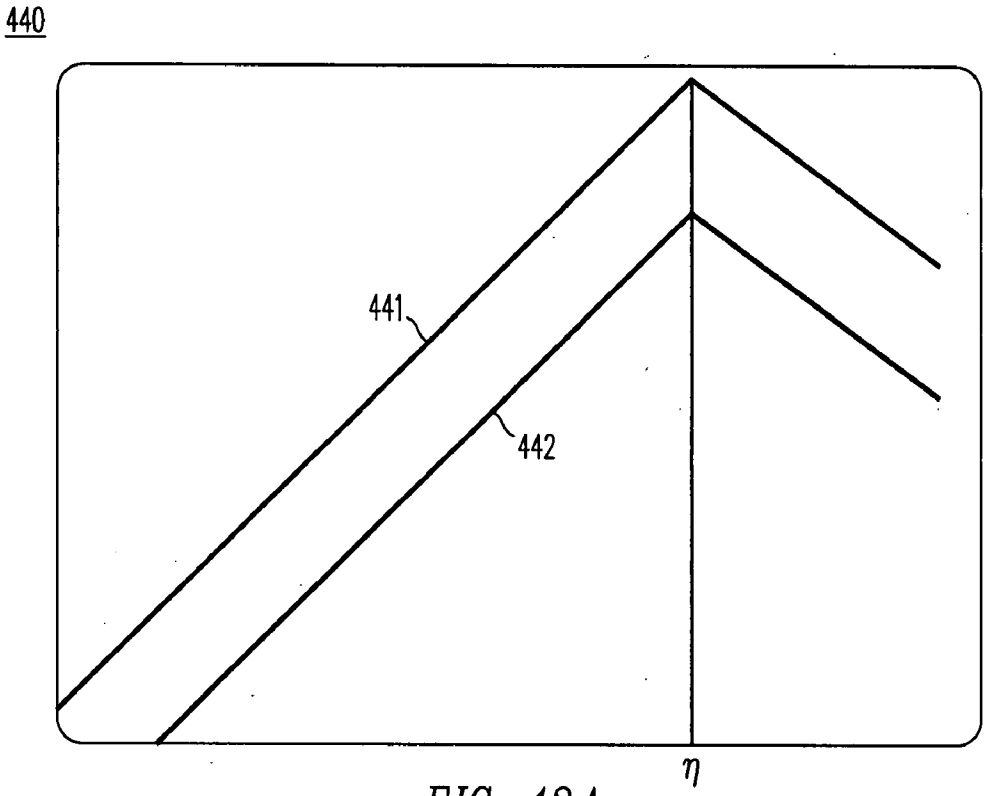

FIG. 13A

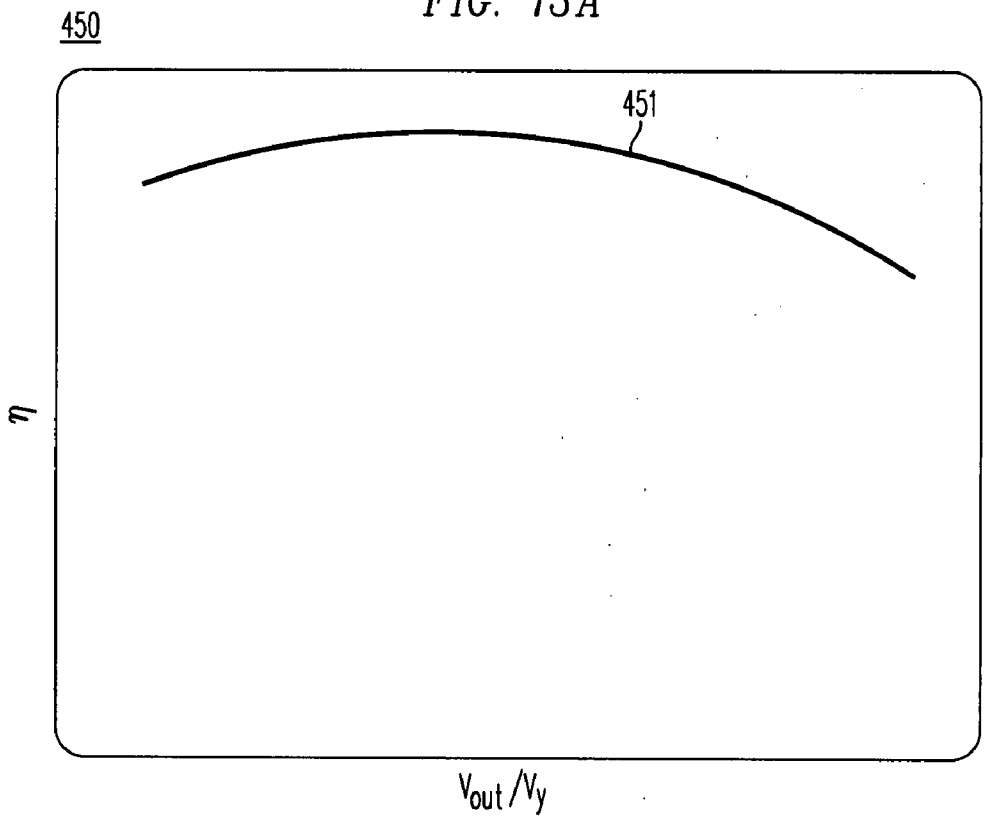

FIG. 13B

NOCO Exhibit 2011
ADC v. NOCO
IPR2024-00671

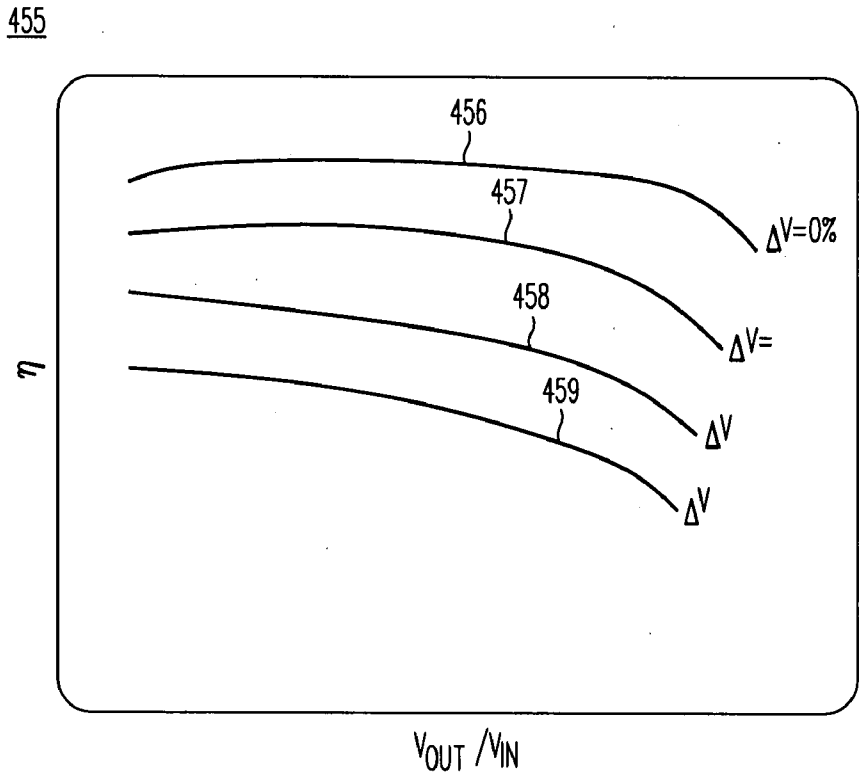

FIG. 13C

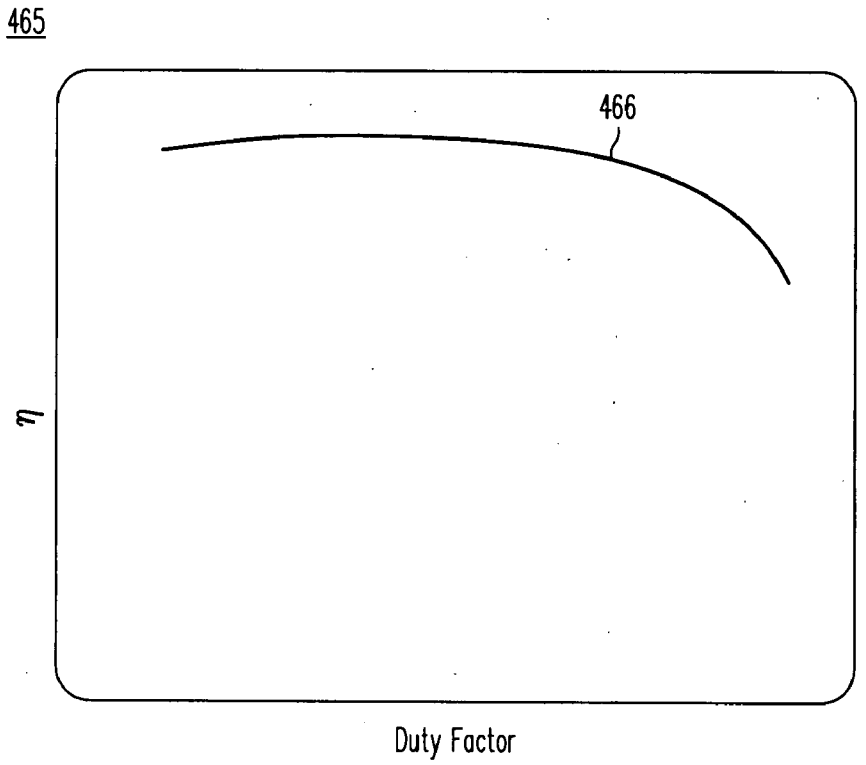

FIG. 13D

NOCO Exhibit 2011
ADC v. NOCO
IPR2024-00671

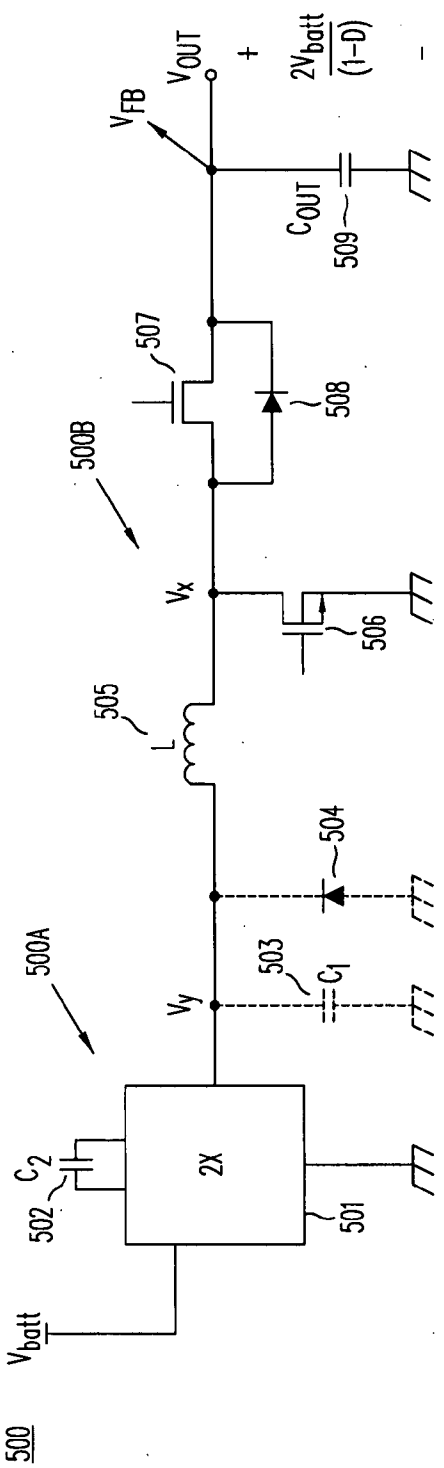

FIG. 14A

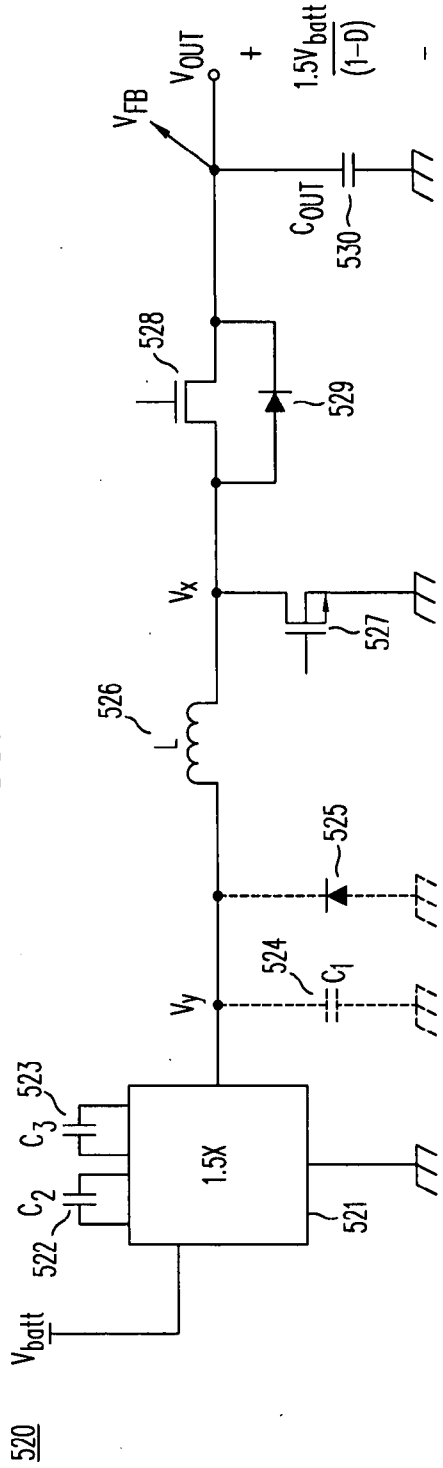

FIG. 14B

NOCO Exhibit 2011
ADC v. NOCO
IPR2024-00671

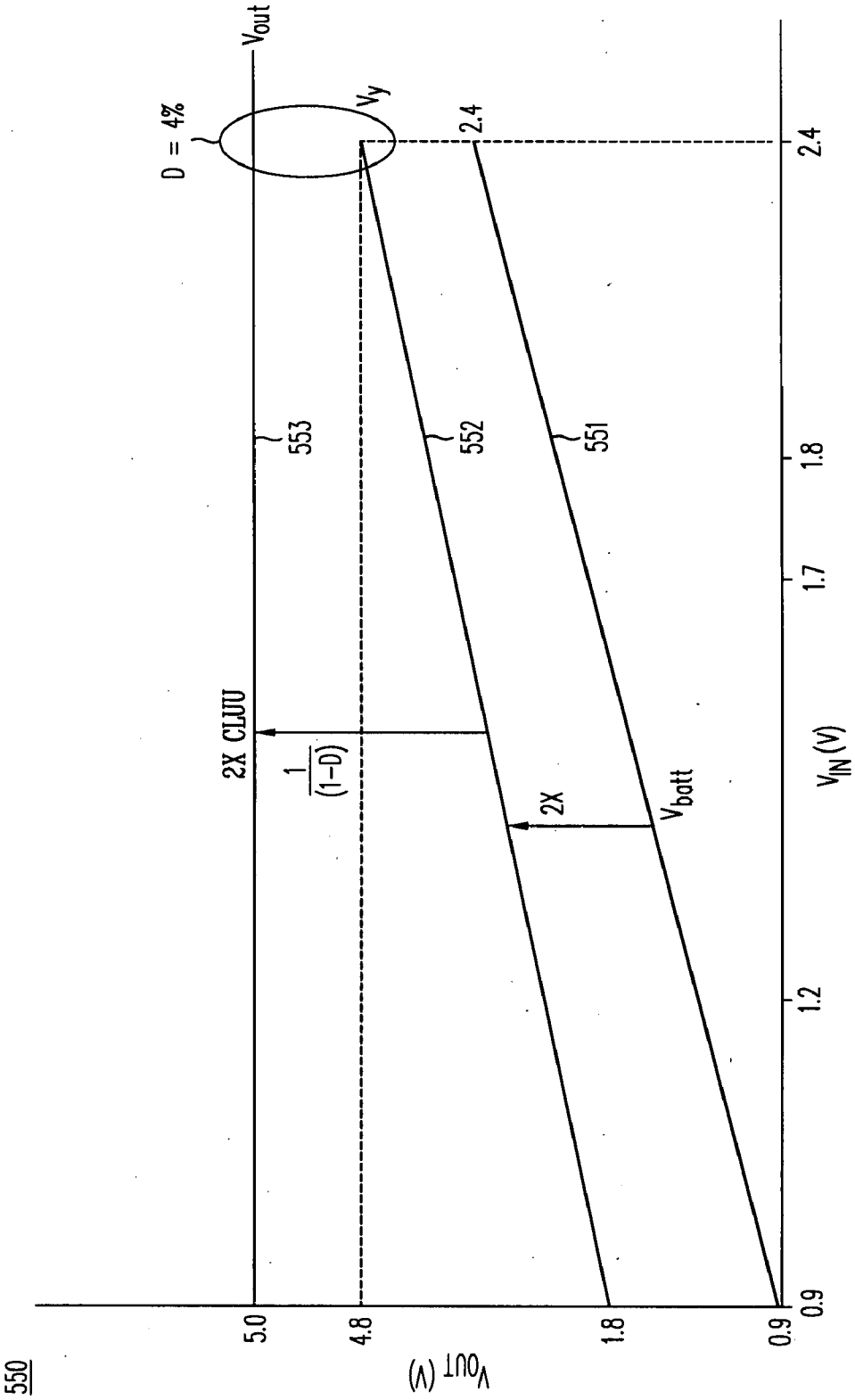
550
V_{out} (V)
5.0
4.8
1.8
0.9
V_{out}
D = 4%
V_y
2.4
553
552
551
2X CLUU
$\frac{1}{(1-D)}$
2X
V_{batt}
0.9
1.2
1.7
1.8
2.4
V_{IN} (V)

FIG. 15A

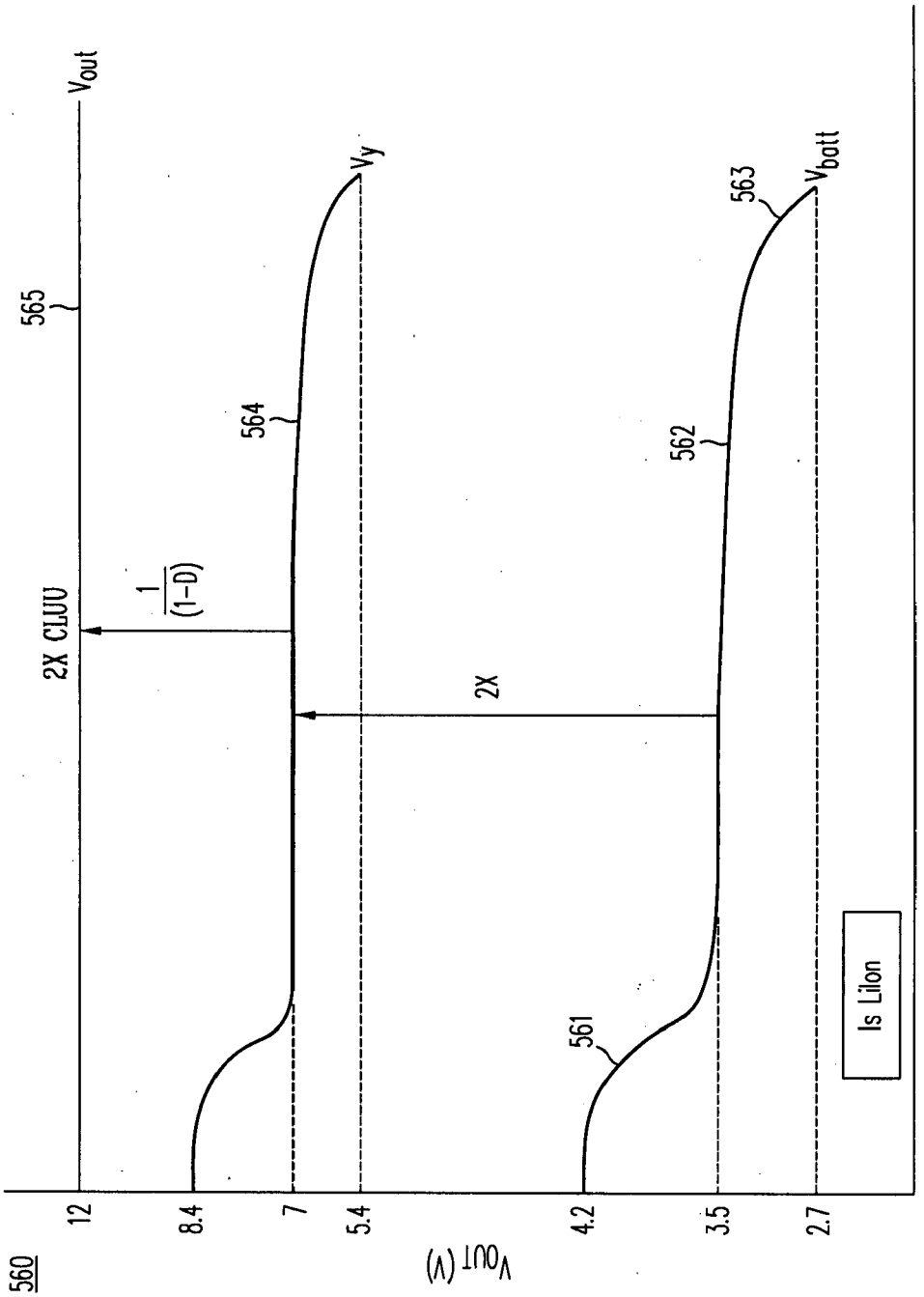
560
V_{out}
565
2X CLUU
$\frac{1}{(1-D)}$
564
V_y
2X
562
563
V_{batt}
561
Is LiIon
12
8.4
7
5.4
4.2
3.5
2.7
V_{OUT} (V)
time t

FIG. 15B

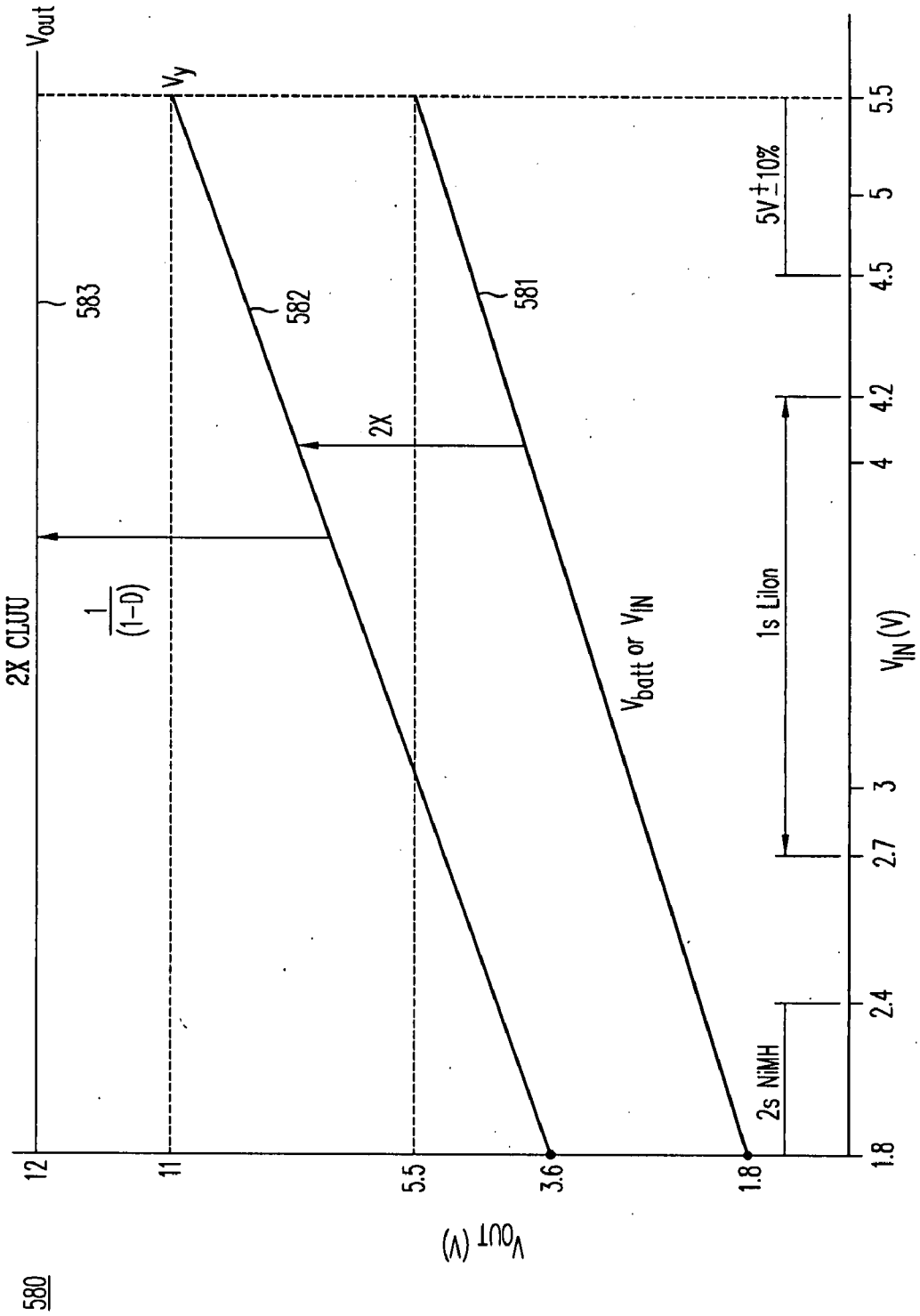
580
2X CLUU
V_{out}
V_y
583
582
581
$\frac{1}{(1-D)}$
2X
V_{batt} or V_{IN}
2s NiMH
1s LiIon
5V±10%
V_{OUT} (V)
12
11
5.5
3.6
1.8
V_{IN} (V)
1.8
2.4
2.7
3
4
4.2
4.5
5
5.5

FIG. 15C

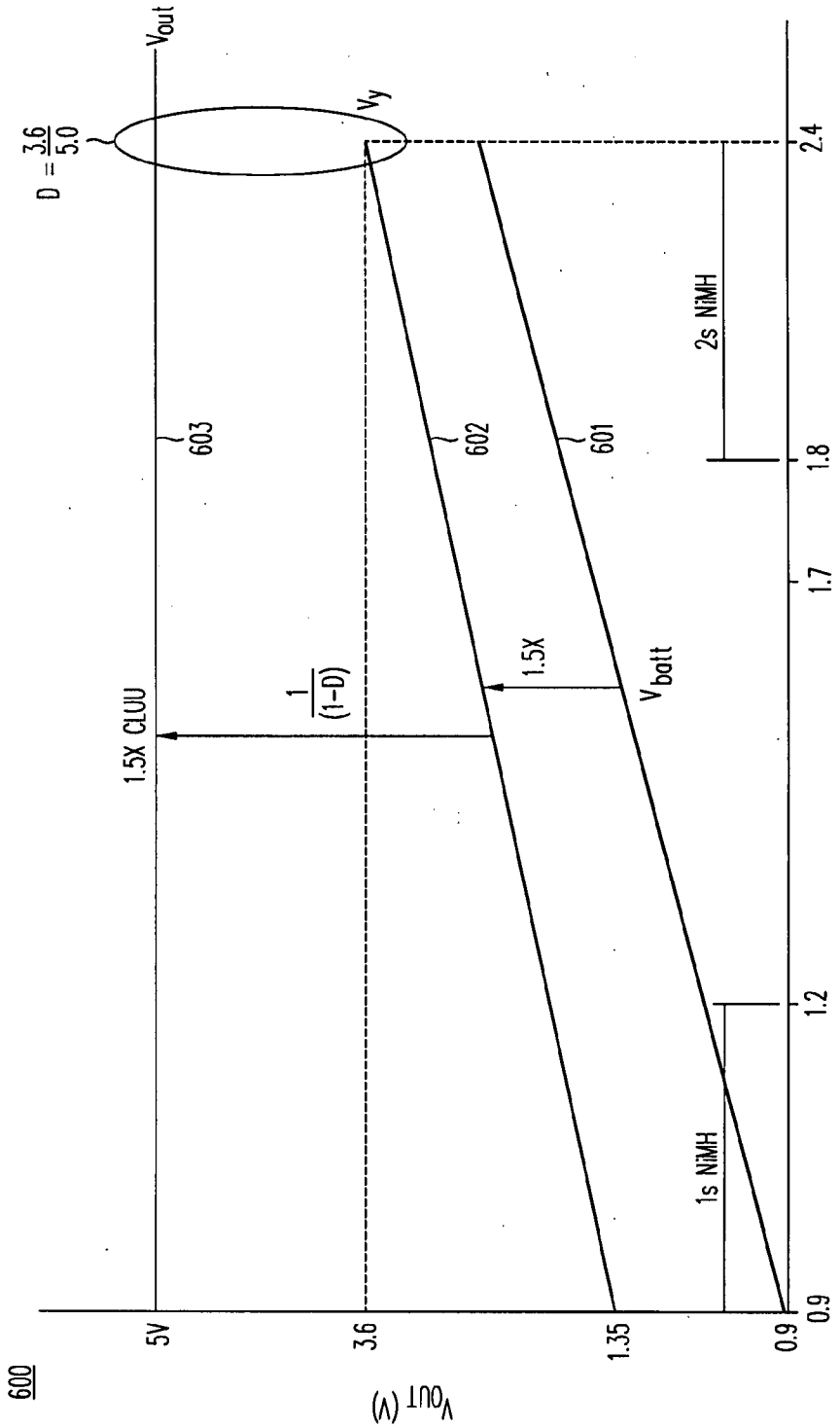
600
V_{out} (V)
5V
3.6
1.35
0.9
V_{out}
V_y
$D = \frac{3.6}{5.0}$
603
602
601
1.5X CLUU
$\frac{1}{(1-D)}$
1.5X
V_{batt}
1s NiMH
2s NiMH
0.9
1.2
1.7
1.8
2.4
V_{IN} (V)

FIG. 15D

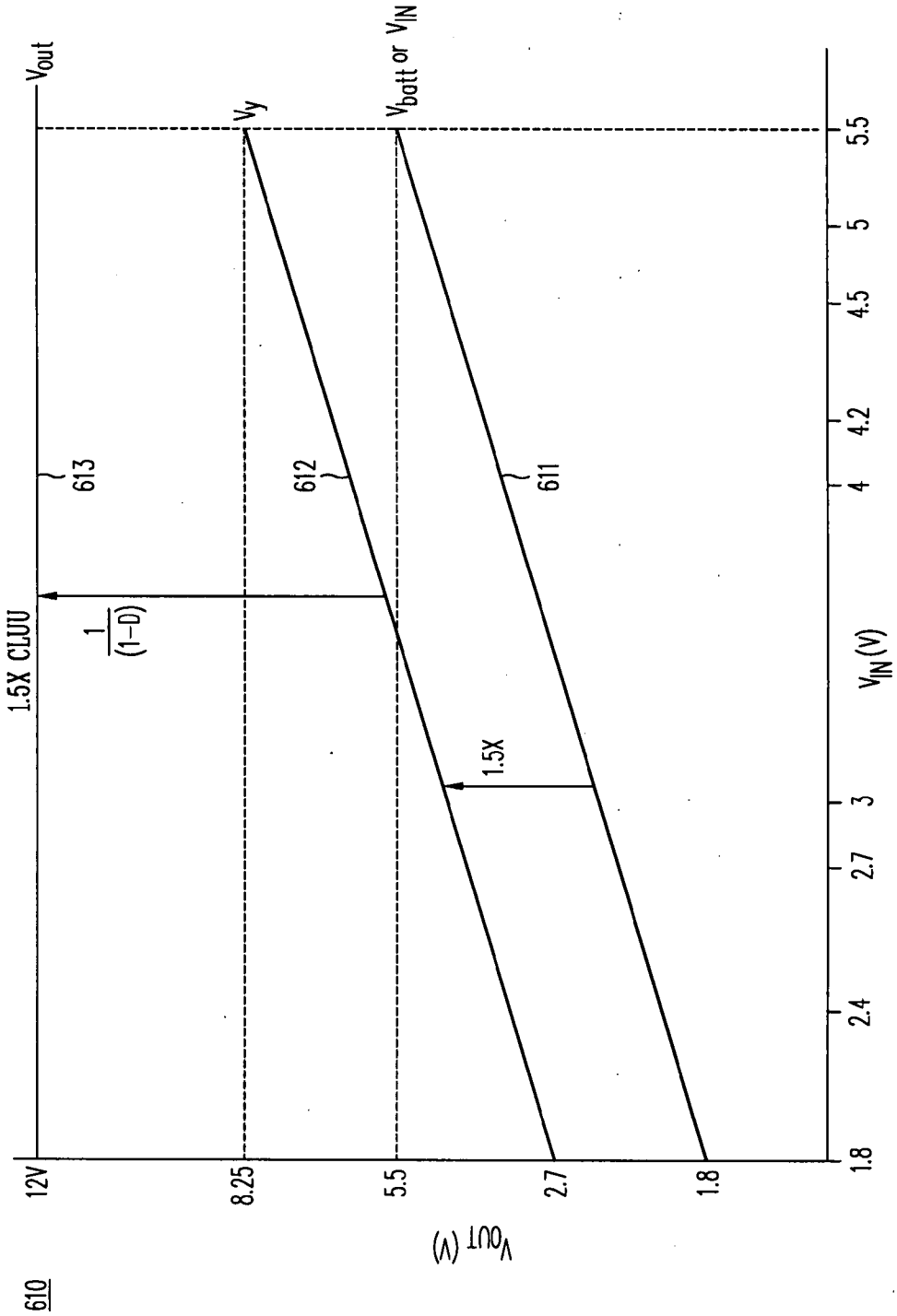
610
V_{out} (V)
12V
8.25
5.5
2.7
1.8
1.5X CLUU
$\frac{1}{(1-D)}$
613
612
611
V_y
V_{batt} or V_{IN}
1.5X
1.8
2.4
2.7
3
4
4.2
4.5
5
5.5
V_{IN}(V)

FIG. 15E

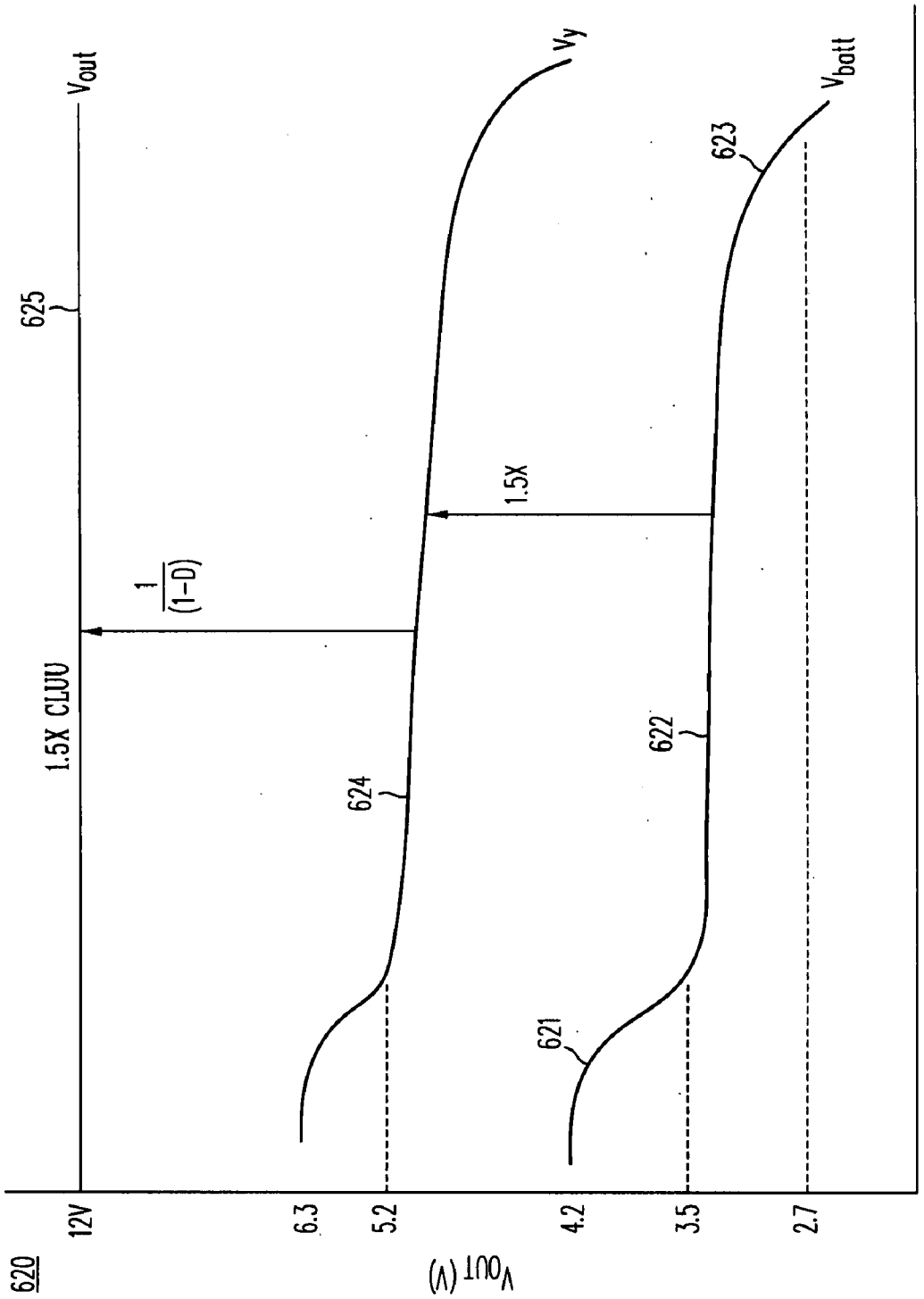
620
V_{out} (V)
12V
6.3
5.2
4.2
3.5
2.7
time t
V_{out}
625
1.5X CLUU
$\frac{1}{(1-D)}$
V_y
624
1.5X
V_{batt}
623
622
621

FIG. 15F

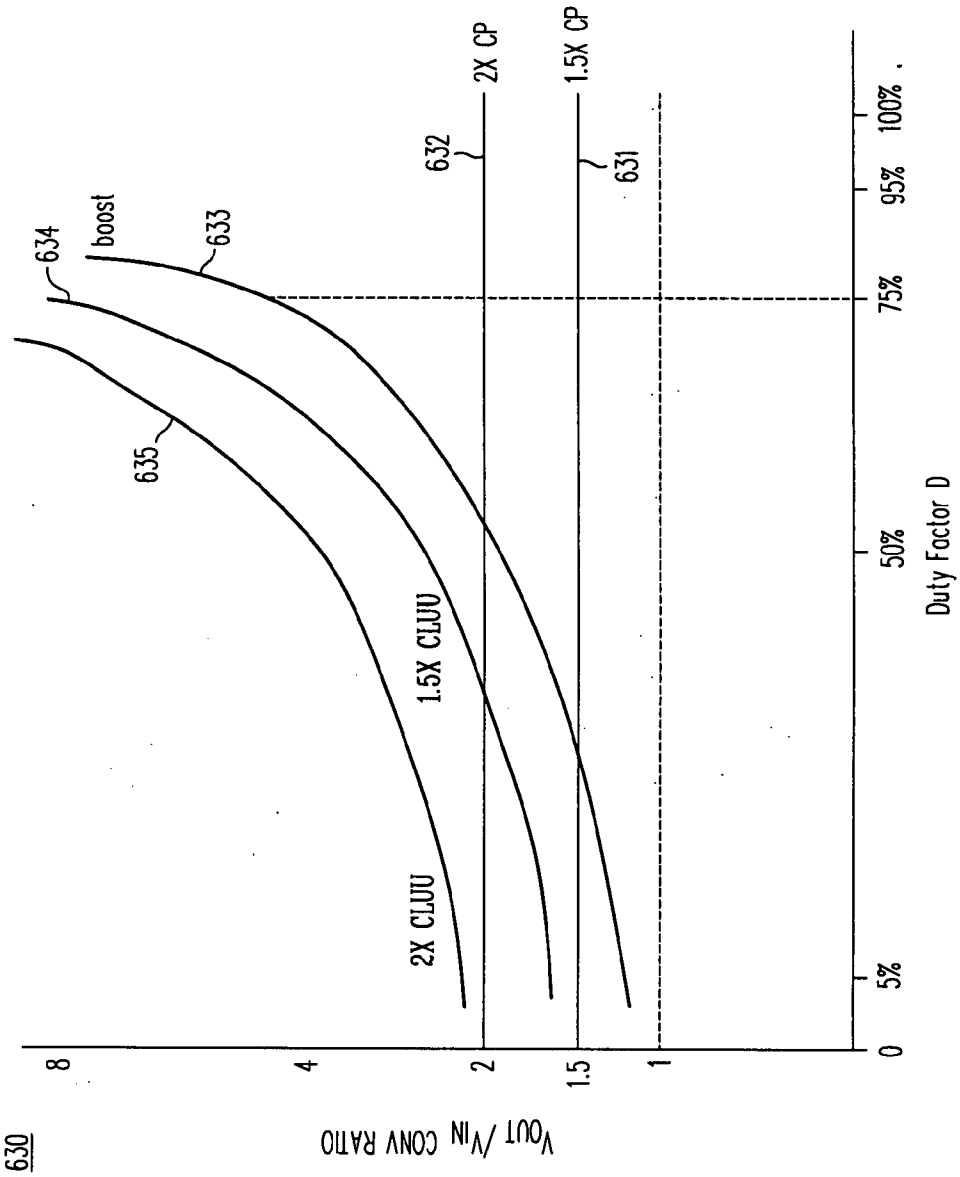
630
V_{OUT}/V_{IN} CONV RATIO
8
4
2
1.5
1
0
5%
50%
75%
95%
100%
Duty Factor D
2X CLUU
1.5X CLUU
boost
634
633
635
632
2X CP
631
1.5X CP

FIG. 15G

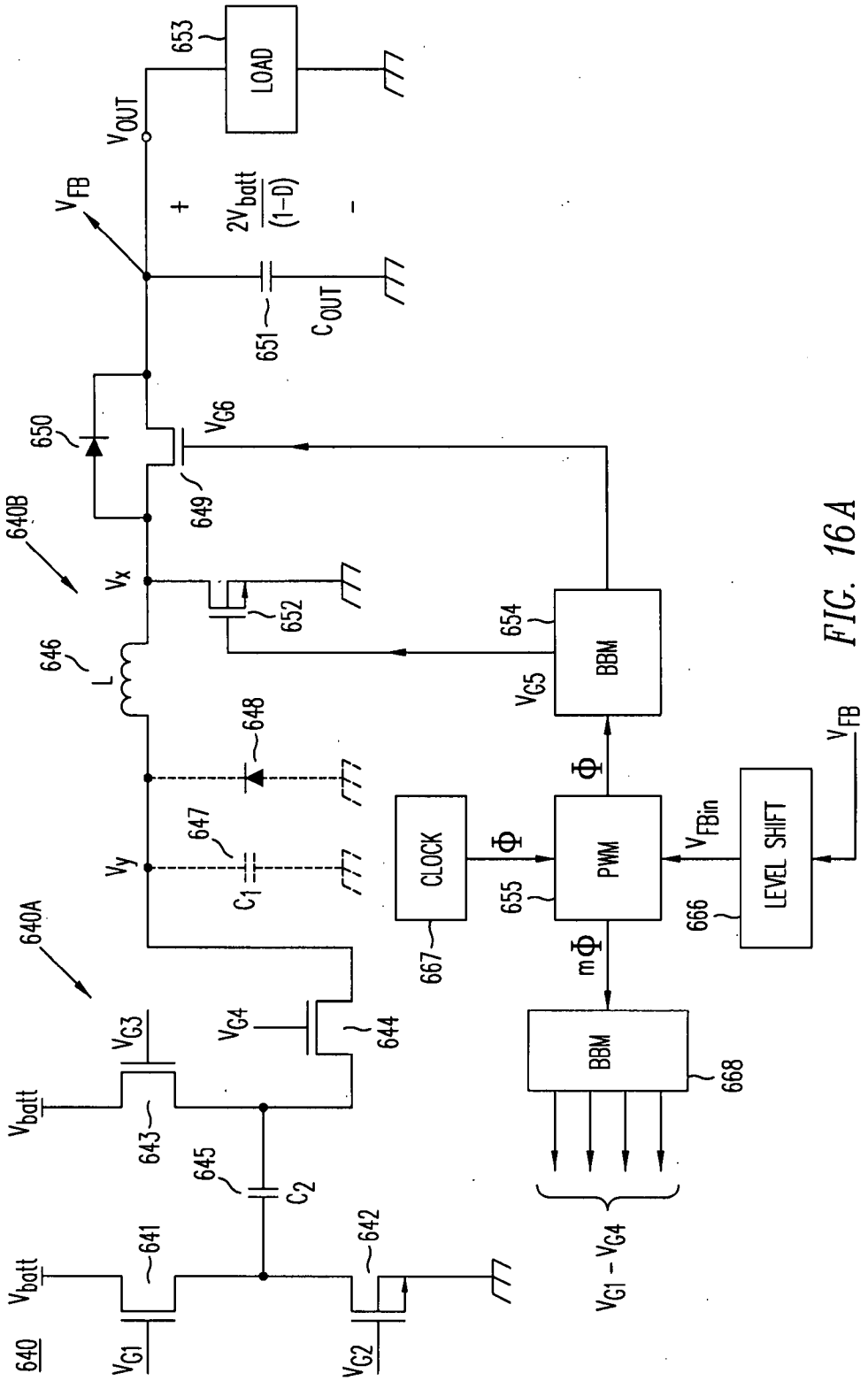

FIG. 16A

NOCO Exhibit 2011
ADC v. NOCO
IPR2024-00671

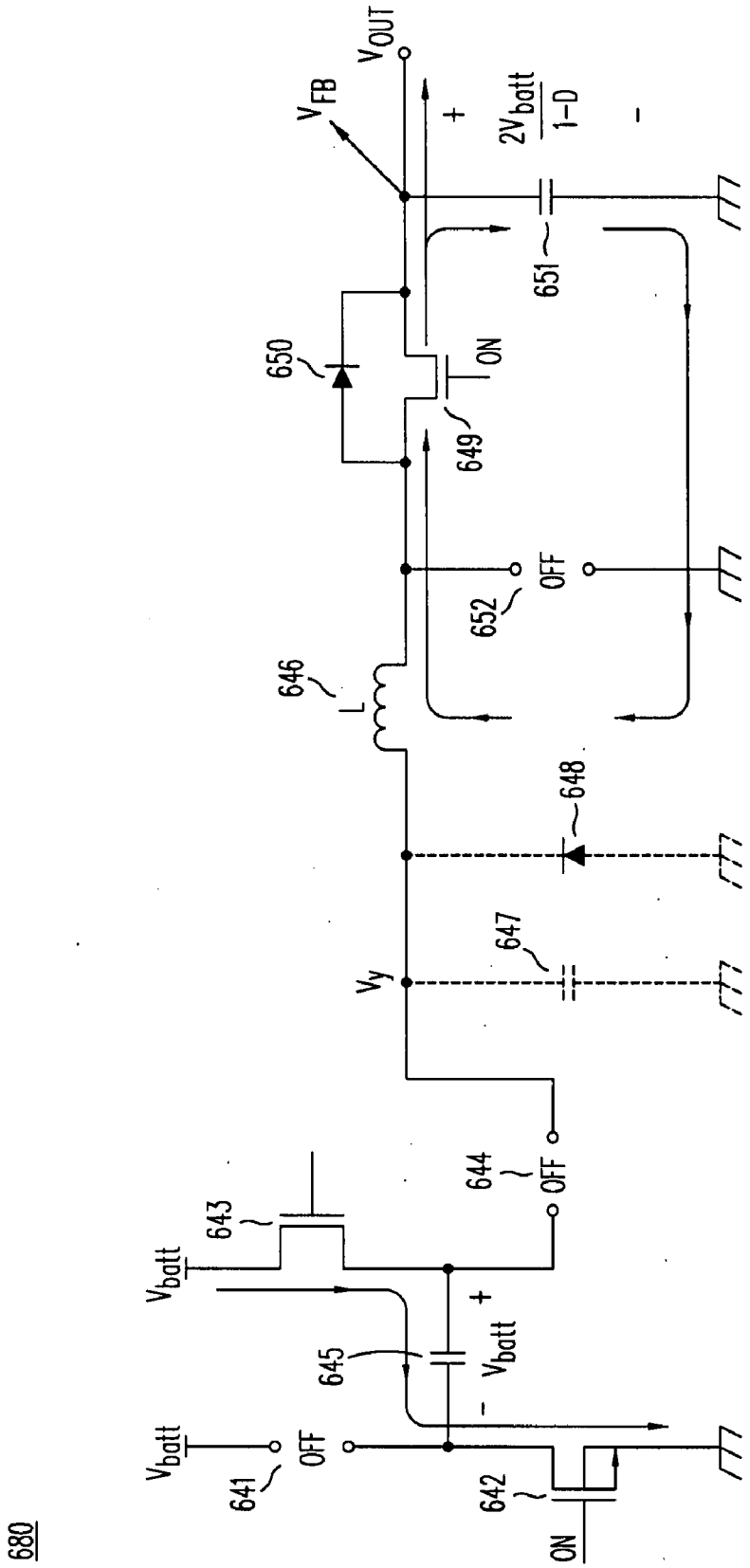
680
V_{batt}
641
OFF
642
ON
V_{batt}
643
645
V_{batt}
644
OFF
V_y
647
648
646
L
652
OFF
649
ON
650
651
V_{FB}
V_{OUT}
$\frac{2V_{batt}}{1-D}$

FIG. 16B

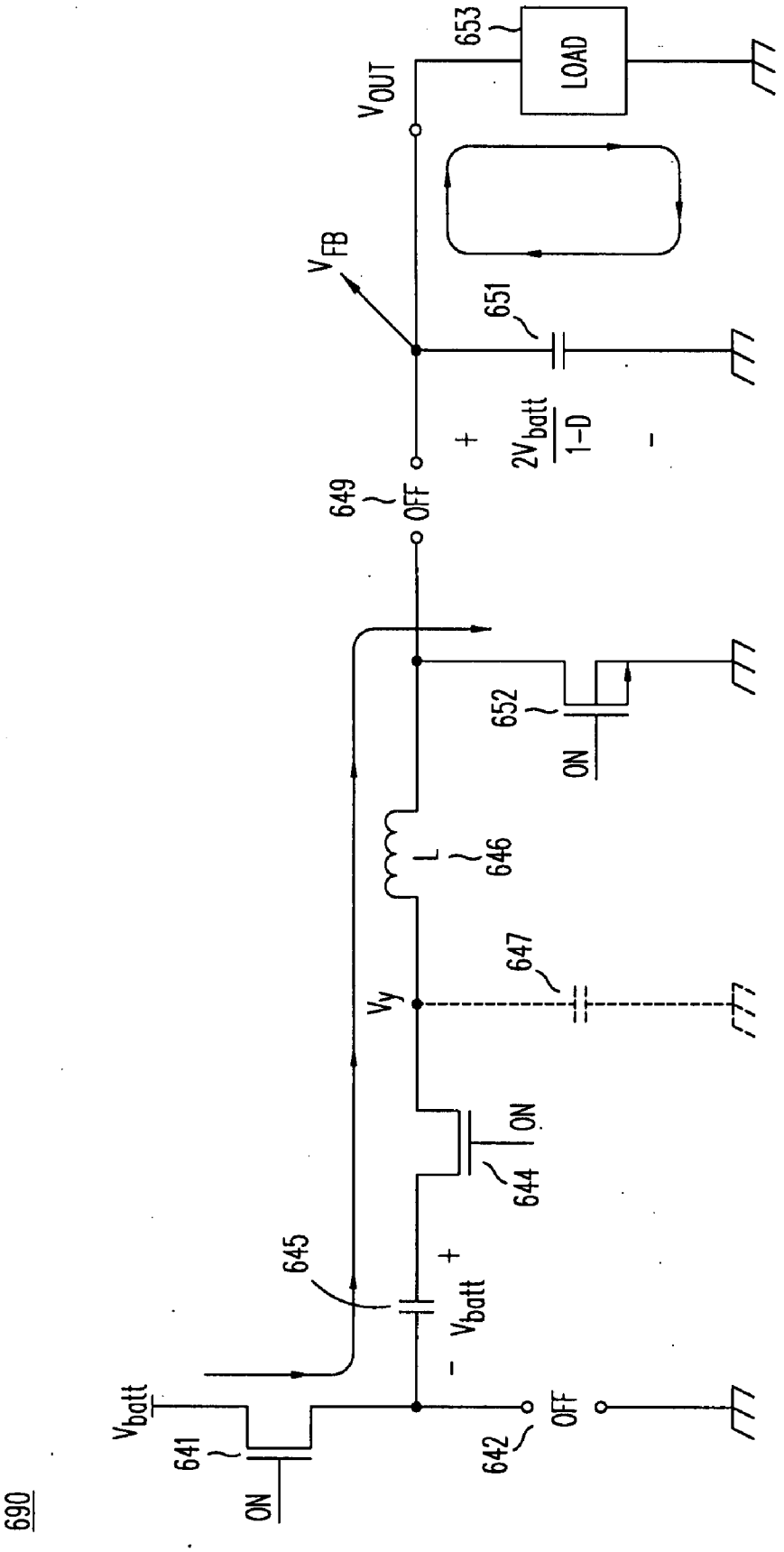
690
V_{batt}
641
ON
642
OFF
645
V_{batt}
644
ON
V_y
647
L
646
652
ON
649
OFF
V_{FB}
651
$\frac{2V_{batt}}{1-D}$
V_{OUT}
653
LOAD

FIG. 16C

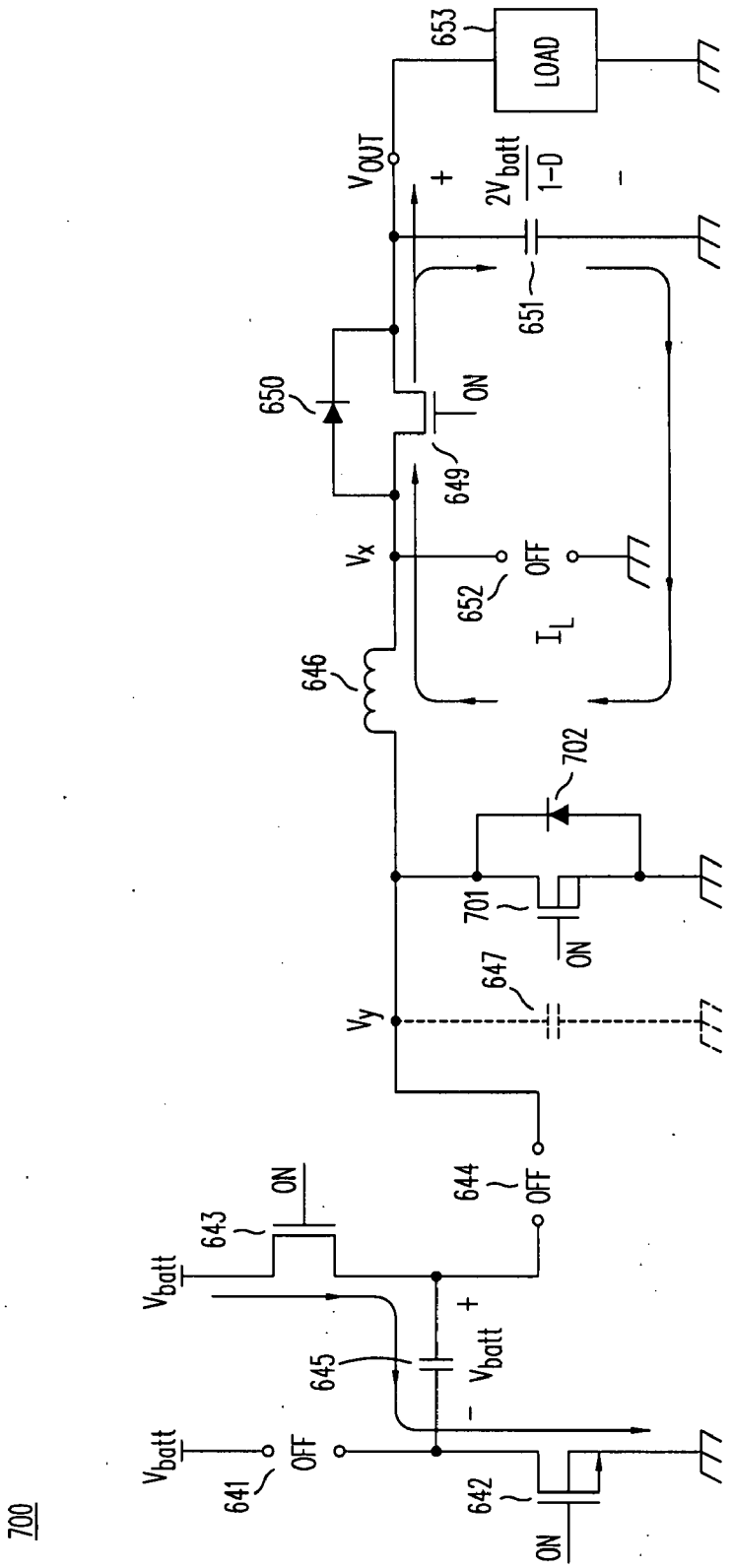

FIG. 16D

NOCO Exhibit 2011
ADC v. NOCO
IPR2024-00671

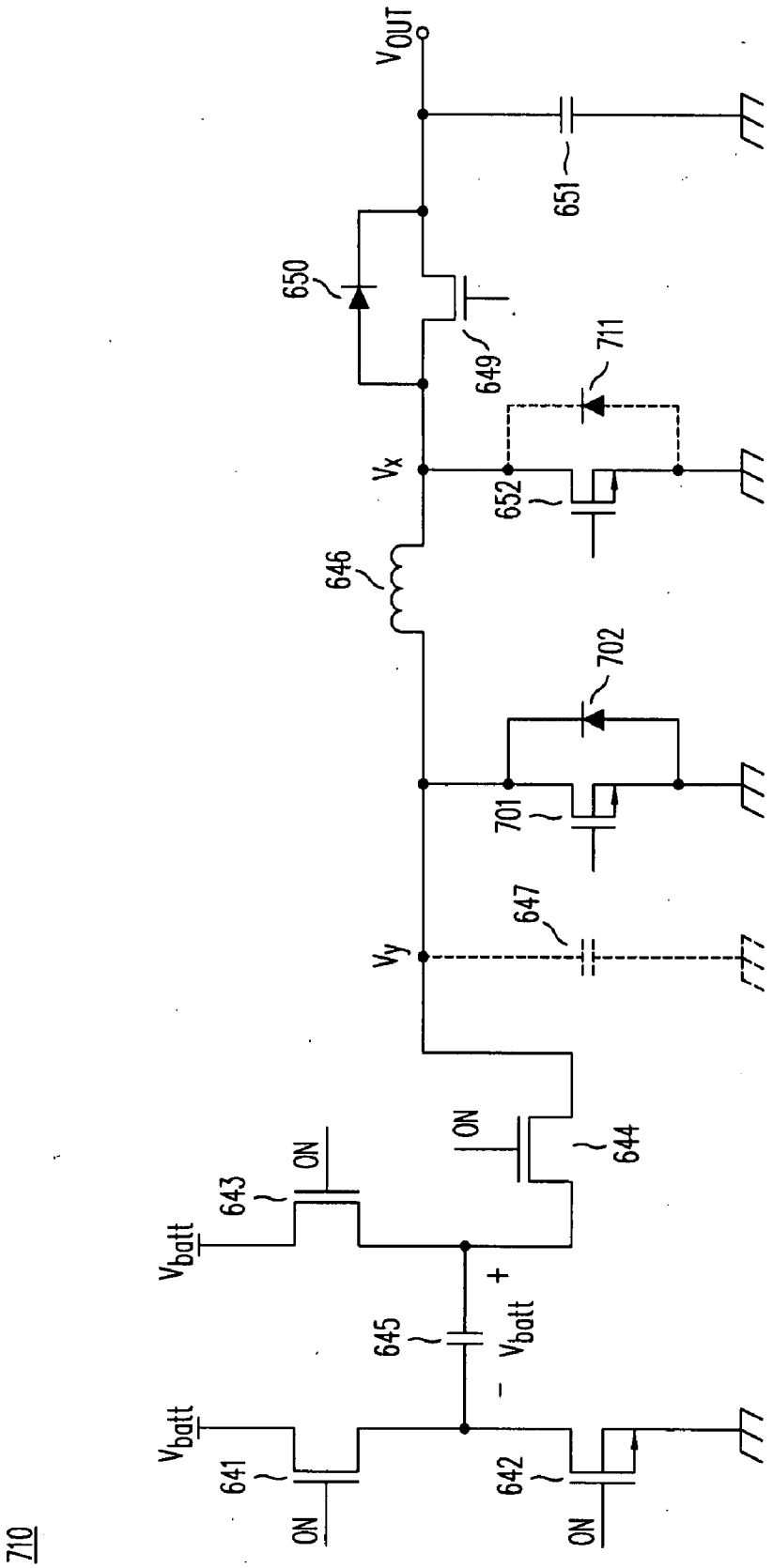

FIG. 16E

NOCO Exhibit 2011
ADC v. NOCO
IPR2024-00671

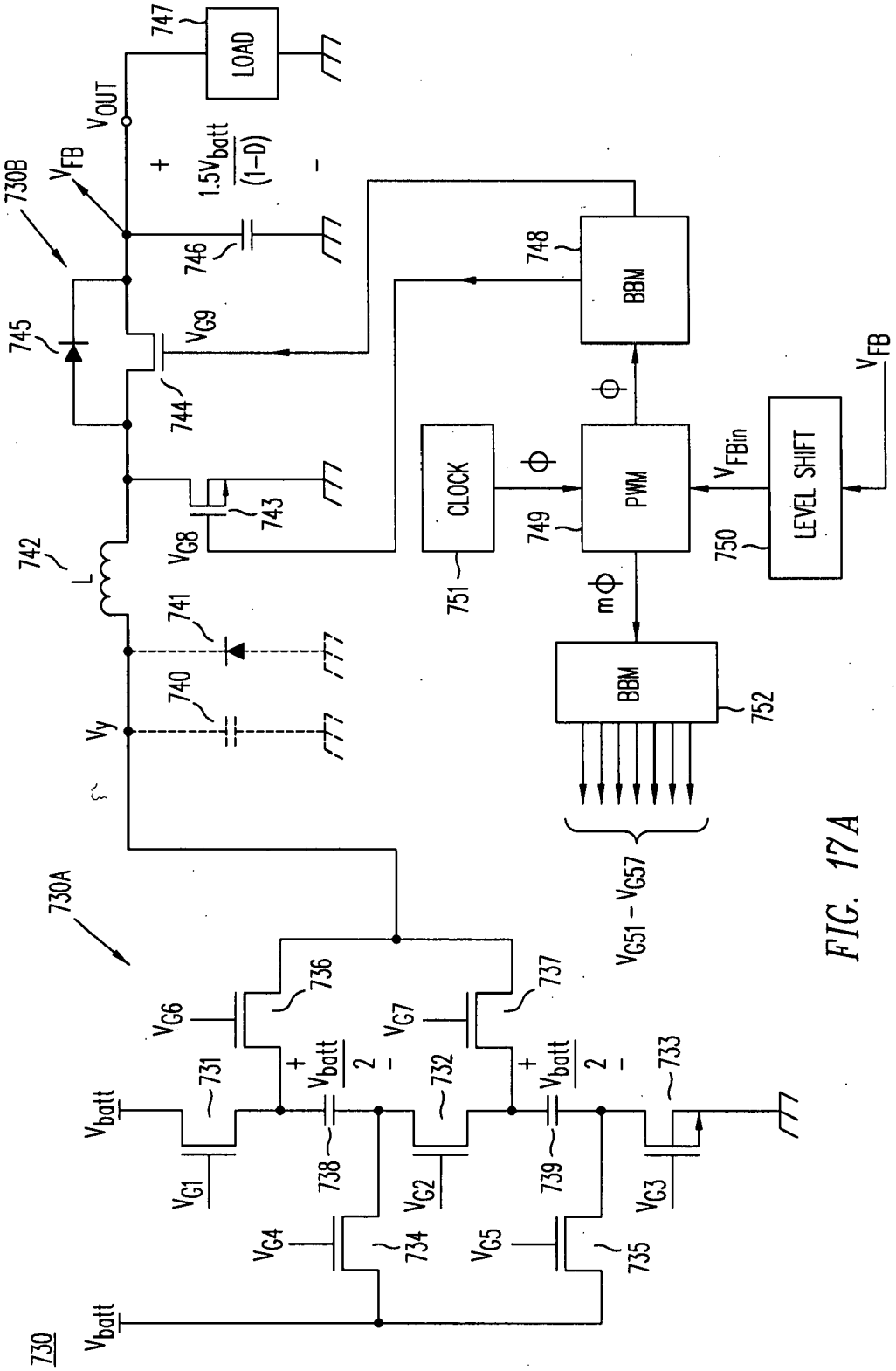

FIG. 17A

NOCO Exhibit 2011
ADC v. NOCO
IPR2024-00671

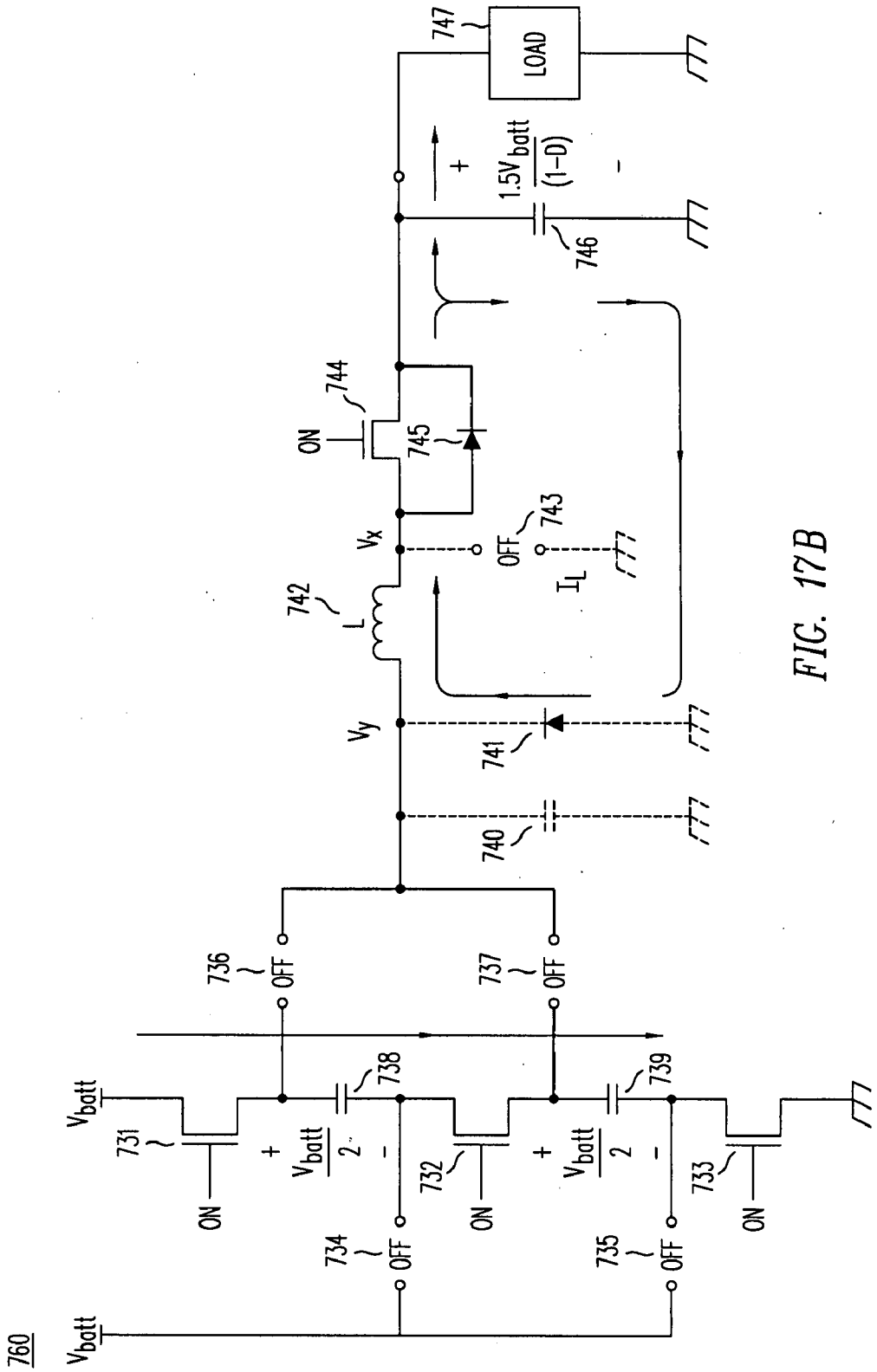

FIG. 17B

NOCO Exhibit 2011
ADC v. NOCO
IPR2024-00671

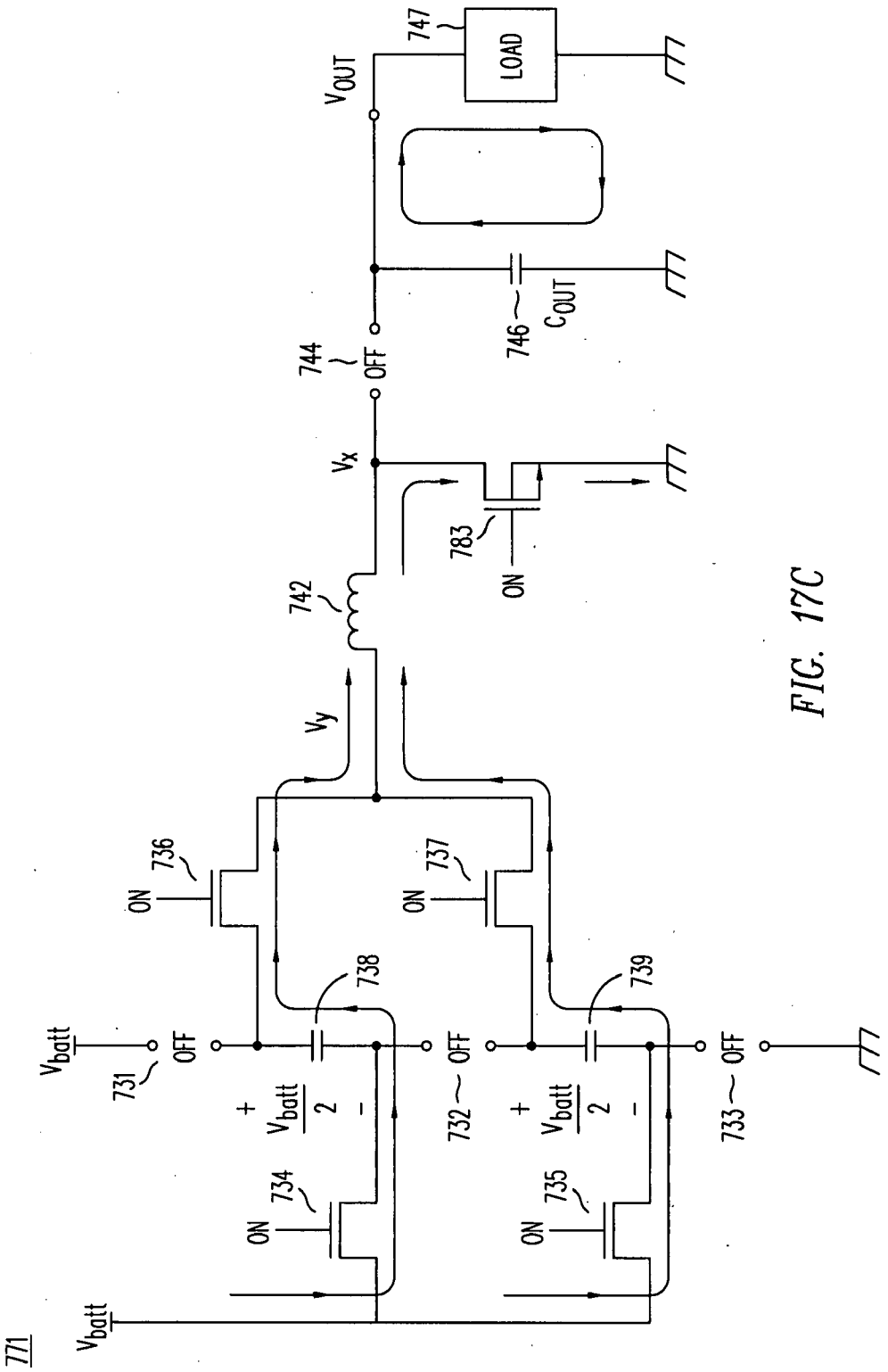
771
V_{batt}
V_{batt}
731
OFF
+
$\frac{V_{batt}}{2}$
-
734
ON
736
ON
738
V_y
742
732
OFF
+
$\frac{V_{batt}}{2}$
-
735
ON
737
ON
739
733
OFF
V_x
783
ON
744
OFF
V_{OUT}
746
C_{OUT}
747
LOAD

FIG. 17C

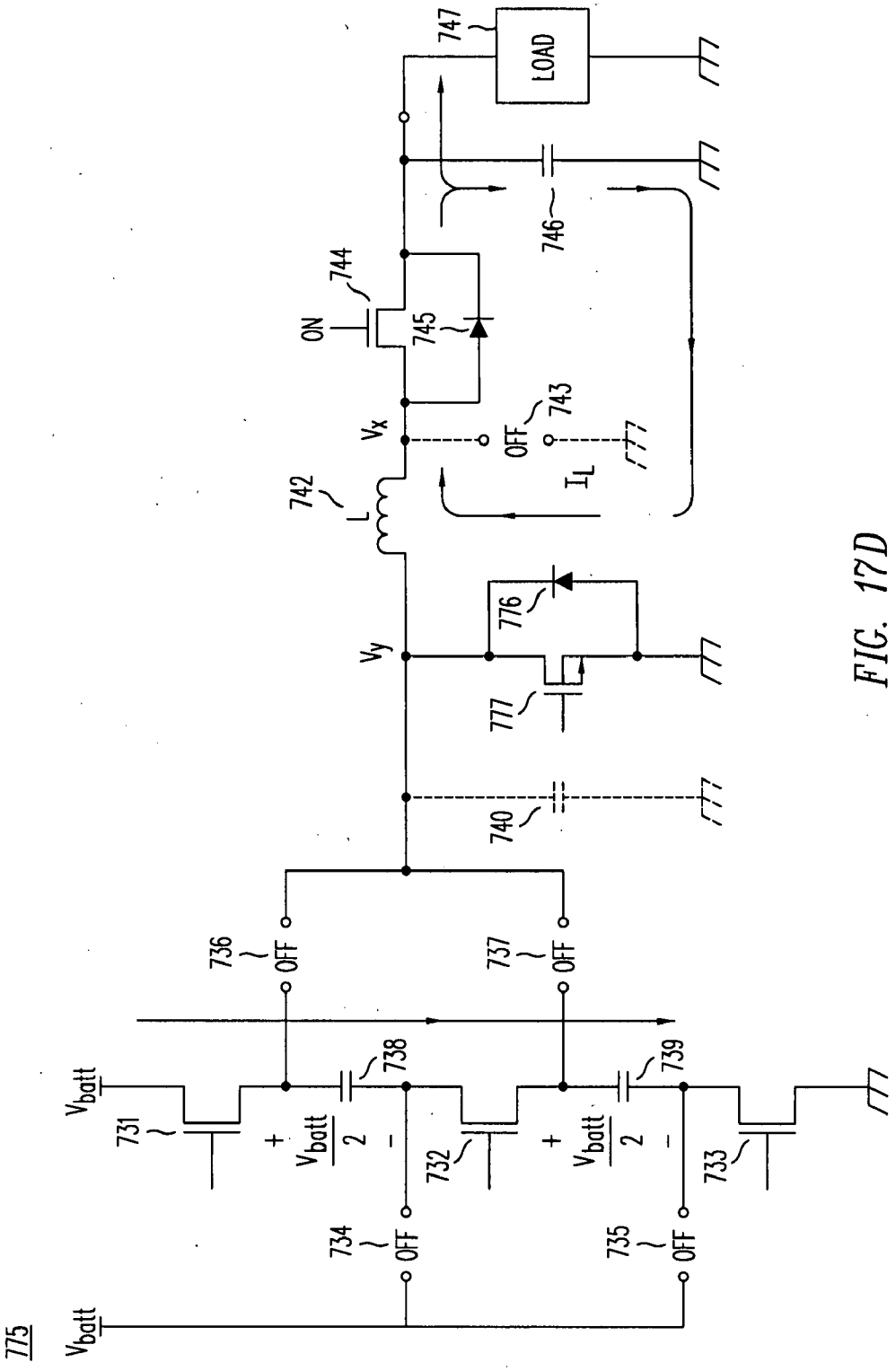

FIG. 17D

NOCO Exhibit 2011
ADC v. NOCO
IPR2024-00671

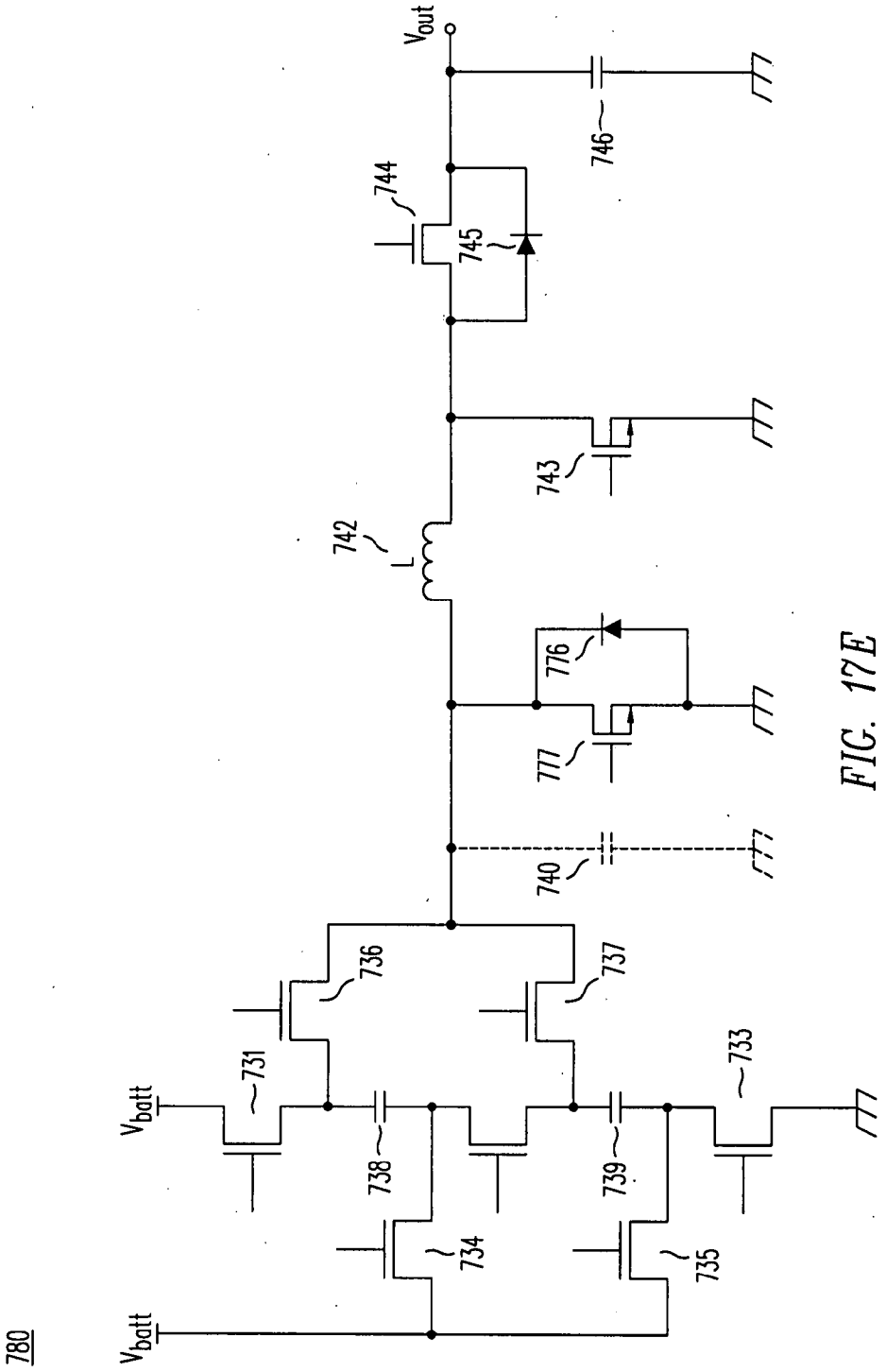
780
V_{batt}
V_{batt}
731
736
737
738
739
733
734
735
740
742
L
743
744
745
746
V_{out}
776
777

FIG. 17E

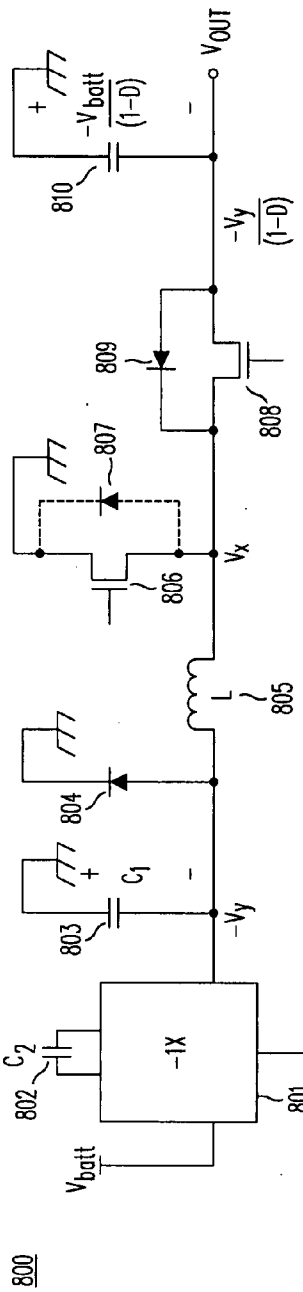

FIG. 18A

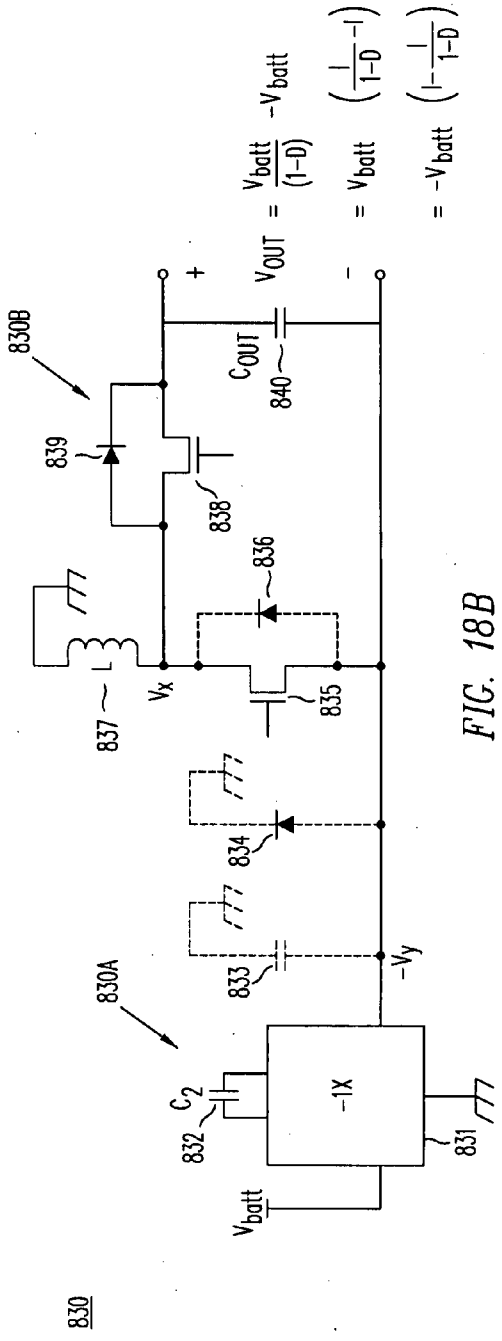

FIG. 18B

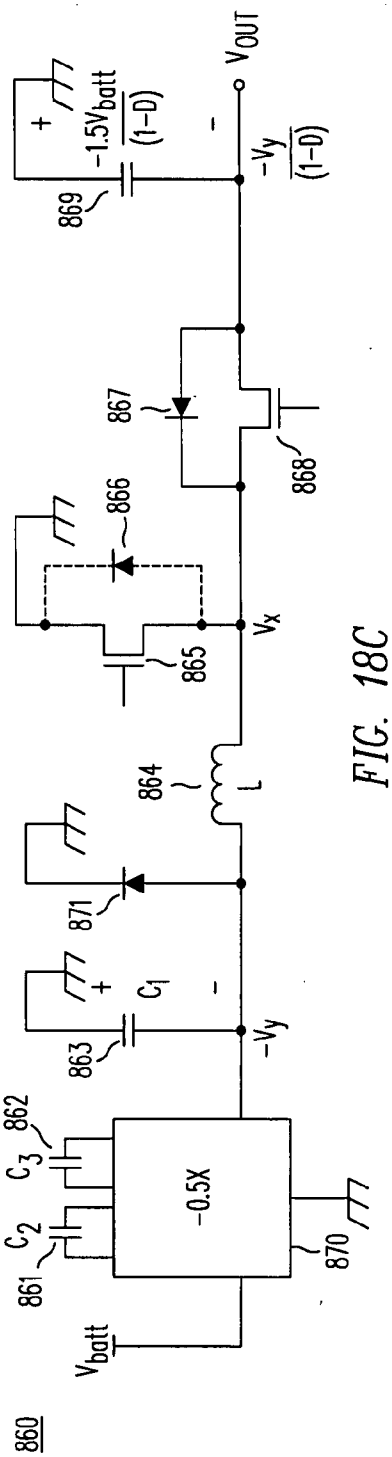

FIG. 18C

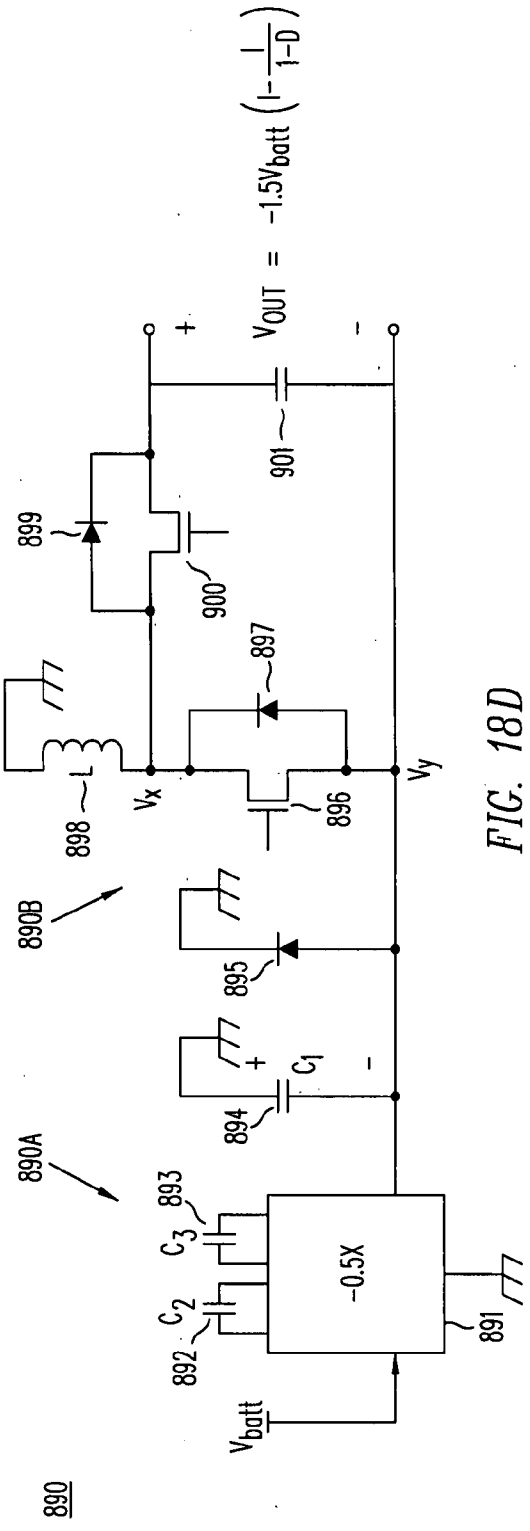

FIG. 18D

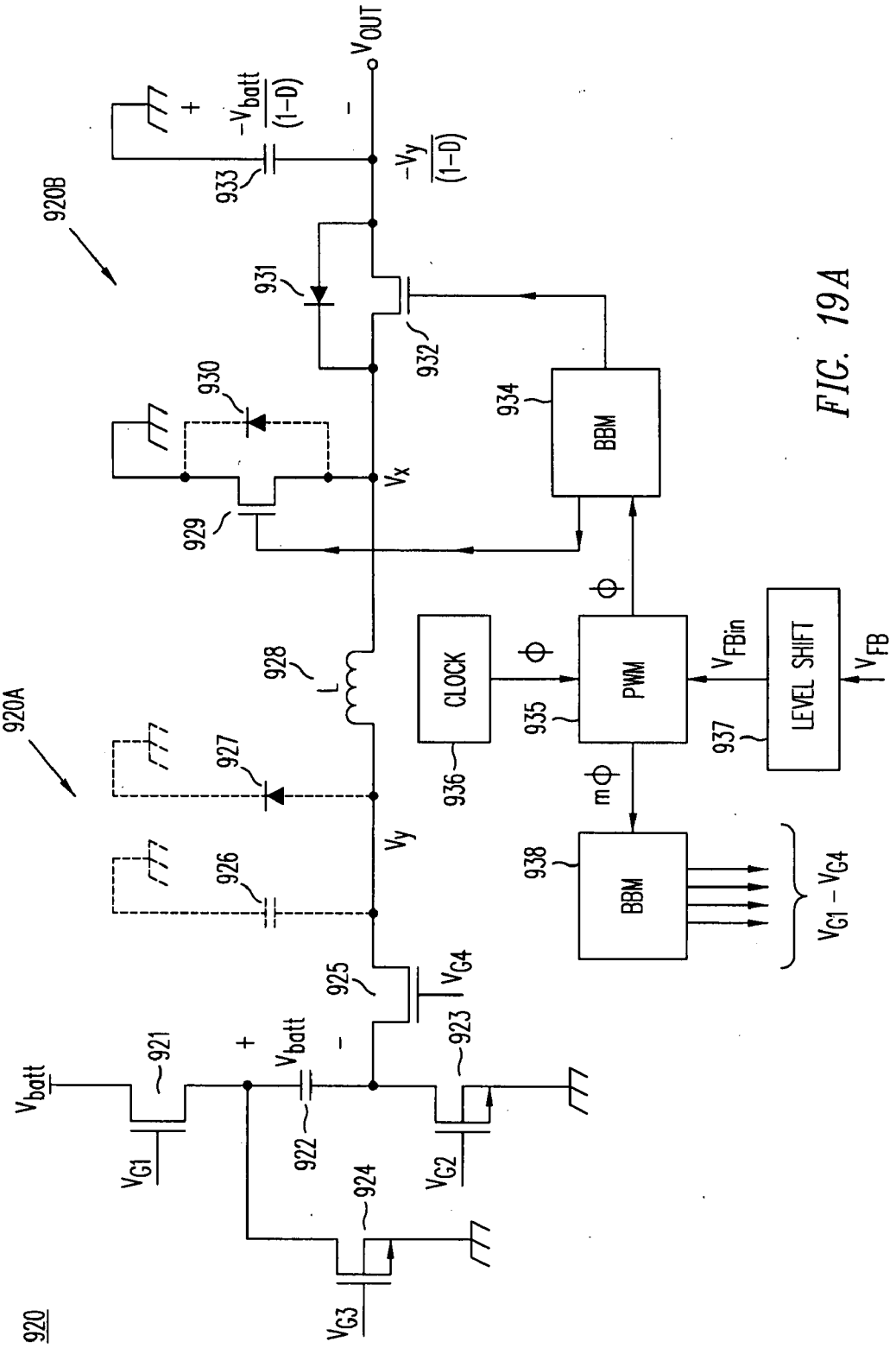
920
920A
920B
V_{batt}
921
922
923
924
925
926
927
928
929
930
931
932
933
934
935
936
937
938
V_{G1}
V_{G2}
V_{G3}
V_{G4}
V_{batt}
V_y
V_x
V_{OUT}
$-\frac{V_{batt}}{(1-D)}$
$-\frac{V_y}{(1-D)}$
L
BBM
CLOCK
PWM
LEVEL SHIFT
BBM
ϕ
$m\phi$
V_{FBin}
V_{FB}
$V_{G1} - V_{G4}$

FIG. 19A

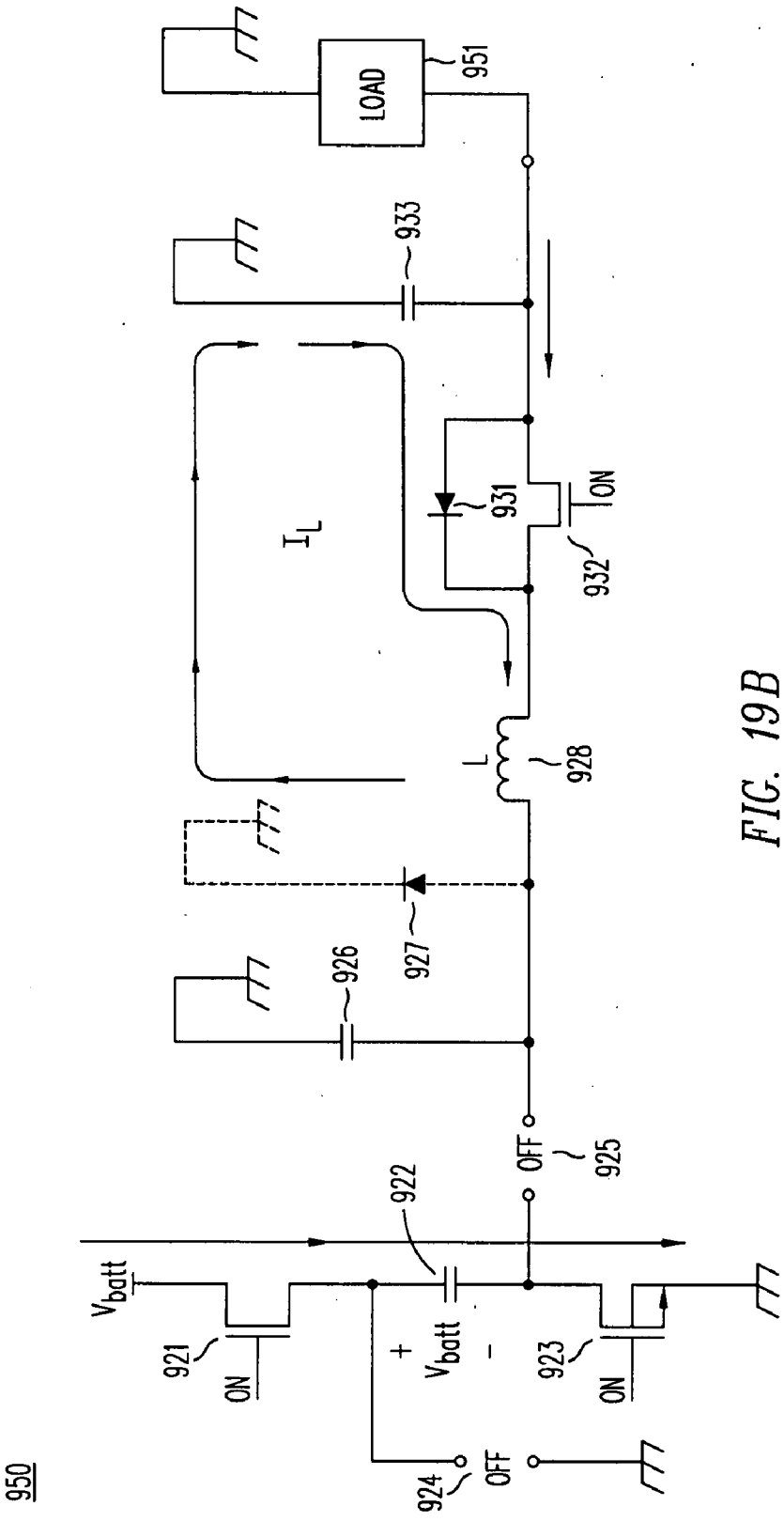
950
LOAD
951
933
931
ON
932
I_L
L
928
927
926
OFF
925
922
V_{batt}
921
ON
+
V_{batt}
-
923
ON
924
OFF

FIG. 19B

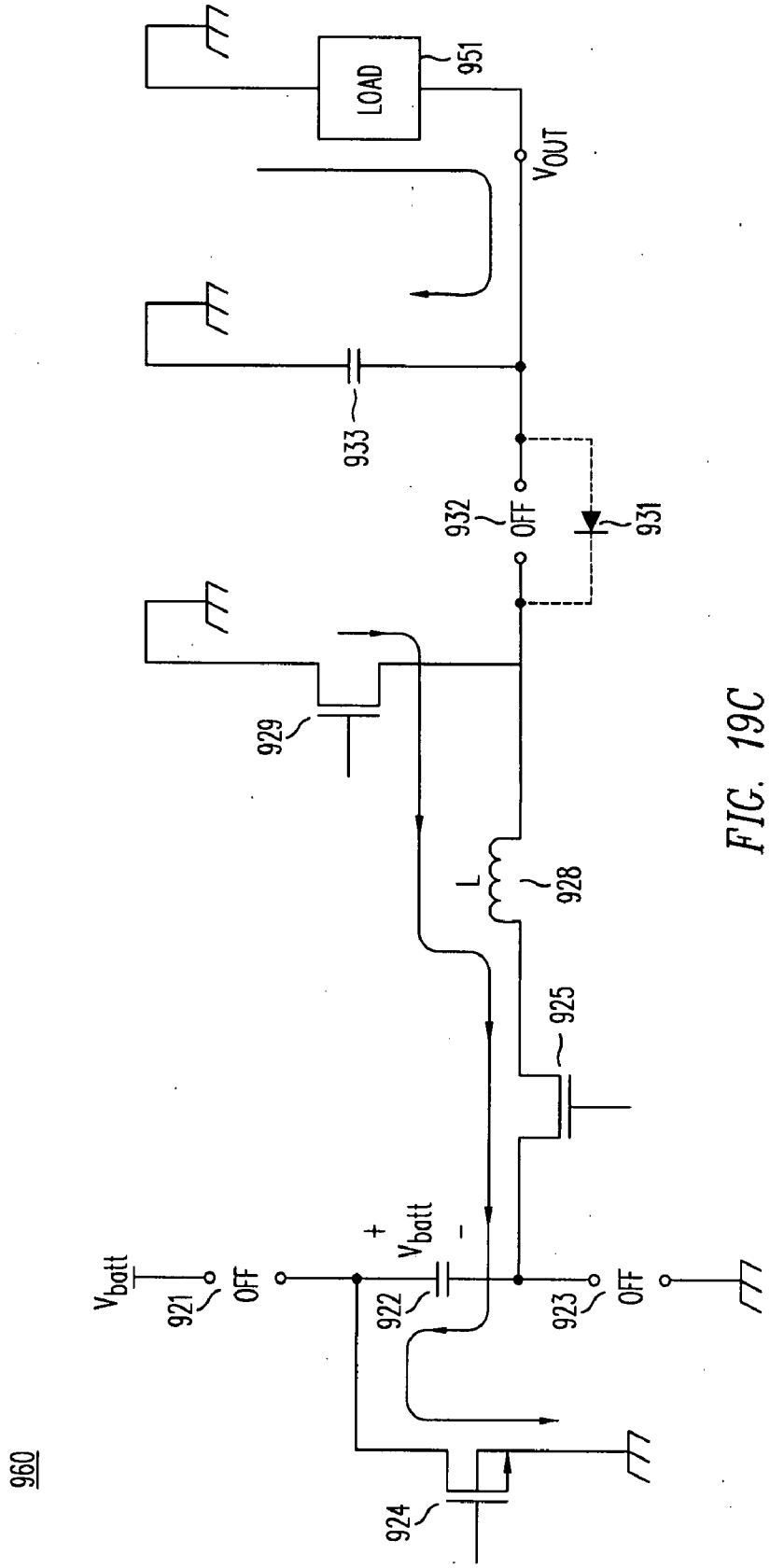
960
LOAD
951
V_{OUT}
933
932
OFF
931
929
L
928
925
V_{batt}
921
OFF
+
V_{batt}
-
922
923
OFF
924

FIG. 19C

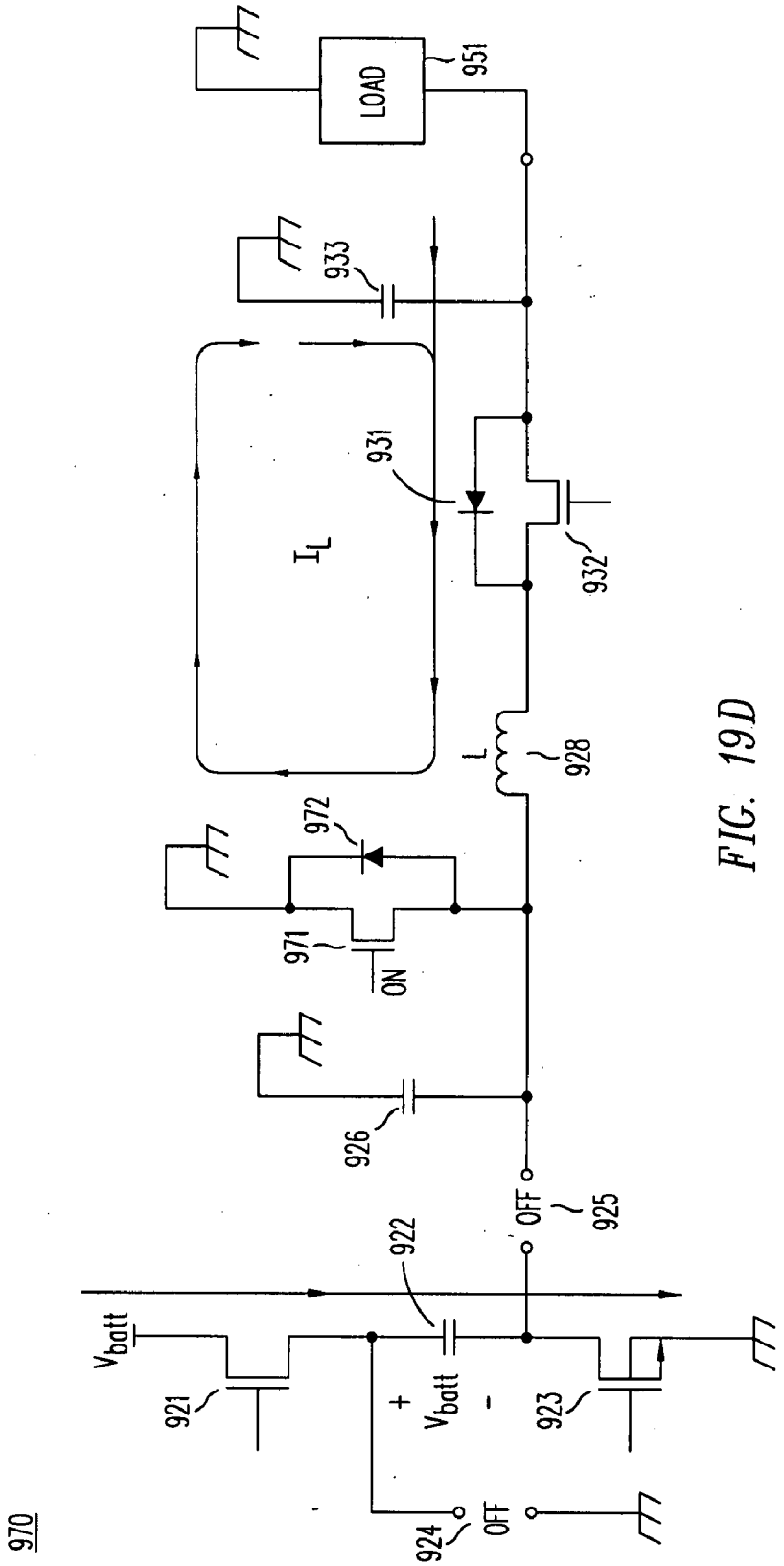
970
LOAD
951
933
931
932
I_L
L
928
972
971
ON
926
OFF
925
922
V_{batt}
921
+
V_{batt}
-
923
924
OFF

FIG. 19D

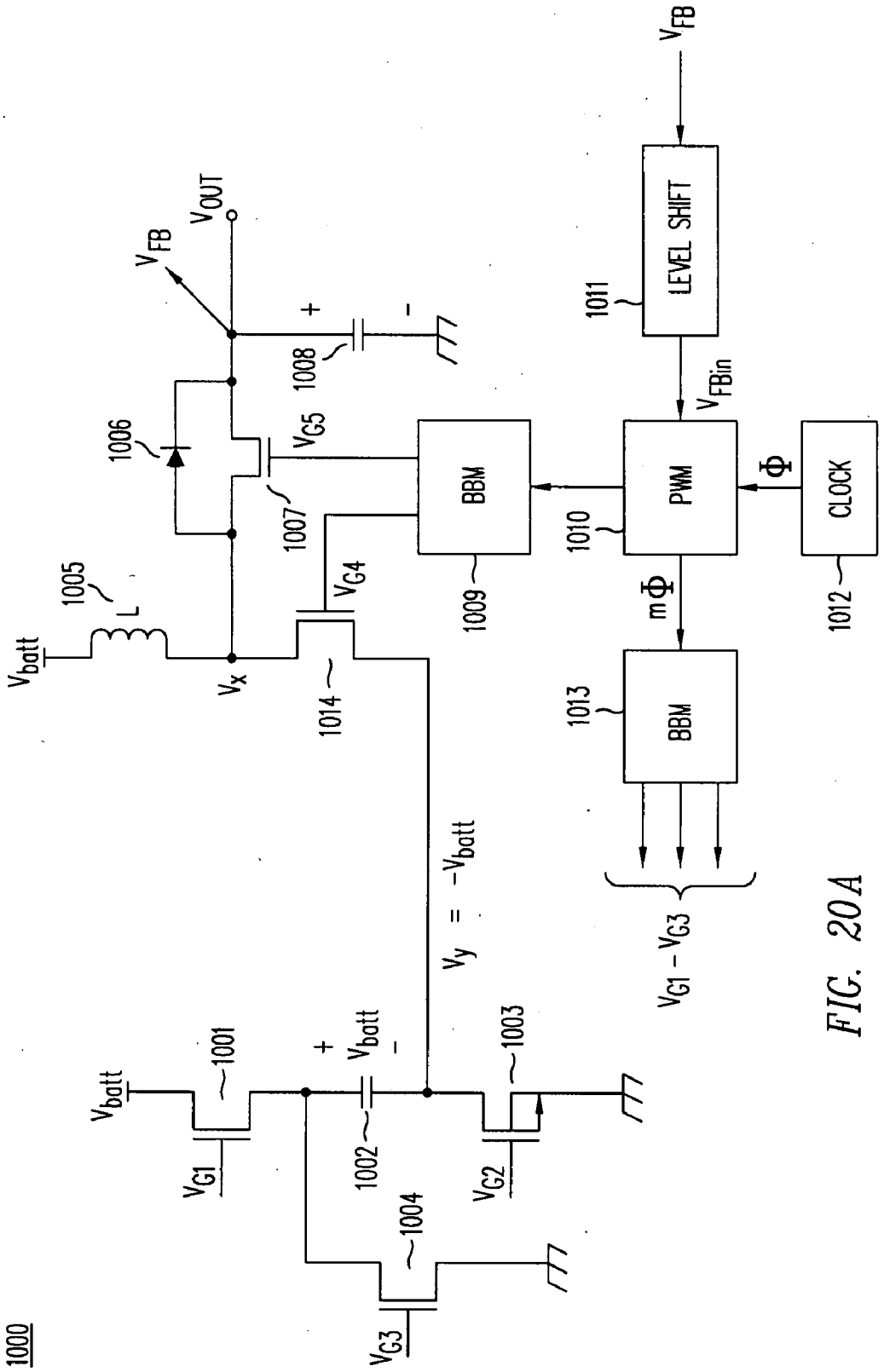
1000
V_{batt}
1001
V_{G1}
1002
V_{batt}
+
-
1003
V_{G2}
1004
V_{G3}
$V_y = -V_{batt}$
1005
L
V_x
1006
1007
V_{G5}
V_{G4}
1014
V_{FB}
V_{OUT}
1008
+
-
BBM
1009
PWM
1010
V_{FBin}
LEVEL SHIFT
1011
V_{FB}
CLOCK
1012
Φ
mΦ
BBM
1013
$V_{G1} - V_{G3}$

FIG. 20A

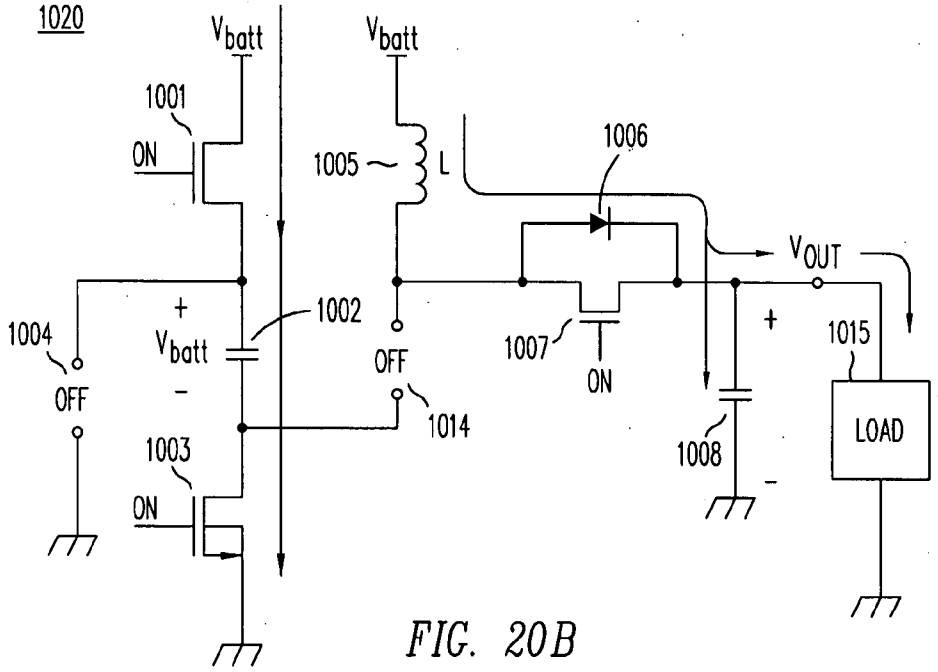

FIG. 20B

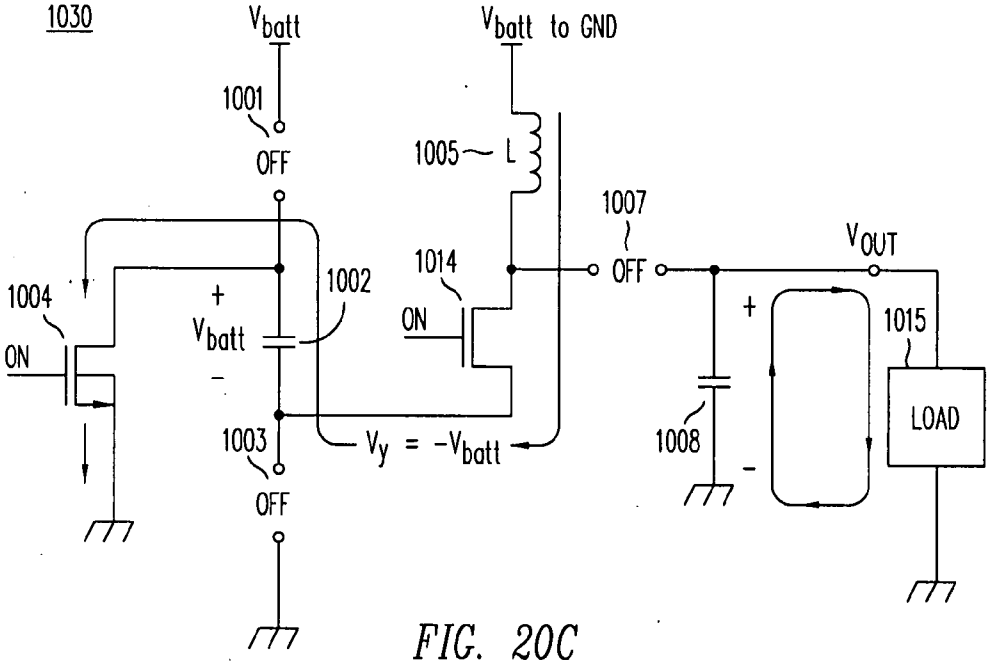

FIG. 20C

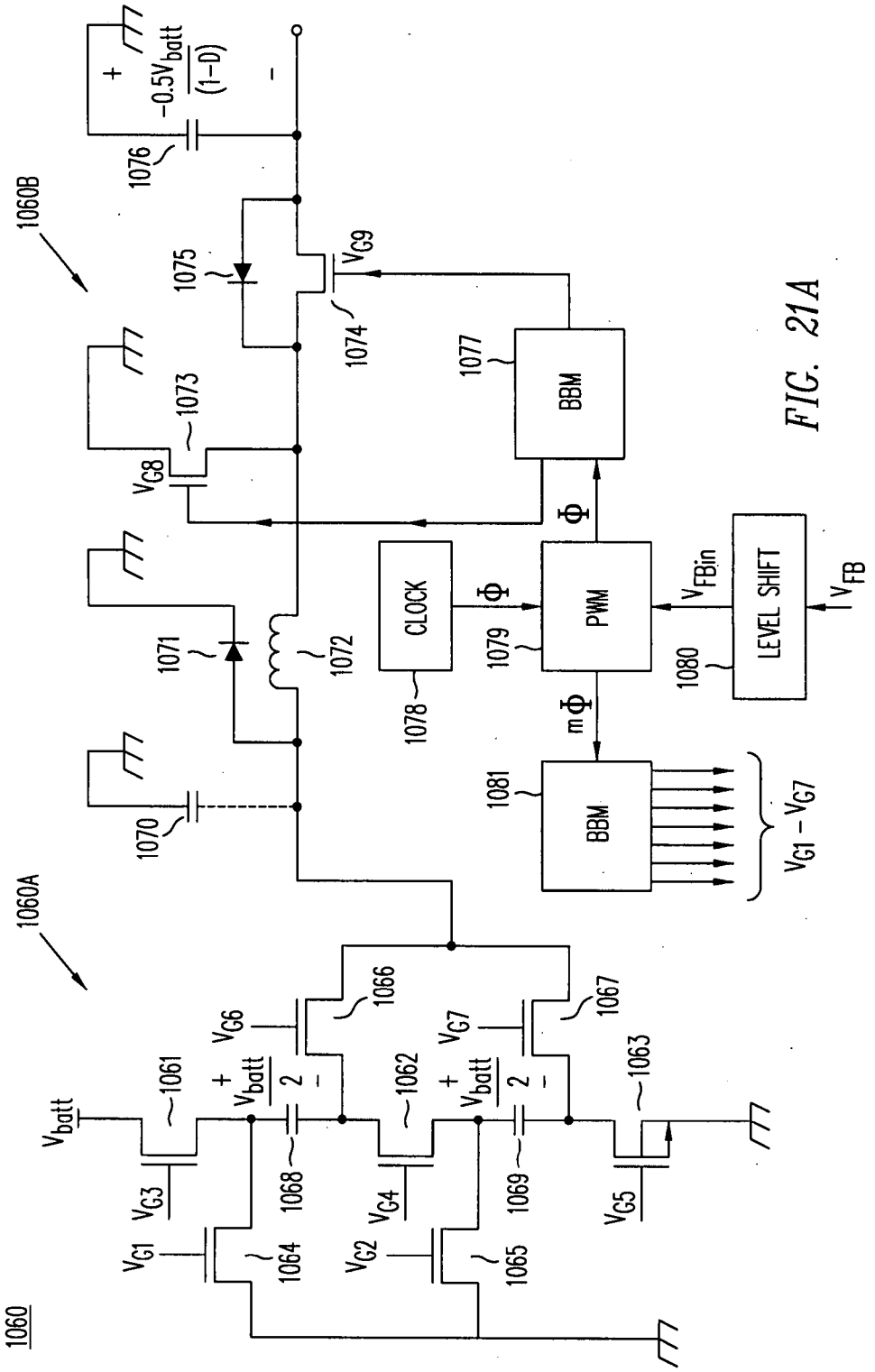
1060
1060A
1060B
V_{batt}
1061
1062
1063
1064
1065
1066
1067
1068
1069
V_{G1}
V_{G2}
V_{G3}
V_{G4}
V_{G5}
V_{G6}
V_{G7}
$\frac{V_{batt}}{2}$
1070
1071
1072
1073
1074
1075
1076
V_{G8}
V_{G9}
$-0.5\frac{V_{batt}}{(1-D)}$
1077
BBM
1078
CLOCK
1079
PWM
1080
LEVEL SHIFT
1081
BBM
Φ
$m\Phi$
V_{FBin}
V_{FB}
$V_{G1} - V_{G7}$

FIG. 21A

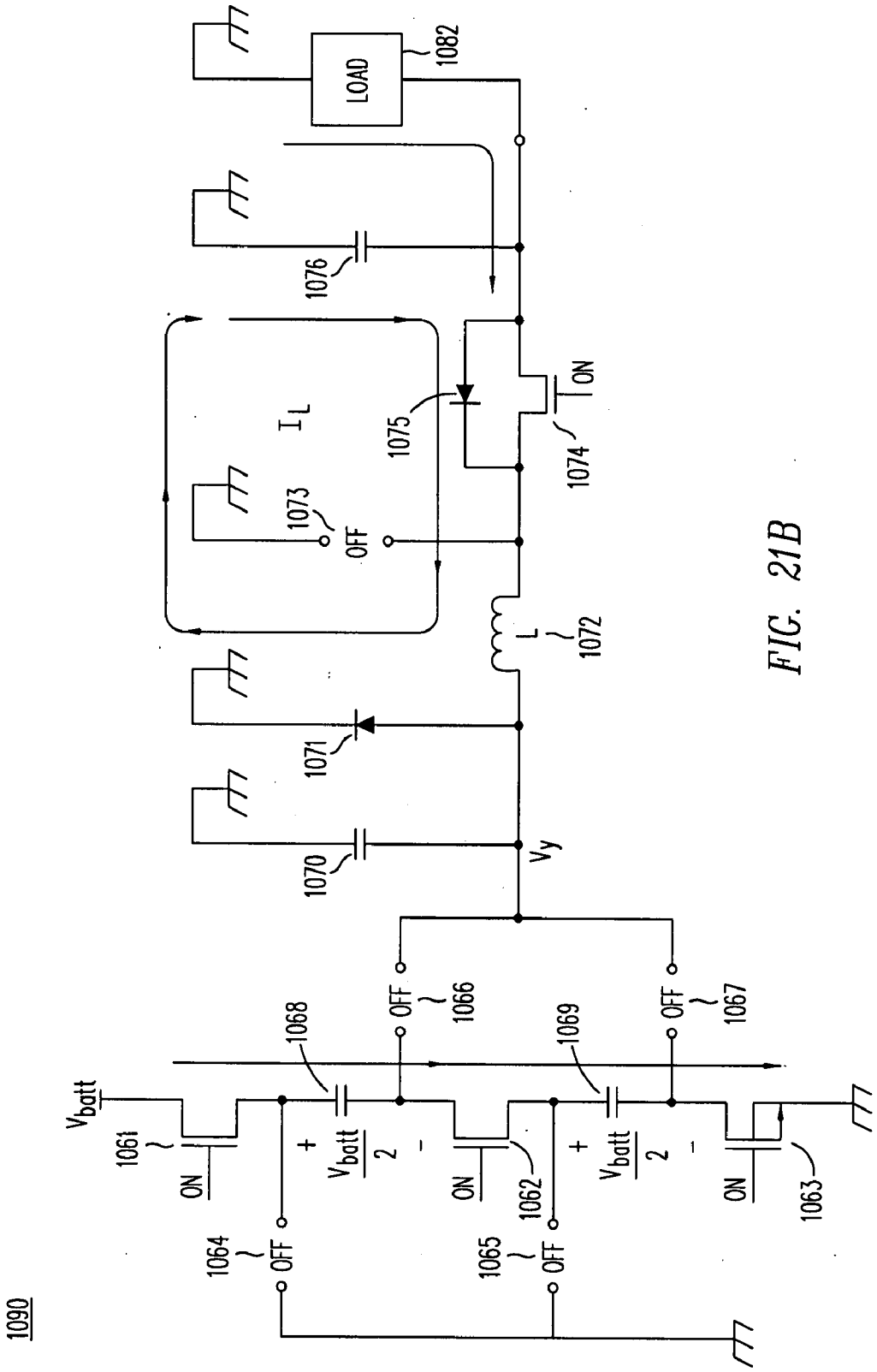
1090
V_{batt}
1061
ON
1064
OFF
1068
+
$\frac{V_{batt}}{2}$
-
OFF
1066
ON
1062
1065
OFF
1069
+
$\frac{V_{batt}}{2}$
-
OFF
1067
ON
1063
1070
V_y
1071
L
1072
1073
OFF
I_L
1075
1074
ON
1076
LOAD
1082

FIG. 21B

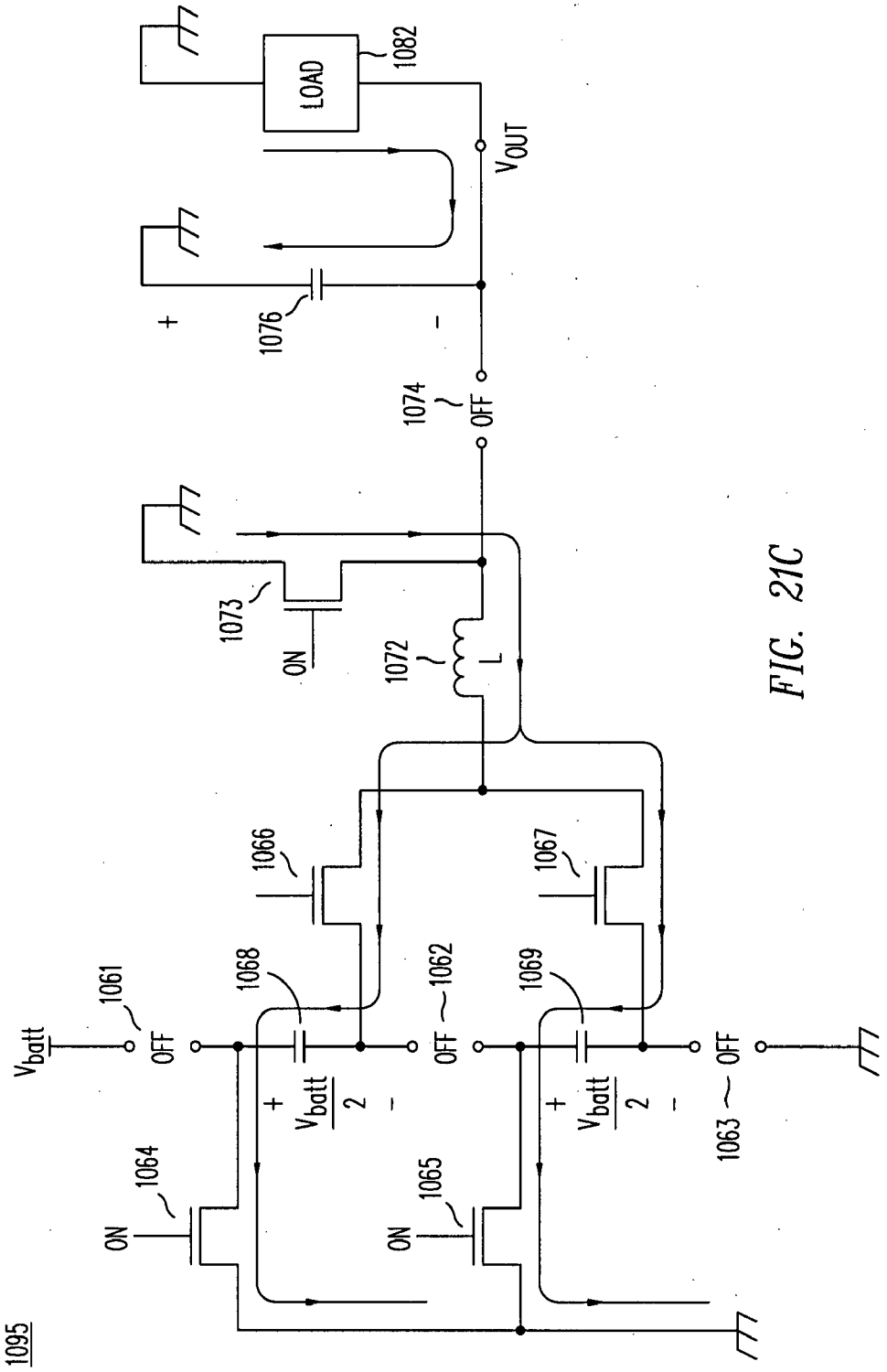
1095
V_{batt}
1061
OFF
ON
1064
1068
+
$\frac{V_{batt}}{2}$
-
1066
1073
ON
1072
L
1074
OFF
1076
+
-
LOAD
1082
V_{OUT}
1062
OFF
ON
1065
1069
+
$\frac{V_{batt}}{2}$
-
1067
1063
OFF

FIG. 21C

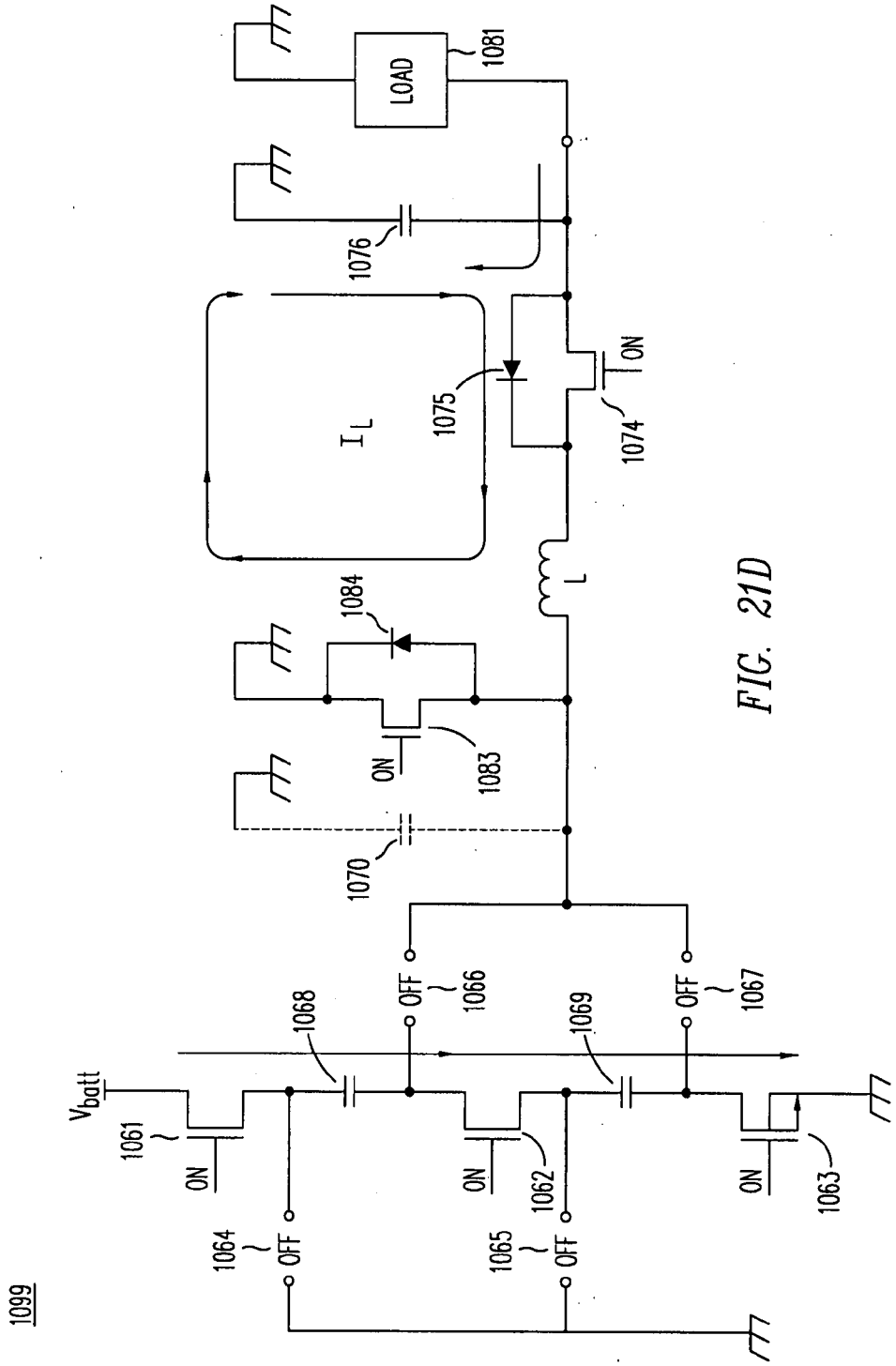
1099
V_{batt}
1061
ON
1064
OFF
1068
OFF
1066
1062
ON
1065
OFF
1069
OFF
1067
1063
ON
1070
1083
ON
1084
I_L
1075
1076
LOAD
1081
1074
ON
L

FIG. 21D

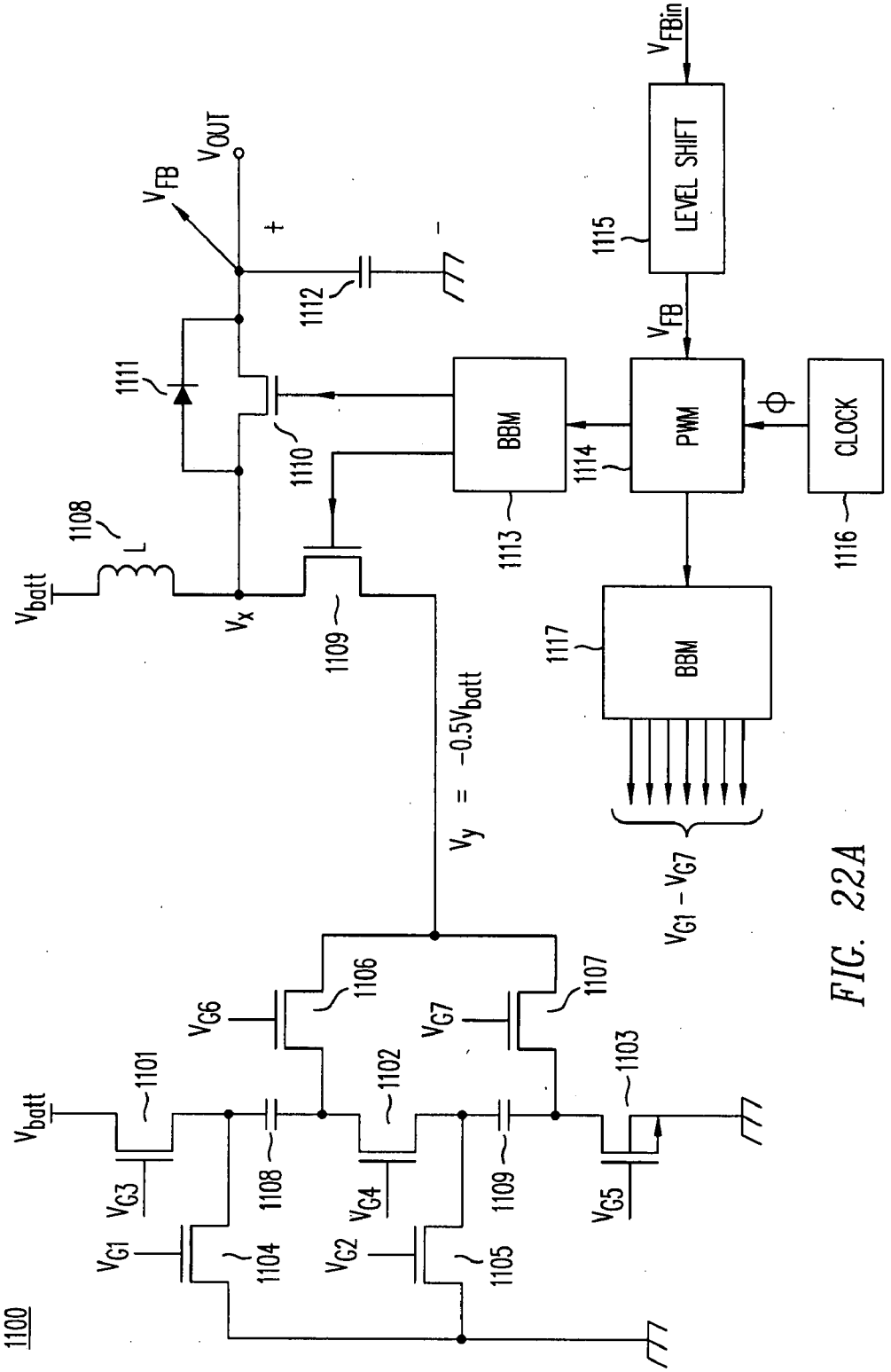
1100
V_{batt}
V_{G1}
V_{G2}
V_{G3}
V_{G4}
V_{G5}
V_{G6}
V_{G7}
1101
1102
1103
1104
1105
1106
1107
1108
1109
V_x
$V_y = -0.5V_{batt}$
1108
L
1110
1111
1112
V_{OUT}
V_{FB}
+
-
1113
BBM
1114
PWM
1115
LEVEL SHIFT
V_{FBin}
V_{FB}
1116
CLOCK
Φ
1117
BBM
$V_{G1} - V_{G7}$

FIG. 22A

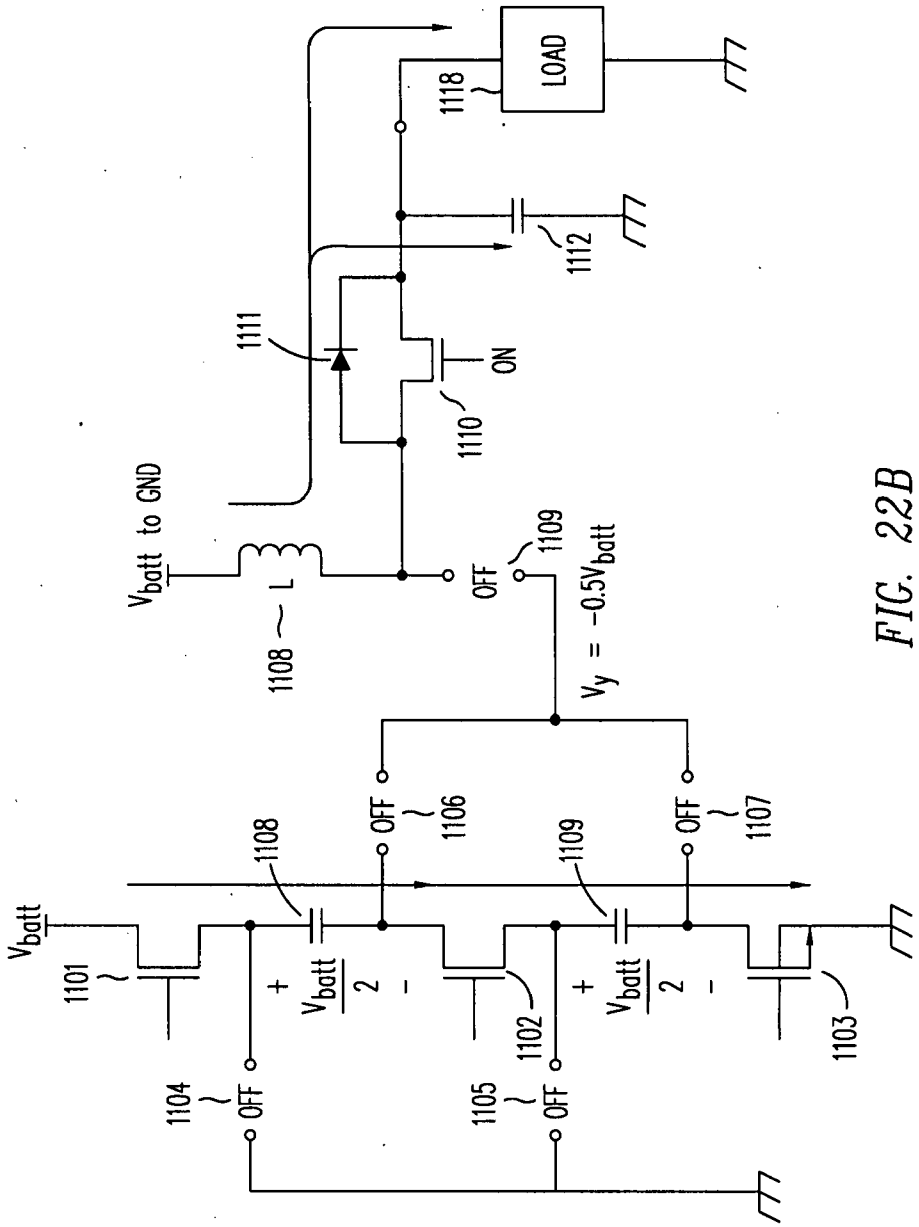
LOAD
1118
1112
1111
ON
1110
V_{batt} to GND
1108
L
OFF
1109
$V_y = -0.5V_{batt}$
OFF
1106
OFF
1107
1108
1109
V_{batt}
1101
+
$\frac{V_{batt}}{2}$
-
1102
+
$\frac{V_{batt}}{2}$
-
1103
1104
OFF
1105
OFF

FIG. 22B

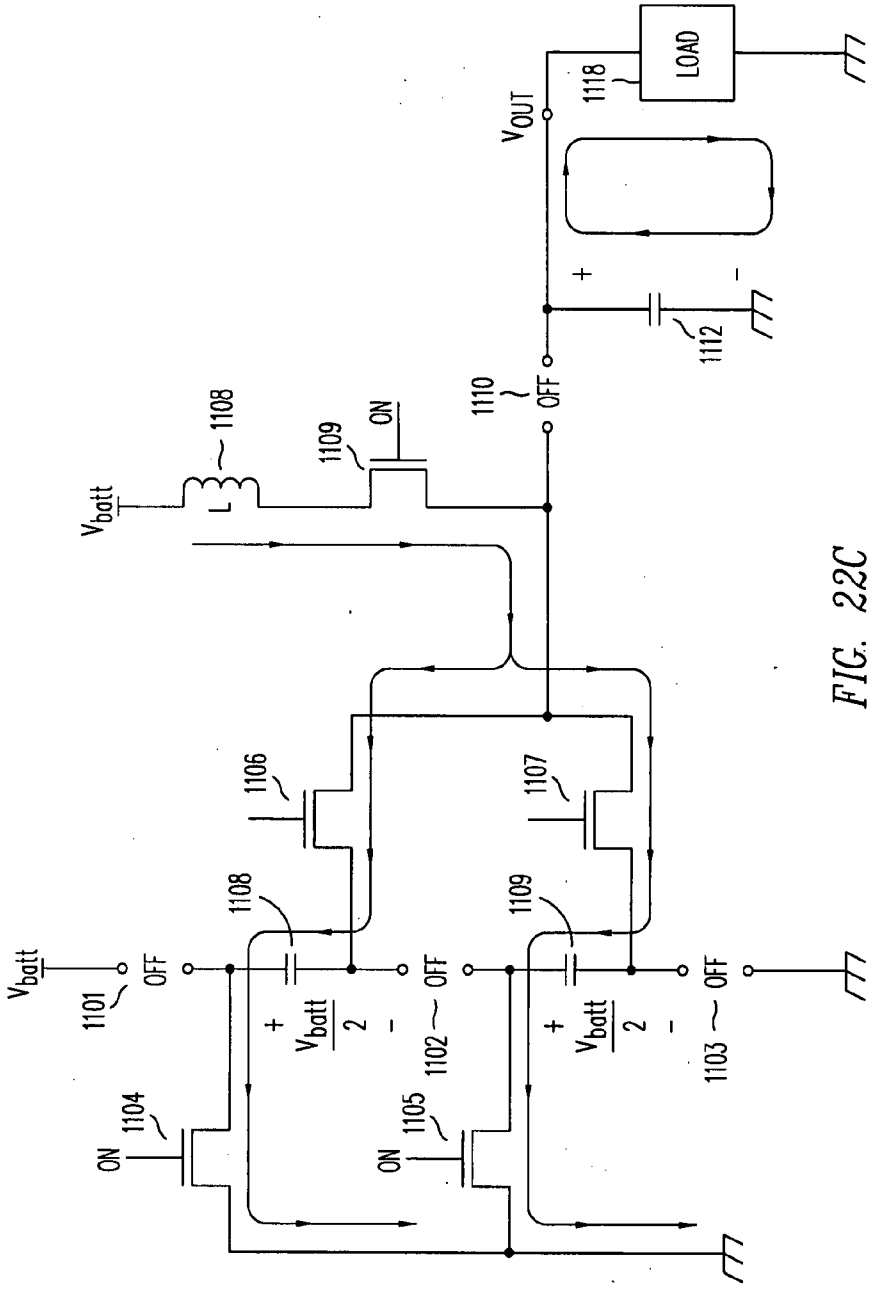

FIG. 22C

NOCO Exhibit 2011
ADC v. NOCO
IPR2024-00671

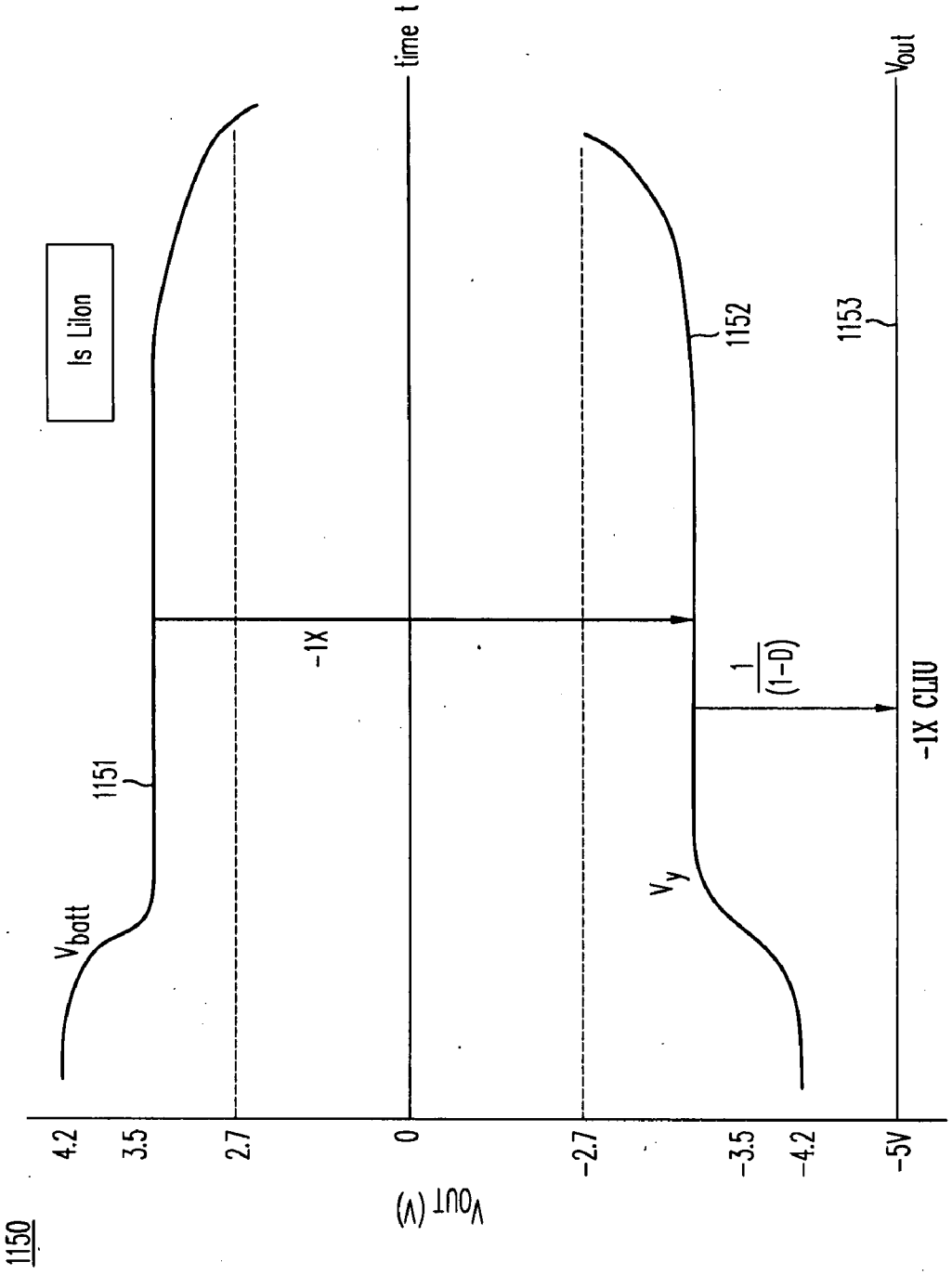
1150
Is LiIon
V_{batt}
1151
-1X
time t
V_y
1152
$\frac{1}{(1-D)}$
-1X CLIU
V_{out}
1153
4.2
3.5
2.7
0
-2.7
-3.5
-4.2
-5V
V_{OUT} (V)

FIG. 23A

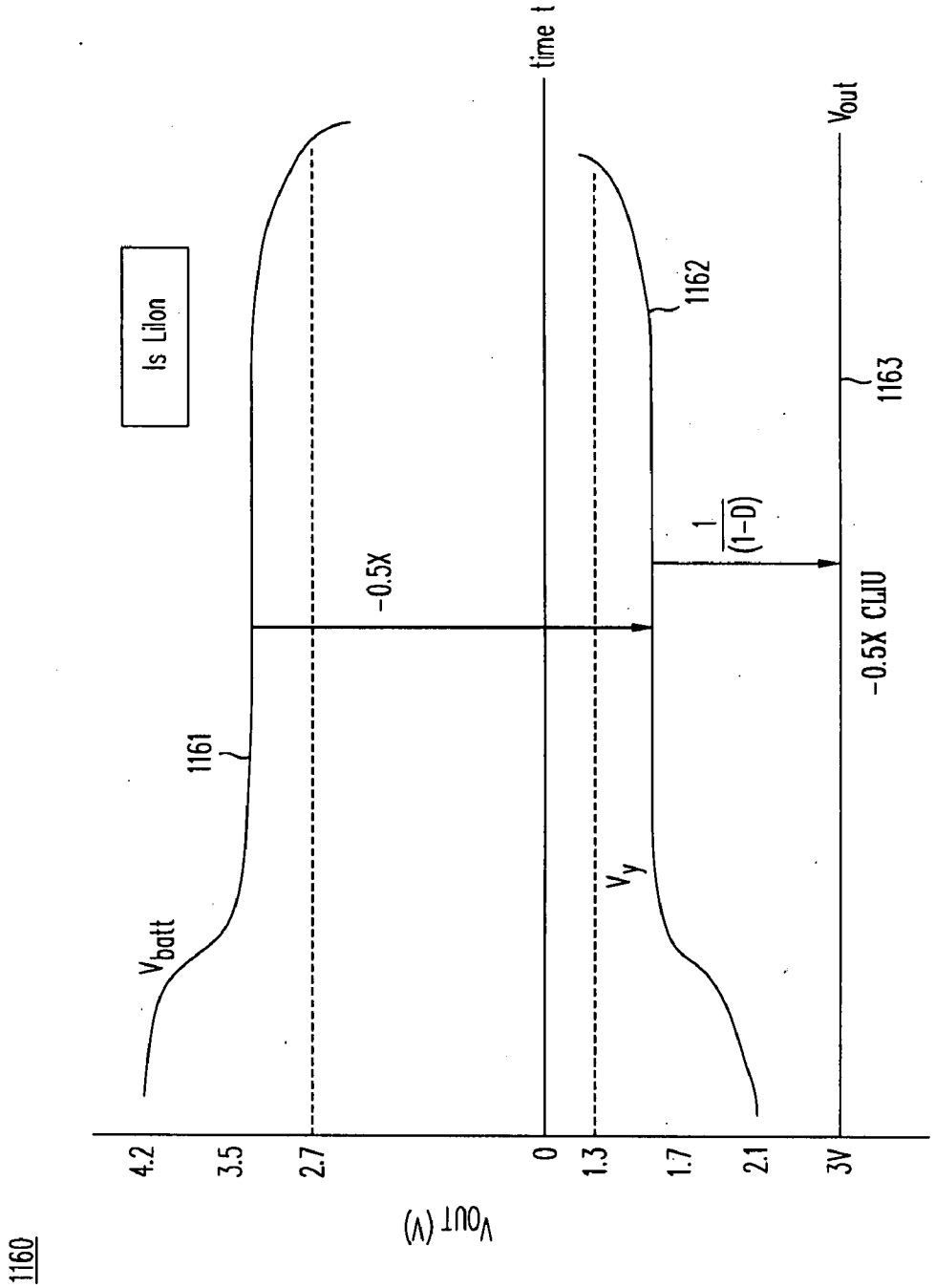

FIG. 23B

NOCO Exhibit 2011
ADC v. NOCO
IPR2024-00671

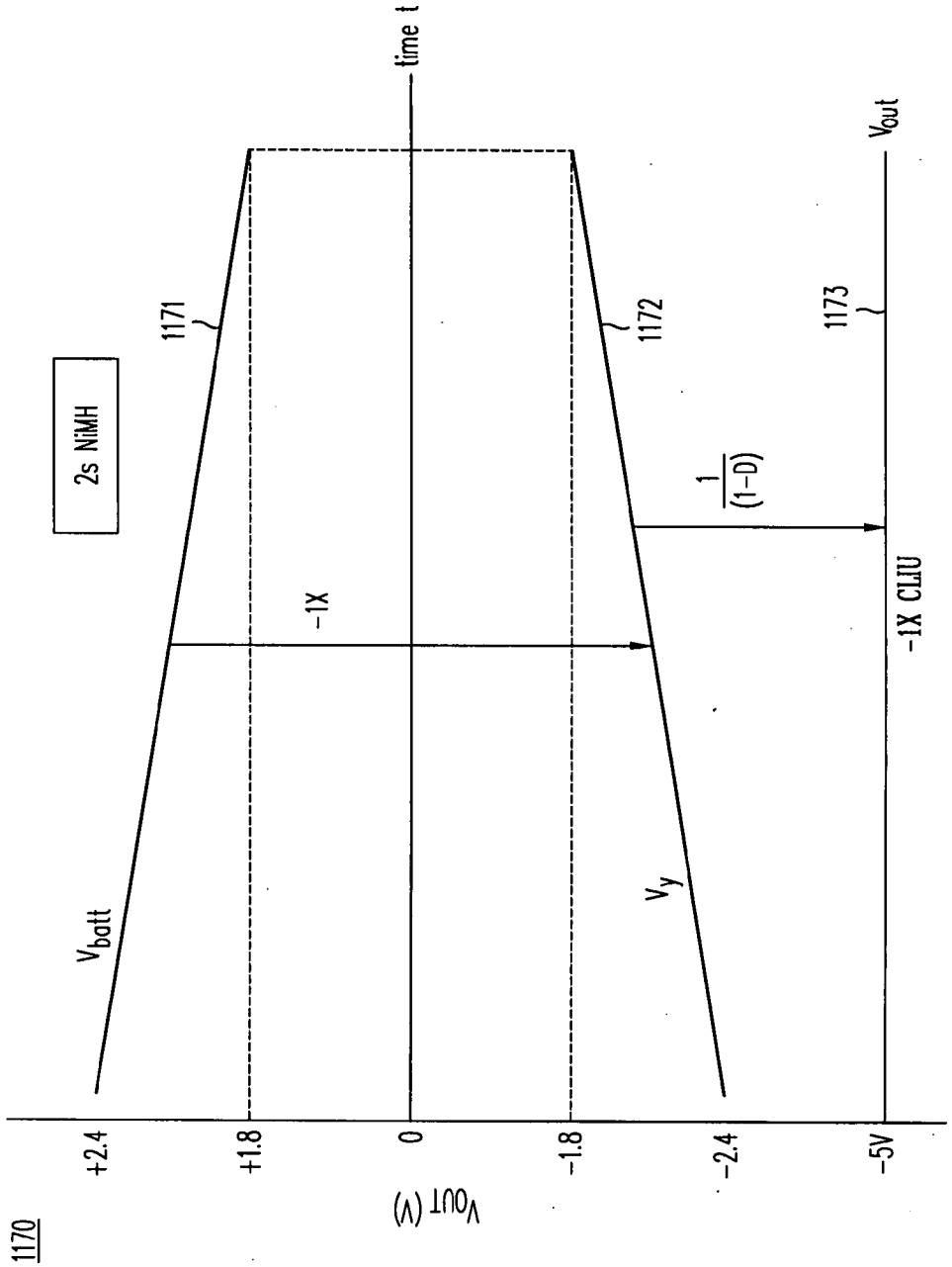
1170
2s NiMH
1171
1172
1173
time t
V_{out}
V_{batt}
V_y
-1X
$\frac{1}{(1-D)}$
-1X CLIU
+2.4
+1.8
0
-1.8
-2.4
-5V
V_{OUT} (V)

FIG. 23C

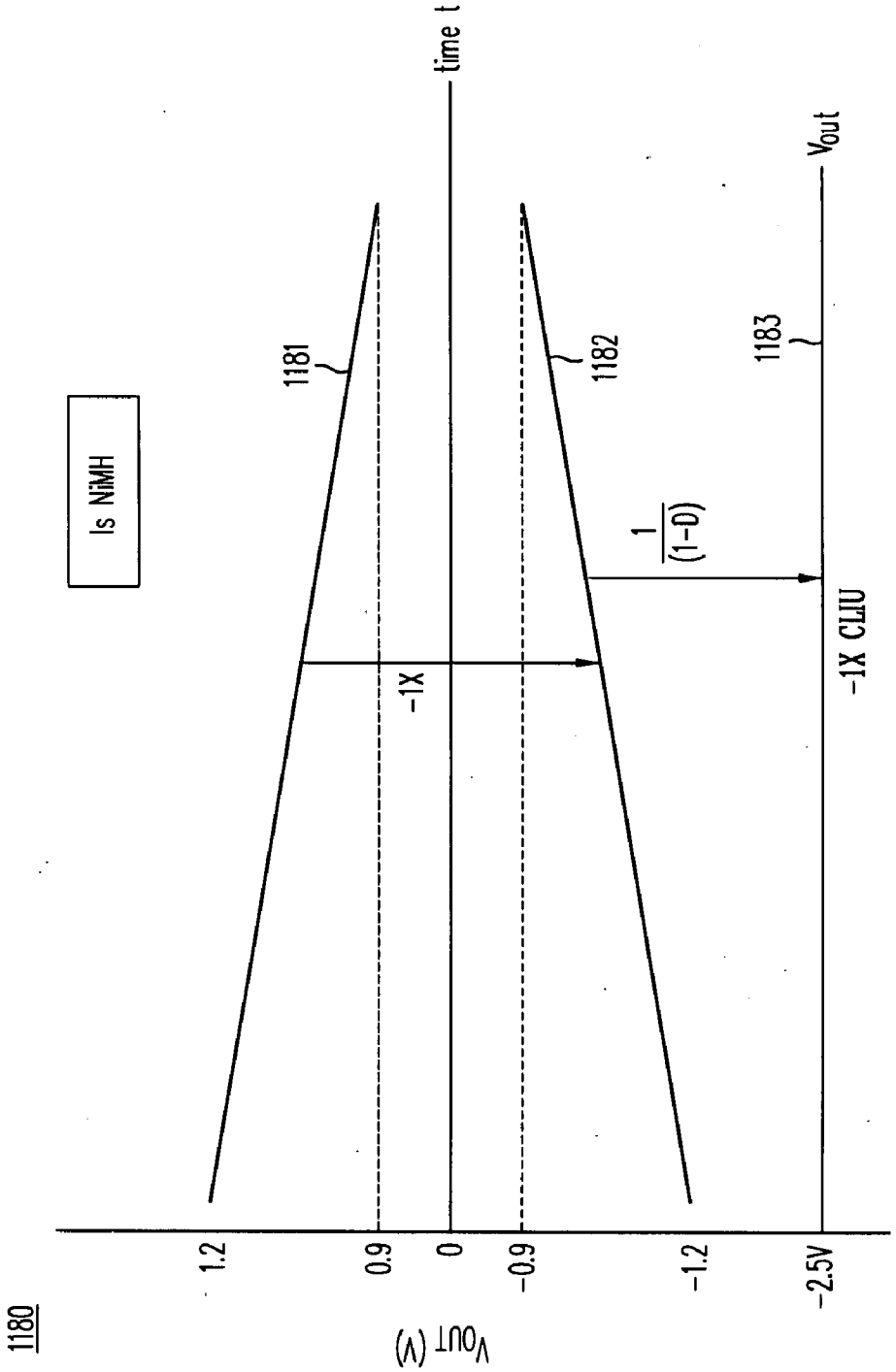
1180
Is NiMH
1181
1182
1183
time t
V_{out}
V_{OUT} (V)
1.2
0.9
0
-0.9
-1.2
-2.5V
-1X
$\frac{1}{(1-D)}$
-1X CLIU

FIG. 23D

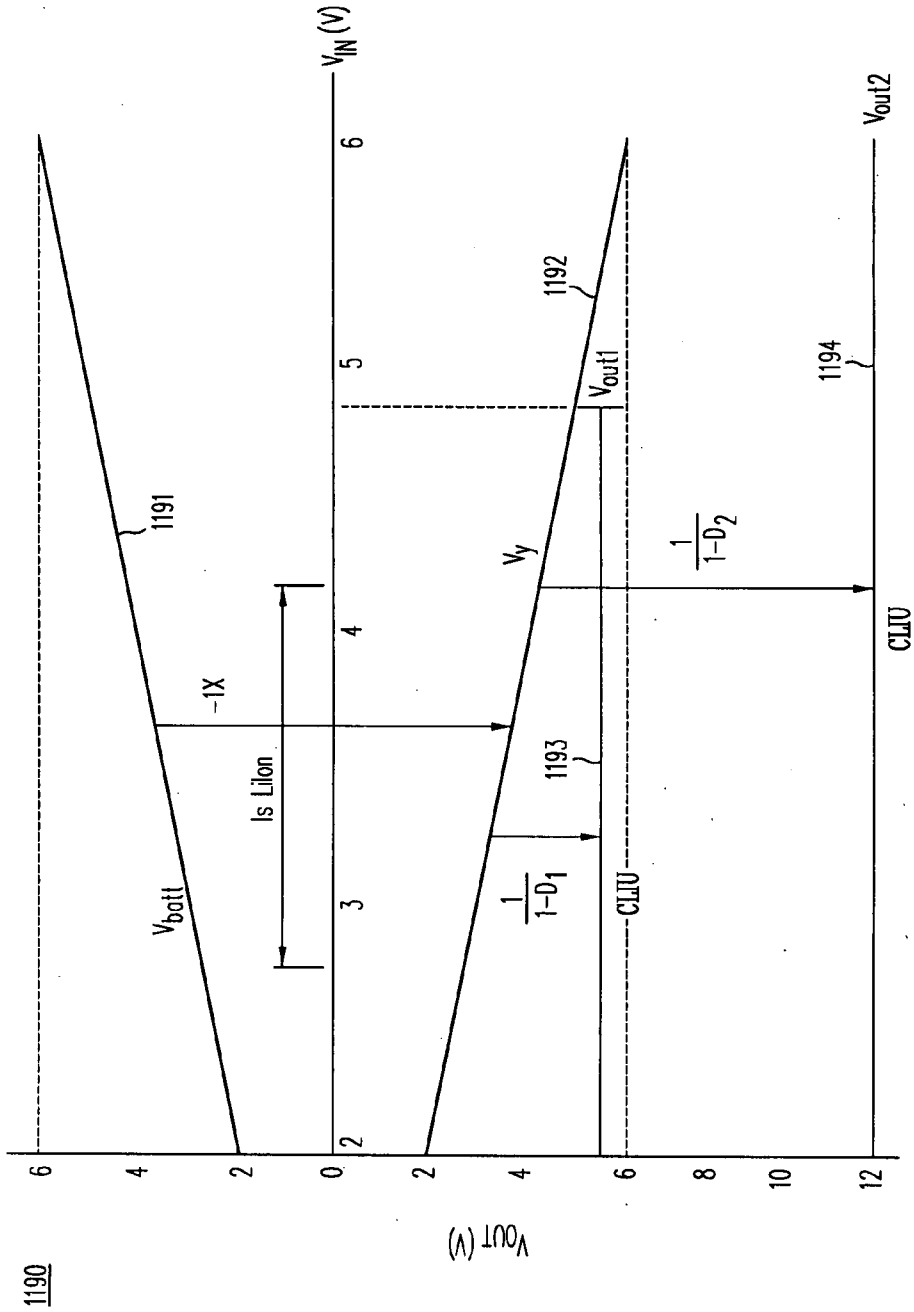

FIG. 23E

NOCO Exhibit 2011
ADC v. NOCO
IPR2024-00671

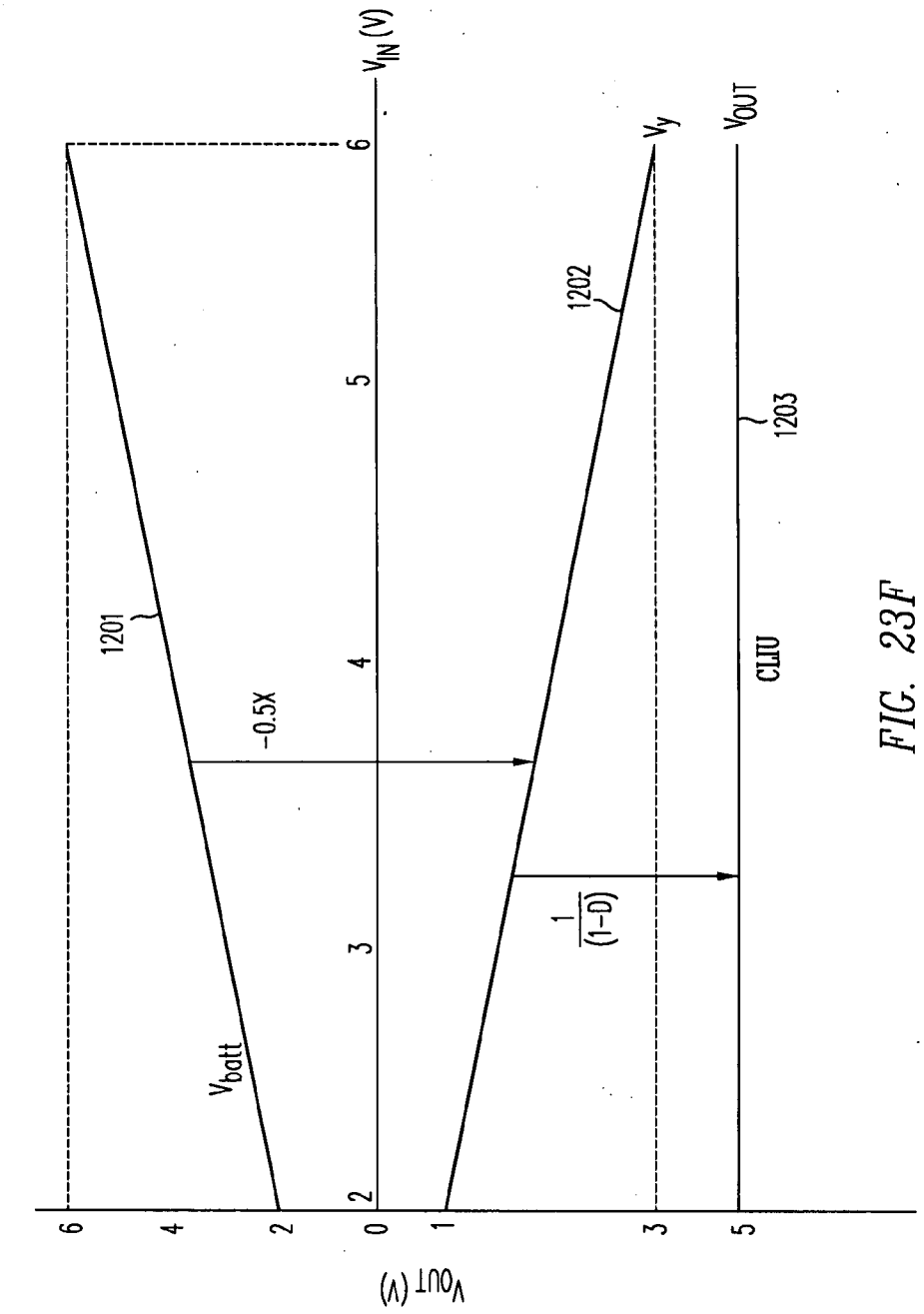
1200
V_{OUT} (V)
6
4
2
0
1
3
5
2
3
4
5
6
V_{IN} (V)
V_{batt}
1201
−0.5X
$\frac{1}{(1-D)}$
1202
V_y
V_{OUT}
1203
CLIU

FIG. 23F

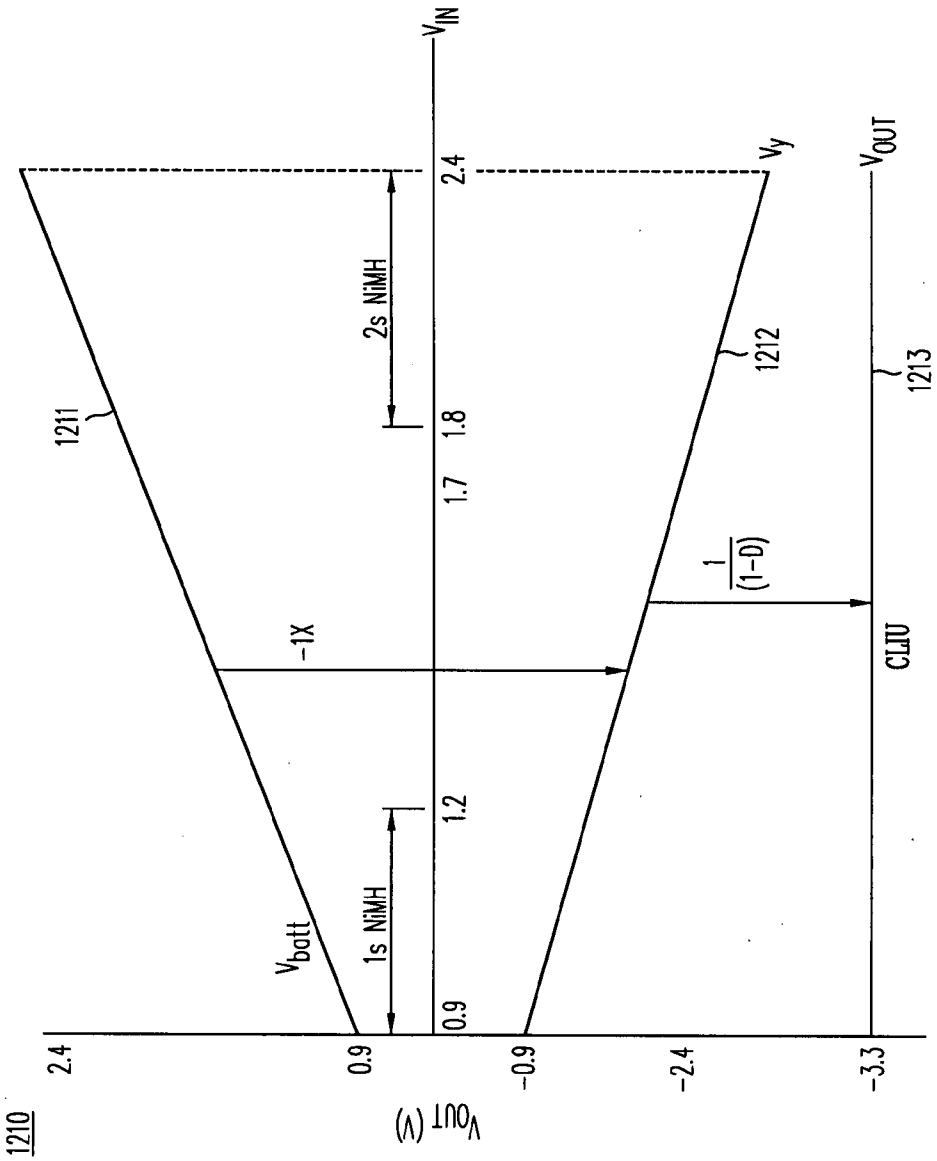

FIG. 23G

NOCO Exhibit 2011
ADC v. NOCO
IPR2024-00671

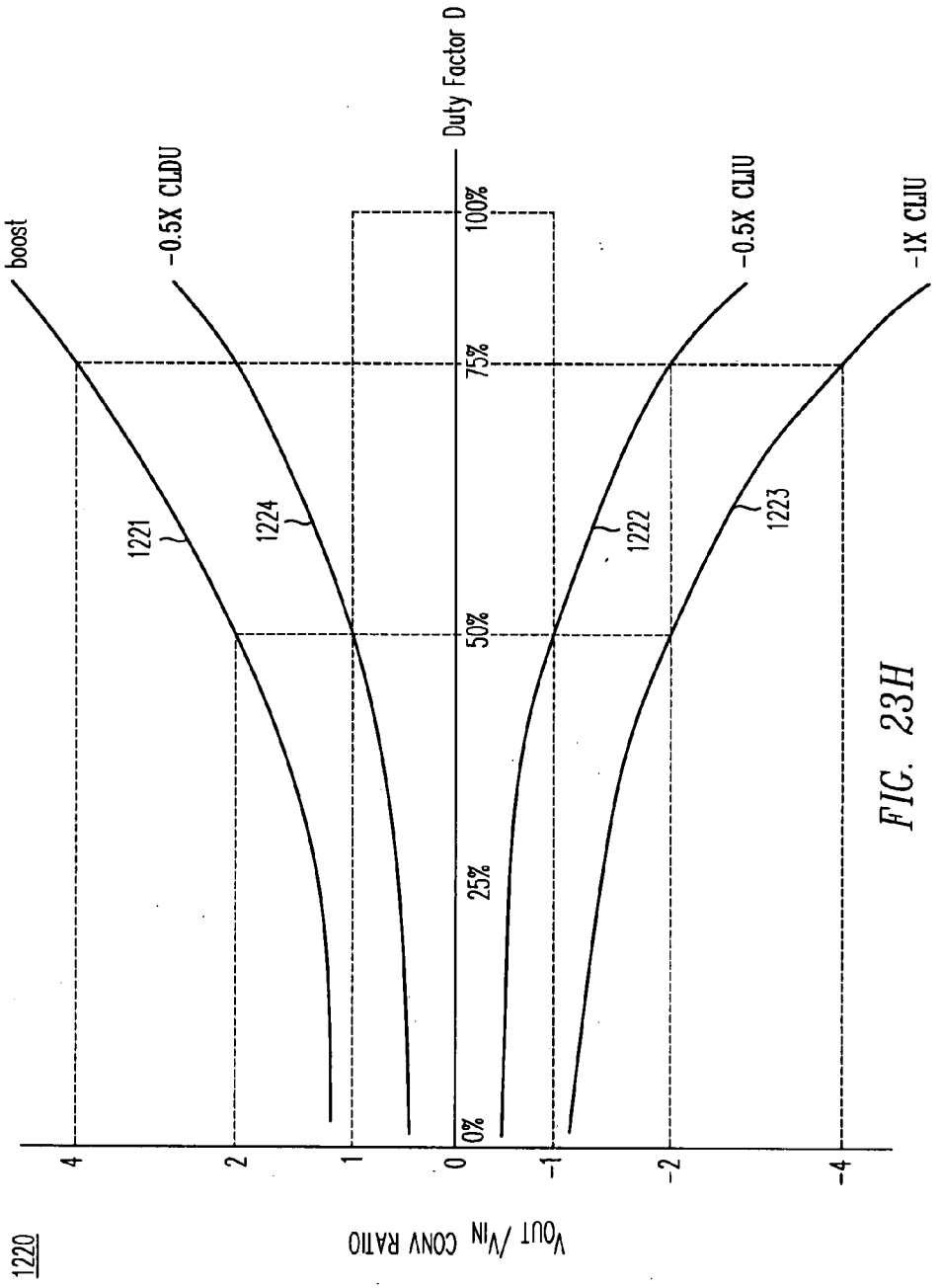

FIG. 23H

NOCO Exhibit 2011
ADC v. NOCO
IPR2024-00671

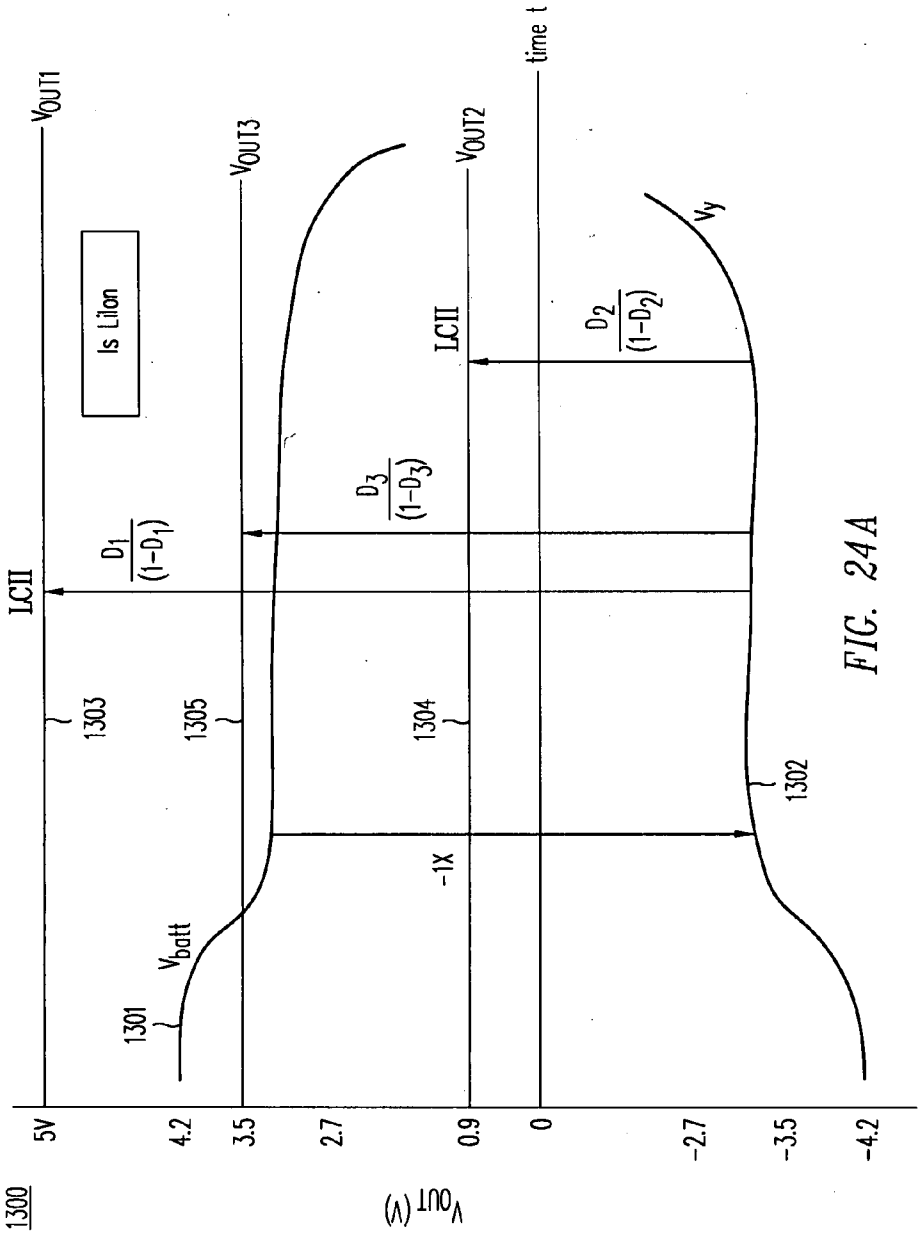
1300
V_{OUT} (V)
5V
4.2
3.5
2.7
0.9
0
-2.7
-3.5
-4.2
V_{OUT1}
V_{OUT3}
V_{OUT2}
time t
Is Lilon
LCII
LCII
$\frac{D_1}{(1-D_1)}$
$\frac{D_3}{(1-D_3)}$
$\frac{D_2}{(1-D_2)}$
V_{batt}
V_y
-1X
1301
1302
1303
1304
1305

FIG. 24A

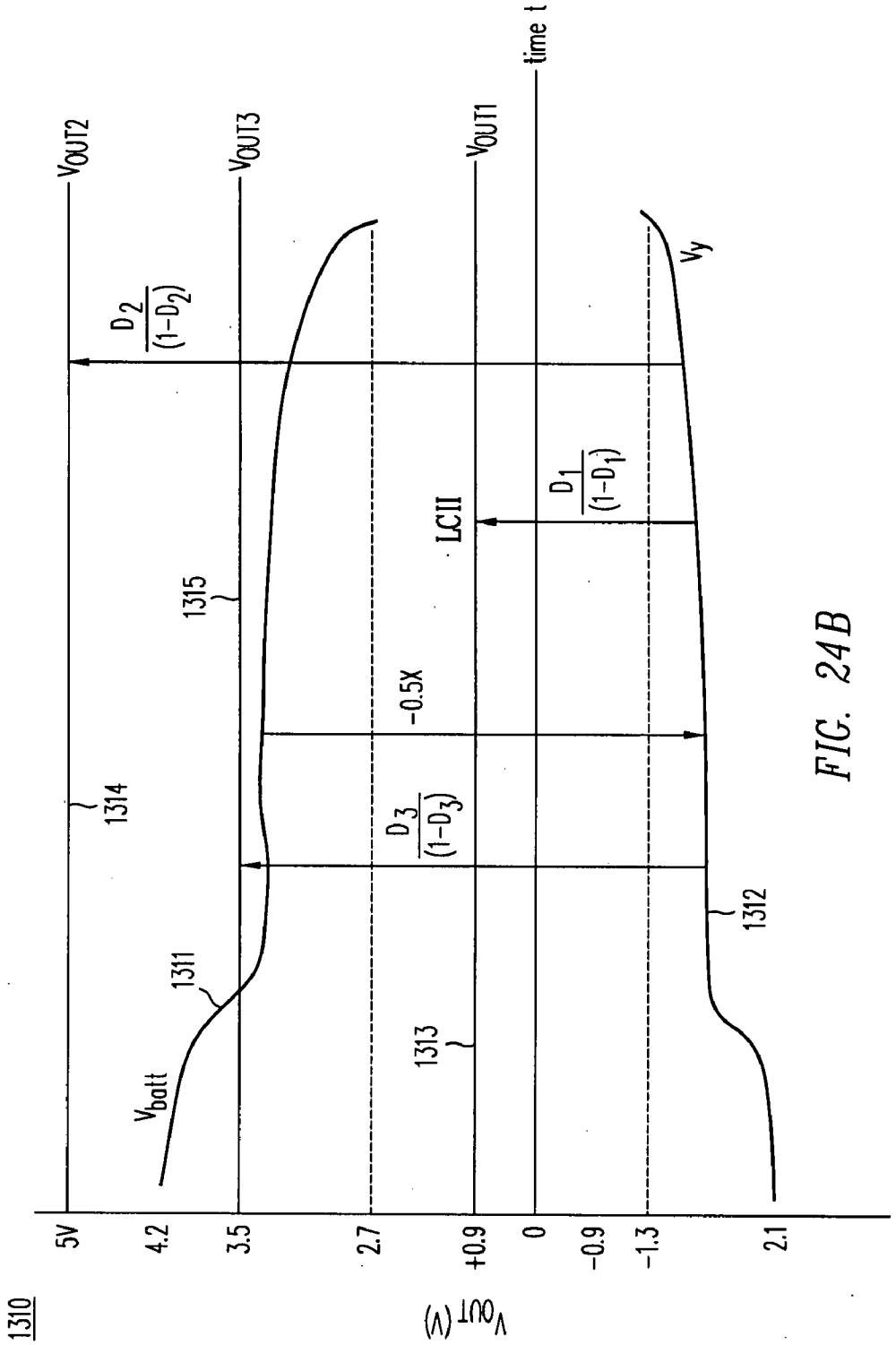
1310
V_{OUT} (V)
5V
4.2
3.5
2.7
+0.9
0
-0.9
-1.3
2.1
V_{OUT2}
V_{OUT3}
V_{OUT1}
time t
V_{batt}
1311
1314
1315
1313
1312
V_y
$\frac{D_2}{(1-D_2)}$
$\frac{D_3}{(1-D_3)}$
$\frac{D_1}{(1-D_1)}$
-0.5X
LCII

FIG. 24B

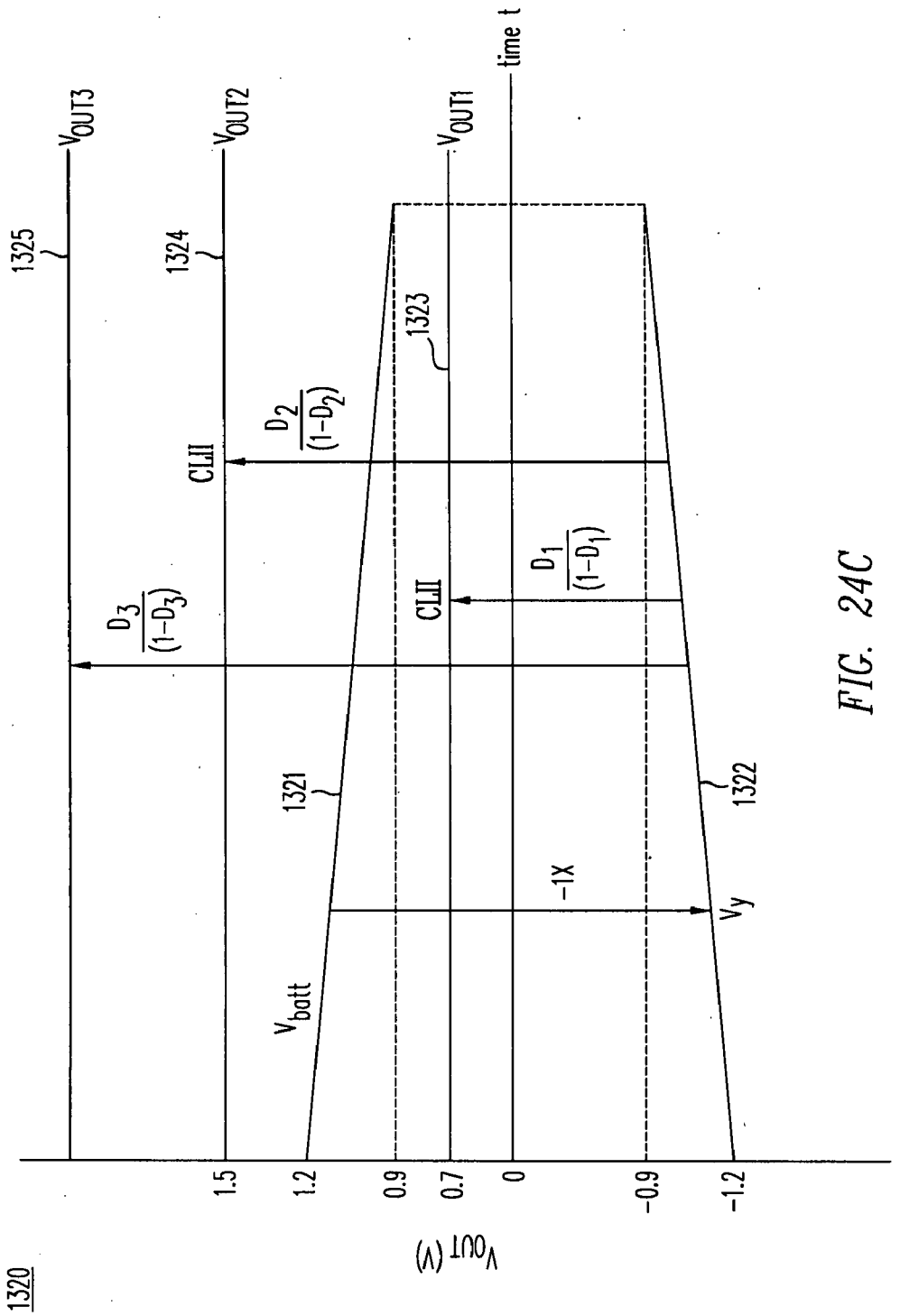
1320
V_{OUT} (V)
1.5
1.2
0.9
0.7
0
-0.9
-1.2
V_{OUT3}
V_{OUT2}
V_{OUT1}
time t
1325
1324
1323
1321
1322
V_{batt}
V_y
-1X
CLII
CLII
$\frac{D_3}{(1-D_3)}$
$\frac{D_2}{(1-D_2)}$
$\frac{D_1}{(1-D_1)}$

FIG. 24C

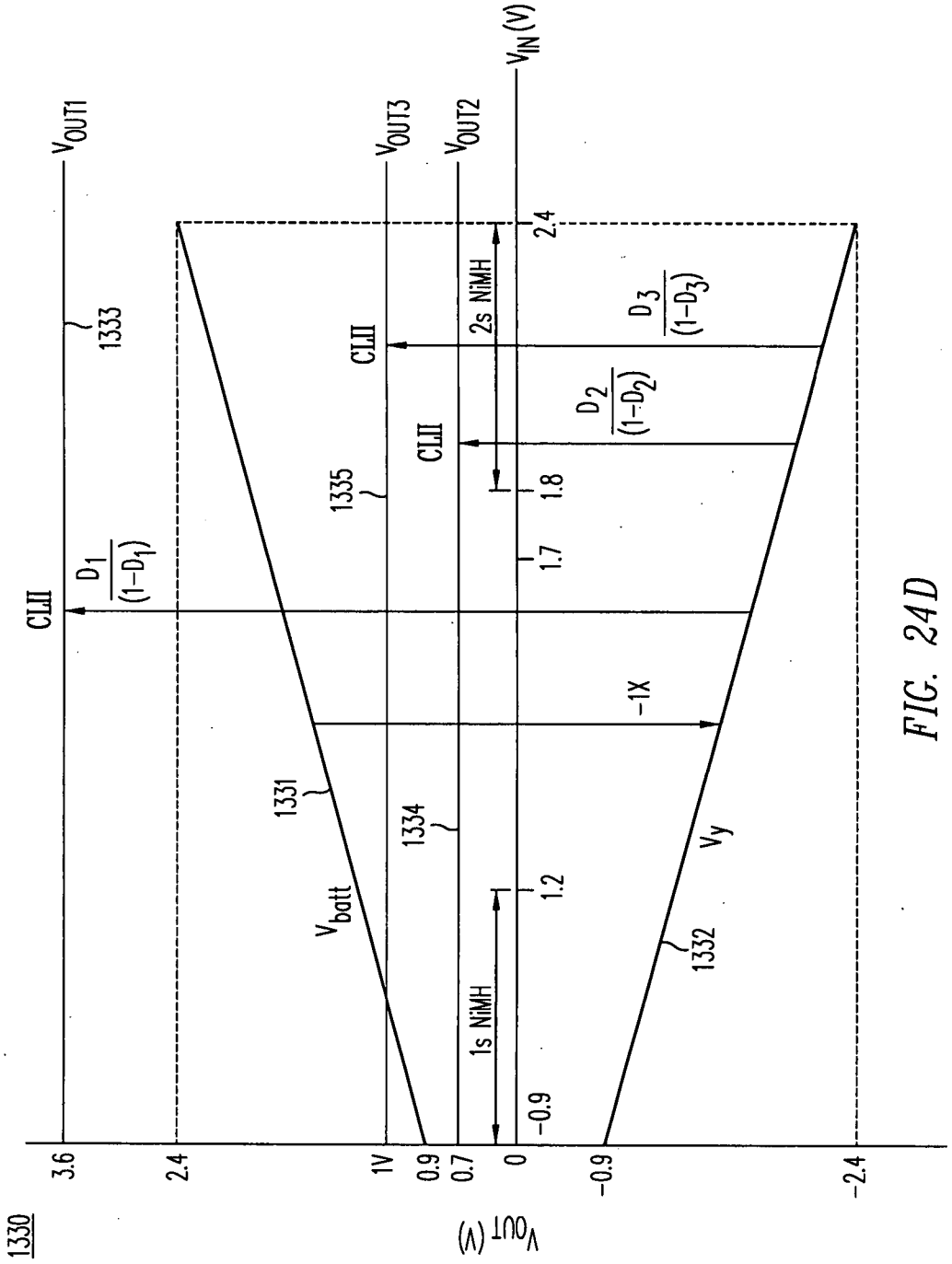
1330
V_{OUT} (V)
3.6
2.4
1V
0.9
0.7
0
-0.9
-2.4
V_{OUT1}
V_{OUT3}
V_{OUT2}
V_{IN} (V)
1333
1335
1331
1334
1332
CLII
CLII
CLII
$\frac{D_1}{(1-D_1)}$
$\frac{D_2}{(1-D_2)}$
$\frac{D_3}{(1-D_3)}$
V_{batt}
V_y
-1X
1s NiMH
2s NiMH
-0.9
1.2
1.7
1.8
2.4

FIG. 24D

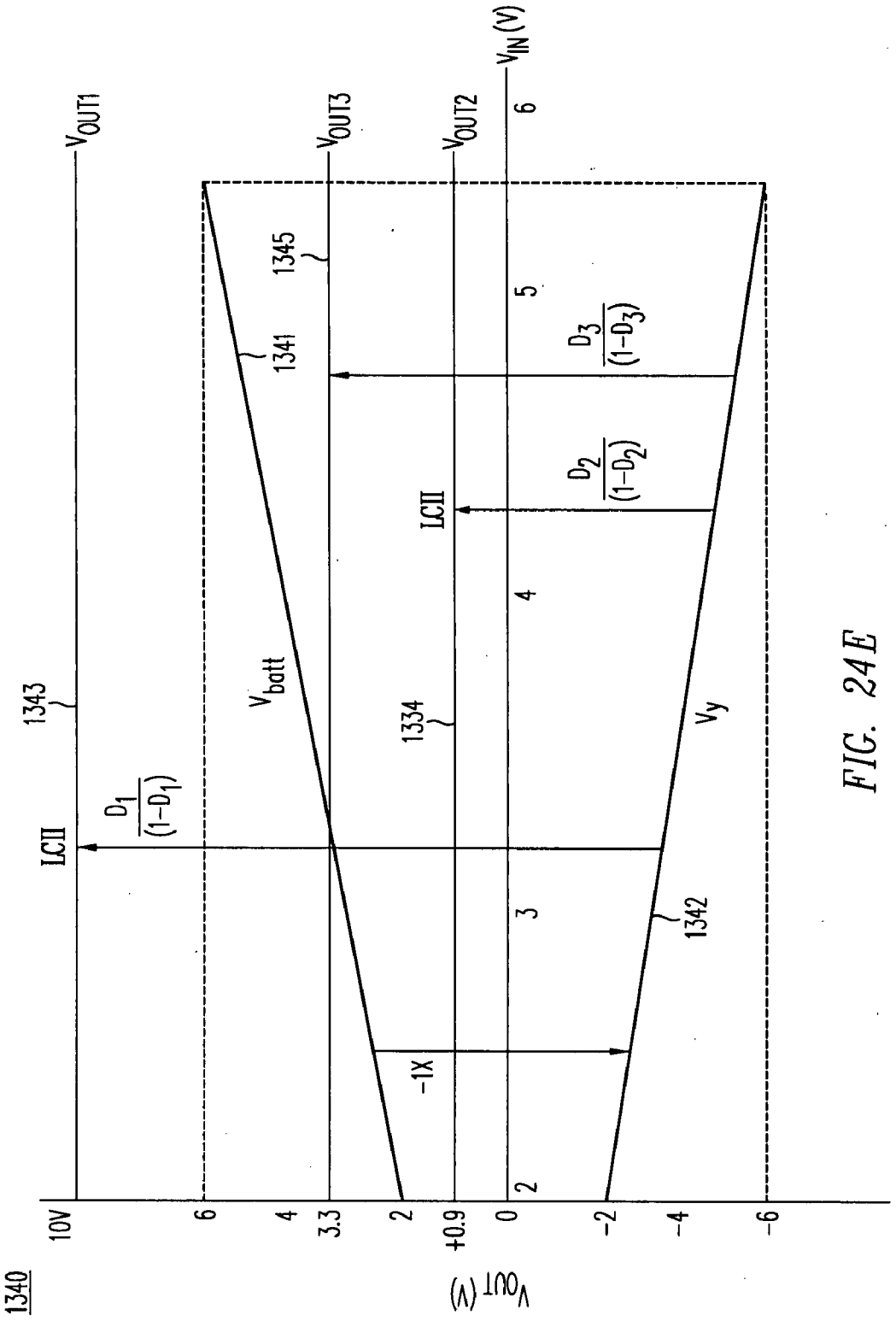

FIG. 24E

NOCO Exhibit 2011
ADC v. NOCO
IPR2024-00671

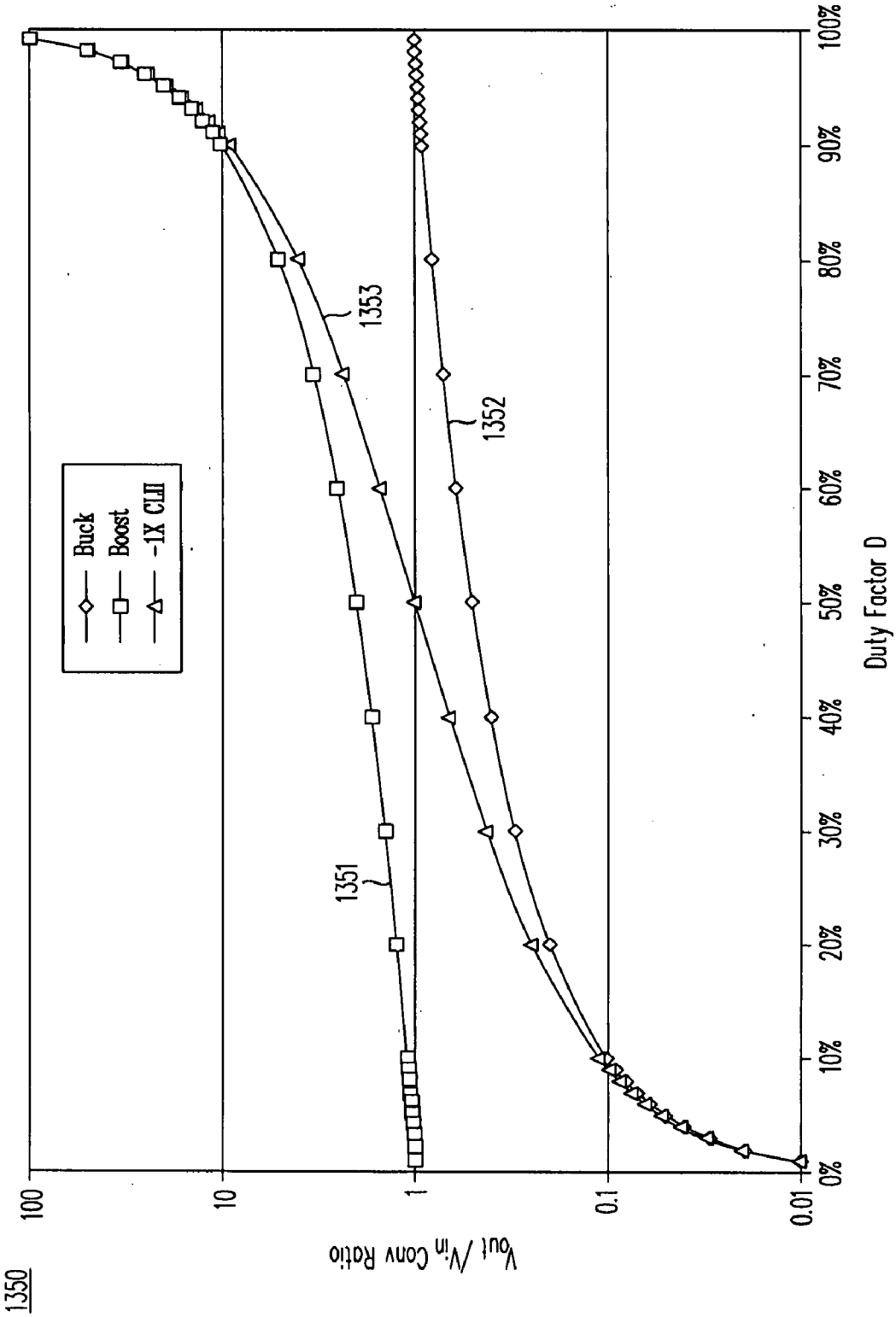

FIG. 24F

NOCO Exhibit 2011
ADC v. NOCO
IPR2024-00671

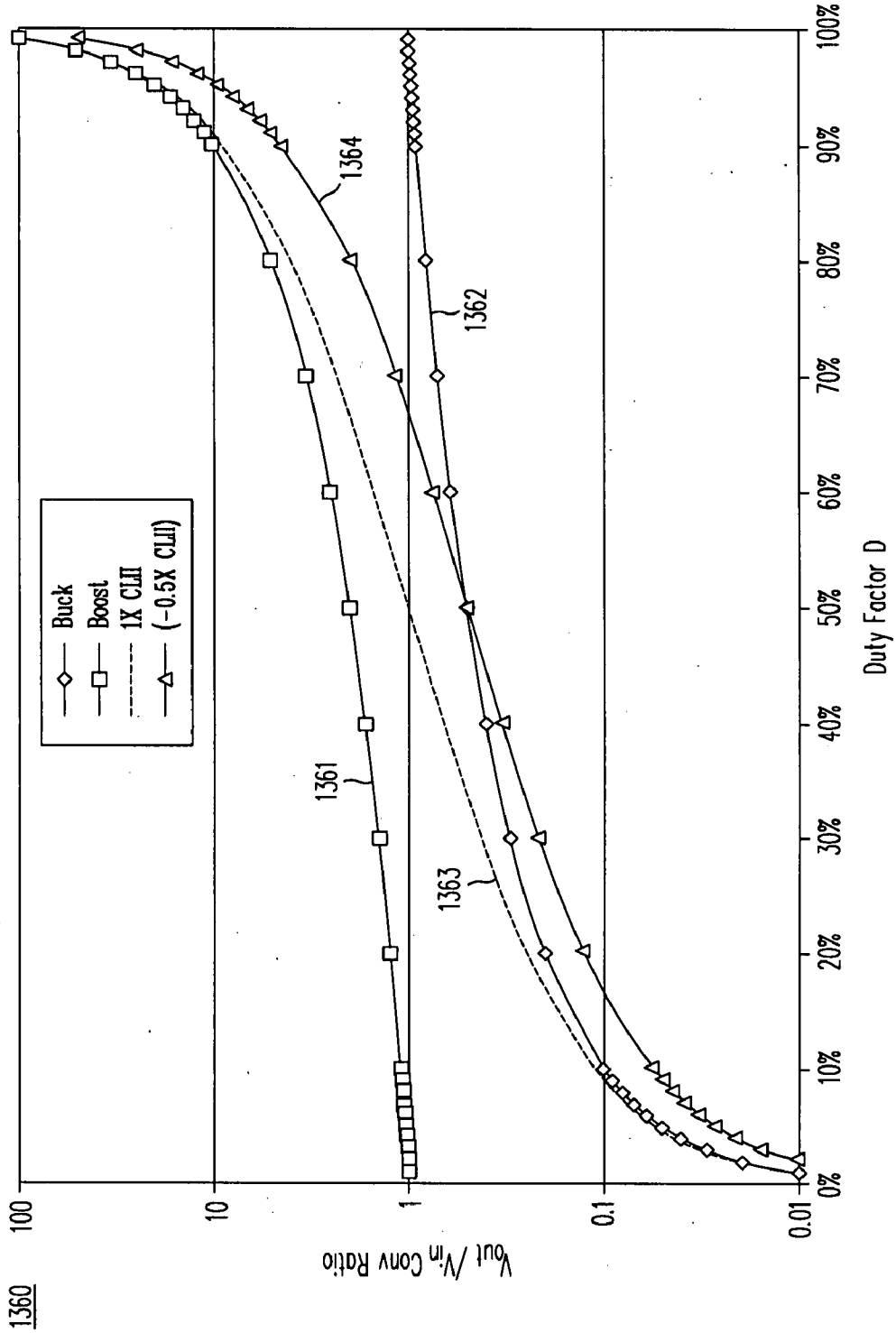
1360
Buck
Boost
1X CLII
(-0.5X CLII)
1361
1362
1363
1364
100
10
1
0.1
0.01
Vout /Vin Conv Ratio
0%
10%
20%
30%
40%
50%
60%
70%
80%
90%
100%
Duty Factor D

FIG. 24G

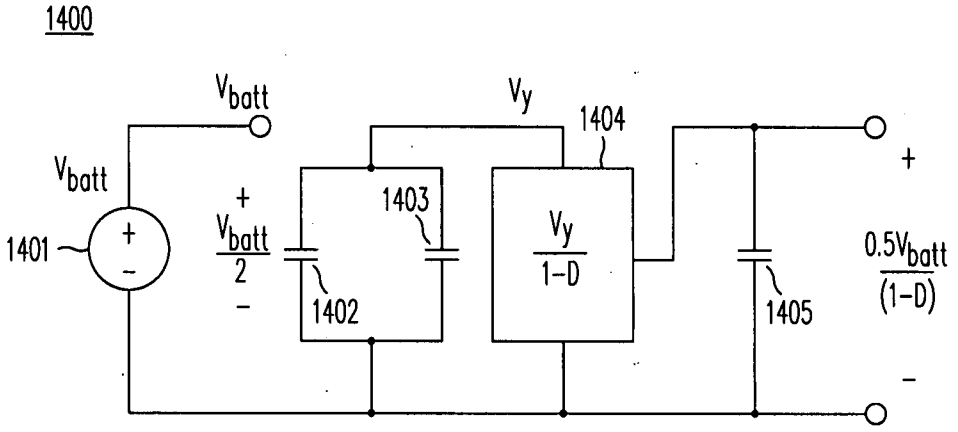

FIG. 25A

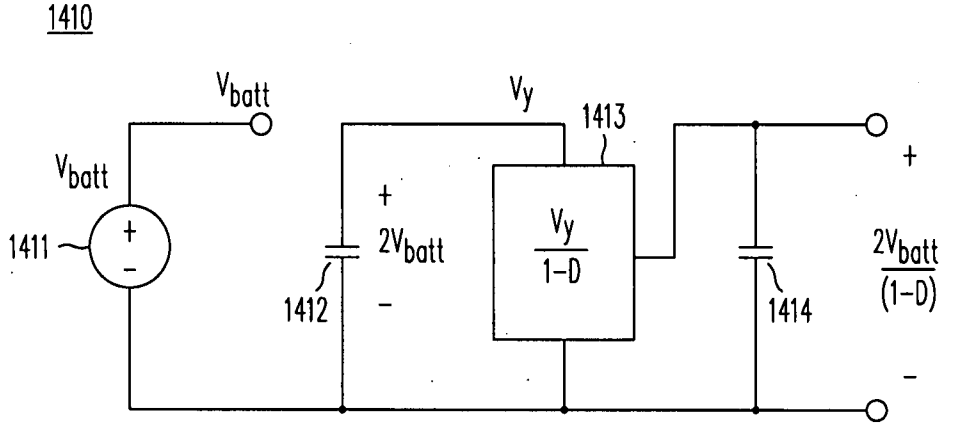

FIG. 25B

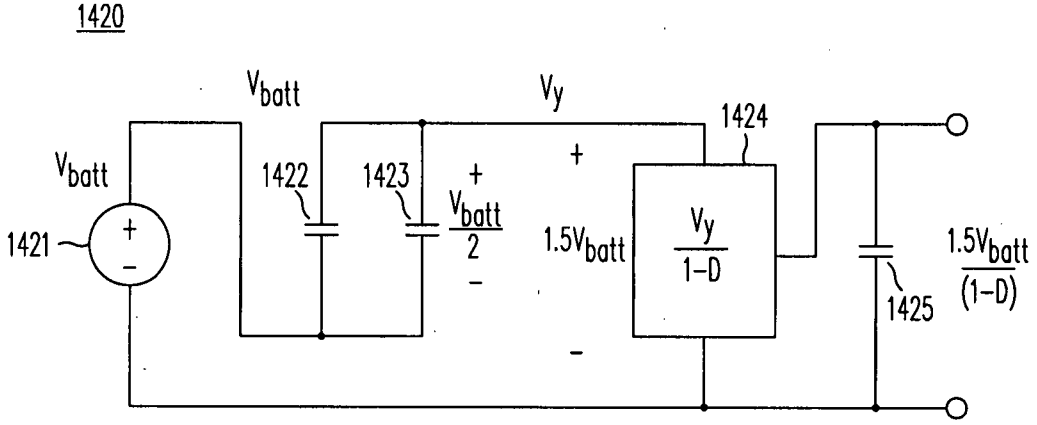

FIG. 25C

NOCO Exhibit 2011
ADC v. NOCO
IPR2024-00671

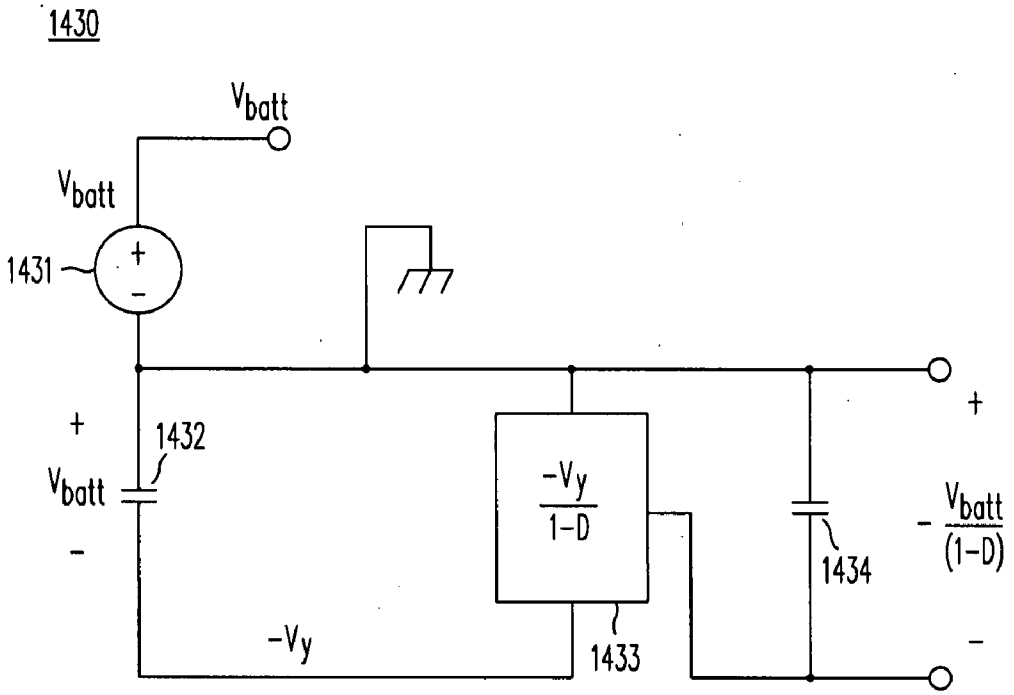

FIG. 25D

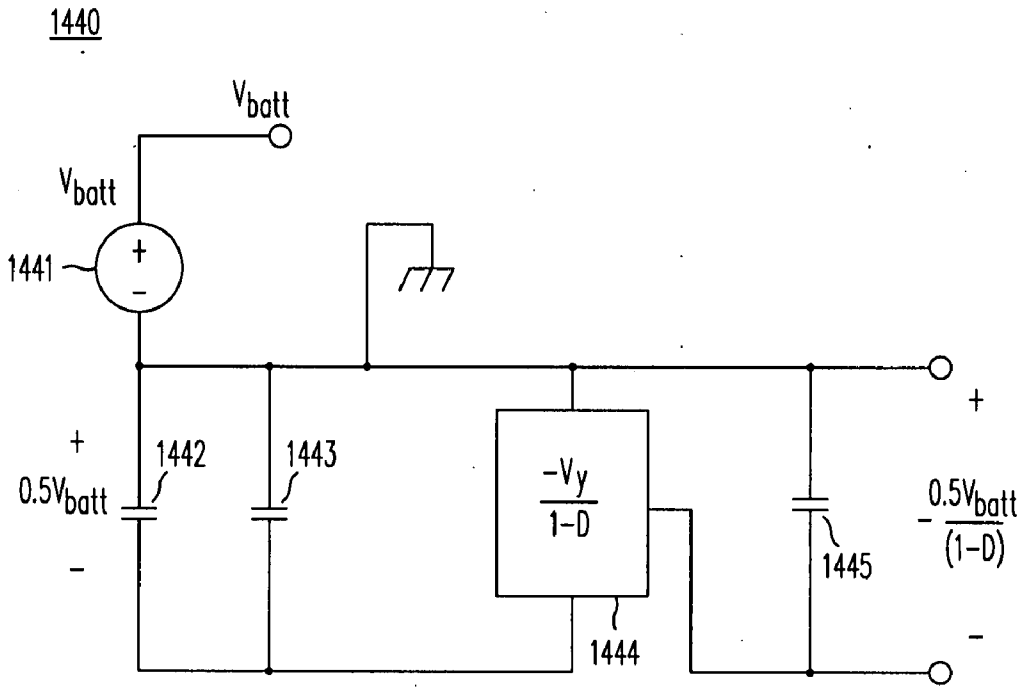

FIG. 25E

NOCO Exhibit 2011
ADC v. NOCO
IPR2024-00671

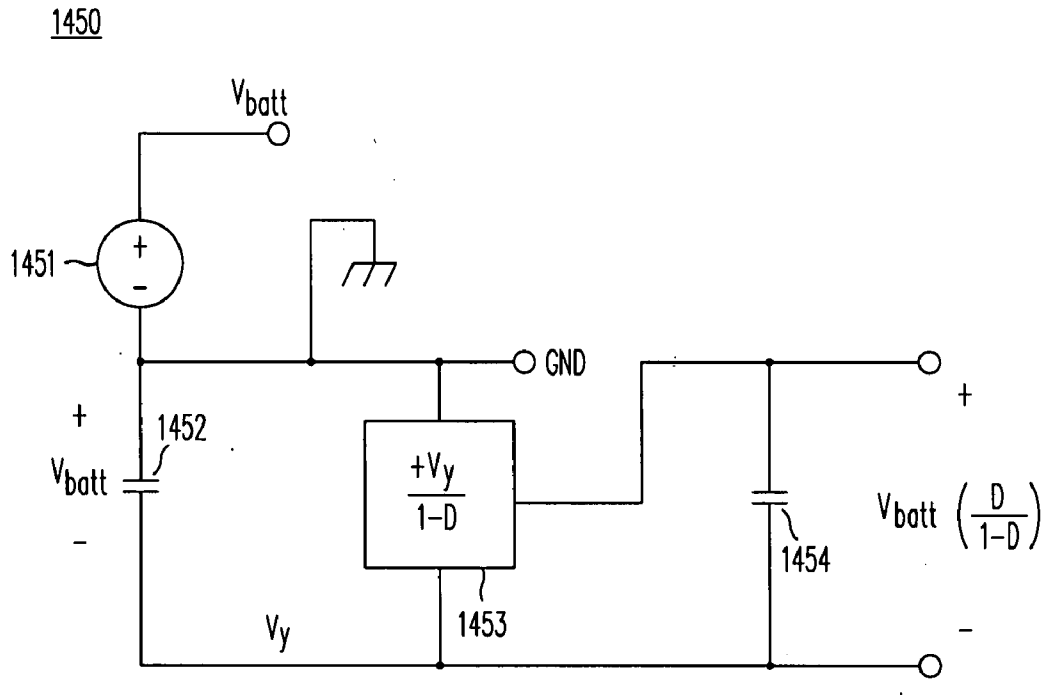

FIG. 25F

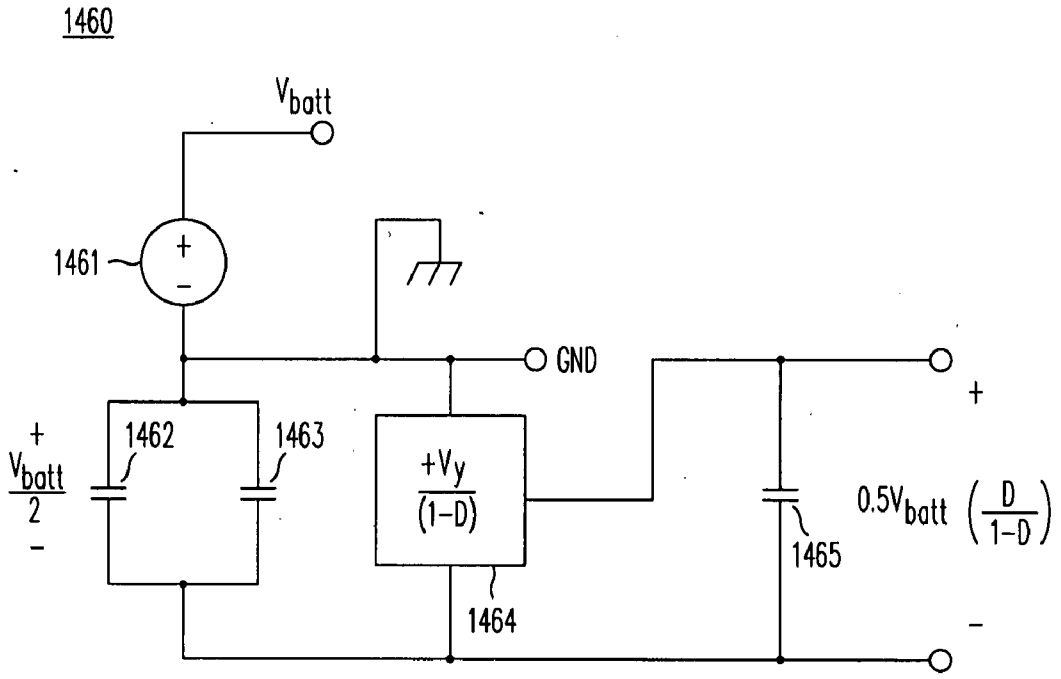

FIG. 25G

HIGH-EFFICIENCY DC/DC VOLTAGE CONVERTER INCLUDING CAPACITIVE SWITCHING PRE-CONVERTER AND UP INDUCTIVE SWITCHING POST-REGULATOR

CROSS-REFERENCE TO RELATED APPLICATIONS

[0001] This application claims the priority of Provisional Applications Nos. 60/877,952 and 60/877,720, both titled "High-Efficiency Down-Up And Related DC/DC Converters" and filed on Dec. 30, 2006, each of which is incorporated herein by reference in its entirety.

FIELD OF THE INVENTION

[0002] This invention pertains to the design, operation and performance of switching power supplies for use in DC/DC conversion and voltage regulation, and to the semiconductor components used in such converters.

BACKGROUND OF THE INVENTION

[0003] Voltage regulation is commonly required to prevent variation in the supply voltage powering various microelectronic components such as digital ICs, semiconductor memories, display modules, hard disk drives, RF circuitry, microprocessors, digital signal processors and analog ICs, especially in battery-powered applications such as cell phones, notebook computers and consumer products.

[0004] Since the battery or DC input voltage of a product often must be stepped-up to a higher DC voltage, or stepped-down to a lower DC voltage, such converters are referred to as DC-to-DC converters. Step-down converters, commonly referred to as "Buck converters," are used whenever a battery's voltage is greater than the desired load voltage. Step-down converters may comprise inductive switching converters, capacitive charge pumps, and linear converters. Conversely, step-up converters, commonly referred to as "boost converters," are needed whenever a battery's voltage is lower than the voltage needed to power its load. Step-up converters may comprise inductive switching converters or capacitive charge pumps.

[0005] Another type of converter may operate as either a step-up or a step-down converter depending on whether the power input to the converter has a voltage above or below its output voltage. Commonly referred to Buck-boost converters, such circuitry is needed whenever a converter's input and output are similar in voltage, where variations in the input voltage preclude the use of a simple boost or Buck converter.

[0006] One example of such an application requiring both step-up and step-down conversion is supplying a regulated 3.3V output from a lithium ion (Lilon) battery. A Lilon battery exhibits a terminal voltage which decays from 4.2V when fully charged to below 3V when discharged. Since the initial battery voltage is above 3.3V and the final battery voltage is below 3.3V, the converter must be able to step-down initially and step-up later.

Inductive Switching Converters

[0007] Of the aforementioned voltage converters, the inductive switching converter can achieve superior performance over the widest range of currents, input voltages and output voltages. The operating principles of the inductive switching converter are described in Application No. [Attorney Docket No. AATI-19-DS-US], titled "High-Efficiency DC/DC Voltage Converter Including Down Inductive Switching Pre-Regulator And Capacitive Switching Post-Converter," filed contemporaneously herewith and incorporated herein by reference. Two examples of non-isolated inductive switching converters, a synchronous Buck step-down converter and synchronous boost step-up converter, are shown in FIGS. **1**A and **1**B.

[0008] An illustrative synchronous Buck converter **1**, shown in FIG. **1**A, comprises a power MOSFET switch **3**, an inductor **5**, a synchronous rectifier power MOSFET **4** with rectifier diode **8**, and a capacitor **6**. Operation of MOSFET **3** is controlled by a pulse-width modulation (PWM) control circuit **2**, driving the gate of MOSFET **3**. The gate drive may vary in polarity and voltage depending on whether MOSFET **3** is N-channel or P-channel. Synchronous rectifier MOSFET **4**, generally an N-channel MOSFET, is driven out of phase with MOSFET **3**, but MOSFET **4** is not necessarily on the entire time when MOSFET **3** is off. In general, MOSFET **4** conducts only during times when diode **8** is conducting.

[0009] While the control circuit controlling the converter's operation is referred to as a "PWM control," implying fixed-frequency variable-pulse-width operation, it may alternatively operate in a variable frequency mode where the clock period is allowed to vary, or alternatively it may alternate between varying and fixed frequency modes depending on load and input conditions.

[0010] The energy delivered from the power source, battery or power input into the DC/DC converter **1** is switched or gated through MOSFET **3**. With its positive terminal connected to the battery or input, MOSFET **3** acts like a "high-side" switch controlling the current in inductor **5**. Diode **7** is a P-N junction parasitic to MOSFET **3**, in parallel to the transistor's drain and source, which remains reverse biased under normal Buck converter operation. Since diode **7** does not carry current under normal operation, it is illustrated by dotted lines.

[0011] By controlling the current in the inductor **5** through the switching and on-time control of MOSFET **3**, the energy stored in the inductor coil's magnetizing field can be adjusted dynamically to control the voltage on output filter capacitor **6**. The output voltage V_{out} is fed back to the input of PWM control circuit **2**, which controls the current I_L in inductor **5** through the repeated switching of MOSFET **3**. The electrical load connected to the converter's output is not shown.

[0012] Driven out of phase with MOSFET **3**, synchronous rectifier MOSFET **4** conducts some portion of the time when MOSFET **3** is off. With its positive terminal connected to the inductor **5**, i.e. to node V_x, and its negative terminal connected the circuit ground, MOSFET **4** acts like a "low-side" switch, shunting the current flowing through diode **8**. Diode **8** is a P-N junction parasitic to synchronous rectifier MOSFET **4**, in parallel to the transistor's drain and source. Diode **8** conducts substantial inductor current only during intervals when both MOSFETs **3** and **4** are turned off.

[0013] One common condition when both MOSFETs **3** and **4** are off occurs during every switching transition to prevent shorting of the input power source to circuit ground. This so-called break-before-make interval prevents shoot through conduction by guaranteeing that both transistors do not conduct simultaneously and short or "crow-bar" the converter's input and power source to ground.

[0014] During this brief break-before-make (BBM) interval, diode **8** in parallel to synchronous rectifier MOSFET **4**

NOCO Exhibit 2011
ADC v. NOCO
IPR2024-00671

must, along with any parasitic capacitance associated with diode **8**, carry the inductor's current I_L. Unwanted noise can occur during the transitions associated BBM operation.

[0015] If we define the converter's duty factor D as the time during which energy flows from the battery or power source into the DC/DC converter, i.e. the time that MOSFET switch **3** is on, then the output to input voltage ratio of the Buck converter **1** is proportionate to its duty factor, i.e.

$$\frac{V_{out}}{V_{in}} = D \equiv \frac{t_{sw}}{T}$$

where t_{sw} is the time during which MOSFET **3** is turned on and T is the duration of the total clock cycle.

[0016] This relationship for a Buck or synchronous Buck converter is illustrated by curve **17** in graph **15** of FIG. **2**A. Notice the Buck converter cannot smoothly reach a zero or unity transfer characteristic without exhibiting some discontinuities **19** and **21** at the extremes of the duty factor D. This phenomenon is due to switching delays in the power MOSFET switch and its control and gate drive circuitry.

[0017] As long as the Buck converter's power MOSFET is still switching, t_{sw} is limited to some portion of the clock period T, e.g. 5%<D<95%, essentially due to turn-on and turn-off delay within the MOSFETs **3** and **4** and their control loop. For example at 95% duty factor and a 3 MHz clock, the off time for the high-side MOSFET **3** is only five percent of the 333 nsec period, or just 16 nsec. This means the high side MOSFET **3** must turn off and back in only 16 nsec—too rapidly to regulate over a 95% output-to-input conversion ratio. The minimum off time problem impacts either synchronous or non-synchronous Buck converters. The problem is, however, further exacerbated in synchronous DC/DC converter **1**, since no time remains for the synchronous rectifier MOSFET **4** to turn on and then off again and still exhibit BBM operation.

[0018] Referring again to curve **17** in FIG. **2**A, above some maximum duty factor D_{max}, there is not adequate time to maintain switching operation and the converter must jump from D_{max} to a 100% duty factor, as shown by discontinuity **21**. Above D_{max}, the converter turns MOSFET **3** on and leaves it on for the entire clock period T. The abrupt transition **21** causes a glitch in the output voltage of Buck converter **1**. Moreover, at a 100% duty factor, $V_{out}=V_{in}$ as shown by line **16**, and all regulation is lost as long as the switching is halted.

[0019] Synchronous boost converter **10** shown in FIG. **1**B includes a low-side power MOSFET **12**, a battery connected inductor **13**, an output capacitor **15**, and a "floating" synchronous rectifier MOSFET **14** with parallel rectifier diode **16**. The gates of the MOSFETs **12** and **14** are driven by break-before-make circuitry (not shown) and controlled by PWM controller **11** in response to voltage feedback V_{FB} from the output of converter **10**, present across output capacitor **15**. BBM operation is needed to prevent shorting the terminals of output capacitor **15**.

[0020] The synchronous rectifier MOSFET **14**, which may be an N-channel or P-channel MOSFET, is considered floating in the sense that its source and drain terminals are not permanently connected to any supply rail, i.e. to ground or V_{batt}. Diode **16** is a P-N diode intrinsic to synchronous rectifier MOSFET **14**, regardless whether synchronous rectifier MOSFET **14** is a P-channel or an N-channel device. A Schottky diode may be included in parallel with MOSFET **16** but with series inductance may not operate fast enough to divert current from forward biasing intrinsic diode **16**. Diode **17**, which is a P-N junction diode intrinsic to N-channel low-side MOSFET **12**, remains reverse biased under normal boost converter operation. Since diode **17** does not conduct under normal boost operation, it is shown with dotted lines.

[0021] If we again define the duty factor D of boost converter **10** as the time during which energy flows from the battery or power source into the converter, i.e. during the time that low-side MOSFET **12** is on and inductor **13** is being magnetized, then the output to input voltage ratio of a boost converter is proportionate to the inverse of 1 minus its duty factor, i.e.

$$\frac{V_{out}}{V_{in}} = \frac{1}{1-D} \equiv \frac{1}{1 = t_{sw}/T}$$

where t_{sw} is the time during which MOSFET **12** is turned on and T is the duration of the total clock cycle.

[0022] This relationship for a boost or synchronous boost converter is illustrated by curve **18** in FIG. **2**A. Notice that the boost converter cannot smoothly reach a unity transfer characteristic without exhibiting some discontinuity at the extremes of D. This phenomenon occurs due to switching delays in the power MOSFET **12** and its control and gate drive circuitry.

[0023] As long as power MOSFET **12** is still switching, t_{sw} is limited to some portion of the clock period T, e.g. 5%<D<95%, essentially due to turn-on and turn-off delay within the MOSFET **12** and its control loop. For example at 5% duty factor and a 3 MHz clock, the off time for the low-side MOSFET **12** is only five percent of the 333 nsec period, or just 16 nsec. This means the low side MOSFET **12** must turn on and back off in only 16 nsec—too rapidly to regulate below a 5% output-to-input conversion ratio. This minimum on time problem impacts either synchronous or non-synchronous boost converters.

[0024] Referring again to curve **18** in FIG. **2**A, below some minimum duty factor D_{min}, there is not adequate time to maintain switching operation and the converter **10** must jump from D_{min} to a 0% duty factor, as shown by discontinuity **20**. Below D_{min}, the converter turns on the synchronous rectifier MOSFET **14** and leaves it on for the entire clock period T. The abrupt transition **20** causes a glitch in the output voltage of boost converter **10**. Moreover, at a 100% duty factor, $V_{out}=V_{in}$ as shown by line **16**, all regulation is lost as long as the switching is halted.

[0025] So for both synchronous Buck converter **1** and synchronous boost converter **10**, operation near a unity transfer characteristic where $V_{out}\approx V_{in}$, shown by line **16** in FIG. **2**A, is problematic.

[0026] The efficiency η of a DC/DC converter can be given by:

$$\eta = \frac{P_{out}}{P_{in}} = \frac{I_{out} \cdot V_{out}}{I_{in} \cdot V_{in}}$$

[0027] An analysis of inductive switching converter efficiencies is described in the above-referenced Application No. [Attorney Docket No. AATI-19-DS-US].

NOCO Exhibit 2011
ADC v. NOCO
IPR2024-00671

[0028] Graph **25** of FIG. **2**B illustrates examples of typical conversion efficiencies for synchronous Buck and synchronous boost converters as a function of the converter's voltage conversion ratio V_{out}/V_{in}. As shown, line **26** illustrates the unity conversion condition where $V_{out}=V_{in}$. Conversion ratios less than unity, on the left side of line **26** in graph **25**, represent step-down conversion. Efficiency curve **27** represents an example of a Buck converter performing step-down voltage conversion. Conversion ratios greater than unity, on the right side of line **26** in graph **25** represent step-up conversion. Efficiency curve **28** represents an example of a boost converter performing step-up voltage conversion.

[0029] In general boost converters exhibit lower efficiencies than Buck converters for comparable load currents, as illustrated by curves **27** and **28**. This disparity is primarily due to the fact that boost converters exhibit higher peak currents than Buck converters. This problem is further accentuated for high V_{out}/V_{in} voltage conversion ratios, especially for output voltages approaching ten times their input, as illustrated by the efficiency decline of curve **28** with increasing conversion ratios.

[0030] Furthermore, in graph **25**, Buck efficiency **27** is not shown for conversion ratios below 0.1 and above 0.9 and likewise boost efficiency **29** is not shown for conversion ratios below 1.1 and above 10, because these ranges require switching converter operation below a 10% or above a 90% duty factor, an operating condition difficult to achieve, especially at high switching frequencies.

Buck-Boost Switching Converter

[0031] The problem of non-isolated DC/DC switching converter operation near unity transfer is especially difficult in applications when the input voltage may vary either above or below the desired output voltage. Examples of this application include the output of noisy AC adapters or in circuitry which must operate by battery back-up during emergency conditions when a main source of power has failed.

[0032] Another scenario where a unity conversion ratio is required occurs when a battery's operating voltage range extends above and below the desired regulated voltage.

[0033] For example, the discharge characteristic of a Lilon battery starts at 4.2V at full charge, initially decays rapidly to around 3.6V, then decays slowly from 3.6V to 3.4V, and finally drops quickly to its cutoff at or below 3V. In the event that a DC/DC converter is needed to produce a well-regulated 3.3V output during the entire duration, a sub-unity conversion ratio of 3.3V/4.2V, or 0.79, is needed at the outset, indicating that a Buck converter is required. At the battery's end-of-life, the conversion ratio exceeds unity becoming 3.3V/3V, or 1.1, requiring a boost converter to achieve regulation. Such an application demanding both step-up and step-down conversion requires a Buck-boost, or up-down converter.

[0034] In the case where the user wants to avoid the complexities of up-down conversion, one possible approach is to use only a Buck converter and give up some battery life by cutting of the battery early, e.g. at 3.3V, but in practice when considering battery manufacturing variations and converter drop-out and duty factor limitations, too much battery life is sacrificed to rely on a Buck-only converter solution.

[0035] If up-down conversion cannot be avoided, one possible solution involves Buck-boost conversion and regulation. The Buck-boost converter can easily be derived from combining synchronous Buck and boost converters into a merged circuit. In the Buck-boost converter **35** of FIG. **3**A, for example, a synchronous Buck converter comprising a P-channel or N-channel MOSFET **36**, an inductor **38**A, an N-channel synchronous rectifier MOSFET **37**, an intrinsic rectifier diode **39**, and a capacitor **44** is used to power a synchronous boost converter comprising a low-side N-channel MOSFET **40**, an inductor **38**B, a synchronous rectifier MOSFET **41**, an intrinsic rectifier diode **42**, and a filter capacitor **43**. Buck-boost converter **35** first steps down the input voltage to an intermediate voltage lower than the desired output, then steps this voltage up to produce V_{out}.

[0036] Conversely, in the synchronous boost-Buck converter **45** of FIG. **3**B, a boost converter comprising a low-side N-channel MOSFET **46**, an inductor **47**, an N-channel or P-channel synchronous rectifier MOSFET **48**A, an intrinsic diode **49**, and a capacitor **54** is used to power a synchronous Buck converter comprising a MOSFET **48**B, an inductor **52**, an N-channel synchronous rectifier MOSFET **50**, an intrinsic rectifier diode **51**, and a filter capacitor **53**. The cascade boost-Buck converter **45** drives a load (not shown). In this approach the input voltage is first stepped-up to an intermediate voltage higher than the desired output, then back down to produce V_{out}.

[0037] The overall efficiency of either Buck-boost converter **35** or boost-Buck converter **45** is given by the product of the boost converter's efficiency η_{boost} multiplied by the Buck converter's efficiency η_{Buck}, mathematically as $\eta_{cascade}=\eta_{Buck}\cdot\eta_{boost}$. Even if both converters are 85% efficient, the combined cascade converter only reaches an overall efficiency of roughly 70%, significantly lower than the efficiency of an individual Buck converter or boost converter. The overall loss of either a Buck-boost or boost-Buck cascade is worse than a synchronous Buck or synchronous boost alone, because there are more transistors in series between input and output, and because all the transistors are switching all the time.

[0038] As shown, boost-Buck converter **45** of FIG. **3**B includes series-connected MOSFETs **48**A and **48**B with intermediate capacitor **54**. Since in steady-state, the current in series-connected MOSFETs must be equal, MOSFET **48**B is redundant and can be eliminated without impacting circuit operation. Even so, boost-Buck converter **45** requires two inductors **47** and **52**, a characteristic highly undesirable from a user's point-of-view.

[0039] Similarly, Buck-boost converter **35** of FIG. **3**A includes inductors **38**A and **38**B with intermediate capacitor **44**. Since in steady state the current in inductors **38**A and **38**B is the same, inductor **38**B is redundant and may be eliminated without changing the function of the circuit. In fact, capacitor **44** may also be eliminated without significantly altering the converter's operation.

[0040] The resulting simplified prior-art Buck-boost converter **55** is illustrated in FIG. **3**C, comprising a single-inductor **59**; four MOSFETs **57**, **56**, **60**, and **61**; diodes **58** and **62** and filter capacitor **63**. The PWM control circuitry and break-before-make and gate buffer circuits are not shown. Depending on its terminal conditions, such a converter can operate in three distinct modes, Buck, boost, and Buck-boost.

[0041] In FIG. **3**D, schematic diagram **65** represents the operation of Buck-boost converter **55** as a Buck converter, where MOSFETs **57** and **56** are switched out-of-phase by a PWM control unit (not shown), while MOSFET **61** remains turned-on, represented as resistance **67**, and MOSFET **60** is turned off, shown as open circuit **66**. The overall power loss in converter **55** is greater than the power loss in a synchronous

Buck converter because it now includes the conduction loss in MOSFET **61**, i.e. power lost continuously in resistance **67**. As a result of this increased power loss, Buck-boost converter **55** operating in its Buck mode has a lower efficiency than conventional Buck converter **1** shown in FIG. **1**A.

[0042] In FIG. **3**E, schematic diagram **70** represents the operation of Buck-boost converter **55** as a boost converter, where MOSFETs **60** and **61** are switched out-of-phase under a PWM control unit (not shown), while MOSFET **57** remains turned-on, represented as resistance **71**, and MOSFET **56** is turned off, shown as open circuit **72**. The overall power loss in converter **55** is greater than the power loss in a synchronous boost converter because it now includes the conduction loss in MOSFET **57**, i.e. power lost continuously in resistance **71**. As a result of this increased power loss, Buck-boost converter **55** operating in its boost mode has a lower efficiency than conventional boost converter **10** shown in FIG. **1**B.

[0043] The loss of efficiency using Buck-boost converter **55** is illustrated in FIG. **4** in the plot of efficiency η for various output-to-input voltage conversion ratios V_{out}/V_{in}. For convenience, conventional Buck and boost efficiency curves **27** and **28** from FIG. **2**B are illustrated by curves **81** and **82** respectively.

[0044] Curve **83** illustrates the efficiency of Buck-boost converter **55** operating in Buck-only mode shown in equivalent circuit **65**. Because of series resistance **67** associated with on-state MOSFET **61**, the efficiency of Buck-boost converter **65** in the Buck only mode is lower than that of a simple Buck converter, represented by curve **81**. This loss of efficiency can range from a few percent to over ten percent, depending on operating conditions. Curve **85** illustrates Buck-boost converter **55** operating in full Buck-boost mode where all four switches are switching constantly, and as a result exhibits even greater losses and poorer efficiency than Buck mode curve **83**.

[0045] Curve **84** illustrates the efficiency of Buck-boost converter **55** operating in boost-only mode shown in equivalent circuit **70**. Because of series resistance **71** associated with on-state MOSFET **57**, the efficiency of a Buck-boost converter **65** in the boost-only mode is lower than that of a simple boost converter, represented by curve **82**. This loss of efficiency can range from a few percent to over ten percent depending on operating conditions. Curve **86** illustrates Buck-boost converter **55** operating in full Buck-boost mode where all four switches are switching constantly, and as a result exhibits even greater losses and poorer efficiency than boost mode curve **84**.

[0046] Operating near unity conversion ratios, where the output voltage is slightly above or below its input, i.e. where $V_{out} \approx V_{in}$, Buck-boost converter **55** must operate in the Buck-boost mode, where all four transistors are switching constantly. The resulting efficiency, represented by curve **87**, can be ten to twenty percent lower than the efficiency of conventional Buck and boost converters, represented by curves **81** and **82**.

[0047] Thus, the efficiency penalty for a prior art Buck-boost converter operating over a wide range of voltage conversion ratios is substantial. Moreover, the converter must change its operating mode whenever operating near unity voltage conversion ratios.

Charge Pump Converters

[0048] An alternative to the switched-inductor converter is a charge pump, a voltage conversion circuit using only switches and capacitors to perform voltage translation through repeated charge redistribution, i.e. the continuous charging and discharging of a capacitor network driven by a clock or oscillator.

[0049] The advantage of a charge pump is that specific voltage conversion ratios, it can exhibit extremely high conversion efficiencies approaching 100%. The disadvantage is that it can only efficiently generate voltages that are selected multiples of the input voltage, determined by the number of "flying capacitors" used in its circuit. At output voltages other than selected multiples of the input voltage, the charge pump exhibits low efficiencies.

[0050] An example of a common charge pump **90** is illustrated in FIG. **5**A, where a single "flying capacitor" **93** is employed as a "doubler", i.e. to double the battery's input voltage. Charge pump **90** comprises four MOSFETs, **92**, **91**, **94** and **95** configured in an H-bridge arrangement, except that one terminal, the source of MOSFET **95** is connected to the charge pump output V_{CP} and reservoir capacitor **96** rather than to ground.

[0051] Operation of charge pump **90** involves repeatedly charging and discharging flying capacitor **93**. During the charging phase, diagonal MOSFETs **94** and **91** are turned on, charging capacitor **93** to the voltage V_{batt} while MOSFETs **92** and **95** remain turned off. Alternatively, in the charge transfer phase, MOSFETs **94** and **91** are turned off, MOSFETs **92** and **95** are turned on, and energy is transferred from the flying capacitor **93** to the output reservoir capacitor **96**, pumping the V_{CP} voltage to a value twice the battery voltage or $2 \cdot V_{batt}$.

[0052] The purpose of the switch network is essentially to place the flying capacitor in parallel with the battery during charging and in series, i.e. stacked on top of the battery's positive terminal, during discharging, as illustrated by equivalent circuit **100** in FIG. **5**B, where voltage source **101** represents the battery input and capacitor **102** charged to V_{batt} represents the flying capacitor. By stacking one voltage atop the other, the output voltage of the charge pump is the sum of the voltages, hence doubling the voltage input. The cycle then repeats with another charging phase.

[0053] FIG. **5**C illustrates a charge pump **110** utilizing two flying capacitors **114** and **115** and a network of seven MOSFETs **111**, **112**, **113**, **116**, **117**, **118** and **119**. This network charges the flying capacitors **114** and **115** in series, charging each flying capacitor to one-half the battery voltage, i.e. $V_{batt}/2$. During the charging stage, MOSFETs **111**, **112** and **113** are turned on and MOSFETs **116**, **117**, **118** and **119** are turned off. After the charging is completed, the two charged capacitors are connected in parallel to the positive terminal of the battery. This connection is accomplished by turning on MOSFETs **116**, **117**, **118** and **119**. The resulting output, shown in equivalent circuit **121** of FIG. **5**D, is then $V_{batt}+V_{batt}/2$, for an output voltage of $1.5V_{batt}$ as illustrated by battery voltage source **124** with capacitors **122** and **123** stacked atop one another. Because the output is 1.5 times its input this charge pump is sometimes referred to as a "fractional" charge pump.

[0054] Actually many charge pump topologies are possible, but most concentrate on using only one or two flying capacitors. A single flying capacitor charge pump is capable only of efficiently delivering an output voltage equal to twice its input voltage, or alternatively, if the capacitor is connected to the negative terminal of the battery, to produce a mirror-image negative voltage of the battery, i.e. $-V_{batt}$. In this topology, the device is known as an inverter. The inverting case is illustrated in equivalent circuit **130** of FIG. **5**E, where battery

NOCO Exhibit 2011
ADC v. NOCO
IPR2024-00671

131 is used to charge capacitor **132** to a voltage below ground, i.e. a voltage referenced to the negative terminal of battery **131**. Two-transistor fractional charge pumps may also be used to produce an output voltage equal to positive or negative one-half the input voltage, as shown in equivalent circuit **135** of FIG. **5**F, where capacitors **137** and **138**, after being charged to one-half of the battery voltage **136** are then referenced to ground to produce either a positive potential $+0.5V_{batt}$ or a negative potential $-0.5V_{batt}$.

[0055] The problem with charge pump converters is they operate efficiently only at specific multiples of the number of flying capacitors. In other words, they are not true voltage converters. Specifically, as a desired load voltage V_{out} drops below the voltage V_{CP} the capacitor network produces, the converter cannot adapt. The voltage-differential between the charge pump's output voltage V_{CP} and the regulated output voltage of the converter V_{out} requires a resistor or current source to support the voltage mismatch, and the voltage across that lossy element results in lost power and reduced efficiency. An analysis of charge pump efficiencies is described in detail in the above-referenced Application No. [Attorney Docket No. AATI-19-DS-US].

[0056] This efficiency equation for single-mode charge pumps is illustrated graphically in FIG. **6**A for various multipliers, including a doubler (curve **151**), an inverter (curve **152**), and fractional charge pumps (curves **153**, **154** and **155**). Curve **156** represents a direct battery connection, identical to a linear converter's maximum theoretical efficiency, i.e. assuming no quiescent operating current. In each case, as the input to output ratio approaches an integral multiple of $\pm\frac{1}{2}V_{batt}$, the efficiency increases. Above that voltage, the charge pump is not capable of delivering a higher voltage and a different capacitor multiplier, i.e. a different operating mode must be employed.

[0057] Each curve shown in graph **150** of FIG. **6**A represents a specific charge pump circuit, e.g. including those shown in FIGS. **5**A-**5**F. Unless a load operates at an exact half-volt integral multiple of the input voltage, however, the efficiency of the charge pump converter using one or two capacitors will suffer. This behavior is especially problematic for battery powered products where the battery voltage changes markedly as the cell discharges. In the case of Lilon batteries, the voltage can decay more than 1V during discharge, representing a 25% change. Even if the peak efficiency may be high at one specific operating condition and battery voltage, the overall efficiency of the converter averaged over the battery discharge curve is poor. Weighted average efficiencies can be lower than 60% using a single-mode charge pump.

[0058] One way to improve the average efficiency of the converter is to switch modes between 1×, 1.5× and 2× automatically within one circuit. This feature is particularly useful to supply a fixed voltage over a wide input range. An example of the efficiency of a mode changing charge pump is illustrated in graph **160** of FIG. **6**B, which shows the efficiency of a tri-mode converter circuit as it switches from 1×-battery-direct mode having an efficiency shown by line **163**, to 1.5×-fractional-mode with efficiency curve **162**, and again to 2×-doubler-mode with an efficiency curve **161** as the battery decays. By switching modes in this zigzag pattern, the efficiency of the charge pump converter is improved because the output is not pumped to an excessively high value compared to the load.

[0059] Unfortunately, conditions still exist where the efficiency suffers substantially. The mode transitions exhibit dramatic shifts in efficiency shown by curve **163** at a conversion ratio of one, and again by curve **162** at a 1.5× conversation ratio. The mode transitions may also result in sudden current and voltage discontinuities, or produce instability or noise. To determine what conversion ratio is required, graph **160** also includes curves **166**, **165**, and **164** relating the required input voltage range and conversion ratios to produce an output voltage of 3V, 3.5V and 4V respectively.

[0060] Specifically, the charge pump converter in 1.5× mode does not perform well for conditions slightly above a unity conversion ratio, manifesting even lower efficiencies than the aforementioned inductive Buck-boost converter.

Dropout in Prior Art Converters

[0061] Whenever the input and the output of a voltage converter approach a range of several hundred millivolts of one another, i.e. $V_{out} \approx V_{in} \pm 200$ mV, the quality of the converter's regulating ability suffers. Loss of regulation quality may be manifested in several ways, either by a one-time or repeated glitch or discontinuity in output voltage, by increased ripple, or by complete loss of regulation within some narrow voltage band. The phenomenon of degraded regulation whenever V_{out} approaches V_{in} is referred to as "dropout", meaning the converter drops out of regulation.

[0062] As shown in FIG. **2**A, the Buck converter **1** of FIG. **1**A momentarily loses regulation as its switching duty factor jumps from D_{max} to 100% or D_{min} to 0% and the boost converter **10** of FIG. **1**B momentarily loses regulation as its switching duty fact jumps from D_{min} to 0%. Both converters completely lose regulation while D=0% since the input is essentially resistively connected to the output during the dropout condition.

[0063] While a Buck-boost converter doesn't really exhibit permanent dropout, it can easily suffer a voltage glitch whenever the converter switches from its Buck mode into its Buck-boost mode, or from its Buck-boost mode to its boost mode. Mode transitions occur whenever the converter changes from a circuit having two power devices switching into one where four devices are switching, or vice versa.

[0064] To avoid the mode switching transition problem, a Buck-boost converter can be run continuously in Buck-boost mode with all four power devices switching continuously but, as shown in FIG. **4**, when this happens the efficiency is degraded under all input-output conditions and conversion ratios.

[0065] As stated above, the charge pump is incapable of regulating voltage without the use of a series connected linear converter to provide the regulation function. Unfortunately, it is well known phenomenon that all linear converters exhibit loss of regulation, i.e. dropout, whenever the ΔV across the linear converter's input and output terminals becomes too small. In essence, dropout occurs in a linear converter because the loop gain of the amplifier performing regulation drops precipitously as its transistor pass element changes from behaving as a current source into acting like a variable resistor. If the pass element is a bipolar transistor, the loss of gain occurs at small values of V_{CE} as the device transitions from its active operating region into saturation. In many bipolar linear converters, this dropout condition occurs at more than 400 mV.

[0066] In so-called "low dropout" linear converters or "LDOs", a MOSFET capable of operating as a current source

at a lower ΔV is substituted for the bipolar pass element, but the linear converter still drops out at 200 to 300 mV as the power MOSFET pass element transitions from its saturation, i.e. constant current, region into its linear, i.e. resistive, region of operation.

[0067] In conclusion, all prior-art non-isolated high-efficiency converters exhibit dropout at voltage conversion ratios approaching unity. Mode switching, loss of regulation and dropout can be avoided, but only by sacrificing efficiency. Isolated converters such as the flyback and forward converter are able to operate at high efficiencies near unity conversion without the need switching modes, but their use of physically-large tapped inductors, coupled inductors, and transformers precludes their application in most portable products.

Summary of Prior-Art Down-Up Converters

[0068] In conclusion, no existing charge pump converter, Buck-boost switching converter or other inductive switching converter is able to both step-up and step-down DC voltages efficiently, especially for conversion ratios near unity, where $V_{in} \approx V_{out}$. What is needed is an up-down converter that is efficient over a wide range of input and output voltages, and that does not need to change its operating mode as it approaches or operates near unity voltage conversion ratios. Furthermore, the converter should be free from dropout problems, maintaining high quality regulation even while biased with an output voltage within a 200 mV of its input, i.e. within the range $V_{out} \approx V_{in} \pm 200$ mV.

SUMMARY OF THE INVENTION

[0069] A DC/DC voltage converter according to this invention includes a pre-converter and a post-regulator. The pre-converter includes a switched capacitive circuit: and a post-regulator includes a switched inductive circuit. An output terminal of the pre-converter is coupled to an input terminal of the post-regulator. An input terminal of the pre-converter comprises an input terminal of the DC/DC voltage converter, and an output terminal of the post-regulator comprises an output terminal of the DC/DC voltage converter. In many embodiments the pre-converter includes a charge pump and the post-regulator includes a boost converter.

[0070] Within this broad structure, many variations are possible within the scope of the invention. In one group of embodiments, the pre-converter includes a voltage-reducing fractional charge pump and the post-regulator includes a non-inverting boost converter. In another group of embodiments, the pre-converter includes a voltage-increasing charge pump and the post-regulator includes a non-inverting boost converter. In another group of embodiments, the pre-converter includes a voltage-inverting charge pump and the post-regulator includes a non-inverting boost converter. In yet anther group of embodiments, the pre-converter includes a voltage-inverting charge pump and the post-regulator includes an inverting boost converter.

[0071] DC/DC converters according to this invention are capable of operating over a wide range of voltage conversion ratios ranging from step-up to step-down conversion without the need for mode switching. Free from mode switching and dropout problems when $V_{out} \approx V_{in}$, the converter does not suffer from noise glitches, poor regulation, and instability, even near unity input-to-output voltage conversion ratios. While the converter includes switched inductor operation, it avoids the minimum pulse width problem plaguing conventional switching converters at very high and very low duty factors, including converter dropout, narrow pulses and associated high-current spikes, variable frequency operation, inadequate time to perform break-before-make transitions. In contrast, prior-art non-isolated DC/DC converters suffer from one or more of the aforementioned problems at extreme duty factors, and their use near unity voltage conversion ratios remains problematic.

[0072] The method and apparatus of this invention can be used in applications requiring up-down conversion, and avoid the problems of existing Buck-boost and flyback converters. While preferred embodiments of this invention specifically address the implementation of up-down converters, variants include improved down-only regulating converters and DC/DC inverters capable of producing negative, i.e. below ground, supply voltages.

BRIEF DESCRIPTION OF THE DRAWINGS

[0073] FIG. **1**A is a circuit diagram of a prior-art synchronous Buck converter.

[0074] FIG. **1**B is a circuit diagram of a prior art synchronous boost converter.

[0075] FIG. **2**A is a graph of the voltage conversion ratio versus duty factor of conventional Buck and boost converters.

[0076] FIG. **2**B is a graph of efficiency versus voltage conversion ratio of conventional Buck and boost converters.

[0077] FIG. **3**A is a circuit diagram of a cascaded Buck-boost converter.

[0078] FIG. **3**B is a circuit diagram of a cascaded boost-Buck converter.

[0079] FIG. **3**C is a circuit diagram of a simplified Buck-boost converter.

[0080] FIG. **3**D is an equivalent circuit diagram of a Buck-boost converter in Buck-only mode.

[0081] FIG. **3**E is an equivalent circuit diagram of a Buck-boost converter in boost-only mode.

[0082] FIG. **4** is a graph of efficiency versus voltage conversion ratio for Buck, boost, and Buck-boost converters.

[0083] FIG. **5**A is a circuit diagram of a 2× doubler charge pump.

[0084] FIG. **5**B is an equivalent circuit diagram of the doubler during discharge.

[0085] FIG. **5**C is a circuit diagram of a 1.5× fractional charge pump.

[0086] FIG. **5**D is an equivalent circuit diagram of the 1.5× circuit during discharge.

[0087] FIG. **5**E is an equivalent circuit diagram of a −× inverter circuit during discharge.

[0088] FIG. **5**F is an equivalent circuit diagram of a 0.5× circuit during discharge.

[0089] FIG. **6**A is a graph of efficiency versus conversion ratio for a single-mode charge pump.

[0090] FIG. **6**B is a graph of efficiency versus conversion ratio for a tri-mode charge pump.

[0091] FIG. **7** is a graph of the voltage conversion ratio versus input voltage for various output voltages for DC/DC converters.

[0092] FIG. **8** is a general schematic circuit diagram of a switched CLXU converter according to the invention.

[0093] FIG. **9** is a diagram of a behavioral model of the switched CLXU converter of FIG. **8**.

[0094] FIG. **10** is a circuit diagram of a switched 0.5× CLDU converter.

NOCO Exhibit 2011
ADC v. NOCO
IPR2024-00671

[0095] FIG. **11**A is a graph illustrating the operation of converter according to this invention with a 1-cell Lilon battery.

[0096] FIG. **11**B is a graph illustrating 2V to 5V input transfer characteristics.

[0097] FIG. **11**C is a graph illustrating the V_{out}/V_{in} ratio as a function of the duty factor.

[0098] FIG. **12**A is a more detailed circuit diagram of a 0.5× CLDU converter.

[0099] FIG. **12**B is a circuit diagram illustrating the charging and recirculation stages of the converter.

[0100] FIG. **12**C is a circuit diagram illustrating the transfer and magnetizing stages of the converter.

[0101] FIG. **12**D is an alternative circuit diagram illustrating the transfer and magnetizing stages of the converter.

[0102] FIG. **12**E is an alternative circuit diagram illustrating the transfer and output stages of the converter.

[0103] FIG. **13**A is a graph showing the efficiency of the pre-converter stage and a function of the voltage conversion ratio V_y/V_{in}.

[0104] FIG. **13**B is a graph showing the efficiency of the post-regulator stage as a function of the conversion ratio V_{out}/V_y.

[0105] FIG. **13**C is a graph showing the efficiency of the converter as a function of the conversion ratio V_{out}/V_{in} for different duty factors.

[0106] FIG. **13**D is a graph showing the efficiency of the converter as a function of the duty factor.

[0107] FIG. **14**A is a functional diagram of a CLUU converter containing a 2× pre-converter.

[0108] FIG. **14**B is a functional diagram of a CLUU converter containing a 1.5× pre-converter.

[0109] FIG. **15**A is a graph showing the low-voltage transfer characteristics of a 2× CLUU converter.

[0110] FIG. **15**B is a graph showing the discharge of a 1s Lilon battery in a 2× CLUU converter.

[0111] FIG. **15**C is a graph showing the higher-voltage transfer characteristics of a 2× CLUU converter.

[0112] FIG. **15**D is a graph showing the low-voltage transfer characteristics of a 1.5× CLUU converter.

[0113] FIG. **15**E is a graph showing the higher-voltage transfer characteristics of a 1.5× CLUU converter.

[0114] FIG. **15**F is a graph showing the discharge of a 1s Lilon battery in a 1.5× CLUU converter.

[0115] FIG. **15**G is a graph showing the voltage conversion ratio V_{out}/V_{in} as a function of duty factor for a 2× CXUU converter, a 1.5× CXUU converter and a boost converter.

[0116] FIG. **16**A is a more detailed circuit diagram of a 2× CLUU converter.

[0117] FIG. **16**B is a circuit diagram showing the charging and recirculation stages of the 2× CLUU converter.

[0118] FIG. **16**C is a circuit diagram showing the transfer and magnetizing stages of the 2× CLUU converter.

[0119] FIG. **16**D is a circuit diagram showing the recirculation through the V_y MOSFET in the alternative embodiment of the 2× CLUU converter shown in FIG. **16**E.

[0120] FIG. **16**E is a circuit diagram of an alternative embodiment of the 2× CLUU converter.

[0121] FIG. **17**A is a more detailed circuit diagram of a 1.5× CLUU converter.

[0122] FIG. **17**B is a circuit diagram showing the charging and recirculation stages of the 1.5× CLUU converter.

[0123] FIG. **17**C is a circuit diagram showing the transfer and magnetizing stages of the 1.5× CLUU converter.

[0124] FIG. **17**D is a circuit diagram showing the recirculation through the V_y MOSFET in the alternative embodiment shown in FIG. **17**E.

[0125] FIG. **17**E is a circuit diagram of an alternative embodiment of the 1.5× CLUU converter.

[0126] FIG. **18**A is a functional diagram of a −1× pre-converter and non-inverting boost converter.

[0127] FIG. **18**B is a functional diagram of a −1× pre-converter and inverting boost converter.

[0128] FIG. **18**C is a functional diagram of a −0.5× pre-converter and non-inverting boost converter.

[0129] FIG. **18**D is a functional diagram of a −0.5× pre-converter and inverting boost converter.

[0130] FIG. **19**A is a more detailed circuit diagram of a −1× CLIU converter.

[0131] FIG. **19**B is an equivalent circuit diagram of the −1× CLIU converter during the charging and recirculating stage.

[0132] FIG. **19**C is an equivalent circuit diagram of the −1× CLIU converter during the magnetizing and discharging stage.

[0133] FIG. **19**D is a circuit diagram of an alternative embodiment of a =1× CLIU converter with MOSFET circulation.

[0134] FIG. **20**A is a circuit diagram of a −1× CLII converter.

[0135] FIG. **20**B is an equivalent circuit diagram of the −1× CLII converter during the charging stage.

[0136] FIG. **20**C is an equivalent circuit diagram of the −1× CLII converter during the magnetizing and discharging stage.

[0137] FIG. **21**A is a more detailed circuit diagram of a −0.5× CLIU converter.

[0138] FIG. **21**B is an equivalent circuit diagram of the −0.5× CLIU converter during the magnetizing and discharging stages.

[0139] FIG. **21**C is an equivalent circuit diagram of the −0.5× CLIU converter during the charging stage.

[0140] FIG. **21**D is a circuit diagram of an alternative embodiment of a −0.5× CLIU converter with MOSFET circulation.

[0141] FIG. **22**A is a circuit diagram of a −0.5× CLII converter.

[0142] FIG. **22**B is an equivalent circuit diagram of the −0.5× CLII converter during the charging stage.

[0143] FIG. **22**C is an equivalent circuit diagram of the −0.5× CLII converter during the magnetizing and discharging stage.

[0144] FIG. **23**A is a graph showing the transfer characteristic of a −1× type CLIU converter regulating a 1s Lilon battery.

[0145] FIG. **23**B is a graph showing the transfer characteristic of a −0.5× type CLIU converter regulating a 1s Lilon battery.

[0146] FIG. **23**C is a graph showing the transfer characteristic of a −1× type CLIU converter regulating a 2s NiMH battery.

[0147] FIG. **23**D is a graph showing the transfer characteristic of a −1× type CLIU converter regulating a 1s NiMH battery.

[0148] FIG. **23**E is a graph showing the higher voltage transfer characteristic of a −1× type CLIU converter.

[0149] FIG. **23**F is a graph showing the higher voltage transfer characteristic of a −0.5× type CLIU converter.

[0150] FIG. **23**G is a graph showing the low voltage transfer characteristic of a −1× type CLIU converter.

NOCO Exhibit 2011
ADC v. NOCO
IPR2024-00671

[0151] FIG. **23**H is a graph showing the voltage conversion ratio V_{out}/V_{in} as a function of duty factor for various CLIU converters.

[0152] FIG. **24**A is a graph showing the transfer characteristic of a −1× type CLII converter regulating a 1s Lilon battery.

[0153] FIG. **24**B is a graph showing the transfer characteristic of a −0.5× type CLII converter regulating a 1s Lilon battery.

[0154] FIG. **24**C is a graph showing the transfer characteristic of a −1× type CLII converter regulating a is NiMH battery.

[0155] FIG. **24**D is a graph showing the low voltage transfer characteristic of a −1× type CLII converter.

[0156] FIG. **24**E is a graph showing the higher voltage transfer characteristic of a −1× type CLII converter.

[0157] FIG. **24**F is a graph showing the voltage conversion ratio V_{out}/V_{in} as a function of duty factor for a −1× CLII converter.

[0158] FIG. **24**G is a graph showing the voltage conversion ratio V_{out}/V_{in} as a function of duty factor for a −0.5× CLII converter.

[0159] FIG. **25**A shows an equivalent circuit diagram of a 0.5× CLDU converter during discharge.

[0160] FIG. **25**B shows an equivalent circuit diagram of a 2× CLUU converter during discharge.

[0161] FIG. **25**C shows an equivalent circuit diagram of a 1.5× CLUU converter during discharge.

[0162] FIG. **25**D shows an equivalent circuit diagram of a −1× CLIU converter during discharge.

[0163] FIG. **25**E shows an equivalent circuit diagram of a −0.5× CLIU converter during discharge.

[0164] FIG. **25**F shows an equivalent circuit diagram of a −1× CLII converter during discharge.

[0165] FIG. **25**G shows an equivalent circuit diagram of a −0.5× CLII converter during discharge.

DESCRIPTION OF THE INVENTION

[0166] FIG. **7** graphically illustrates the requisite voltage conversion ratio V_{out}/V_{in} of a DC/DC converter operating at a variety of voltage output voltages for input voltages ranging from 1.8V to 6.6V. Curve **181**, for example, shows that for a 4.5V to 5.5V range of input voltages, regulating a 5V output to ±1% accuracy requires operation above and below a unity conversion ratio, meaning an up-down regulating converter is required to hold a tighter tolerance than the ±5% or ±10% accuracy commonly guaranteed by low cost AC/DC wall adapters.

[0167] Another need for up-down conversion occurs when using a lithium ion battery to produce a voltage intermediate to its wide voltage range. As examples, curves **182**, **183**, **184** in FIG. **7** illustrate output voltages of 4V, 3.6V, and 3.3V respectively. Since these outputs fall within the Lilon battery's normal discharge voltage range of 4.2V to 3V, the converter must regulate in step-down mode with a voltage conversion ratio below unity at the beginning of the cell's discharge cycle, and in step-up mode with a conversion ratio above unity later as the cell's voltage decays.

[0168] Curve **185** illustrates a 3V output, which theoretically should require only step down conversion, but because of the aforementioned problem of dropout, a Lilon battery supplying a 3V output must be cut off above 3.2V, thereby wasting useful battery life. New generation Lilon cells under development may allow operation down to 2.7V, requiring the need to utilize up-down conversion for 2.7 V outputs, as shown by curve **186**. At a 2.5V battery condition, dropout issues may also require the use of an up-down converter even to supply a regulated 2.5V output, as shown by curve **187**. If, however, up-down conversion results in a loss of efficiency exceeding the extra operating time gained by the extended battery range, then the user lifetime benefit of using a battery capable of lower voltage operation is lost entirely.

[0169] Similarly, dropout concerns make it difficult to guarantee a 1.8V regulated output shown by curve **188** from 2-cell-connected nickel-metal-hydride or nickel-cadmium, i.e. NiMH or NiCd, batteries, since those their output voltages range from 2.4V down to 1.8V. Stopping battery usage at a 2V condition unacceptably wastes more than half the battery's charge life.

[0170] Other examples of battery arrangements needing an efficient low dropout up-down converter are two NiMH dry-cells, two alkaline cells, or a single cell Lilon battery. Since 2-series-cell NiMH battery packs supply a voltage ranging from 1.8V to 2.4V, 2-series-cell alkaline batteries supply a voltage ranging from 1.8V up to 3.4V during charging, and single-cell Lilon batteries supply a voltage ranging from 4.2V down to 3V or even 2.7V, any output between 4.2V and 1.8V needs an up-down converter to maximize efficiency and battery life, as shown by curves **188** through **182** in FIG. **7**.

[0171] If we also consider that some systems allow the DC output from the AC/DC wall adapter to be connected without a battery present, the input voltage supplied to a system's DC/DC converter input can be considerably higher than if the battery were present, and may reach as high as 6.5V. When the battery is present and the charger disconnected, the input voltage may be as low as 1.8V. In such cases, every output curve ranging from curve **181** to **188**, i.e. from 5V down to a 1.8V output, requires an up-down converter.

[0172] Today most electrical loads are supplied by an up-only or down-only converter, and the battery is cut off prematurely to avoid requiring up-down conversion at the expense of wasting usable stored charge in a battery. Up-down conversion is avoided at any cost except in extreme situations. With the poor efficiency, mode switching, noise glitches, regulation dropout, and poor regulation offered by existing up-down converters, be they DC/DC converters, charge pumps, or linear converters; a requirement for up-down conversion and regulation is extremely problematic. In short, present up-down converters cannot meet the need of today's efficiency-focused consumer marketplace.

A New DC/DC Converter Topology

[0173] The new non-isolated DC/DC converter and voltage regulation topology described herein is capable of operating over a wide range of voltage conversion ratios ranging from step-up to step-down conversion without the need for mode switching. Free from mode switching and dropout problems when $V_{out} \approx V_{in}$, the converter does not suffer from noise glitches, poor regulation, and instability, even near unity input-to-output voltage conversion ratios. While the converter includes switched inductor operation, it avoids the minimum pulse width problem plaguing conventional switching converters at very high and very low duty factors, including converter dropout, narrow pulses and associated high-current spikes, variable frequency operation, inadequate time to perform break-before-make transitions. In contrast, prior-art non-isolated DC/DC converters suffer from one or

more of the aforementioned problems at extreme duty factors, and their use near unity voltage conversion ratios remains problematic.

[0174] The method and apparatus of this invention can be used in applications requiring up-down conversion, and avoid the problems of existing Buck-boost and flyback converters. While preferred embodiments of this invention specifically address the implementation of up-down converters, variants include improved down-only regulating converters and DC/DC inverters capable of producing negative, i.e. below ground, supply voltages.

[0175] Collectively, the new DC/DC converters disclosed herein comprise four new converter topologies and variants thereof, referred to herein by acronym as

[0176] CLDU—switched capacitor-inductor down-up converter

[0177] CLUU—switched capacitor-inductor up-up converter

[0178] CLIU—switched capacitor-inductor inverting-up converter (inverter)

[0179] CLII—switched capacitor-inductor inverting-inverting converter

[0180] Specifically this invention focuses on switched capacitor-inductor regulating converters comprising a switched-capacitor step-up, step-down, or inverting pre-converter feeding an inductively implemented step-down post-regulator. As a matter of nomenclature, the first C in the acronym represents the capacitive energy storage element in the pre-converter and the L represents the energy storage element, i.e. the coil or inductor, in the converter's second, or post-regulator, stage.

[0181] The third character in the converter's name, either: D, U or I, indicates whether the pre-converter is stepping the input or battery voltage, down, up, or inverting respectively, before supplying it to the post-regulator. The last character U describes the post-regulator as a step-up converter, meaning the magnitude of the voltage is increased without changing its relative polarity. For example, "up" for a positive voltage means making a larger positive voltage, while "up" for a negative voltage, the output of an inverting pre-converter, means a greater negative voltage. Thus, "up" means an increase in the absolute value of the voltage, whether the voltage is positive or negative.

[0182] These topologies, described by the acronyms CLDU, CLUU, and CLIU vary in the utility for differing applications, and as such this new switched capacitor-inductor family of DC/DC converter topologies can be collectively described as CLXU regulating converters, the X referring to a variable U for up, D for down, and I for inverting, respectively.

[0183] Another converter related to the CLIU inverter, the CLII converter uses an inverting post-regulator to produce a positive voltage which may vary above and below unity conversion ratios.

[0184] Related U.S. Application No. [Attorney Docket No. AATI-22-DS-US], titled "High-Efficiency DC/DC Voltage Converter Including Capacitive Switching Pre-Converter And Down Inductive Switching Post-Regulator," filed contemporaneously herewith and incorporated herein by reference, describes other switched capacitor-inductor converters comprising a switched capacitor step-down, step-up, or inverting pre-converter followed by a switched inductive step-down type post-regulator. Collectively these CLXD type regulating converters include the following:

[0185] CLUD—switched capacitor-inductor up-down converter

[0186] CLDD—switched capacitor-inductor down-down converter

[0187] CLID—switched capacitor-inductor inverting-down converter (inverter)

[0188] CLII—switched capacitor-inductor inverting-inverting converter

[0189] Related U.S. Application No. [Attorney Docket No. AATI-19-DS-US] and Application No. [Attorney Docket No. AATI-21-DS-US], titled "High-Efficiency DC/DC Voltage Converter Including Up Inductive Switching Pre-Regulator And Capacitive Switching Post-Converter," each of which is filed contemporaneously herewith and each of which is incorporated herein by reference, describe other switched inductor-capacitor regulating converters, where pre-regulation is achieved by a switched inductor stage and post-conversion is accomplished by a switched capacitor stage.

Switched Capacitor-inductor (CLXU) Converters

[0190] FIG. **8** illustrates a switched CLXU converter **200** comprising a switched-capacitor pre-converter **200**A with a conversion ratio n supplying an intermediate voltage V_y to a switched-inductor post-regulator **200**B comprising a step-up switched inductor converter, where the output voltage is further used as feedback to control the operating condition and output of the post-regulator. The output voltage V_y of pre-converter **200**A thereby follows the input at an n× multiple for optimum efficiency while post-regulator **200**B dynamically adjusts the output voltage to produce a well-regulated output at a desired voltage V_{out}.

[0191] In converter **200**, a charge pump **201** scales the input voltage V_{batt} by a factor "n" to produce an intermediate voltage V_y. Charge-pump **201** including a capacitor **207** and optionally a capacitor **208** or more, comprises a switched-capacitor network producing any variety of multiplier, including a doubler, an inverter, or a fractional or fractional-inverting circuit. The node at which the intermediate voltage V_y appears may also include a filter capacitor **209** and a diode **210**, depending on various design considerations.

[0192] Within converter **200**, the switched-inductor post-regulator **200**B comprises a PWM controller **213**, a break-before-make gate buffer **212**, a low-side N-channel power MOSFET **202**, a floating synchronous rectifier power MOSFET **204** with intrinsic PN diode **211**, and an inductor **203**. A filter capacitor **205** is connected across the output of converter **200** to insure stability, reduce ripple, and improve transient response. In this embodiment of the invention, the step-up switched-inductor post-regulator **200**B is topologically configured as a synchronous boost converter although any step-up switched inductor DC/DC converter may be used. For example MOSFET **204** may be eliminated and diode **211** replaced by a Schottky rectifier to implement a conventional boost converter in lieu of the synchronous boost converter shown.

[0193] A PWM controller **213** controls the on-time of low-side N-channel MOSFET **202** by varying the duty factor D in response to its feedback input, operating at a fixed frequency Φ as determined by ramp generator clock **215**. Alternatively PWM controller **213** may operate at a variable frequency with either a fixed or variable on-time for N-channel MOSFET **202**.

[0194] Whenever N-channel MOSFET **202** is on, current flows from the output terminal of the charge pump **201**

NOCO Exhibit 2011
ADC v. NOCO
IPR2024-00671

through inductor **203**. Inductor **203** is thereby magnetized, storing energy in an amount equal to $\frac{1}{2}LI^2$ and resisting any rapid changes in current. At the switching frequency Φ, current in inductor **203** cannot react to the rapid switching of MOSFET **202** so that the inductor behaves as a nearly lossless current source, whose average current changes slowly, over many clock cycles in response to pulse width modulation controlled by PWM controller **213**.

[0195] Whenever low-side MOSFET **202** is not conducting, inductor **203** drives the voltage V_x to a level above the output voltage V_{out}, forward biasing diode **211** and allowing current in the inductor **203** to flow uninterrupted, i.e. to recirculate. With both of MOSFETs **202** and **204** off, the power dissipated in diode **211** is $I_L \cdot V_f$ where V_f is the forward voltage of P-N junction in diode **211**. Floating synchronous rectifier MOSFET **204** conducts all or some portion of the time whenever N-channel MOSFET **202** is off, shunting diode **211** and redirecting the recirculation current through the channel of MOSFET **204**. Since MOSFET **204** only conducts when rectifier diode **211** is conducting, it operates as a "synchronous" rectifier, even though conduction in the channel of MOSFET **204** occurs only during a portion of the time conduction takes place in diode **211**. During conduction, the voltage drop across the synchronous rectifier MOSFET **204** is given by $I_L \cdot R_{DS}(on)$ and its instantaneous power dissipation is $IL^2 \cdot R_{DS}(on)$.

[0196] A break-before-make (BBM) buffer **212** insures that low-side power MOSFET **202** and floating power MOSFET **204** never conduct simultaneously to prevent shoot-through conduction, shorting out the load **206**. Shoot through conduction, the crow barring of the input from overlapping conduction, is an undesirable condition leading to wasted power and a loss of efficiency and potentially resulting in damage to the MOSFETs. While BBM intervals must be sufficiently long to prevent shoot-through conduction, excessively long BBM intervals are also undesirable since they force diode **211** to carry current for longer times and to dissipate more power.

[0197] Except for the BBM period, synchronous rectifier MOSFET **204** ideally should be turned on and conducting whenever low-side MOSFET **202** is off. In some circumstances, however, it may be advantageous to turn off MOSFET **204** prematurely or not to turn it on at all. For example at very low output currents, unwanted oscillations and reverse current flow may occur if MOSFET **204** is left on for an extended duration. Shutting MOSFET **204** off disables channel conduction, and diode **204** under a reverse bias condition prevents reverse current conduction, improving the light load efficiency of converter **200**.

[0198] Alternatively, as described in Application No. [Attorney Docket No. AATI-18-DS-US], titled "Low-Noise DC/DC Converter With Controlled Diode Conduction," filed contemporaneously herewith and incorporated herein by reference, the synchronous rectifier MOSFET **204** may remain on, but controlled in a manner to limit the magnitude of its drain current when it is not being operated as a fully-on device. Alternating between a resistive switch state and a low-current constant-current mode in MOSFET **204** reduces electrical noise in converter **200**.

[0199] Charge pump **201** converts the input voltage V_{batt} to an intermediate voltage nV_y using a switched capacitor network with flying capacitors **207** and (optionally) **208**. The conversion ratio n× of charge pump **201** may be step-up, step down, or inverting.

[0200] In the event that charge pump **201** uses step-down conversion, e.g. a dual-capacitor fractional version where n=0.5, converter **200** operates as a CLDU down-up converter, which may step-up or step-down the input voltage or it may provide a unity voltage conversion ratio, i.e. where $V_{out} \approx V_{in}$.

[0201] Step-up conversion in the pre-converter of a switched CLUU converter may be performed with a single-capacitor doubler, where n=2, or a dual-capacitor fractional implementation, where n=1.5. Dual capacitors may also be configured as a tripler, a method well known to one skilled in the art. CLUU converters can thereby achieve high step-up conversion ratios while maintaining a duty factor much closer to 50% than is possible with a simple inductive boost converter.

[0202] Using an inverter in the pre-converter may be accomplished with a single capacitor circuit, where n=−1, or with a two capacitor circuit, where n=−0.5. Connecting the output of an inverting pre-converter to the input of a post-regulator comprising a non-inverting inductive boost converter results in an output voltage that is even more negative than the intermediate voltage Vy. Such an inverter is referred to as a CLIU converter, the "U" referring to "up" meaning greater in numerical magnitude. Assuming that the input voltage is above ground, a CLIU converter can only deliver a below ground, i.e. negative, output voltage.

[0203] In another alternative, an inverting pre-converter is used to produce a negative supply rail at a voltage V_y of $-0.5V_y$, for example, and then to boost the voltage in a positive polarity, i.e. inverted in polarity a second time, to a positive voltage having an absolute value greater than the absolute value of V_y. Accordingly, this CLII converter is capable of producing voltages both above and below zero, and even to actively regulate precisely at zero volts.

[0204] The output of converter **200**, filtered by reservoir capacitor **205**, supplies load **206** with a regulated voltage V_{out}. In a preferred embodiment this output is used to provide feedback to the PWM controller **213** with a feedback signal V_{FB} which is converted by level shifter **214** to a voltage used to produce V_{FBin}, the control signal input to PWM controller **213**. As shown below, the value of V_y output by the pre-converter is self biasing and allows charge pump **201** to operate at its maximum efficiency point. The negative feedback loop facilitates tight voltage regulation in the post-regulator without significantly affecting the overall efficiency of the CLXU converter.

[0205] In a preferred embodiment, the output voltage of level shifter **214** is V_{out}, i.e. the feedback should force the value of V_{out} to a same voltage V_{out}. In the case of CLUU and CLDU converters this level shifter may comprise a network of two resistors acting as a voltage divider to match the feedback to the converter's internal voltage reference but need not account for the factor n from the pre-converter. In inverting converters, the feedback must be referenced to the converter's ground pin.

[0206] Another feature of CLXU converter **200** is the use of oscillator **215** to control the switching of both MOSFETs **202** and **204** and charge pump **201**. By synchronizing the switched inductor post-regulator and switched capacitor pre-

converter circuits, the size of intermediate filter capacitor **209** can be greatly reduced or in some cases capacitor **209** may be eliminated altogether.

Behavioral Model of CLXU Converters

[0207] To better understand the general operation of CLXU converter **200**, behavioral model **250** of FIG. **9** can be used for control analysis and for estimating efficiency. As shown, step-down pre-converter **200**A is powered from input voltage V_{in} producing an intermediate voltage V_y which in turn powers a switched inductor post-regulator **200**B.

[0208] The conversion ratio of the pre-converter **200**A is given by

$$V_y = n \cdot V_{in}$$

or expressed as a voltage conversion ratio V_y/V_{in} for pre-converter **200**A, the ratio equals

$$\frac{V_y}{V_{in}} = n$$

[0209] Theoretically, since charge pumps are not voltage converters the output voltage V_y of pre-converter **200**A, can be "loaded" by whatever it is driving. Loading means its output is forced to another voltage V_z dissimilar from V_y by an amount ΔV, represented by lossy element **253**. Because voltage V_y is not normally supplying current to any load except post-regulator **200**B, post-regulator **200**B cannot force its input V_z to be substantially different than V_y so that $\Delta V \approx 0$ and $V_y \approx V_z$.

[0210] In the CLXU topology, post-regulator **200**B operates as a step-up or boost converter, given by the relation

$$V_{out} = \frac{V_z}{1-D} \approx \frac{V_y}{1-D}$$

[0211] where D is the duty cycle of the low side MOSFET **202**, ranging between 0% and 100% and with an output similar to curve **18** of FIG. **2**A.

[0212] Combining the two equations gives us the important relationship

$$V_{out} \approx \frac{V_y}{1-D} = \frac{n \cdot V_{batt}}{1-D}$$

[0213] The voltage conversion ratio of the CLXU is therefore given by

$$\frac{V_{out}}{V_{in}} = \frac{n}{1-D}$$

[0214] From this relation, we can make the important observation for the CLXU converter that the converter's output to input ratio is the multiplicative product of its pre-converter's ratio "n" and the post-regulator's duty-factor dependent voltage boost factor 1/(1−D). In essence, to properly regulate an output, the duty factor D, the conversion ratio n, or both must be varied dynamically to compensate for changes in input voltage.

[0215] While the post-regulator of the CLXU converter can only step-up its input to a higher voltage, operating in tandem with the charge pump pre-converter, the combined converter can operate at step-up, step-down, or even unity voltage conversion ratios.

[0216] Specifically, if n<1, the pre-converter **200**A steps down, the post-regulator **200**B steps up and the combination forms an up-down CLDU converter. With a two capacitor fractional charge pump this relation is given by

$$\frac{V_{out}}{V_{in}} = \frac{0.5}{1-D}$$

[0217] FIG. **10** represents a functional diagram of a CLDU down-up converter **300** comprising a 0.5× step-down charge-pump pre-converter **300**A followed by an switched inductor boost converter as a post-regulator **300**B.

[0218] If n>1, the converter **300** operates only as step-up CLUU converter and can achieve high step-up conversion ratios at moderate duty factors. Functional descriptions of single and dual flying capacitors CLUU converters are illustrated in FIGS. **14**A and **14**B. In single capacitor implementations of the pre-converter **501**, as shown in FIG. **14**A, the CLUU converter can be described by the relation

$$\frac{V_{out}}{V_{in}} = \frac{2}{1-D}$$

[0219] In dual capacitor fractional implementations of the pre-converter **521**, as shown in FIG. **14**B, the CLUU converter can be described by the relation

$$\frac{V_{out}}{V_{in}} = \frac{1.5}{1-D}$$

[0220] If n is negative and the post-regulator is non-inverting, the resulting CLIU converter is inverting and supplies a wide range of negative voltages. These inverting CLIU converters are illustrated in FIGS. **18**A and **18**B. For single-capacitor charge-pump implementations such CLIU inverters are described by

$$\frac{V_{out}}{V_{in}} = \frac{-1}{1-D}$$

[0221] Using dual-capacitor fractional inverting charge-pumps, such CLIU inverters are described by

$$\frac{V_{out}}{V_{in}} = \frac{-0.5}{1-D}$$

[0222] In such cases, the boost converter increases the magnitude of the voltage without changing its polarity, i.e. the term "up" refers to increasing the absolute value of a negative voltage without changing its polarity.

[0223] In an alternative embodiment, an inverting boost converter can be used to drive the pre-converter's output more

NOCO Exhibit 2011
ADC v. NOCO
IPR2024-00671

positive and even above zero volts. Strictly speaking, such an implementation uses a positive boost converter referenced to a negative supply voltage—the output of the inverting charge pump. But since the polarity is opposite that of the output of the pre-converter, by convention, this last stage "inverts" the signal a second time.

[0224] A CLXX converter with two inversions is therefore capable of producing and regulating a positive, i.e. above ground, output voltage and is herein referred to as a CLII converter. Such a CLII converter, such as those shown in FIGS. **18**C and **18**D can regulate voltages above and below ground as given by

$$\frac{V_{out}}{V_{in}} = \left[\frac{1}{1-D} - 1\right] = \frac{D}{1-D}$$

for a single capacitor charge pump implementation and by

$$\frac{V_{out}}{V_{in}} = 0.5\left[\frac{1}{1-D} - 1\right] = \frac{0.5 \cdot D}{1-D}$$

for a two-capacitor fractional inverting charge pump.

CLDU Down-Up Converter Operation

[0225] A functional diagram of a CLDU down-up converter **300** is shown in FIG. **10** where converter **300** comprises a 0.5× step-down charge-pump pre-converter **300**A, an inductor **306**, an N-channel low-side switch **307**, a synchronous rectifier **308** with intrinsic P-N diode **308** and an output filter capacitor **310**. Capacitor **304** may range in size depending of the "n" multiple and circuit implementation of charge pump **301** and in some cases can be eliminated. Diode **305** also depends on charge pump **301** design and operation.

[0226] FIGS. **11**A-**11**C illustrate various electrical characteristics of CLDU converter **300**. Specifically, graph **320** in FIG. **11**A illustrates the application of a CLDU converter in regulating the discharge of a single-cell lithium ion battery. The notation "1s Lilon" refers to a single series-connected cell comprising lithium ion electrochemistry.

[0227] As described in graph **320**, a fully charged 1s Lilon battery exhibits a voltage V_{batt} around 4.2V at the onset of discharging illustrated by line segment **321** which settles to a voltage of approximately 3.5V before remaining relatively constant for some extended duration, as revealed by line segment **322**. Later, curve **322** illustrates that the battery voltage decays below 3.5V into a range {Vout<Vbatt<(Vout+δ)} between lines **325** and **326**, a condition where a normal converter would suffer dropout or mode switching problems.

[0228] As the cell approaches full discharge in segment **323**, its voltage drops rapidly to 2.7V, below which it must be cut off to avoid over-discharge induced cell damage. Only specialized Lilon batteries can operate down to 2.7V without growing crystallites and thereby shorting out the cell.

[0229] The output voltage V_y of the 0.5× switched capacitor pre-converter **300**A is illustrated by curve **324**. This intermediate voltage varies in proportion to the battery input voltage discharge characteristic, with a voltage equal to one-half V_{batt}. The inductive boost post-regulator **300**B steps this time-varying intermediate voltage up by a factor 1/(1−D) to produce a constant CLDU output voltage V_{out}, as illustrated by line **325**. The output voltage of CLDU converter **300** can be any voltage greater than the highest value of curve **324**, namely 2.1V. Such an output voltage may be greater than, less than, or within the voltage range of the battery input. For example, as shown V_{out} is 3V, inside the Lilon battery's voltage range of 4.2V to 2.7V.

[0230] Regardless of the Lilon cell voltage, CLDU converter **300** steps the battery voltage down by half with its 0.5× charge-pump pre-converter, a varying voltage V_y represented by line **324**. This voltage is then boosted by a 1/(1−D) duty-factor-dependent boost converter to produce a constant regulated output voltage shown by line **325**. The condition of converter **300** can be described as shown in Table 1:

TABLE 1

Phase	Up/Down	V_{batt}	nX	V_y	D	V_{out}	V_{out}/V_{in}
321. Full charge	Down	4.2 V	0.5X	2.1 V	30%	3 V	0.71
Decay	Down	3.6 V	0.5X	1.8 V	40%	3 V	0.83
322. Plateau	Down	3.5 V	0.5X	1.75 V	42%	3 V	0.86
Discharge $V_{batt} \approx V_{out}$	Unity	3.0 V	0.5X	1.5 V	50%	3 V	1.00
323. Extend Range	Up	2.7 V	0.5X	1.35 V	55%	3 V	1.11

[0231] Using feedback, the duty factor self-adjusts to maintain the proper output voltage and regulation, whereby

$$D = 1 - \frac{V_y}{V_{out}} = 1 - \left[\frac{0.5 \cdot V_{batt}}{V_{out}}\right]$$

[0232] Unlike in conventional Buck-boost converters, as the battery voltage curve **323** passes through the output voltage **325**, i.e. when $V_{in}=V_{out}\approx 3V$, no mode change occurs. CLDU converter **300** therefore remains stable with no dropout and degradation in the quality of regulation.

[0233] Eliminating time as a variable, the transfer characteristic of converter **300** is illustrated in graph **330** of FIG. **11**B, comparing V_{out} to V_{in} for a 3.3V CLDU converter. As shown, unregulated battery input voltage **331** ranging from 2V to 5V is reduced by the 0.5× capacitor pre-converter **300***a* to a lower voltage V_y having a narrower range of 1V to 2.5V, illustrated by line **333**. The slope of line **333** is half that of the input voltage **331**, reducing the sensitivity of converter **300** to noise and other input fluctuations. The intermediate voltage node V_y of line **333** is then stepped up by the inductive boost post-regulator **300**B by a factor 1/(1−D) using a varying duty factor to produce a constant output voltage V_{out}, illustrated by line **334**. Feedback of the output is employed to adjust the duty factor D to maintain V_{out} at 3.3V.

[0234] At point **332**, the input and output voltages are equal and converter **300** is regulating at a unity conversion ratio. When line **331** is above line **334**, i.e. to the right of point **332**, converter **300** is providing a step down regulation. When line **331** is less than **334**, the output voltage is greater than its input and converter **300** is acting as a step-up converter. The mode of operation of converter **300** remains the same throughout all conditions shown, even at point **332**.

[0235] One common application using a single cell Lilon battery and requiring a 3.3V regulated supply is in a cell phone. Unlike a 3V output, where the converter is mostly operating in step-down mode, a 3.3V output requires operation closer to unity conversion and exhibits an extended duration in its step-up mode as shown in Table 2.

NOCO Exhibit 2011
ADC v. NOCO
IPR2024-00671

TABLE 2

Phase	Up/Down	V_{batt}	nX	V_y	D	V_{out}	V_{out}/V_{in}
Full charge	Down	4.2 V	0.5X	2.1 V	36%	3.3 V	0.79
Decay	Down	3.6 V	0.5X	1.8 V	45%	3.3 V	0.92
Plateau	Down	3.5 V	0.5X	1.75 V	47%	3.3 V	0.94
$V_{batt} \approx V_{out}$	Unity	3.3 V	0.5X	1.65 V	50%	3.3 V	1.00
Discharged	Unity	3.0 V	0.5X	1.5 V	55%	3.3 V	1.10
Extend Range	Up	2.7 V	0.5X	1.35 V	59%	3.3 V	1.22

[0236] Despite operating within approximately ±20% of its unity conversion ratio, CLDU converter **300** typically exhibits its duty factors in the narrow range of 36% to 59%, utilizing PWM control circuitry more easily implemented than circuits controlling extreme duty factors, especially at high switching frequencies.

[0237] Unlike the converter of this invention, no present day converter is able to operate with high efficiencies over the battery's entire voltage range. Handset designers today must employ step-down-only Buck converters that cut off around 3.5V, thereby throwing away the battery life in discharge phases (curve **323**) and a portion of voltage-plateau-phase (curve **322**), because the added use-life of these later phases of discharge is completely overcome by the efficiency loss of a conventional Buck-boost converter.

[0238] As previously derived, the conversion ratio of 0.5× CLDU converter **300** is given by

$$\frac{V_{out}}{V_{in}} = \frac{0.5}{1-D}$$

V_{out} is illustrated by line **343** in FIG. **11**C as a function of duty factor and compared to the boost converter's characteristic, shown by line **341**. While the boost converter exceeds the unity voltage conversion ratio, illustrated by dashed line **342**, at all values of the duty factor D, CLDU converter **300** is able to operate both above and below the unity conversion condition. The output voltage V_y of pre-converter **300**A, illustrated by line **344**, however, illustrates that the operation of the pre-converter **300**A does not depend on the duty factor of the boost converter in post-regulator **300**B.

[0239] As shown, a unity conversion ratio occurs in 0.5× CLDU converter **300** when the duty factor D=50%. Under the same condition, a boost converter exhibits a conversion ratio of 2. At low duty factors, where conversion ratio of the boost converter approaches unity, 0.5× CLDU converter **300** is able to supply a regulated output voltage V_{out} roughly equal to one-half the input voltage V_{in}.

[0240] At higher duty factors, e.g. when D=75%, a boost converter manifests a strong dependence on duty factor at a conversion ratio of 4, while CLDU converter **300** exhibits a conversion ratio of only 2. Compared to a boost converter alone, the lower slope of V_{out} in CLDU converter **300** reduces its noise sensitivity to fluctuations in duty factor.

CLDU Converter Implementation

[0241] FIG. **12**A illustrates an implementation of a 0.5× CLDU converter **400**. As shown, switched capacitor pre-converter **400**A comprises MOSFETs **401**, **402**, **403**, **404**, and **405** with flying capacitors **406** and **407**. The gates of MOSFETs **401**, **402**, **403**, **404**, and **405** are controlled by a break-before-make (BBM) unit **415** to alternatively charge and discharge flying capacitors **406** and **407**. The intermediate voltage V_y charges capacitor **408** and powers the input to an inductive post-regulator **400**B, the current flowing into inductor **410**.

[0242] The current flowing through inductor **410** is dynamically adjusted by the duty factor of a low-side N-channel MOSFET **414** with a PWM controller **416** responding to changes in the output voltage of converter **400**. A feedback signal V_{FB} is adjusted in voltage and polarity by a level shift circuit **417** to control PWM controller **416**.

[0243] When low-side MOSFET **414** is conducting, the voltage V_x is biased near ground, at a voltage drop of $I_L \cdot R_{DSN}$, during which time the inductor **410** is magnetized, i.e. stores energy. When MOSFET **414** is turned off, the voltage V_x flies up above the output voltage V_{out} across capacitor **413**, forwarding biasing diode **412** and transferring energy to the output capacitor **413**.

[0244] During some portion of the time while diode **412** is forward biased, a synchronous rectifier MOSFET **411** is turned-on, diverting the current from diode **412**. A break-before-make unit **415** drives the gate of MOSFETs **414** and **411** out-of-phase insuring that the output capacitor **413** is not shorted by the simultaneous conduction of MOSFETs **411** and **414**. In a preferred embodiment, a clock generator **418** synchronizes the switching of MOSFETs **411** and **414** in post-regulator **400**B with the switching of MOSFETs **401**, **402**, **403**, **404**, and **405** in pre-converter **400**A.

[0245] In an alternative embodiment, synchronous rectifier MOSFET **411** is eliminated and the current transfer to output capacitor **413** performed entirely by diode **412**, which is incorporated in converter **400** as a separate device (not an intrinsic diode within MOSFET **411**) and preferably comprises a Schottky metal-semiconductor diode instead of a P-N junction. Schottky diodes are preferred because they exhibit lower forward voltage drops than do junction diodes. In yet another embodiment, a Schottky diode can be placed in parallel with MOSFET **411** and intrinsic P-N diode **412**.

[0246] The operation of CLDU converter **400** is illustrated in FIGS. **12**B and **12**C. In FIG. **12**B, flying capacitors **406** and **407** are charged through the conducting MOSFETs **401** and **403** while MOSFETs **402**, **404** and **405** remain off. Since capacitors **406** and **407** are connected in series, if they have equal capacitance each one charges to a voltage one-half the battery input voltage, i.e. $V_{batt}/2$.

[0247] During this cycle, synchronous rectifier MOSFET **411** is conducting a recirculation current through inductor **410**, thereby moving energy from inductor **410** to output capacitor **413** and load **425**. The phase can be referred to as the "charging and recirculation phase", i.e. the charging of the flying capacitors **406** and **407** and the moving of the energy from the inductor **410** to the output capacitor through inductor recirculation.

[0248] Specifically, during the charging and recirculation phase, the energy in inductor **410** is used to charge output capacitor **413** because inductor **410** forces the voltage V_x to a more positive potential than the output voltage V_{out}, hence the output voltage V_{out} is boosted. Controlled by the inductor **410**, the intermediate voltage V_x changes instantaneously in order to prevent any instantaneous interruption in inductor current I_L. Because charge pump output MOSFETs **404** and **405** are off during this phase, the current transfer path includes filter capacitor **408**. If the capacitance of filter

NOCO Exhibit 2011
ADC v. NOCO
IPR2024-00671

capacitor **408** is substantial, the voltage V_y will remain substantially at $0.5 \cdot V_{batt}$, i.e. the output of the fractional step down charge pump.

[0249] If capacitor **408** is not sufficiently large, the voltage at V_y will decay during the transfer phase and have to be replenished during the subsequent transfer phase. In some instances, e.g. if capacitor **408** is even smaller, the polarity of V_y may actually drop below ground. In such cases, diode **409** can be added to complete the recirculation path of inductor **410** and limit the range of negative voltage on node V_y. In another embodiment, diode **409** may be replaced with a grounded N-channel MOSFET having an intrinsic parallel P-N junction diode and being turned on whenever V_y goes negative.

[0250] FIG. **12**C represents the transfer condition where energy is transferred from flying capacitors **406** and **407** in pre-converter **400**A to inductor **410** in post-regulator **400**B. This transfer is achieved by turning off MOSFETs **401** and **403** and turning on MOSFETs **402**, **404** and **405**, thereby forming a parallel combination of flying capacitors **406** and **407** that is connected in series with inductor **410** and charges capacitor **408** to an voltage V_y equal to the voltage on the flying capacitors **406** and **407**, i.e. $+V_{batt}/2$. The voltage V_y is positive and above ground because the negative terminals of the capacitors are tied to ground—specifically capacitor **407** has its negative terminal hard wired to ground and capacitor **406** has its negative terminal connected to ground through MOSFET **402**.

[0251] Simultaneous with the charging of capacitor **408**, N-channel MOSFET **414** is turned on and conducts a current I_L through inductor **410**, completing the circuit and magnetizing, i.e. storing energy equal to I_L^2L in inductor **410**. Since the voltage at the node V_x is near ground, it is more negative than the output voltage V_{out} and diode **412** is non-conducting, i.e. reversed biased and off. During this cycle MOSFET **411** is turned off and output capacitor **413** must supply the necessary load current I_{out} to electrical load **425**. The voltage across capacitor **413** begins to sag during this cycle and is replenished during the subsequent recirculation cycle shown in FIG. **12**B.

[0252] The two cycles alternate to keep inductor **410** magnetized and flying capacitors **406** and **407** and output capacitors **408** and **413** charged. The entire system is efficient because once the voltage builds up on the capacitors **408** and **413** during start-up, steady-state operation must only replenish enough charge to compensate for the small shifts in voltage resulting from voltage sagging across the capacitors **408** and **413** during their discharge periods.

[0253] As shown in a preferred embodiment, converter **400** is operated using the same switching frequency for all the MOSFETs, with MOSFETs **402**, **403** and **404** switched in phase with MOSFET **414** and out of phase with MOSFETs **401** and **403**. Synchronous rectifier MOSFET **411** may conduct for all or some portion of the time whenever MOSFET **414** is off. Break-before-make unit **415** must guarantee that conduction in transfer MOSFETs **402**, **404**, and **405** never overlaps with conduction in charging MOSFETs **401** and **403**. Similarly, BBM unit **415** must also insure that MOSFETs **414** and **411** never conduct simultaneously.

[0254] The advantage of this embodiment is that energy is transferred from pre-charged flying capacitors **406** and **407** directly into inductor **410** in real time. Converting energy stored in an electric field into energy stored as a magnetic field in real time minimizes the size required for filter capacitor **408**, allowing it to be physically realized as an on-chip capacitor or in some cases even as parasitic junction capacitance.

[0255] In an alternative embodiment of the CLDU converter, the phasing of the MOSFETs comprising the step-up post-regulator may be opposite that of the MOSFETs in the charge pump pre-converter, as illustrated in FIGS. **12**D and **12**E. Specifically, in FIG. **12**D flying capacitors **406** and **407** are charged while the current in inductor **410** re-circulates through conducting MOSFET **414**. During this same time interval, output capacitor **413** must supply load **425** with current. All other MOSFETs including MOSFETs **402**, **404**, **405** and **411**, are turned off.

[0256] This recirculation phase of converter **400** shown in FIG. **12**D is similar to that shown in FIG. **12**B in that the flying capacitors **406** and **407** are charging, but the load **425** is disconnected from inductor **410** rather than taking energy from it. Since Vx is held near ground by on MOSFET **414**, diode **412** remains reversed biased. The size of capacitor **408** must be sufficient to supply power to inductor **410** or the circuit will oscillate and power will be lost.

[0257] In the second phase of this embodiment, shown in FIG. **12**E, flying capacitors **406** and **407** maintain the current in inductor **410** to charge capacitor **408** while inductor **410** is supplying energy to load **425** and output capacitor **413** through conducting synchronous rectifier MOSFET **411**. MOSFETs **401**, **403** and **414** are turned off. With MOSFET **414** off, V_x flies up to a voltage higher than the output voltage V_{out} so that no voltage differential exists to magnetize inductor **410** in this phase, only to maintain current continuity.

[0258] Since in this embodiment inductor **410** is magnetized only when low-side MOSFET **414** is conducting, during which time the only source of stored energy is that present in capacitor **408**, the size of capacitor **408** is typically larger than the size of capacitor **408** in the embodiment shown FIGS. **12**B and **12**C. Whenever a large intermediate capacitor is needed, pre-converter **400**A and post-regulator **400**B are operating more independently and less synergistically than in designs where the energy flow between to the two stages of conversion is more balanced, with less need for storing energy in intermediate capacitor **408**. That balance is best when charge pump pre-converter **400**A and the switched inductor post-regulator **400**B are synchronized to a common clock and phased so that the inductor **410** is magnetized whenever the charge pump within pre-converter **400**A discharges flying capacitors **406** and **407**, as illustrated in FIGS. **12**B and **12**C.

[0259] While charge-pump pre-converter **400**A and switched-inductor post-regulator **400**B are preferably operated at the same frequency and synchronized to a common clock, in an alternative embodiment they may be operated at different frequencies. Referring again to converter **200** shown in FIG. **8**, PWM controller **213** in pre-converter **200**A switches at a clock frequency Φ generated by clock circuit or ramp generator **215** while charge pump **201** switches at a frequency $m \cdot \Phi$, i.e. at a different frequency "m" times the clock frequency. Since m may be greater than or less than unity, charge pump **201** may be operated at a frequency higher or lower than PWM controller **213**. At m=1 pre-converter **200**A and post-regulator **200**B are switching at the same frequency.

[0260] Whenever charge pump pre-converter **200**A is not operating at the same frequency as switched inductor post-regulator **200**B, intermediate filter capacitor **209** becomes increasingly important in storing energy to power post-regulator **200**B and to magnetize inductor **203** as needed. While

the two clocks may "free run" and thereby vary in frequency, unsynchronized operation can lead to excessive switching noise in the system.

[0261] In a preferred embodiment of a multi-frequency implementation of the CLXU converter, the pre-converter and post-regulator circuits switch at different frequencies but are synchronized either by a phase-locked-loop, also known as a PLL, or by using a common clock multiplied-up or divided-down to generate the two dissimilar clock signals. Ideally the clock waveform for the inductive post-regulator comprises a ramp generator rather than oscillating to produce a square wave. The gate drive for the charge pump MOSFETs may, however, comprise square wave signals generated by feeding the output of the ramp generator into a comparator. Alternatively, one or more of the MOSFETs in the charge pump pre-converter may be used to limit the charge pump's inrush current during the charging or discharging of its flying capacitors.

CLXU Converter Efficiency

[0262] One unexpected aspect of a CLXU converter, and in fact any CLXX converter, is the relative independence of its overall efficiency η on input and load conditions. This can better be understood by referring to FIG. **9**, where charge-pump pre-converter **200**A produces an intermediate voltage V_y that provides the input to switched inductor post-regulator **200**B.

[0263] The lossy element **253** is included in the behavioral model to illustrate that because the charge-pump within pre-converter **200**A cannot actually regulate voltage, any voltage mismatch ΔV between its output voltage V_y and the desired input voltage V_z needed to power post-regulator **200**B will result in a further loss of efficiency. In "LC class" converters like those described in related U.S. Application No. [Attorney Docket No. AATI-19-DS-US], closed loop feedback from the output terminal of the entire DC/DC converter is beneficial to counter any "loading" effects on the charge pump. But in "CL class" converters like converter **250** shown in FIG. **9** the output voltage V_y of the charge pump within pre-converter **200**A is internal to converter **250** and unless the input to post-regulator **200**B is used to supply an external load, V_z will naturally operate at the voltage V_y the optimum efficiency condition.

[0264] Specifically, in CLXX type converters, the switched capacitor pre-converter may operate in an open-loop manner to produce an output voltage V_y that is some fixed multiple "n" of its input. For example, using one or two flying capacitors, the multiplier will be an integral multiple of 0.5V. As long as V_z can be maintained near the voltage $n \cdot V_{in}$, i.e. where $V_y \approx V_z$, the efficiency of charge pump pre-converter **20**A will remain high. Any deviation ΔV from this optimum condition will result in a loss of charge pump efficiency, where the mismatch is given by $\Delta V = V_z - V_y$ resulting in a loss that has the same mathematical form $\Delta V/V_{in}$ as the losses in a linear converter, even though lossy element **253** is not really regulating voltage per se. Specifically, the loss may be defined as

$$P_{loss2} = I_y \cdot \Delta V = I_y \cdot |(V_y - V_z)|$$

[0265] The efficiency η_2 of element **253**, is then given by

$$\eta_2 = \frac{P_z}{P_y} = \frac{P_y - P_{loss2}}{P_y} = \frac{I_y \cdot V_y - I_y(V_y - V_z)}{I_y \cdot V_y} = \frac{V_z}{V_y}$$

and where $V_z \leqq V_y$, i.e. the maximum theoretical efficiency of the second element is 100%. From the converter transfer function $V_y = n \cdot V_{in}$ then

$$\eta_2 = \frac{V_z}{V_y} = \frac{V_z}{nV_{in}}$$

[0266] Line **441** in the efficiency graph **440** of FIG. **13**A illustrates η_2 as a function of the input-to-output charge pump voltage conversion ratio. In reality however, the maximum efficiency of charge pump pre-converter **200**A is not 100%. Charge pump pre-converter **200**A typically has a maximum efficiency in the range of 96% when delivering power to a load operating at a voltage V_z. Assuming for the sake of simplicity that this efficiency remains relatively constant, the conversion efficiency of the first two stages is given by

$$\eta_{CP} = \eta_1 \cdot \eta_2 = \eta_2 \frac{V_z}{V_y} = \frac{\eta_2 \cdot V_z}{n \cdot V_{in}}$$

[0267] This equation is illustrated by line **442** in FIG. **13**A. Note that the maximum voltage conversion ratio is limited to the ratio "n". The dashed line above that cannot physically be realized but illustrates the impact of the lossy element **253** is mathematically symmetric, i.e. purely a lossy element. When n=1, the charge pump is not actually stepping up voltage and the efficiency equation defaults to that of linear converter.

[0268] Referring again to behavioral model **250**, the overall efficiency of the CLXU converter shown can be estimated the product of the aforementioned charge pump efficiency $\eta_1 \cdot \eta_2$ and the efficiency of the switched inductor post-regulator η_3.

[0269] The power input to post-regulator **200**B is given by $P_z = I_z \cdot V_z$, while $P_{out} = I_{out} \cdot V_{out}$. The efficiency η_3 of the post-regulator **200**B can thus be expressed as

$$\eta_3 = \frac{P_{out}}{P_z} = \frac{I_{out} \cdot V_{out}}{I_z \cdot V_z}$$

[0270] The voltage dependence of the post-regulator efficiency given by the above equation is illustrated for a given load current by example curve **451**, shown in graph **450** of FIG. **13**B. Typical values range from 94% to 89% depending on operating conditions, power MOSFET resistance and operating currents. Since post-regulator efficiency η_3 depends on the voltage conversion ratio, and since the conversion ratio depends on duty factor D, then it follows logically that the switching converter's efficiency depends on duty factor, i.e. $\eta_3 = f(D)$.

[0271] Overall CLXX converter efficiency is thus given by the efficiency product of the charge-pump pre-converter and the switching post-regulator converter.

$$\eta = \eta_{CP} \cdot \eta_3 = \eta_1 \cdot \eta_3 \frac{V_z}{V_y} = \eta_1 \cdot \eta_3 \frac{V_z}{n \cdot V_{in}}$$

[0272] Graph **455** in FIG. **13**C illustrates the overall efficiency of a CLXX converter for various values of V_z, expressed as a percentage of V_y. Since feedback within post-

NOCO Exhibit 2011
ADC v. NOCO
IPR2024-00671

regulator **200**B maintains the targeted output voltage V_{out} by adjusting its duty factor for a wide range of intermediate voltages V_z then, unloaded, $V_z=V_y=n\cdot V_{in}$ and the above equation simplifies to

$$\eta=\eta_{CP}\cdot\eta_3=\eta_1\cdot\eta_3$$

where η_3 is a function of the duty factor D. Using a step-up, boost converter topology for the post-regulator stage, the CLXU converter transfer function is given by $V_{out}=V_y/1-D=[n/(1-D)]V_{in}$. As such, the efficiency can be re-plotted in terms of duty factor D rather than by conversion ratio V_{out}/V_{in} as illustrated by line **466** in efficiency graph **465** of FIG. **13**D.

[0273] Switched CLXX and CLXU converters of this invention can produce a well regulated output with efficiencies relatively insensitive to the V_{out}/V_{in} voltage conversion ratio. In the event that the charge-pump pre-converter is a step-down fractional charge pump, e.g. where n=½, the resulting CLDU converter is able to operate in either step-up or step-down modes without exhibiting any mode changes, narrow pulse, or dropout effects near unity voltage conversion ratios, i.e. when $V_{out}\approx V_{in}$. The CLDU converter is able to operate over a range of output to input voltage ratios far beyond that of a Buck converter, boost converter or charge pump. Assuming a practical limitation on duty factor ranges between 10% and 90%, Table 3 compares the usable range of voltage conversion ratios of the CLDU converter to those of a charge pump doubler, Buck converter, and boost converter.

TABLE 3

Converter Topology	Range of V_{out}/V_{in}	Range of Efficiency	Unity Ratio Efficiency
2X Charge Pump	0.1 to 2.0	Above 1.8	Poor, η < 50%
Boost Converter	1.1 to 15	Good up to ~8-10	Dropout below 1.1
Buck Converter	0.1 to 0.9	Good over range	Dropout above 0.9
0.5X CLDU	0.1 to ~10	Good up to ~4-5	Good, η > 88%

[0274] Despite its high efficiency characteristic, a Buck converter operating between a 10% to 90% duty factor is only capable of step-down conversion ratios, i.e. where $V_{out}=\{0.1V_{in}$ to $0.9V_{in}\}$ as shown by curve **471**. Similarly a boost converter operating between a 10% to 90% duty factor is only capable of step-up conversion ratios, i.e. where $V_{out}=\{1.1V_{in}$ to $8V_{in}\}$ as shown by curve **472**. Furthermore 2× charge pump efficiency, shown by curve **473**, is high only for conversion ratios exceeding 1.8.

[0275] In contrast, the efficiency of a CLDU converter (curve **474**) is high over a wide range of voltage conversion ratios, i.e. where $V_{out}=\{0.1V_{in}$ to $4V_{in}\}$. This result is unexpected considering that the CLDU converter combines elements of a charge pump and a boost converter, yet regulates over a much wider range of operating conditions than either of them.

Switched Capacitor-Inductor Up-Up (CLUU) Regulating Converters

[0276] A CLXU converter topology is useful for step-up voltage regulation. By utilizing a step-up charge-pump as a pre-converter, step-up voltage conversion is performed in two stages, or as a CLUU converter. Examining the implementation of CLUU converters in greater detail, FIGS. **14**A and **14**B illustrate the functional block representation of two different switched LCUU regulating converters, a 2× type shown in FIG. **14**A and a fractional 1.5× type shown in FIG. **14**B.

[0277] In FIG. **14**A, 2×-type LCUU converter **500** comprises a pre-converter **500**A and a post-regulator **500**B. Pre-converter **500**A comprises a doubler charge pump **501** with a flying capacitor **502** and a filter capacitor **503**. The output of charge pump **501** supplies an intermediate voltage V_y which in turn powers the step-up switched-inductor post-regulator **500**B, comprising an inductor **505**, an N-channel MOSFET **506**, a synchronous rectifier MOSFET **507** with an intrinsic diode **508**, and an output capacitor **509**. In some cases and depending on the magnitude of capacitance C_1, a diode **504** is included to clamp the voltage range of V_y. Since $V_y=2\cdot V_{batt}$ and $V_{out}=V_y/1-D$), then the voltage conversion ratio of the 2×-type CLUU converter is given by

$$\frac{V_{out}}{V_{batt}}=\frac{2}{1-D}$$

[0278] An example of the CLUU converter's ability to regulate a wide range of input voltages is illustrated in graph **550** of FIG. **15**A, where a battery or input voltage **551** varying from 0.9 to 2.4V is used to produce a regulated 5V output **553**. The input range from 0.9V to 1.2V represents the voltage typically supplied by single cell NiMH batteries, the range from 0.9V to 1.7V represents alkaline batteries, while the range from 1.8V to 2.4V represents 2s configured NiMH batteries.

[0279] As shown, the battery input **551** is doubled in voltage by pre-converter **500**A to an intermediate voltage V_y shown by line **552**, and then further stepped up by switched inductor post-regulator **500**B by a varying amount 1/(1−D) to produce regulated output voltage **553**. At battery input voltages as low as 0.9V a 5V input can be produced with a duty factor of only 64% despite delivering a voltage conversion ratio of 5.6. The 2.4V input condition is more difficult since by using a 2× pre-converter, V_y=4.8V, requiring a duty factor in the post-regulator as low as 4%.

[0280] Another example of CLUU regulation is illustrated in graph **560** of FIG. **15**B where the output voltage V_{batt} of a 1s Lilon battery is stepped up and regulated to 12V. The Lilon battery fully charged starts with a 4.2V condition that decays over time (curve **561**) to a plateau voltage of approximately 3.5V (curve **562**) and then eventually reaches its discharged condition of 2.7V (curve **563**). The doubling pre-converter **500**A produces time varying voltage V_y, shown by curve **564**, ranging from 8.4V to 5.4V, which is then further stepped up to 12V by an a varying amount 1/(1−D) by step-up post-regulator **500**B to produce a constant 12V output (curve **565**).

[0281] The wide range of input voltages useful to create and regulate a 12V output is illustrated in graph **580** of FIG. **15**C, where the input voltage ranges from 1.8V, the low condition of a 2s NiMH battery, across the 1s Lilon range of 2.7 to 4.2V, and up to 5.5V, the +10% tolerance condition of a 5V regulated supply.

[0282] As shown in graph **580**, the battery or input voltage (curve **581**) is doubled to produce V_y (curve **582**) and is then boosted by a varying factor of 1/(1−D) to produce a regulated output shown as 12V (curve **583**). Using a 2× type CLUU converter, the duty factor of post-regulator **500**B for 1.8V to 12V conversion is only 70% while the 5V+10% condition requires a duty factor of around 8.3%.

NOCO Exhibit 2011
ADC v. NOCO
IPR2024-00671

[0283] In some cases, 2× pre-converter **500**A produces an undesirably high intermediate voltage V_y at high input voltage conditions, and which forces boost post-regulator **500**B to operate at low duty factors. One way to avoid this problem is to employ a 1.5×-type charge pump pre-converter instead of a doubler.

[0284] For example, as shown in FIG. **14**B, a 1.5×-type LCUU converter **520** comprises a pre-converter **520**A and a post-regulator **520**B. Pre-converter **520**A comprises a fractional charge pump **521** with flying capacitors **522** and **523** and a filter capacitor **524**. The output of charge pump **521** supplies an intermediate voltage V_y which in turn powers step-up switched-inductor post-regulator **520**B, comprising an inductor **526**, an N-channel MOSFET **527**, a synchronous rectifier MOSFET **528** with an intrinsic P-N rectifier diode **529**, and an output capacitor **530**. In some cases and depending on the magnitude of the capacitance C_1 of filter capacitor **524**, diode **525** is included to clamp the voltage range of V_y. Since $V_y=1.5\cdot V_{batt}$ and $V_{out}=V_y/(1-D)$, then the voltage conversion ratio of the 1.5×-type CLUU converter is given by

$$\frac{V_{out}}{V_{batt}} = \frac{1.5}{1-D}$$

[0285] Analogous to the doubler LCUU regulation shown in FIG. **15**A, an example of the ability of 1.5× CLUU converter **520** to regulate a wide range of input voltages is illustrated in graph **600** of FIG. **15**D, where a battery or input voltage varying from 0.9 to 2.4V (curve **601**) is used to produce a regulated 5V output (curve **603**).

[0286] As shown, the battery voltage (curve **601**) is increased by 1.5× by fractional pre-converter **520**A to intermediate voltage V_y shown by line **602**, and then further stepped up by switched inductor post-regulator **520**B by a varying amount 1/(1−D) to produce regulated output voltage (curve **603**). At battery input voltages as low as 0.9V a 5V input can be produced with a duty factor of only 73% despite delivering a voltage conversion ratio of 5.6. Compared to 2× CLUU converter **500**, the 2.4V input condition is not difficult to handle with 1.5× type pre-converter **520**A since an intermediate voltage V_y=3.6V requires a duty factor no lower than 28% in the post-regulator to provide a 5V output.

[0287] The wide range of input voltages that can be used to provide a 12V output using 1.5× CLUU converter **520** is illustrated in graph **610** of FIG. **15**E, where the input voltage shown ranges from 1.8V, the low condition of a 2s NiMH battery, across the 1s Lilon range of 2.7 to 4.2V, and up to 5.5V, the +10% tolerance condition of a 5V regulated supply. The battery or input voltage (curve **611**) is multiplied by 1.5× to produce V_y (curve **612**) then boosted by a varying factor of 1/(1−D) to produce a regulated output (curve **613**) shown as 12V. Using 1.5× type CLUU converter **520**, the duty factor of 1.8V to 12V conversion is only 78%, while the 5V+10% condition requires a duty factor of around 31%, a condition considerably easier to realize than the 8.3% duty factor mandated by the doubler type CLUU converter **500**.

[0288] An example of CLUU regulation using 1.5× type pre-converter **520**A is illustrated in graph **620** of FIG. **15**F where the discharge of a 1s Lilon battery is stepped up and regulated to 12V. The Lilon battery fully charged starts with a 4.2V condition that decays over time (curve **621**) to a plateau voltage of approximately 3.5V (curve **622**) and then eventually reaches its discharged condition of 2.7V (curve **623**). The 1.5×-type fractional pre-converter **520**A produces a time-varying voltage V_y shown by curve **624** ranging from 6.3V to 4.0V which is then further stepped up to 12V by an a varying amount 1/(1−D) by istep-up post-regulator **520**B to produce a constant 12V output (curve **625**).

[0289] The duty factor D of a CLUU converter is lower than that of a boost or CLDU converter, making it ideally suited for providing high voltage conversion ratios. This feature is illustrated in graph **630** in FIG. **15**G showing the voltage conversion ratio at various duty factors. The graph compares the characteristic of 2×-type CLUU converter **500** (curve **635**) to the characteristic of 1.5× type CLUU converter **520** (curve **634**). Both of these characteristics are contrasted with the characteristics of a conventional boost converter (curve **633**), a 1.5× charge pump (curve **631**), and a 2× charge pump (curve **632**).

[0290] None of the converters shown operates below a unity conversion ratio, meaning they are all limited to step-up operation. At low duty factors, the conversion ratio of a boost converter (curve **633**) asymptotically approaches unity, the conversion ratio of 1.5× CLUU converter **520** (curve **634**) approaches 1.5, and the conversion ratio of 2× CLUU converter **500** (curve **635**) approaches 2. At a 50% duty factor, a boost converter provides a conversion ratio of 2, 1.5×-type CLUU converter **520** provides a conversion ratio of 3 and 2×-type CLUU converter **500** provides a conversion ratio of 4. From the relationship

$$D = 1 - \frac{V_y}{V_{out}} = 1 - \left[n\frac{V_{in}}{V_{out}}\right]$$

describing D as function of the reciprocal of the voltage conversion ratio and the pre-converter factor n×, it is clear that larger values of "n" increase the minimum required duty factor for any given conversion ratio. For example, at a 75% duty factor, 2× CLUU converter **500** can step up its input by a factor of 8, double that of a boost converter, but it is limited to providing output voltages greater than twice its input voltage. A 0.5× CLDU converter is usable only for providing output voltages up to twice its input voltage but can provide an output voltage down to half its input voltage, meaning that it is capable of regulating at unity conversion ratio.

[0291] Table 4 summarizes some of these conditions.

TABLE 4

Condition	2X CLUU	1.5X CLUU	Boost	0.5X CLDU
D = 75%	V_{out}/V_{in} = 8	V_{out}/V_{in} = 6	V_{out}/V_{in} = 4	V_{out}/V_{in} = 2
D = 50%	V_{out}/V_{in} = 4	V_{out}/V_{in} = 3	V_{out}/V_{in} = 2	V_{out}/V_{in} = 1
lim D → 0%	V_{out}/V_{in} = 2	V_{out}/V_{in} = 1.5	V_{out}/V_{in} = 1	V_{out}/V_{in} = 0.5
1sNiMH → 12 V	80% < D < 85%	85% < D < 88%	90% < D < 93%*	95%* < D < 96%*

NOCO Exhibit 2011
ADC v. NOCO
IPR2024-00671

TABLE 4-continued

Condition	2X CLUU	1.5X CLUU	Boost	0.5X CLDU
2sNiMH → 12 V	60% < D < 70%	70% < D < 78%	80% < D < 85%	90% < D < 93%*
1sNiMH → 5 V	52% < D < 64%	64% < D < 73%	76% < D < 82%	88% < D < 91%*
Lilon → 12 V	30% < D < 55%	48% < D < 66%	65% < D < 78%	83% < D < 89%
5 ± 10% → 12 V	8%* < D < 25%	31% < D < 44%	54% < D < 63%	77% < D < 81%
2sNiMH → 5 V	4%* < D < 28%	28% < D < 46%	52% < D < 64%	76% < D < 82%

[0292] For input voltages that are a large percentage of the desired output, such as a 5V to 12V, or a Lilon battery to 12V converter, 2×-type CLUU converter **500** may be forced to operate at extremely low duty factors, which may limit the its maximum frequency of operation. In contrast, a CLDU up-down converter has no problem operating at such conditions but is more limited at very high conversion ratios, e.g. generating 12V from a 1s or 2s NiMH dry cell battery pack.

[0293] Those conditions marked with an asterisk (*) may require limiting the converter's operating frequency in order to meet the full range in required duty factors.

[0294] Doubler CLUU Converter: A CLUU converter **640** using a 2×-type pre-converter **640**A is shown in FIG. **16**A. As shown, charge pump doubler pre-converter **640**A comprises MOSFETs **641**, **642**, **643** and **644** and a flying capacitor **645** to provide intermediate output voltage V_y, and an optional filter capacitor **647**. A diode **648** may be included to limit the V_y negative voltage swing and may be omitted depending on the value C_1 of capacitor **647**. Intermediate voltage V_y is connected to inductor **646** of a boost-type post-regulator **640**B, with a low-side N-channel MOSFET **652**, a floating synchronous rectifier MOSFET **649** with an intrinsic P-N diode **650** and an output capacitor **651** driving a load **653**.

[0295] The output of converter **640** is given by the equation

$$V_{out} = \frac{2 \cdot V_{batt}}{(1 - D)}$$

[0296] Post-regulator **640**B is controlled by a PWM controller **655** driving MOSFET **652** in response to the feedback signal V_{FB} from the output terminal of converter **640**, shifted to the appropriate value V_{FBin} by a level shift circuit **666**. The level shift circuit **666** is needed to convert the output voltage V_{out}, which is higher than the battery voltage V_{batt}, to a voltage within the range of the PWM controller **655**. One convenient method to implement level shift circuit **666** involves a resistor divider. The implementation of a feedback circuit is described in the above-referenced Application No. [Attorney Docket No. AATI-19-DS-US].

[0297] As shown, a clock and ramp generator **667** is used to switch PWM controller **655** at a frequency Φ and is used to drive MOSFETs **641**, **642**, **643** and **644** in pre-converter **640**A at a frequency m·Φ, which may be higher or lower than the switching frequency of the MOSFETs **649** and **652** in post-regulator **640**B. In a preferred embodiment, m=1 and charge pump pre-converter **640**A and switched inductor post-regulator **640**B are clocked at the same frequency and synchronized to the same clock. A break-before-make (BBM) circuit **668** provides the gate drive and necessary level shifting V_{G1} to V_{G4} to the charge pump MOSFETs **641**, **642**, **643** and **644**. A BBM circuit **654** drives low-side MOSFET **642** and synchronous rectifier MOSFET **649** in accordance with PWM controller **655**, preventing significant shoot-through conduction, i.e. simultaneous conduction in both MOSFET **649** and MOSFET **659**, to prevent damage to and improve the efficiency of converter **640**.

[0298] As shown in FIGS. **16**B and **16**C, operation of converter **640** occurs in two alternating phases. In the charging and recirculating phase, shown in FIG. **16**B, flying capacitor **645** is charged to substantially the full battery voltage Vbatt through on MOSFETs **643** and **642** while current I_L in inductor **646** re-circulates through diode **650**, on-state synchronous rectifier MOSFET **649** and output capacitor **651** to the load. The recirculation path is completed by capacitor **647**, and if the voltage at V_y sags below ground, by diode **648**. MOSFETs **641**, **644** and **652** remain off in this phase of operation. The on-time of synchronous rectifier MOSFET **649** may be shorter than the entire period when diode **650** is conducting and its beginning and end may be determined by control signals other than simply the gate drive of low-side MOSFET **652**.

[0299] In the second phase, shown in FIG. **16**C, MOSFETs **642**, **643** and, if applicable, **649** are turned off and MOSFETs **641**, **644** and **652** are turned on to connect flying capacitor **645** to inductor **646**, thereby magnetizing inductor **646**. During this phase, output capacitor **651** must supply load **653**. After a prescribed time, determined by PWM controller **655**, converter **640** reverts to the first phase, alternating according to the duty factor set by PWM controller **655**.

[0300] In an alternative converter **710** shown in FIG. **16**E, diode **648** is replaced by a MOSFET **701** and a diode **702**, which are timed to conduct whenever the voltage V_y falls below ground. The operation of MOSFET **701** during recirculation phase **700** is illustrated in FIG. **16**D.

[0301] Alternatively, the synchronous rectifier MOSFET **649** and low-side MOSFET **652** are switched in phase opposite to the charge pump MOSFETs **641**, **642**, **643** and **644**, but this alternative typically requires a larger value C_1 of capacitor **647**. In another embodiment, the synchronous rectifier MOSFET **649** is never turned off fully but only reduced to low current operation, in the range of a few microamperes to reduce noise, as described in the above-referenced Application No. [Attorney Docket No. AATI-18-DS-US].

[0302] Fractional CLUU Converter: A CLUU converter **730** containing a 1.5×-type pre-converter **730**A is shown in FIG. **17**A. As shown, fractional charge pump pre-converter **730**A comprises MOSFETs **731** through **737** and flying capacitors **738** and **739** to provide an intermediate output voltage V_y, and an optional filter capacitor **740**. A diode **741** may be included to limit the V_y negative voltage swing and may be omitted depending on the capacitance value C_1 of capacitor **740**. Intermediate voltage V_y is connected to inductor **742** of a boost-type post-regulator **730**B, with a low-side N-channel MOSFET **743**, a floating synchronous rectifier MOSFET **744** with an intrinsic P-N diode **745**, and an output

NOCO Exhibit 2011
ADC v. NOCO
IPR2024-00671

capacitor **746** driving a load **747**. The output of 1.5×-type LCUU converter **730** is given by the equation:

$$V_{out} = \frac{1.5 \cdot V_{batt}}{(1-D)}$$

[0303] Post-regulator **730**B is controlled by a PWM controller **749**, driving low-side MOSFET **743** in response to a feedback signal V_{FB} from the output terminal of converter **730**, level-shifted to the appropriate value V_{FBin} by a level shift circuit **750**. Level shift circuit **750** is needed to convert the output voltage V_{out}, which is higher than the battery voltage V_{batt}, to a voltage within the range of PWM controller **749**. One convenient method to implement level shift circuit **750** involves a resistor divider. The implementation of a feedback circuit is described in the above-referenced Application No. [Attorney Docket No. AATI-19-DS-US].

[0304] As shown, a clock and ramp generator **751** is used to switch PWM controller **749** at a frequency Φ and is used to drive the MOSFETs **731** through **737** within charge pump pre-converter **730**A at a frequency m·Φ, which may be higher or lower than the switching frequency used to drive post-regulator **730**B. In a preferred embodiment m=1 and charge pump pre-converter **730**A and switched inductor post-regulator **730**A are clocked at the same frequency and synchronized to the same clock. A BBM circuit **752** provides the necessary level shifting for the gate voltages V_{G1} to V_{G7} for the charge pump MOSFETs **731** through **737**. BBM circuit **748** drives low-side MOSFET **743** and synchronous rectifier MOSFET **744** in accordance with PWM controller **749**, preventing significant shoot-through conduction, i.e. simultaneous conduction in both MOSFET **743** and MOSFET **744**, to prevent damage and improve converter efficiency.

[0305] As shown in FIGS. **17**B and **17**C, operation of converter **730** occurs in two alternating phases. In the charging and recirculating phase, shown in FIG. **17**B, each of flying capacitors **738** and **739** is charged to substantially half the battery voltage, i.e. $V_{batt}/2$, through MOSFETs **731**, **732**, and **733**, while current I_L in inductor **742** re-circulates through diode **745**, synchronous rectifier MOSFET **744** and output capacitor **746**, to the load **747**. The recirculation path is completed by capacitor **740** and if the voltage at V_y sags below ground, by diode **741**. MOSFETs **734**, **735**, **736**, **737** and **743** remain off in this phase of operation. The on-time of synchronous rectifier MOSFET **744** may be shorter than the entire period when diode **745** is conducting and its beginning and end may be determined by control signals other than simply the gate drive of low-side MOSFET **743**.

[0306] In the second phase, shown in FIG. **17**C, MOSFETs **731**, **732**, and **733** and, if applicable, **744** are turned off and MOSFETs **734**, **735**, **736**, **737** and **783** are turned on to connect flying capacitors **738** and **739** to inductor **742**, thereby magnetizing inductor **742**. During this phase, output capacitor **746** must supply load **747**. After a prescribed time, determined by PWM controller **749**, converter **730** reverts to the first phase, alternating according to the duty factor set by PWM controller **749**.

[0307] In an alternative embodiment of converter **730** shown in FIG. **17**E, diode **741** is replaced by MOSFET **777** and diode **776**, which are timed to conduct whenever the voltage V_y falls below ground. The operation of MOSFET **777** during recirculation phase **775** is illustrated in FIG. **17**D.

[0308] Alternatively, the synchronous rectifier MOSFET **744** and low-side MOSFET **743** are switched in phase opposite to the charge pump MOSFETs **731** through **737** but require a larger value C_1 of capacitor **740**. In another embodiment, the synchronous rectifier MOSFET **744** is never turned off fully but only reduced to low current operation, in the range of a few microamperes to reduce noise, as described in the above-referenced Application No. [Attorney Docket No. AATI-18-DS-US].

Switched Capacitor-inductor (CLIX) Regulating Inverters

[0309] The generic CLXU converter topology of FIG. **8** is also useful for producing regulated voltages below ground. By utilizing an inverting charge-pump as a pre-converter, inverting voltage conversion is performed in two stages, or as a CLIX converter. While the switched-inductor post-regulator as described comprises an up converter, meaning the magnitude of the voltage is increased, there are two possible polarities later defined as CLIU and CLII, which are referred to herein generically as CLIX inverting converters.

[0310] Examining the implementation of the CL type inverters in greater detail, FIGS. **18**A-**18**D illustrate a functional block representation of four different switched CLIX regulating inverters, comprising −1× type pre-converters in FIGS. **18**A and **18**B, and fractional −0.5× type pre-converters in FIGS. **18**C and **18**D. In FIGS. **18**A and **18**C, the post-regulator comprises a non inverting boost converter, a circuit that increases the absolute value of the magnitude of the negative output voltage, i.e. a more negative voltage, without inverting its polarity. Such circuit topologies are referred top herein as CLIU converters.

[0311] In FIGS. **18**B and **18**D, the post-regulator comprises an inverting boost converter, a circuit that increases the magnitude of the output voltage in a polarity more positive than its intermediate voltage V_y. The output voltage may be below or above ground, i.e. positive or negative polarity so long as V_{out} is more positive than intermediate voltage V_y. Such circuit topologies are referred top herein as CLII converters.

[0312] Non-inverting Boost Post-regulators: In FIG. **18**A, a −1× type CLIU converter **800** comprises a charge pump **801** with a flying capacitor **802** and a filter capacitor **803**. The output of charge pump **801** supplies a negative, i.e. below ground, intermediate voltage V_y which in turn powers a non-inverting step-up switched-inductor post-regulator comprising an inductor **805**, an N-channel MOSFET **806**, a synchronous rectifier MOSFET **808** with intrinsic rectifier diode **809** and an output capacitor **810**. MOSFET **806** includes P-N diode **807**, which remains reverse biased since $V_x \leqq 0$. In some cases, depending on the magnitude of capacitance C_1 of filter capacitor **803**, a diode **804** is included to clamp the positive voltage range of V_y. Since $V_y = -1 \cdot V_{batt}$ and $V_{out} = V_y/(1-D)$, then the voltage conversion ratio of converter **800** is given by

$$\frac{V_{out}}{V_{batt}} = \frac{-1}{1-D} = \frac{1}{D-1}$$

[0313] An example of CLIU conversion using a −1× type CLIU converter is illustrated in graph **1150** of FIG. **23**A, where the discharge of a 1s Lilon battery is inverted and regulated to −5V. The Lilon battery fully charged starts with a 4.2V condition that decays over time to a plateau voltage (curve **1151**) of approximately 3.5V and then eventually

NOCO Exhibit 2011
ADC v. NOCO
IPR2024-00671

reaches its discharged condition of 2.7V. The single-capacitor pre-converter produces a time varying negative voltage $-V_y$, shown by curve **1152**, ranging from −4.2V to −2.7V, which is stepped up in (absolute) magnitude to −5V by a varying amount 1/(1−D), using a non-inverting step-up post-regulator to produce a constant −5V output (curve **1153**).

[0314] A similar graph **1170** of FIG. **23**C illustrates the discharge of a two-series cell connected nickel-metal-hydride battery, or 2s NiMH, regulated by the −1×-type LCIU inverter to −5V. The input voltage (curve **1171**) ranging in value from 2.4V to 1.8V during discharge is inverted to produce $-V_y$ (curve **1172**) ranging from −2.4V to −1.8V. V_y is then regulated by a factor 1/(1−D) by a non-inverting boost converter to produce a regulated output voltage of −5V (curve **1173**). Operation to produce −12V would require similar operation but at different duty factors.

[0315] The ability of the −1× LCIU inverter to create a −5V or −12V output from a wide range of input voltages is illustrated in graph **1190** of FIG. **23**E, with inputs as shown ranging from 2V up to 6V, a range including a 1s Lilon discharge condition. As shown, battery or input voltage (curve **1191**) is inverted to produce intermediate voltage V_y, shown by curve **1192**. Using a non-inverting boost type post-regulator operating a duty factor D_1, a regulated −5V output (curve **1193**) is produced, or at a different duty factor D_2, a −12V output (curve **1194**) may be produced.

[0316] Another example of the CLIU converter's flexibility to invert and regulate a wide range of input voltages is illustrated in graph **1210** of FIG. **23**G, where a battery or input voltage (curve **1211**) varying from 0.9 to 2.4V is used to produce a regulated −3.3V output (curve **1213**). The input range from 0.9V to 1.2V represents single cell NiMH batteries, the range from 0.9V to 1.7V represents alkaline batteries, while the range from 1.8V to 2.4V represents 2s configured NiMH batteries.

[0317] As shown in graph **1210**, the battery or input voltage (curve **1211**) is inverted by the charge pump pre-converter to produce V_y (curve **1212**) and is then boosted by a varying factor of 1/(1−D) to produce an output voltage (curve **1213**), shown here as −3.3V. Alternatively, a different duty factor range could be employed to produce a −12×V output (not shown).

[0318] In some cases, a −1× pre-converter produces an undesirably large negative intermediate voltage Vy at high input voltage conditions, and forcing the boost post-regulator to operate at low duty factors. One way to avoid this problem is to employ a −0.5×-type fractional charge pump inverting pre-converter instead of a −1× type pre-converter.

[0319] In FIG. **18**C, a −0.5× type CLIU converter **860** includes a fractional charge pump **872** with flying capacitors **861** and **862** and a filter capacitor **863**. The output of charge pump **870** supplies a negative, i.e. below ground, intermediate voltage V_y which in turn powers a non-inverting step-up post-regulator comprising an inductor **864**, an N-channel MOSFET **865**, a synchronous rectifier MOSFET **868** with intrinsic rectifier diode **867** and an output capacitor **869**. MOSFET **865** includes a P-N diode **866** which remains reverse biased since $V_x \leqq 0$. In some cases, depending on the capacitance C_1 of capacitor **863**, a diode **871** is included to clamp the positive voltage range of V_y. Since $V_y = -0.5 \cdot V_{batt}$ and $V_{out} = V_y/(1-D)$, then the voltage conversion ratio of the −0.5×-type CLIU converter is given by

$$\frac{V_{out}}{V_{batt}} = \frac{-0.5}{1-D} = \frac{0.5}{D-1}$$

[0320] An example of CLIU conversion using a −0.5× type CLIU converter is illustrated in graph **1150** of FIG. **23**B where the discharge of a 1s Lilon battery is inverted and regulated to −3V. The Lilon battery fully charged starts with a 4.2V condition that decays over time to a plateau voltage (curve **1161**) of approximately 3.5V and then eventually reaches its discharged condition of 2.7V. The double-capacitor pre-converter produces a time varying negative voltage $-V_y$, shown by curve **1152**, ranging from −2.1V to −1.35V. V_y is then stepped up in magnitude to −3V by an a varying amount 1/(1−D) using a non-inverting step-up post-regulator to produce a constant −3V output (curve **1163**).

[0321] The ability of the −0.5× CLIU inverter to create and regulate a −5V output from a wide range of input voltages is illustrated in graph **1200** of FIG. **23**F, with inputs as shown ranging from 2V up to 6V, a range including a is Lilon discharge condition. As shown, battery or input voltage (curve **1201**) is inverted and halved to produce intermediate voltage V_y, shown by curve **1202**, ranging from 1 to 3V. Using a non-inverting boost type post-regulator operating at a duty factor D_1, a regulated −5V output (curve **1203**) is produced, or at a different duty factor, a −3.3V output (not shown) may be produced.

[0322] Another example of the CLIU converter's flexibility to invert and regulate a wide range of input voltages is illustrated in graph **1210** of FIG. **23**G, where a battery or input voltage (curve **1211**) varying from 0.9 to 2.4V is used to produce a regulated −3.3V output (curve **1213**). The input range from 0.9V to 1.2V represents single cell NiMH batteries, the input range from 0.9V to 1.7V represents alkaline batteries, while the input range from 1.8V to 2.4V represents 2s configured NiMH batteries.

[0323] The duty factor for CLIX inverters can be derived by rearranging the formula for the CLXU converter to yield

$$D = 1 - \left[n\frac{V_{in}}{V_{out}}\right]$$

[0324] Since n<0 and $V_{in}/N_{out}<0$, both numbers are negative and the duty factor equation mathematically behaves the same as a non-inverting converter. This principle is illustrated in graph **1220** of FIG. **23**H where curve **1221** represents a boost converter's conversion ratio as a function of duty factor. The conversion ratio of a −1×-type CLIU inverter (curve **1223**) is the negative mirror image of curve **1221** and the conversion ratio of a −0.5×-type CLIU inverter is half that value, or a mirror image of the conversion ratio of a +0.5× CLDU converter, described previously. In some sense, the −0.5× CLIU converter is analogous to an inverted form of a down-up converter since it can produce voltages above and below $-V_{batt}$.

[0325] Table 5 contrasts the D=50% preferred conversion ratio for the −1× CLIU and −0.5× CLIU converters and illustrates the duty factor range needed to output several negative output voltages from a Lilon battery.

NOCO Exhibit 2011
ADC v. NOCO
IPR2024-00671

TABLE 5

Condition	−0.5X LCDU	−1X LCDU	Boost (Positive)
D = 50%	V_{out}/V_{in} = −0.55	V_{out}/V_{in} = −1.0	V_{out}/V_{in} = 1.0
Lilon → 3.0 V	N/A	71% < D < 100%*	71% < D < 100%*
Lilon → 2.7 V	N/A	64% < D < 90%	64% < D < 90%
Lilon → 1.8 V	N/A	43% < D < 60%	43% < D < 60%
Lilon → 0.9 V	42% < D < 60%	21% < D < 30%*	21% < D < 30%*

[0326] Those conditions marked with an asterisk (*) may require limiting the converter's operating frequency in order to meet the full range in required duty factors. Those marked with N/A require both step-up and step-down inversion.

[0327] CLIU Converter Implementation: A CLIU converter **920** using a −1×-type pre-converter **920**A is shown in FIG. **19**A. As shown, charge pump inverting pre-converter **920**A includes MOSFETs **921**, **923**, **924**, and **925** and a flying capacitor **922** and provides an intermediate negative output voltage $-V_y$. A filter capacitor **926** is optional. Also, a diode **927** may be included to limit the positive voltage swing of V_y and may be omitted depending on the capacitance value C_1 of a capacitor **926**. Intermediate voltage V_y is connected to an inductor **928** of a non-inverting boost-type post-regulator **920**B with a ground-connected MOSFET **929**, a floating synchronous rectifier MOSFET **932** with an intrinsic P-N diode **931** and an output capacitor **933** driving the load. Since $V_x \leqq 0$, the output of converter **920** is given by the equation

$$V_{out} = -\frac{V_{batt}}{(1-D)} = \frac{V_{batt}}{(D-1)}$$

[0328] Post-regulator **920**B is controlled by a PWM controller **935** driving MOSFET **929** in response to the feedback signal V_{FB} from the output terminal of converter **920**, level shifted to the appropriate value V_{FBin} by a level shift circuit **937**. The level shift circuit **937** is needed to convert the output voltage V_{out} which is negative, i.e. below circuit ground, to a voltage within the range of PWM controller **935**. One convenient method to implement level shift circuit **937** involves a current mirror. The implementation of various feedback circuits is described in the above-referenced Application No. [Attorney Docket No. AATI-19-DS-US].

[0329] As shown in FIG. **19**A, a clock and ramp generator **936** is used to switch PWM controller **935** at a frequency Φ and is used to drive the charge pump MOSFETs **921**, **923**, **924**, and **925** at a frequency m·Φ, which may be higher or lower than the switching frequency used to drive post-regulator **920**B. In a preferred embodiment m=1 and charge pump pre-converter **920**A and switched inductor post-regulator **920**B are clocked at the same frequency and synchronized to the same clock. A BBM circuit **938** provides the gate drive and necessary level shifting to generate the gate voltages V_{G1} to V_{G4} of the charge pump MOSFETs **921**, **923**, **924**, and **925**, respectively. A BBM circuit **934** drives MOSFET **929** and synchronous rectifier MOSFET **932** in accordance with PWM controller **935**, preventing significant shoot-through conduction, i.e. simultaneous conduction in both MOSFET **929** and MOSFET **932**, to prevent damage to and improve the efficiency of converter **920**.

[0330] FIGS. **19**B and **19**C show that the operation of converter **920** occurs in two alternating phases. In the charging and recirculating phase, shown in FIG. **19**B, flying capacitor **922** is charged to substantially the full battery voltage Vbatt through on MOSFETs **921** and **923**, while the current I_L in inductor **928** re-circulates through diode **931**, the on-state synchronous rectifier MOSFET **932**, output capacitor **933**, and load **951**. The recirculation path is completed by capacitor **926**, and if the voltage V_y rises above ground, diode **927** will also conduct. MOSFETs **924**, **923** and **929** remain off in this phase of operation. The on-time of synchronous rectifier MOSFET **932** may be shorter than the entire period when diode **931** is conducting and control signals other than simply the gate drive of ground connected MOSFET **929** may determine when it begins and ends.

[0331] In the second phase, shown in FIG. **19**C, MOSFETs **921**, **923** and **932** are turned off and MOSFETs **924**, **925** and **929** are turned on to connect flying capacitor **922** to inductor **928**, thereby magnetizing inductor **928**. During this phase, output capacitor **933** must supply load **931**. After a prescribed time determined by the PWM controller **935**, converter **920** reverts to the first phase.

[0332] In an alternative embodiment shown in circuit diagram **970** of FIG. **19**D, diode **927** is replaced by a MOSFET **971** and a diode **972** which are timed to conduct whenever the voltage V_y falls below ground.

[0333] Alternatively the synchronous rectifier MOSFET **932** and ground-connected MOSFET **929** may be switched in a phase opposite to that of the charge pump MOSFETs **921**, **923**, **924**, and **925**, but this alternative may require a larger value of the capacitance C_1 of capacitor **926**. In another embodiment the synchronous rectifier MOSFET **932** is never turned off fully but only reduced to low current operation, in the range of a few microamperes to reduce noise, as described in the above-referenced Application No. [Attorney Docket No. AATI-18-DS-US].

[0334] Fractional CLIU Converter: A CLIU converter **1060** using a −0.5×-type pre-converter **1060**A is shown in FIG. **21**A. As shown, the fractional charge pump pre-converter **1060**A includes MOSFETs **1061** through **1067** and flying capacitors **1068** and **106**, with an intermediate output voltage V_y. A filter capacitor **1070** is optional. Also, a diode **1071** may be included to limit the positive swing of the voltage V_y and may be omitted depending on the capacitance C_1 of capacitor **1070**. Intermediate voltage V_y is provided to an inductor **1072** of a non-inverting boost-type post-regulator **1060**B, which also includes a ground-connected MOSFET **1073**, a floating synchronous rectifier **1074** MOSFET with an intrinsic P-N diode **1075** and an output capacitor **1076** driving a load. The output of converter **1060** is given by the equation

$$V_{out} = -\frac{0.5 \cdot V_{batt}}{(1-D)} = \frac{0.5 \cdot V_{batt}}{(D-1)}$$

[0335] Post-regulator **1060**B is controlled by a PWM controller **1079** driving MOSFET **1073** in response to the feedback signal V_{FB} from the output terminal of converter **1060**, level-shifted to the appropriate value V_{FBin} by a level shift circuit **1080**. Level shift circuit **1080** is needed to convert the output voltage V_{out} which is negative, i.e. below ground, to a positive signal within the range of PWM controller **1079**. One convenient method to implement level shift circuit **1080** involves a current mirror. The implementation of various

feedback circuits is described in the above-referenced Application No. [Attorney Docket No. AATI-19-DS-US]

[0336] As shown in FIG. **21**A, a clock and ramp generator **1078** is used to switch PWM controller **1079** at a frequency Φ and to drive the charge pump MOSFETs **1061** through **1067** at a frequency m·Φ which may be higher or lower than the switching frequency of post-regulator **1060**B. In a preferred embodiment m=1, and charge pump pre-converter **1060**A and switched inductor post-regulator **1060**B are clocked at the same frequency and synchronized to the same clock. A BBM circuit **1081** provides the gate drive and necessary level shifting to generate the gate voltages V_{G1} to V_{G7} of the charge pump MOSFETs **1061** through **1067**. respectively. A BBM circuit **1077** drives low-side MOSFET **1073** and synchronous rectifier MOSFET **1074** in accordance with PWM controller **1079**, preventing significant shoot-through conduction, i.e. simultaneous conduction in both MOSFET **1073** and MOSFET **1074**, to prevent damage to and improve the efficiency of converter **1060**.

[0337] FIGS. **21**B and **21**C show that the operation of converter **1060** occurs in two alternating phases. In the charging and recirculating phase, shown in FIG. **21**B, each of flying capacitors **1068** and **1069** is charged to substantially half the battery voltage, i.e. $V_{batt}/2$, through MOSFETs **1061**, **1062**, and **1063**, while the current I_L in inductor **1072** re-circulates through diode **1075**, synchronous rectifier MOSFET **1074**, output capacitor **1076**, and the load **1082**. The recirculation path is completed by capacitor **1070** and if the voltage at V_y rises above ground, diode **1071** also conducts. MOSFETs **1064**, **1065**, **1066**, **1067** and **1073** remain off in this phase of operation. The on-time of synchronous rectifier MOSFET **1074** may be shorter than the period when diode **1075** is conducting and control signals other than simply the gate drive of ground-connected MOSFET **1073** may be used to determine when it begins and ends.

[0338] In the second phase, shown in FIG. **21**C, MOSFETs **1061**, **1062**, **1063** and **1074** are turned off and MOSFETs **1064**, **1065**, **1066**, **1067** and **1063** are turned on to connect flying capacitors **1068** and **1069** to inductor **1072**, thereby magnetizing inductor **1072**. During this phase, output capacitor **1076** must supply load **1082**. After a prescribed time, determined by the PWM controller **1079**, converter **1060** reverts to the first phase.

[0339] In an alternative embodiment, shown in circuit diagram **1099** of FIG. **21**D, diode **1071** is replaced by MOSFET **1083** and diode **1084** which are timed to conduct whenever the voltage V_y rises above ground.

[0340] Alternatively, the synchronous rectifier MOSFET **1074** and ground connected MOSFET **1073** may be switched in phase opposite to the charge pump MOSFETs **1061** through **1067**, but this alternative may require a larger value of the capacitance C_1 of capacitor **1070**. In another embodiment, the synchronous rectifier MOSFET **1074** is never turned off fully but only reduced to low current operation, in the range of a few microamperes to reduce noise, as described in the above-referenced Application No. [Attorney Docket No. AATI-18-DS-US], filed contemporaneously herewith and incorporated herein by reference.

[0341] Inverting Boost Post-regulators: An alternative implementation of a CLXX type converter utilizes a boost post-regulator referenced to a negative supply rail to produce a voltage more positive than that rail. The resulting output voltage may be above or below ground, but it will be more positive than the negative supply rail to which the boost post-regulator is referenced. Since the boost post-regulator boosts voltage in an opposite direction to the charge pump and may even produce a positive output voltage, the post-regulator is also inverting. The resulting converter is referred to herein as a CLII converter.

[0342] A functional diagram of a LCII converter **830** is illustrated in FIG. **18**B. Converter **830** includes pre-converter **830**A which contains a −1× type charge pump **831** with a flying capacitor **832** and a filter capacitor **833**. The output of charge pump **831** supplies a negative, i.e. below ground, intermediate voltage V_y which in turn forms a negative supply rail and powers a step-up switched-inductor post-regulator **830**B comprising an inductor **837**, a $-V_y$ rail-connected MOSFET **835**, a synchronous rectifier MOSFET **838** with an intrinsic rectifier diode **839**, and an output capacitor **840**. MOSFET **835** includes a P-N diode **836** which remains reverse biased since $V_y<0$ and $V_x>0$. In some cases, depending on the magnitude of capacitance C_1 of capacitor **833**, a diode **834** is included to clamp the positive voltage range of V_y.

[0343] In converter **830**, the negative supply rail to which the boost converter within post-regulator **830**B is referenced is given by $V_y=-1\cdot V_{batt}$. If the input powering the boost converter is defined as V_{inb}, then $V_{out}=[Vy+|V_{inb}|/(1-D)]$ or as $V_{out}=[-V_{batt}+|V_{inb}|/(1-D)]$. Theoretically any voltage V_{inb} can power the boost converter to, e.g. V_y, $V_y/2$ or $V_{batt}+V_y/2$, but the most negative potential in the circuit is not ground—it is V_y which in this application is equal to $-V_{batt}$.

[0344] One of the most convenient inputs is to power the boost stage between ground and the negative supply rail V_y, as shown in FIG. **18**B, so that in the case of the −1×-type LCII converter, $V_{inb}=V_{batt}$. Given that condition, so that $V_{out}=[Vy+|V_y|/(1-D)]$, then the voltage conversion ratio of the −1×-type CLII converter is given by

$$\begin{aligned} V_{out} &= y + \frac{|Vy|}{1-D} \\ &= -V_{batt} + \frac{|V_{batt}|}{1-D} \\ &= V_{batt}\left(\frac{1}{1-D} - 1\right) \\ &= V_{batt}\left(\frac{D}{1-D}\right) \end{aligned}$$

yielding the transfer function

$$\frac{V_{out}}{V_{batt}} = \frac{D}{1-D}$$

which evaluated over a range from 0% to 100% has a positive value of approximately 0 volts, i.e. ground, at duty factors approaching 0% and at duty factors approaching 100% grows exponentially.

[0345] FIG. **24**A shows, for example, the discharge of the Lilon battery from 4.2V down to 2.7V along curve **1301**. In the −1× type LCII inverter, a negative mirror image voltage V_y of the battery input V_{batt}, shown by curve **1302**, is then used to produce a positive output voltage. At a duty factor D_1, the output V_{out1} is maintained by feedback at 5V, shown by curve **1303**, a voltage greater than the battery's voltage range. By varying the duty factor to D**2**, feedback maintains the output

V_{out2} at +0.9V, shown by curve **1304**, below the range of V_{batt} (curve **1301**). By varying the duty factor to D_3, a V_{out3} at a voltage within the range of V_{batt} is obtained (curve **1305**).

[0346] FIG. **24**C illustrates the use of a −1× CLII converter with a 1s NiMH dry cell. As shown the battery discharge (curve **1321**) powers the −1× charge pump inverter to create a varying negative V_y rail (curve **1322**), a negative mirror image of the battery voltage. This rail is then used to power one of several possible up converters. At a duty factor D_1, feedback is used to maintain a V_{out1} **1323** of 0.7V (curve **1323**). At duty factor D_2, feedback is used to maintain a V_{out2} of 1.5V (curve **1324**). At duty factor D_3, feedback is used to maintain a V_{out3} of 5V (curve **1325**). One CLII converter is thus capable of operating over a wide range of conditions.

[0347] The operating range of −1×-type CLII converter **830** is also illustrated in FIGS. **24**D and **24**E. In graph **1330** of FIG. **24**D, a range of input voltages from 0.9 to 2.4V, illustrated as curve **1331**, is inverted by the charge pump pre-converter **830**A to a voltage range shown by curve **1332**. The range shown as curve **1332** is then used to power the boost post-regulator **830**B to produce various output voltages. At a duty factor D_1, a V_{out1}, of 3.6V (curve **1333**), a voltage above the battery input, is produced. At a duty factor D_2, a V_{out2} of 0.7V (curve **01334**), a voltage below the battery input, is produced. At a duty factor D_3, a V_{out3} of 1.0V (curve **1335**), a voltage within the battery input range, is produced.

[0348] Similarly, −1× LCII regulation for 2V to 5.5V inputs is illustrated in graph **1340** of FIG. **24**E, where the battery input (curve **1341**) is inverted by charge pump pre-converter **830**A to a varying negative voltage rail V_y, shown by curve **1342**. At a duty factor D_1, an output voltage V_{out1} of 310V (curve **1343**), a voltage above the input range, is produced. At a duty factor D_2, an output voltage V_{out2} of 0.9V (curve **1344**), a voltage well below the battery input, is produced. At a duty factor D_3, an output voltage V_{out3} of 3.3V (curve **1344**), a voltage within the specified battery input range is produced.

[0349] Since the negative voltage produced by the charge pump is the voltage powering the boost post-regulator, and since a boost converter can only output a voltage greater than its input voltage, the minimum output voltage of the LCII converter is zero volts. But its maximum output voltage is limited only by its duty factor. Capable of output-to-input voltage conversion ratios less than and greater than unity, the LCII converter can be considered a special implementation of a down-up converter. This feature of the CLII converter is illustrated in graph **1350** of FIG. **24**F by curve **1353**, showing its ability to regulate at unity conversion ratios, a feature not available in boost converters (curve **1351**) and Buck converters (curve **1352**).

[0350] A circuit diagram of a CLII converter **1000** using a −1×-type pre-converter **1000**A is shown in FIG. **20**A. As shown, charge pump inverting pre-converter **1000**A includes MOSFETs **1001**, **1003**, and **1004** and a flying capacitor **1002** and provides an intermediate negative output voltage $V_y = -V_{batt}$. Intermediate voltage V_y is connected to a MOSFET **1014** in an inverting boost-type post-regulator **1000**B with a ground-connected inductor **1005**, a floating synchronous rectifier MOSFET **1007** with an intrinsic P-N diode **1006** and an output capacitor **1008** driving the load.

[0351] Post-regulator **1000**B is controlled by a PWM controller **1010** driving MOSFET **1014** in response to the feedback signal V_{FB} from the output terminal of converter **1000**, level shifted to the appropriate value V_{FBin} by a level shift circuit **1011**. The level shift circuit **1011** is needed to convert the output voltage V_{out} to a voltage within the range of PWM controller **1010**. One convenient method to implement level shift circuit **1010** involves a current mirror. The implementation of various feedback circuits is described in the above-referenced Application No. [Attorney Docket No. AATI-19-DS-US].

[0352] As shown in FIG. **20**A, a clock and ramp generator **1012** is used to switch PWM controller **1010** at a frequency Φ and is used to drive the charge pump MOSFETs **1001**, **1003**, and **1004** at a frequency m·Φ, which may be higher or lower than the switching frequency used to drive post-regulator **1000**B. In a preferred embodiment m=1 and charge pump pre-converter **1000**A and switched inductor post-regulator **1000**B are clocked at the same frequency and synchronized to the same clock. A BBM circuit **1013** provides the gate drive and necessary level shifting to generate the gate voltages V_{G1} to V_{G3} of the charge pump MOSFETs **1001**, **1003**, and **1004**, respectively. A BBM circuit **1009** drives MOSFET **1014** and synchronous rectifier MOSFET **1007** in accordance with PWM controller **1010**, preventing significant shoot-through conduction, i.e. simultaneous conduction in both MOSFET **1007** and MOSFET **1014**, to prevent damage to and improve the efficiency of converter **1000**.

[0353] FIGS. **20**B and **20**C show that the operation of converter **1000** occurs in two alternating phases. In the charging and recirculating phase, shown in FIG. **20**B, flying capacitor **1002** is charged to substantially the full battery voltage Vbatt through MOSFETs **1001** and **1003**, while the current I_L in inductor **1005** re-circulates through diode **1006**, the on-state synchronous rectifier MOSFET **1007**, output capacitor **1008**, and load **1015**. The recirculation path is completed by capacitor **1008**. MOSFET remains off in this phase of operation. The on-time of synchronous rectifier MOSFET **1007** may be shorter than the entire period when diode **1006** is conducting and control signals other than simply the gate drive of ground connected MOSFET **929** may determine when it begins and ends.

[0354] In the second phase, shown in FIG. **20**C, MOSFETs **1001**, **1003** and **1007** are turned off and MOSFETs **1004** and **1014** are turned on to connect flying capacitor **1002** to inductor **1005**, thereby magnetizing inductor **1005**. During this phase, output capacitor **1008** must supply load **1015**. After a prescribed time determined by the PWM controller **1010**, converter **1000** reverts to the first phase.

[0355] Alternatively the synchronous rectifier MOSFET **1007** and V_y-connected MOSFET **1014** may be switched in a phase opposite to that of the charge pump MOSFETs **1001**, **1003**, and **1003**, but this alternative may require that a capacitor be connected between the node V_y and ground. In another embodiment the synchronous rectifier MOSFET **1007** is never turned off fully but only reduced to low current operation, in the range of a few microamperes to reduce noise, as described in the above-referenced Application No. [Attorney Docket No. AATI-18-DS-US].

[0356] Another LCII converter **890** is illustrated in functional blocks in FIG. **18**D. Converter **890** includes a pre-converter **890**A containing a −0.5× fractional type charge pump **891** with flying capacitors **892** and **893** and a filter capacitor **894**. The output of charge pump **891** supplies a negative, i.e. below ground, intermediate voltage V_y which in turn forms a negative supply rail and powers a step-up switched-inductor post-regulator **890**B, which includes a MOSFET **896** connected between an inductor **898** and $-V_y$, a synchronous rectifier MOSFET **900** with an intrinsic diode

899, and an output capacitor **901**. MOSFET **896** includes a P-N diode **897** which remains reverse biased since $V_y<0$ and $V_x>0$. In some cases, depending on the magnitude of capacitance C_1 of capacitor **894**, a diode **895** is included to clamp the positive voltage range of V_y. While any input voltage may be used to power the boost converter, FIG. **18**D illustrates a case where the input voltage is equal to the positive polarity of the V_y supply rail. The transfer characteristic for such a converter is

$$\frac{V_{out}}{V_{batt}} = \frac{0.5 \cdot D}{1 - D}$$

a ratio that that of the −1× CLII converter described previously.

[0357] The operation of −0.5× type CLII converter **890** is illustrated by graph **1310** in FIG. **24**B, where a Lilon battery voltage ranging from 4.2V to 2.7V (curve **1311**) is inverted by a −0.5× type fractional charge pump to produce a varying V_y negative supply rail (curve **1312**). At a duty factor D_1, a V_{out1} of +0.9V (curve **1313**), a voltage below the battery, is produced. At a duty factor D_2, a V_{out2} of 5V (curve **1314**), a voltage well above the battery input, is produced. At a duty factor D_3, a V_{out3} of 3.3V (curve **1315**), a voltage within the Lilon battery input range, is produced.

[0358] The −0.5× CLII converter **890** is also capable of output to input voltage conversion ratios less than and greater than unity, and can therefore be considered a special implementation of a down-up converter. This feature of the CLII converter is illustrated in graph **1360** of FIG. **24**G by curve **1364** showing its ability to regulate at unity conversion ratios, a feature not available a in boost converter (curve **1361**) or a Buck converter (curve **1362**). The conversion ratios for a −1×-type CLII converter (curve **1363**) is included as a reference.

[0359] A circuit diagram of a CLIU converter **1100** using a −0.5×-type pre-converter **1100**A is shown in FIG. **22**A. As shown, charge pump inverting pre-converter **1100**A includes MOSFETs **1101**, **1102**, **1103**, **1104**, **1105**, **1106**, and **1107** and flying capacitors **1108** and **1109** and provides an intermediate negative output voltage $V_y=-0.5V_{batt}$. Intermediate voltage V_y is connected to a MOSFET **1119** of an inverting boost-type post-regulator **1100**B with a V_{batt}-connected inductor **1118**, a floating synchronous rectifier MOSFET **1110** with an intrinsic P-N diode **1111** and an output capacitor **1112** driving the load.

[0360] Post-regulator **1100**B is controlled by a PWM controller **1114** driving MOSFET **1119** in response to the feedback signal V_{FB} from the output terminal of converter **1100**, level shifted to the appropriate value V_{FBin} by a level shift circuit **1115**. The level shift circuit **1115** is needed to convert the output voltage V_{out} to a voltage within the range of PWM controller **1114**. One convenient method to implement level shift circuit **1114** involves a current mirror. The implementation of various feedback circuits is described in the above-referenced Application No. [Attorney Docket No. AATI-19-DS-US].

[0361] As shown in FIG. **22**A, a clock and ramp generator **1116** is used to switch PWM controller **1114** at a frequency Φ and is used to drive the charge pump MOSFETs **1101**, **1102**, **1103**, **1104**, **1105**, **1106**, and **1107** at a frequency m·Φ, which may be higher or lower than the switching frequency used to drive post-regulator **1100**B. In a preferred embodiment m=1 and charge pump pre-converter **1100**A and switched inductor post-regulator **1100**B are clocked at the same frequency and synchronized to the same clock. A BBM circuit **1117** provides the gate drive and necessary level shifting to generate the gate voltages V_{G1} to V_{G7} of the charge pump MOSFETs **1101**, **1102**, **1103**, **1104**, **1105**, **1106**, and **1107**, respectively. A BBM circuit **1113** drives MOSFET **1119** and synchronous rectifier MOSFET **1110** in accordance with PWM controller **1114**, preventing significant shoot-through conduction, i.e. simultaneous conduction in both MOSFET **1119** and MOSFET **1110**, to prevent damage to and improve the efficiency of converter **1100**.

[0362] FIGS. **22**B and **22**C show that the operation of converter **1100** occurs in two alternating phases. In the charging and recirculating phase, shown in FIG. **22**B, each of flying capacitors **1108** and **1109** is charged to substantially one-half the battery voltage Vbatt through MOSFETs **1101**, **1102** and **1103**, while the current I_L in inductor **1118** re-circulates through diode **1111**, the on-state synchronous rectifier MOSFET **1110**, output capacitor **1112**, and load **1120**. MOSFETs **1104**, **1105**, **1106**, **1107** and **1119** remain off in this phase of operation. The on-time of synchronous rectifier MOSFET **1110** may be shorter than the entire period when diode **1111** is conducting and control signals other than simply the gate drive of MOSFET **1110** may determine when it begins and ends.

[0363] In the second phase, shown in FIG. **22**C, MOSFETs **921**, **923** and **932** are turned off and MOSFETs **1104**, **1105**, **1106**, **1107** and **1119** are turned on to connect flying capacitors **1108** and **1109** to inductor **1118**, thereby magnetizing inductor **1118**. During this phase, output capacitor **1112** must supply load **1120**. After a prescribed time determined by the PWM controller **1114**, converter **1100** reverts to the first phase.

[0364] Alternatively the synchronous rectifier MOSFET **1110** and MOSFET **1119** may be switched in a phase opposite to that of the charge pump MOSFETs **1101**, **1102**, **1103**, **1104**, **1105**, **1106**, and **1107**, but this alternative may require a capacitor to be connected to node V_y. In another embodiment the synchronous rectifier MOSFET **1110** is never turned off fully but only reduced to low current operation, in the range of a few microamperes to reduce noise, as described in the above-referenced Application No. [Attorney Docket No. AATI-18-DS-US].

Conclusion

[0365] The family of CLXX converters is capable of producing a well regulated output for a wide range of output to input voltage conversion ratios. These various CLXX topologies are illustrated during their discharge phase in FIGS. **25**A-**25**G.

[0366] In the 0.5×-type fractional CLDU converter **1400** of FIG. **25**A, the input voltage from a battery **1401** is used to repeatedly charge two flying capacitors **1402** and **1403** to a voltage $+V_{batt}/2$ to produce an intermediate voltage V_y equal to $V_{batt}/2$. The intermediate voltage V_y is then used to magnetize a switched inductor in a boost converter **1404** to step up V_y by a factor of 1/(1−D). The resulting output voltage is given by $+0.5 \cdot V_{batt}/(1-D)$, and converter **1400** is capable of down-up operation and voltage regulation at unity voltage conversion ratios.

[0367] In the 2×-type CLUU converter **1410** of FIG. **25**B, the input voltage from a battery **1411** is used to repeatedly charge one flying capacitor **1412** to a voltage $+V_{batt}$ to pro-

NOCO Exhibit 2011
ADC v. NOCO
IPR2024-00671

duce an intermediate voltage V_y equal to $2 \cdot V_{batt}$. The intermediate voltage V_y is then used to magnetize a switched inductor in a boost converter **1413** to step up V_y by a factor of 1/(1−D). The resulting output voltage is given by $+2 \cdot V_{batt}/(1-D)$, and converter **1410** is capable of up-up voltage regulation with extreme voltage conversion ratios at moderate duty factors.

[0368] In the 1.5×-type fractional CLUU converter **1420** of FIG. **25**C, the input voltage from a battery **1421** is used to repeatedly charge two flying capacitors **1422** and **1423** to a voltage $+V_{batt}/2$ to produce an intermediate voltage V_y equal to $1.5 \cdot V_{batt}$. The intermediate voltage V_y is then used to magnetize a switched inductor in a boost converter **1424** to step up V_y by a factor of 1/(1−D). The resulting output voltage is given by $+1.5 \cdot V_{batt}/(1-D)$, and converter **1420** is capable of up-up voltage regulation with extreme voltage conversion ratios at moderate duty factors.

[0369] In the −1×-type CLID converter **1430** of FIG. **25**D, the input voltage from a battery **1431** is used to repeatedly charge one flying capacitor **1432** to a voltage $+V_{batt}$ to produce an inverted intermediate voltage V_y equal to $-V_{batt}$. The intermediate voltage V_y is then used to magnetize a switched inductor in a non-inverting boost converter **1433** to increase the magnitude of V_y by a factor of 1/(1−D) without changing its polarity, i.e. to make a larger negative voltage. The resulting output voltage is given by $-V_{batt}/(1-D)$, and converter **1430** is capable of inverted step-up voltage regulation with extreme negative voltage conversion ratios at moderate duty factors.

[0370] In the −0.5×-type inverting fractional CLDU converter **1440** of FIG. **25**E, the input voltage from a battery **1441** is used to repeatedly charge two flying capacitors **1442** and **1443** to a voltage $+V_{batt}/2$ to produce an intermediate voltage V_y equal to $-V_{batt}/2$. The intermediate voltage V_y is then used to magnetize a switched inductor in a boost converter **1444** to increase the magnitude of V_y by a factor of 1/(1−D) without changing its polarity, i.e. to make a larger negative voltage. The resulting output voltage is given by $-0.5 \cdot V_{batt}/(1-D)$, and converter **1440** is capable of inverted step-up voltage regulation with extreme negative voltage conversion ratios at moderate duty factors.

[0371] In the −1×-type double inverting CLII converter **1450** of FIG. **25**F, the input voltage from a battery **1431** is used to repeatedly charge one flying capacitor **1452** to a voltage $+V_{batt}$ to produce an inverted intermediate voltage V_y equal to $-V_{batt}$. The intermediate voltage V_y is then used as a negative supply rail and to magnetize a switched inductor in a non-inverting boost converter **1453** to increase the magnitude of V_y by a factor of 1/(1−D) without changing its polarity, i.e. to make a larger positive voltage. The resulting output voltage is given by $V_{batt}[D/(1-D)]$, and converter **1450** is capable of above ground up-down voltage conversion and voltage regulation at unity voltage ratios.

[0372] In the −0.5×-type fractional double inverting CLII converter **1460** of FIG. **25**G, the input voltage from a battery **1461** is used to repeatedly charge two flying capacitors **1462** and **1463** to a voltage $+V_{batt}/2$ to produce an inverted intermediate voltage V_y equal to $-V_{batt}/2$. The intermediate voltage V_y is then used as a negative supply rail and to magnetize a switched inductor in a non-inverting boost converter **1464** to increase the magnitude of V_y by a factor of 1/(1−D) without changing its polarity, i.e. to make a larger positive voltage. The resulting output voltage is given by $0.5 \cdot V_{batt}[D/(1-D)]$, and converter **1460** is capable of above ground up-down voltage conversion and voltage regulation at unity voltage ratios.

[0373] While a number of embodiments according to this invention have been described above, these embodiments are intended to be illustrative and not limiting. Persons of skill in the art will be able to devise numerous alternative embodiments within the broad principles of this invention from the descriptions herein.

1. A DC/DC voltage converter comprising:

a pre-converter comprising a switched capacitive circuit: and

a post-regulator comprising a switched inductive circuit,

wherein an output terminal of the pre-converter is coupled to an input terminal of the post-regulator, an input terminal of the pre-converter comprising an input terminal of the DC/DC voltage converter, an output terminal of the post-regulator comprising an output terminal of the DC/DC voltage converter.

2. The DC/DC voltage converter of claim **1** further comprising a feedback path, a first terminal of the feedback path being coupled to the input terminal of the pre-converter, a second terminal of the feedback path being coupled to the output terminal of the post-regulator.

3. (canceled)

4. The DC/DC voltage converter of claim **1** wherein the post-regulator comprises a high-side switch connected in a series path with a low-side switch and an inductor connected to a point in the series path between the high-side switch and the low-side switch.

5. The DC/DC voltage converter of claim **4** wherein the high-side switch comprises a high-side MOSFET and the low-side switch comprises a low-side MOSFET.

6. The DC/DC voltage converter of claim **5** wherein the post-regulator comprises a break-before-make unit coupled to a gate of the high-side MOSFET and a gate of the low-side MOSFET and a pulse width modulation unit coupled to the break-before-make unit.

7. (canceled)

8. The DC/DC voltage converter of claim **6** comprising a clock generator coupled to the pulse width modulation unit and to the pre-converter.

9. (canceled)

10. The DC/DC voltage converter of claim **6** wherein the post-regulator comprises a level shift unit coupled to the pulse width modulation unit.

11. The DC/DC voltage converter of claim **10** comprising a feedback path, a first terminal of the feedback path being coupled to the level shift unit.

12. The DC/DC voltage converter of claim **11** wherein a second terminal of the feedback path is coupled to the output terminal of the post-regulator.

13. The DC/DC voltage converter of claim **1** wherein the pre-converter comprises a charge pump, the charge pump producing an output voltage equal to a predetermined multiple of an input voltage.

14. The DC/DC voltage converter of claim **13** wherein the charge pump produces an output voltage equal to 0.5 times the input voltage.

15. The DC/DC voltage converter of claim **14** wherein the post-regulator comprises a boost converter.

16. The DC/DC voltage converter of claim **15** wherein the post-regulator comprises:

NOCO Exhibit 2011
ADC v. NOCO
IPR2024-00671

an inductor and a low-side MOSFET connected in a series conduction path being an output terminal of the pre-converter and ground; and

a synchronous rectifier MOSFET connected between a common node in the series conduction path between the inductor and the low-side MOSFET and the output terminal of the DC/DC converter.

17. The DC/DC voltage converter of claim **13** wherein the charge pump produces an output voltage equal to 2 times the input voltage.

18. The DC/DC voltage converter of claim **17** wherein the post-regulator comprises a boost converter.

19. The DC/DC voltage converter of claim **18** wherein the post-regulator comprises:

an inductor and a low-side MOSFET connected in a series conduction path being an output terminal of the pre-converter and ground; and

a synchronous rectifier MOSFET connected between a common node in the series conduction path between the inductor and the low-side MOSFET and the output terminal of the DC/DC converter.

20. The DC/DC voltage converter of claim **13** wherein the charge pump produces an output voltage equal to 1.5 times the input voltage.

21. The DC/DC voltage converter of claim **20** wherein the post-regulator comprises a boost converter.

22. The DC/DC voltage converter of claim **21** wherein the post-regulator comprises:

an inductor and a low-side MOSFET connected in a series conduction path being an output terminal of the pre-converter and ground; and

a synchronous rectifier MOSFET connected between a common node in the series conduction path between the inductor and the low-side MOSFET and the output terminal of the DC/DC converter.

23. The DC/DC voltage converter of claim **13** wherein the charge pump produces an inverted output voltage equal to −1 times the input voltage.

24. The DC/DC voltage converter of claim **23** wherein the post-regulator comprises a non-inverting boost converter.

25. The DC/DC voltage converter of claim **23** wherein the post-regulator comprises an inverting boost converter.

26. The DC/DC voltage converter of claim **13** wherein the charge pump produces an inverted output voltage equal to −0.5 times the input voltage.

27. The DC/DC voltage converter of claim **26** wherein the post-regulator comprises a non-inverting boost converter.

28. The DC/DC voltage converter of claim **26** wherein the post-regulator comprises an inverting boost converter.

* * * * *